Breathing and locomotion in birds.

A thesis submitted to the University of Manchester for the degree of Doctor of Philosophy in the Faculty of Life Sciences.

2010

Peter George Tickle

Contents

Chapter 1

Abstract of a thesis by Peter George Tickle submitted to the University of Manchester for the degree of PhD in the Faculty of Life Sciences and entitled 'Breathing and Locomotion in Birds'.

September 2010

Birds are a diverse group of vertebrates, with over 10,000 extant species. Diversification into volant, aquatic and terrestrial environmental niches has precipitated a remarkable morphological diversity between species. Birds have a unique respiratory system consisting of a rigid lung connected to an air sac system. Air is pumped into the respiratory system via movements of the ribcage and sternum. Previous research identified the uncinate processes, ossified projections extending from the vertebral ribs, as critical respiratory and locomotor structures. Uncinate processes facilitate inspiration and expiration through associated muscles that displace the ribs and therefore sternum. External intercostal muscles project from the processes and function during locomotion to stabilise body roll. Therefore uncinate processes provide a link between breathing and locomotion in birds. The objective of my PhD is to extend beyond this basic research on uncinate processes to investigate how diversity in avian body morphology relates to the fundamental functions of breathing and locomotion.

While the function of uncinate processes in respiration has been identified, the mechanism whereby ventilatory movements are elicited is not known. Therefore I present a model that demonstrates how respiratory movements of the skeleton are facilitated by the lever action of uncinate processes. Furthermore, variation in process and sternal morphology is driven by adaptation to different forms of locomotion. Therefore fundamental differences in breathing mechanics may be associated with specialisation to locomotor behaviour. Detailed developmental studies of the uncinate processes in birds are almost nonexistent. I provide the first detailed description of developmental changes in the uncinate processes in the turkey. Ossification of the uncinate processes begins around the time of hatch. However, the base is cartilaginous upon hatching and so the lever action of the processes may be compromised in the chick. I provide further evidence for a functional link between process length and respiratory physiology, since elongated processes support an elevated resting metabolic rate in birds. This link was further explored in physiological experiments where the energetic cost of walking in the barnacle goose was manipulated by load carrying. Carrying extra mass on the sternum is more energetically costly than an equivalent back load indicating that the cost of breathing increased. A directly proportional relationship exists between increasing mass of back load and metabolic rate, while sternal loads were approximately twice as expensive to carry during locomotion. Leg loads incurred the greatest increase in metabolism. Finally, I demonstrate how uncinate processes functioned as respiratory structures in basal avian species and a theropod ancestor of modern birds. Development of the uncinate processes may have been an important step in the evolution of the avian lung - air sac system.

The principal findings of the five first author research articles presented in this PhD thesis shed important new light on the ventilatory mechanics in birds and highlight interactions between breathing and locomotion. Diversity in avian body morphology driven by adaptation to various locomotor behaviours has resulted in modification of the respiratory system.

Declaration

No portion of the work referred to in this thesis has been submitted in support of an application for another degree or qualification of this or any other university or other institute of learning.

Signed: Date:

Copyright Statement

1) The author of this thesis (including any appendices and/or schedules to this thesis) owns certain copyright or related rights in it (the "Copyright") and he has given The University of Manchester certain rights to use such Copyright, including for administrative purposes.

2) Copies of the thesis, either in full or in extracts and whether in hard or electronic copy, may be made only in accordance with the Copyright, Designs and Patents Act 1988 (as amended) and regulations issued under it or, where appropriate, in accordance with licensing agreements which the University has from time to time. This page must form part of any such copies made.

3) The ownership of certain Copyright, patents, designs, trade marks and other intellectual property (the "Intellectual Property") and any reproductions of copyright works in this thesis, for example graphs and tables ("Reproductions"), which may be described in this thesis, may be owned by the author and may be owned by third parties. Such Intellectual Property and Reproductions cannot and must not be made available for use without prior written permission of the owner(s) of the relevant Intellectual Property and/or Reproductions.

4) Further information on the conditions under which disclosure, publication and commercialisation of this thesis, the Copyright and any intellectual Property and/or Reproductions described in it may take place is available in the University IP Policy (see http://www.campus.manchester.ac.uk/medialibrary/policies/intellectual-property.pdf), in any relevant Thesis restriction declarations deposited in the University Library, University Library's regulations (see http://www.manchester.ac.uk/library/aboutus/regulations) and in The University's policy on presentation of Theses.

Signed: Date:

Author Information

Name: Peter George Tickle

Date of Birth: 13th September 1983

Nationality: British

Address: 50 Norris Road, Sale, Cheshire, M33 3QR, UK

Curriculum Vitae

1989-1996	Brooklands Primary School, Sale, Cheshire, UK
1996-2002	Sale Grammar School, Sale, Cheshire, UK
2002-2005	B.Sc. (Hons), School of Biological Sciences, University of Manchester, UK
2005-2006	Research technician, Faculty of Life Sciences, University of Manchester, UK
2006-2010	PhD, Faculty of Life Sciences, University of Manchester, Manchester, UK. Supervisor: Dr J. R. Codd.

Publications

(1) **Tickle, P. G.**, Ennos, A. R., Lennox, L. E., Perry, S. F. and Codd, J. R. (2007) Functional significance of uncinate processes in birds. *J. Exp. Biol.* **210**, 3955-3961.

(2) **Tickle, P. G.** and Codd, J. R. (2009) Ontogenetic development of the uncinate processes in the domestic turkey (*Meleagris gallopavo*). *Poultry Sci.* **88**, 179-184.

(3) **Tickle, P. G.**, Nudds, R. L. and Codd, J. R. (2009) Uncinate process length in birds scales with resting metabolic rate. *PLoS ONE* **4**(5), e5667.

(4) Nudds, R.L., Gardiner, J.D., **Tickle, P.G.** Codd, J.R. (2010) Energetics and kinematics of walking in the barnacle goose (*Branta leucopsis*). *Comp. Biochem. Physiol. A* . **156**, 318-324.

(5) **Tickle, P. G**., Richardson, M. F. and Codd, J.R. (2010) Load carrying during locomotion in the barnacle goose (*Branta leucopsis*): the effect of load placement and size. *Comp. Biochem. Physiol. A* **156**, 309-317.

(6) Codd, J. R., Heuer, C. and **Tickle, P. G.** (2010) Uncinate processes in birds and other tetrapods. *ZFMK Bonner Zool. Beitr*. *In press*.

(7) Waring, K., **Tickle, P.G.**, Stokkan, K. A.., Codd, J.R. and Sellers, W.I. The musculoskeletal anatomy of the reindeer (*Rangifer tarandus)*: fore and hind limb. *Polar Biol. In press*.

(8) Nudds, R., Folkow, L., Lees, J. **Tickle, P.** Stokkan, K-A and Codd. J. Cost of terrestrial transport in Svalbard rock ptarmigan (*Lagopus muta hyperborea*): first evidence for energy savings from aerial running in a bird. *Proc. R. Soc. B. In review.*

(9) **Tickle, P. G.**, Norell, M. A., Nudds, R. L. and Codd, J. R. A continuum in breathing mechanics from early theropods to living birds. *Proc. R. Soc. Lond. B. In review*.

(10) **Tickle P.G.,** Lean, S., Rose, K. and Codd, J.R. How increasing speed and load carriage affects the energetics and kinematics of locomotion in the tufted duck (*Aythya fuligula*). *In preparation*.

(11) **Tickle, P.G.,** Nudds, R.L. & Codd, J.R. Scaling of uncinate process length, flight muscle mass and breathing frequency in birds. *In preparation*.

Conference Presentations

(1) **Tickle, P. G.** and Codd, J. R. (2007) Accessory breathing structures in birds with different locomotor modes. Society for Experimental Biology, Glasgow, UK, 31st March – 4th April, 2007.

(2) **Tickle, P. G.,** Manning, P. L. and Codd, J. R. (2008) Uncinate processes in extant birds and extinct dinosaurs. Invited Presentation: Progressive Palaeontology, Manchester, UK, 29th May, 2008.

(3) **Tickle, P. G.** (2009) The energetics of load bearing in the barnacle goose (*Branta leucopsis*). Invited Presentation: International Congress of Respiratory Science, Bonn, Germany, 9th-13th August 2009.

Acknowledgements

I would firstly like to thank my supervisor Jonathan Codd for his unstinting support over the course of my PhD. His mentorship, approach to science and friendship throughout my studentship made for a most enjoyable experience, even in the most exacting circumstances.

Secondly I would like to thank Robert Nudds for his patient help and advice over the last few years. His contribution to my research, especially concerning the mysteries of respirometry and statistics proved invaluable. I would also like to thank Roland Ennos for his contribution to this thesis and everyone in the biomechanics laboratory – Jamie, Adam, Dave, Si, John and numerous undergraduate and masters students - who ensured that the last four years were so entertaining and memorable.

Finally I would like to thank my family and friends for all their help and support throughout my greatly extended time as a student!

Organisation of this PhD thesis.

I have submitted this PhD thesis for examination at the University of Manchester in the Alternative Format. The Alternative Format allows inclusion of chapters that are either already published, or in the format of, journal articles. Therefore each chapter is presented in the format particular to the journal where it is either published or submitted. Accordingly, reference lists are provided at the end of each research chapter while citations from the introductory and concluding chapters are listed at the end of the thesis. The first four research chapters presented have been published in peer-reviewed journals while the fifth chapter has been submitted for peer-review. I am the first author on all papers submitted as part of this thesis. However, given the collaborative nature of some of the studies presented here, the contribution of each author to the relevant article is disclosed below.

Chapter 2

Tickle, P. G., Ennos, A. R., Lennox, L. E., Perry, S. F., and Codd, J. R. (2007) Functional significance of the uncinate processes in birds. *Journal of Experimental Biology* 210, 3955-3961

I carried out the research and analysis for this paper. Dr Roland Ennos contributed the mathematical model of uncinate process function that I used to estimate the mechanical advantage of uncinate processes in dissection specimens. Laura Lennox helped to dissect the razorbill, *Alca torda*. This study was based upon an original idea developed by Professor Steven Perry at the University of Bonn. I wrote the article with final editing assistance from Dr Jonathan Codd and co-authors.

Chapter 3

Tickle, P. G. and Codd, J. R. (2009) Ontogenetic development of the uncinate processes in the domestic turkey (*Meleagris gallopavo*). *Poultry Science* 88, 179-184.

I completed and analysed data from all material properties testing and histochemical experiments. Domestic turkey eggs were provided by Dr Grenham Ireland of the University of Manchester. Materials testing experiments were conducted with the technical assistance of Riaz Akhtar, Andrew Forrest and Ken Gyves at the School of Materials, University of Manchester. I wrote the article, while Dr Codd edited and offered advice on the manuscript.

Chapter 4

Tickle, P., Nudds, R. and Codd, J. (2009) Uncinate process length in birds scales with resting metabolic rate. *PLoS ONE* 4, e5667.

Morphological data on uncinate processes from Chapter 2 was augmented by additional measurements of skeletal specimens. I collated data from the literature on metabolic rates in birds. I performed general linear model and phylogenetic independent contrast analyses while Dr Robert Nudds completed regression analyses. I wrote the article for publication, to which suggestions and editing advice were provided by Drs Nudds and Codd.

Chapter 5

Tickle, P. G., Richardson, M. F. and Codd, J. R. (2010) Load carrying during locomotion in the barnacle goose (*Branta leucopsis*): The effect of load placement and size. *Comparative Biochemistry and Physiology, Part A* 156, 309-317.

I completed all respirometry trials and processed all resulting physiological and kinematic data. Mark Richardson assisted with collecting respirometry data on sternally loaded birds. I wrote the article and a final edit was provided by Dr Codd.

Chapter 6

Tickle, P. G., Norell, M. A., Nudds, R. L. and Codd, J. R. A continuum in breathing mechanics from early theropods to living birds. *Proceedings of the Royal Society B: Biological Sciences. (Under review)*

I measured *Confuciusornis sanctus* specimens at the Senckenberg Research Institute, Frankfurt, and applied the geometric model of uncinate process function from Chapter 2 to all species. Dr Mark Norell provided specimen access and contributed photographs of *Oviraptor*. I wrote the submitted manuscript with editorial assistance from Drs Nudds, Norell and Codd.

Chapter 1

General Introduction

1. Introduction

1.1 The Avian Respiratory System

Birds are an extremely diverse group of terrestrial vertebrates with over 10,000 extant species. Diversification into volant, aquatic and terrestrial environmental niches has precipitated a remarkable morphological diversity between species. Whilst of course there are strong underlying similarities among birds, there are obvious differences between, for example, a penguin (a diving bird), an ostrich (a running bird) and a hummingbird (a fast flying hovering bird). Even within a particular group differences can be found. For example, if we look at flying birds, while the wings of soaring species, such as albatross, are long and narrow the wings in a pheasant, a bird that requires short, powerful and manoeuvrable flight, are broad and elliptical (Kardong 2006). Such diversity amongst extant birds presents a challenge for zoologists: what are the biomechanical and physiological consequences of such varied morphology and anatomy?

For the constancy of metabolism and survival, all vertebrates must deliver oxygen to, and remove waste products from, respiring tissues by interaction of circulatory and respiratory systems. The lung is the location of gas exchange with the external environment in air-breathing higher vertebrates. The fundamental challenge of maintaining oxygen supply to the lung in a wide range of terrestrial vertebrate body morphologies and lifestyles is reflected by the morphological diversity of respiratory organs. For example, while some amphibians are able to perform respiratory gas exchange using specialised skin, lizards, mammals and birds have internal gas exchange surfaces. Air from the external environment must therefore be delivered to the internal lung using a ventilatory pump. The highly derived mammalian lung is constructed from numerous bifurcations of the primary airway, which terminate in tiny hollow alveolar cavities. These alveoli are tidally ventilated, so that inhaled air is brought into the lung and removed upon exhalation. In contrast, there is a variety of lung anatomy within the lizards, from lungs consisting of a single sack-like chamber to more complicated multichambered structures. The anatomy of crocodilian and bird lungs has some shared characteristics but also exhibits some important differences. For example, birds and crocodiles have multichambered lungs through which air passes in one direction only (Farmer and Sanders, 2010). However, unlike the crocodilian lung, the avian lung is rigid and connected to a series of air sacs.

While there are broad similarities in the respiratory system of birds, many differences in behaviour and physiology have contributed to a wide diversity of body morphologies. In this thesis, I present original research on how the mechanisms that facilitate airflow in the avian respiratory system are affected by the demands of locomotion. Morphological analysis of the avian skeleton is used in Chapter 2 to highlight the interaction between respiration and locomotion in birds. I present a model that demonstrates how respiratory movements of the skeleton are facilitated by the lever action of osteological characters, the uncinate processes. Furthermore, evidence is presented for variation in thoracic morphology driven by adaptation to different forms of locomotion. In Chapter 3 I present a detailed description of how ventilatory function may be affected during skeletal development. Ossification of uncinate processes was investigated in a precocial species using histochemical and materials testing techniques. I provide evidence for a functional link between respiratory structure morphology and respiratory physiology in Chapter 4. Here I demonstrate the relationship between uncinate process morphology and the rate of energy metabolism in birds. This link was further explored in Chapter 5 where the energetic cost of walking in the barnacle goose was manipulated by load carrying. Interaction between locomotion and respiration was explored by experimentally manipulating the mass of the back, sternum and legs. Comparison of the energetics of locomotion under these conditions highlights the potential metabolic cost of moving the sternum. Finally, in Chapter 6 I considered the evolution of respiratory and locomotor systems in theropod dinosaurs and their avian descendants by comparison of fossil specimens with modern birds. Given the interaction of respiratory and locomotor systems highlighted in earlier chapters, this final research chapter gives an overview of the evolution of the modern avian ventilatory apparatus. I consider how development of the modern avian respiratory pump may have been instrumental in the evolution of energetically expensive locomotor behaviours.

The overall objective of this thesis is to further our understanding of how the diversity in avian morphology and anatomy relates to aspects of their breathing and locomotion.

1.1.1 Structure of the lung and air sacs

The respiratory apparatus in birds consists of a highly derived lung connected to a series of avascular air sacs. In contrast to mammals, birds have a rigid parabronchial lung that is attached to the craniodorsal vertebral column, horizontal septum and vertebral ribs (Maina and King, 1972; Duncker, 1974). Air sacs consist of a simple epithelial wall supported by connective tissue, are not vascularised and play no direct role in gas exchange (Magnussen et al., 1976). Air sacs are divided into an anterior group consisting of the cervical, interclavicular and anterior thoracic sacs, and a posterior group, comprising the posterior thoracic and abdominal air sacs (Duncker, 1974) (Figures 1, 2 and 3). There is diversity in size and number of air sacs in the thoracic cavity of birds (Duncker, 1971). For example, the domestic turkey has 7 air sacs while the white stork has 11 (King and McLelland, 1975). Furthermore, the largest air sac varies between species; in some birds the caudal thoracic air sac is largest, while in others the abdominal air sac has the greatest volume (King and McLelland, 1975; Farmer, 2006). The functional significance of differences in air sac morphology is unknown, although variation may be in some way linked to providing balance and agility during locomotion (Farmer, 2006). Airways that connect the system of air sacs to the lung derive from a bifurcation of the trachea. This split produces two primary bronchi (mesobronchi) that extend to the posterior air sacs via the intrapulmonary bronchus that bypasses the lung (Figures 1 and 3). Four sets of secondary bronchi (medioventral, mediodorsal, lateroventral and laterodorsal) branch from the upper wall of the intrapulmonary bronchus (Maina, 2006) (Figure 1). Narrow (3-10μm) parabronchial tubes extend from the secondary bronchi to form the functional gas exchange surface of the lung (Duncker, 1974). These terminal gas exchanging air capillaries branch off from the parabronchi to form continuous tubules, rather than spherical terminal units as is the case in the mammalian lung, and have a diameter of around 10 to 20 μm (Maina, 2000; West, 2006). In comparison, the diameter of human alveoli is about 300 μm (West, 2006). Therefore the surface density of the blood-gas barrier is far greater in the avian lung compared to the lung in mammals (Maina, 2000). Flow of inspired air in the parabronchial capillaries is perpendicular to the direction of blood flow forming a very effective cross-current gas exchanger. This anatomical arrangement allows oxygenated blood to leave the lung with a higher partial pressure of oxygen than the air leaving the gas exchange tissue. Therefore efficiency of oxygen extraction in the crosscurrent lung of birds is greater than in the mammalian tidal alveolar lung (Scheid and Piiper, 1970). For example, little penguins may be able to extract 50-60% of inspired oxygen whereas the value for bats is in the region of 40-45%

(Stahel and Nicol, 1988; Chappell and Roverud, 1990). Other adaptations of the bird lung include a relatively thin blood-gas barrier, maximising the diffusing capacity of the lung (Maina and King, 1982; Gehr et al., 1980). The highly efficient cross-current system coupled with a very thin blood-gas barrier enables birds to sustain a high rate of metabolism (Maina, 2000) and perform remarkable physiological feats in conditions of low oxygen such as high altitude flight (Butler 2010).

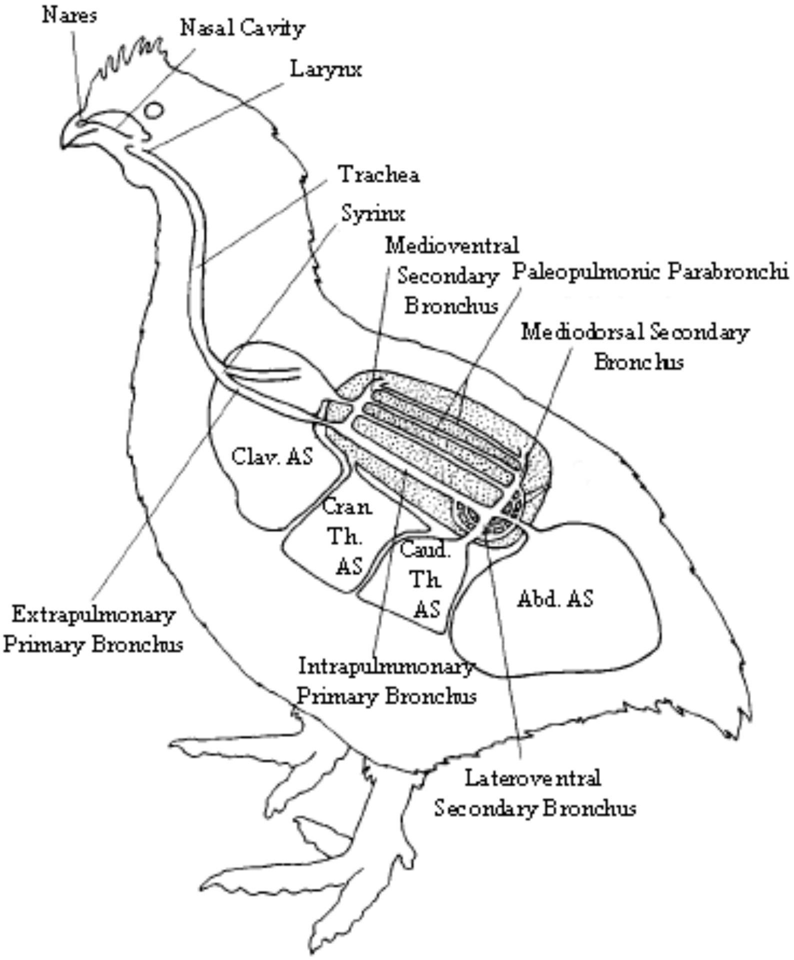

Figure 1: Overview of the respiratory system in a chicken. Position of the lung, air sacs and airways are indicated.

Clav. AS: clavicular air sac; Cran. Th. AS: cranial thoracic air sac; Caud. Th. AS: caudal thoracic air sac; Abd. AS: abdominal air sac.

(from Fedde, 1998)

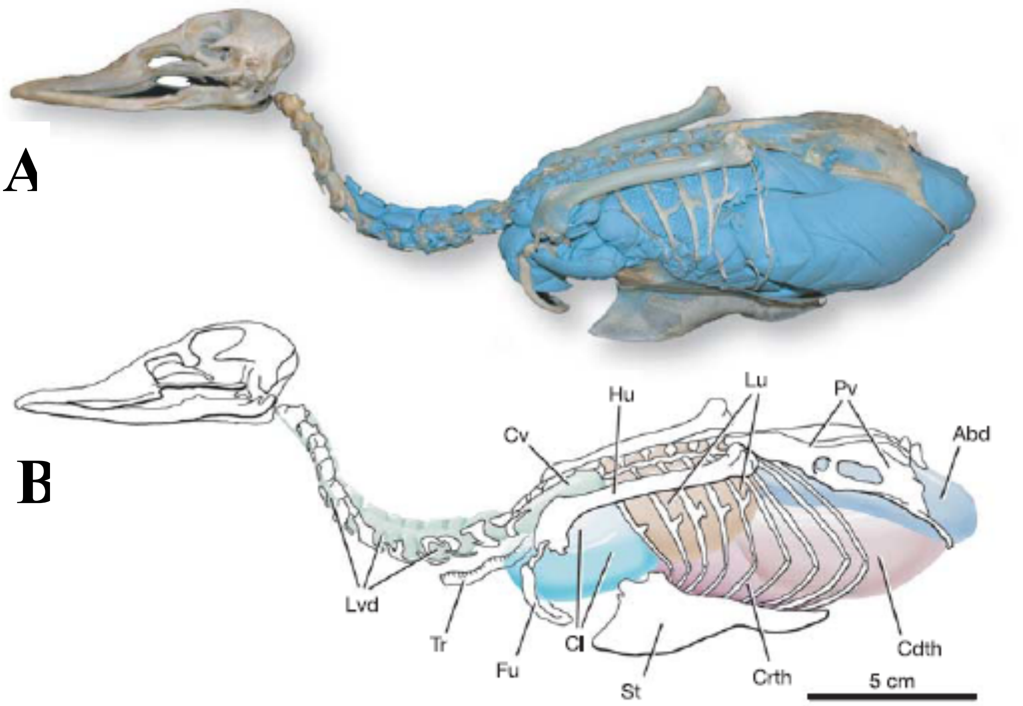

Figure 2: Air-sac system in a duck, *Anas crecca*.

A) Blue latex injection shows the extent of the air sac system in birds. Air sacs invade bone and extend between layers of tissue.

B) Main elements of the avian respiratory system: Abd: abdominal air sac; Cdth: caudal thoracic air sac; Cl - interclavicular air sac; Crth - cranial thoracic air sac; Cv - cervical air sac; Fu - furcula; Hu - humerus; Lu - lung; Lvd - lateral vertebral diverticula; Pv - pelvis; and Tr - trachea

(from O’Connor and Claessens, 2005)

1.1.2 Airflow in the avian respiratory system

Birds use bellows-like movement of air sacs to pump air across the gas exchange tissue (Scheid, 1979). Anatomical complexity within the avian respiratory system has confounded attempts to describe the pattern of airflow around the lung and air sacs. Since the lung is connected to airways at both anterior and posterior ends, contrasting with the blind-ended alveoli found in mammals, it is not clear from morphology alone how inspired air moves across the lung (Maina *et al.*, 2009). Interaction between air sacs, bronchi and the lung coupled with a lack of anatomical valving in the airways means that there is not an obvious pathway that inspired air will follow. Glass models of the avian respiratory system were constructed in early attempts to understand movement of inspired air (Dotterwich, 1936; Hazelhoff, 1951) while other researchers studied changes in gas composition at various sites in the chicken lung (Zeuthen, 1942; Schmidt-Nielsen et al, 1969). Seminal research on the movement of air within the respiratory system of the duck was produced in the early 1970s by Bretz and Schmidt-Nielsen (1971; 1972). The first direct measurements of airflow were determined in the primary bronchus and secondary bronchi using thermistor probes (Bretz and Schmidt-Nielsen 1971). Detection of a marker gas introduced into the respiratory system provided further evidence of the pathways taken by inhaled air. The movement of gas in the respiratory system is suggested to be a two cycle event (Bretz and Schmidt-Nielsen, 1972) (Figure 3):

1) During the inspiratory phase of the first cycle inspired air moves directly from the primary bronchus into the posterior air sacs, bypassing the parabronchial gas exchange tissue. Anterior air sacs do not receive a significant portion of the air inhaled during the first inspiration (Figure 3A).

2) Inhaled air passes into the mediodorsal secondary bronchi and parabronchi during the expiratory phase of the first cycle (Figure 3B).
3) Air in the parabronchi is drawn into the anterior air sacs during the inspiratory phase of the second cycle (Figure 3C).
4) During the expiratory phase of the second cycle, this air is exhaled from the anterior air sacs and from the respiratory system (Figure 3D).

The flow of air through the parabronchial tissue during inhalation and exhalation is therefore suggested to be unidirectional (Bretz and Schmidt-Nielsen, 1971). The operation of the counter-current gas exchange system in birds is made possible by such unidirectional flow.

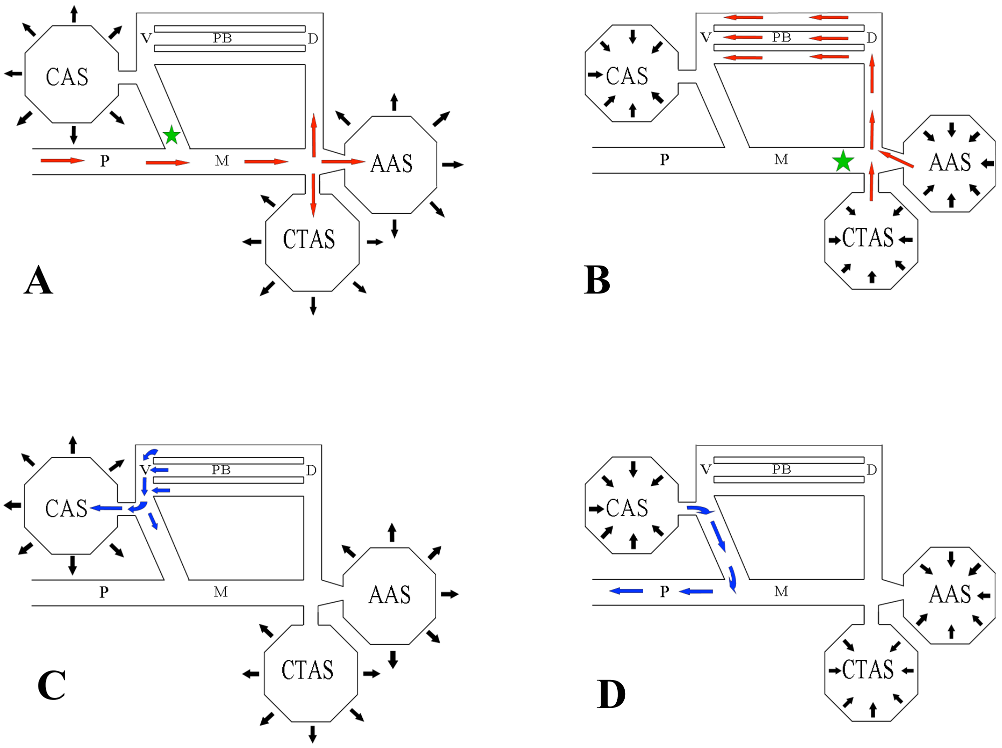

Figure 3: Schematic diagram of airflow in the avian respiratory system. Anterior is to the left. CAS: group of cranial air sacs; AAS: abdominal air sac; CTAS: caudal thoracic air sac; P: primary bronchus; M: meso (intrapulmonary) bronchus; V: medioventral secondary bronchi; PB: parabronchial gas exchange tissue: D: mediodorsal secondary bronchi. Green stars show the locations of inspiratory and expiratory aerodynamic valves. Black arrows indicate air sac volume changes. Arrows show the pathway taken by air through the respiratory system; red arrows: air prior to passage through lung; blue arrows: air that has passed through the lung.

- **A)** Inspiration 1: air is drawn into the posterior air sacs.
- **B)** Expiration 1: air is pumped into the mediodorsal bronchus and parabronchi.
- **C)** Inspiration 2: air in the parabronchi is drawn into the medioventral bronchus and anterior air sacs.
- **D)** Expiration 2: air is exhaled from the anterior air sacs and respiratory system.

Despite the evidence for unidirectional flow in the avian lung, the precise mechanisms that facilitate such airflow remain equivocal. For unidirectional flow to occur, air must pass into the posterior air sacs before being pumped across the lung. Therefore inspired air must be shunted past openings of the medioventral secondary bronchi or else passage of airflow will move into the cranial air sacs bypassing the lung (Figure 3A, green star). Furthermore, upon expiration air must flow over the lung rather than exiting the body via the intrapulmonary mesobronchi (Figure 3B, green star). Absence of anatomical valves in the airways (Scheid *et al*., 1972; Jones *et al*., 1981) means that airflow around the respiratory system must be directed according to aerodynamic principles. Airway geometry and air sac pressure differentials might cause changes in the velocity and pressure of gas-flow, thereby directing air around the respiratory system efficiently (Scheid *et al*., 1972; Fedde, 1998; Maina *et al*., 2009). However, much research on how air moves around the avian respiratory system remains to be completed. Few species have so far been investigated and experiments are typically conducted in resting birds. Therefore little information is available on how differences in respiratory anatomy and the increased demand for oxygen during exercise affects airflow.

1.1.3 The avian aspiration pump.

The ventilatory pump produces airflow over the internal gas exchange surface in birds; muscles function to produce movements of the thoracic skeleton causing pressure changes in the pleural cavities. The vertebral column spanning the thorax is connected to the sternum by ossified ribs consisting of dorsal (vertebral) and ventral (sternal) components. In all extant birds except the screamers (Anhimidae) (Bellairs and Jenkin, 1960) ossified projections, the uncinate processes, extend caudally from several vertebral ribs (Figure 4). A cartilaginous kinetic joint connects the vertebral to the sternal ribs that articulate ventrally along the lateral margins of the sternum. During inspiration, hypaxial muscles associated with the uncinate processes facilitate forward and upward movement of the vertebral ribs (Codd *et al*, 2005), expanding the transverse diameter of the thoracic cavity (Figure 5). Each vertebral rib connects to the thoracic vertebrae by a twin articulation. The capitulum articulates with the diapophysis of the vertebral column while the tuberculum connects to the parapophysis of the processus transversus. Movement of the vertebral ribs is restricted to a fixed plane defined by the arrangement of the articulation points with the vertebrae (Zimmer, 1935). An increase in the angle between vertebral and sternal ribs causes ventral displacement of the sternum (Claessens, 2008). Ventilatory movements of the sternum have typically been described as scissor-like (Kardong, 2006) although recent research in three walking species indicates that displacement in these birds may follow an elliptical trajectory (Figure 5; Claessens, 2008). Since the caudal sternal ribs are relatively long, the caudal sternal margin is displaced further ventrally than the cranial margin (Claessens, 2008). During expiration, reduction in the angle between vertebral and sternal ribs causes cranial and dorsal movement of the sternum, and may be aided by elastic recoil in addition to the expiratory muscles of the thorax (Claessens, 2008).

For birds resting on their sternum, for example when incubating eggs, sternal movement is restricted. Under these conditions reduction in thoracic pressure for inspiration is facilitated by lateral flaring of the ribs (Codd *et al*., 2005) and dorsal displacement of the vertebral column caused by an increase in angle between vertebral and sternal ribs (Claessens, 2008). Therefore body posture has an effect on breathing, indicating that there is plasticity in the ventilatory mechanics of birds. A further mechanism for lung ventilation when sternal movements are restricted has been suggested based upon observations of pelvic movements in birds. In the pigeon (*Columba livia*), pelvic musculature is active during inspiration to facilitate elevation of the pelvis (Baumel, 1990). Depression of the pelvis was caused by expiratory abdominal muscles indicating that pelvic movements can assist in breathing. However, subsequent analyses of birds have failed to find evidence of this putative accessory breathing mechanism. Cineradiographic investigation of walking birds (emu (*Dromaius novaehollandiae*), guinea fowl (*Numida meleagris*) and tinamou (*Nothoprocta perdicaria*)) did not show any contribution of the post-sacral vertebrae to breathing (Claessens, 2004; Claessens, 2008). However, the number of species used remains low and the potential effects on the respiratory system of stress (such as conditions of low oxygen), which may cause a switch to alternative ventilatory mechanisms, remain unknown.

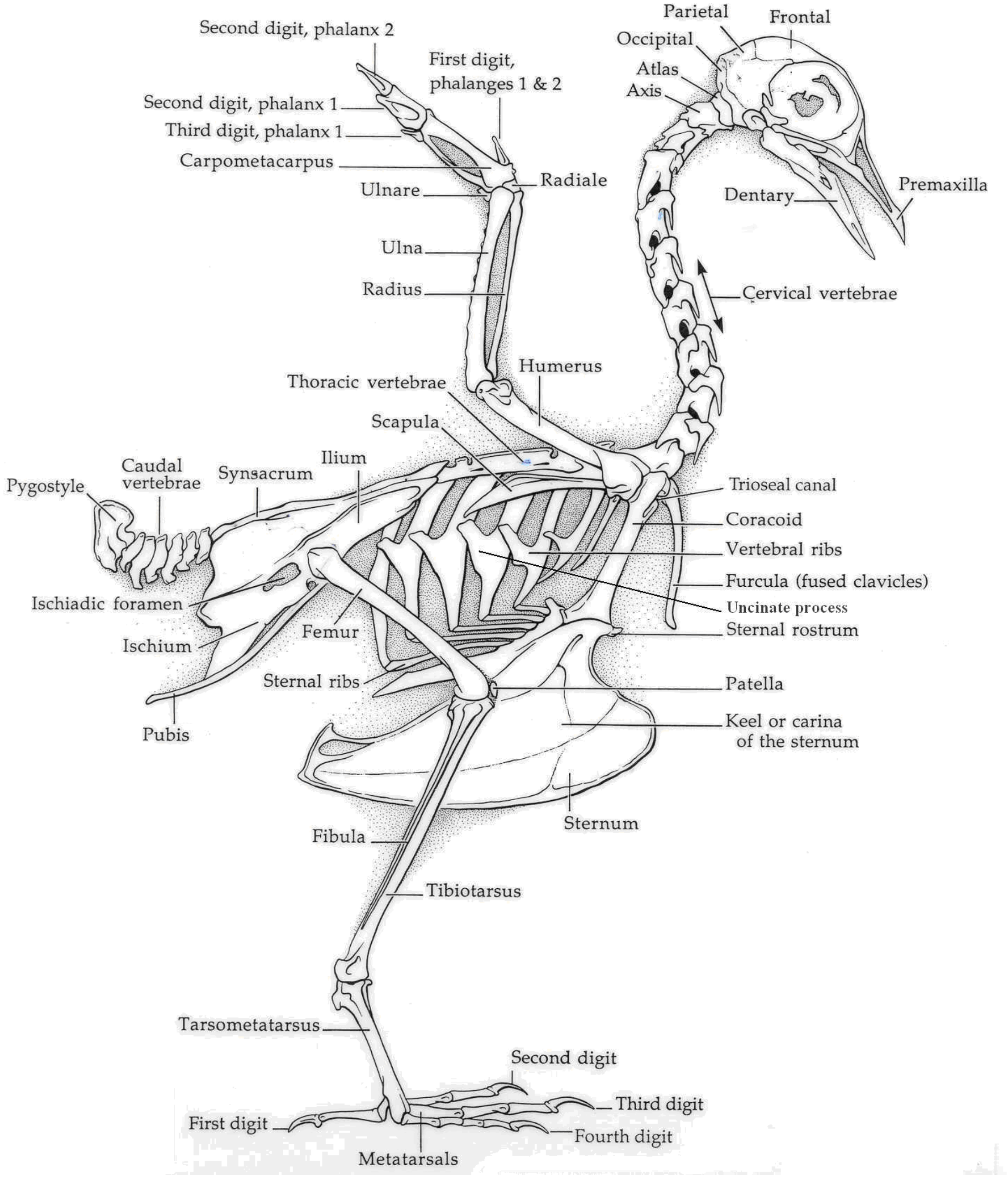

Figure 4: Skeleton of a rock pigeon (*Columba livia*) showing detail of the major structures. The thoracic skeleton and pectoral girdle comprise of the thoracic vertebrae, vertebral and sternal ribs, uncinate processes, sternum, coracoids, furcula and scapula.

(taken from: http://www.zoo.ufl.edu/courses/vertzoo/lab_birds.html)

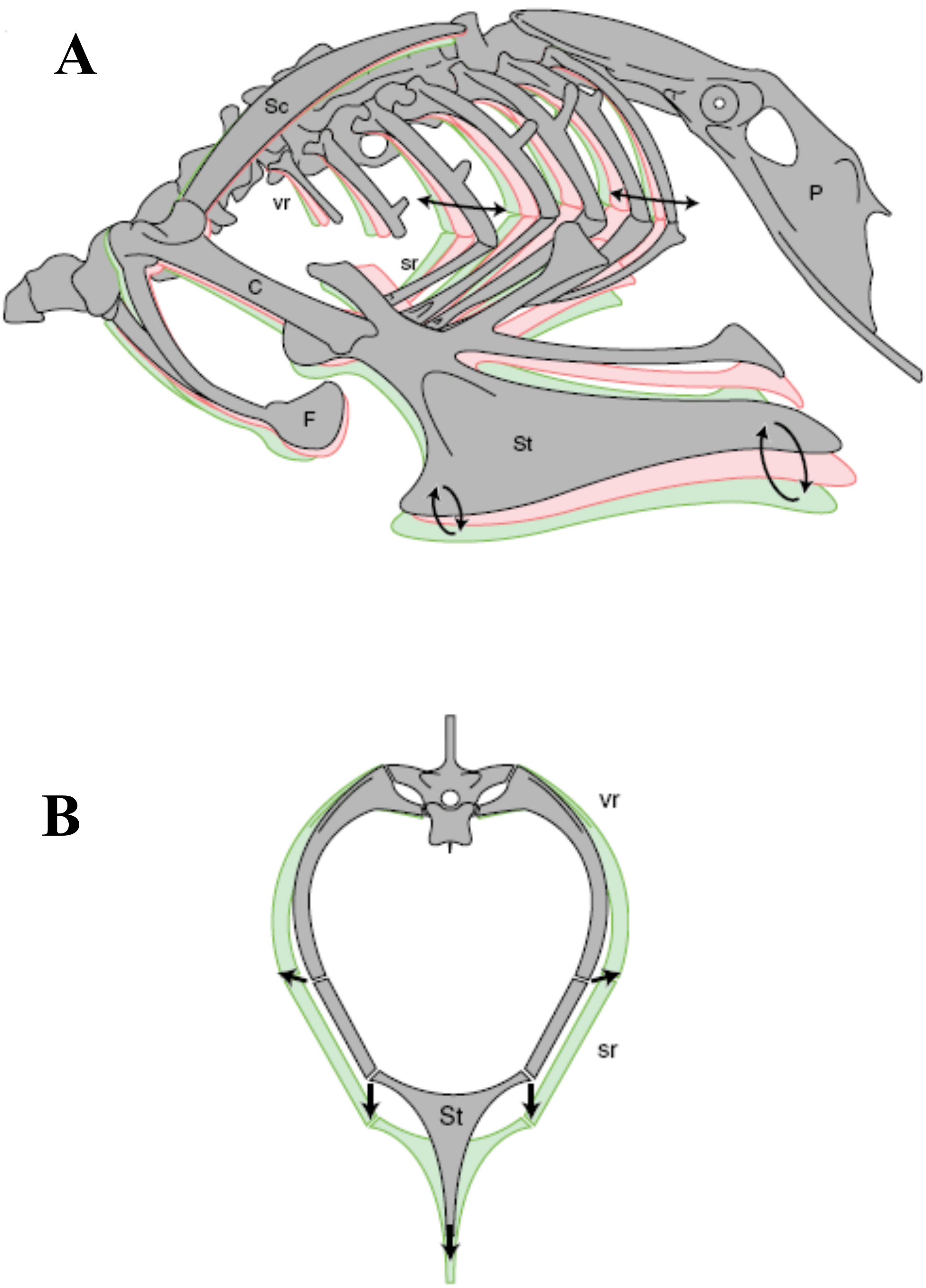

Figure 5: A model of the skeletal aspiration pump in birds (Claessens, 2008). Lateral (**A**) and transverse (**B**) view of skeletal movements during lung ventilation. The sternum moves in an elliptical rotation due to movements of the vertebral ribs (A): grey, end expiration; pink, mid-inspiration; green, peak inspiration. Upon inspiration, the vertebral ribs move forwards and upwards (A; B). St, sternum; sr, sternal rib; vr, vertebral rib; v, vertebral column; sc, scapula; c, coracoid; f, furcula; P, pelvis.

1.2 The uncinate processes in birds

Uncinate processes are hook-shaped (Lat., uncinatus = hooked, from uncus = hook) ossified projections that extend caudo-dorsally from the vertebral ribs in birds (Figures 4 and 6). Hypotheses of uncinate process function include a role in strengthening the rib cage (King and McClelland, 1975; Walker and Liem, 1994; Kardong, 2006), forming a site for the attachment of respiratory and locomotor musculature (Hildebrand, 1982) and as an adaptation for flight (Welty and Baptista, 1988). Zimmer (1935) concluded that the uncinate processes function as levers to facilitate movement of the ribs. These hypotheses were based on the general morphology of the processes rather than experimental evidence. However, recent *in vivo* research confirmed that uncinate processes do indeed have an integral role in ventilation, assisting inspiration and expiration in addition to having a locomotor role (Codd *et al*., 2005).

Codd *et al* (2005) investigated the activity of muscles associated with uncinate processes (the appendicocostal, external oblique and external intercostal muscles: Figure 6) during locomotion and normal quiet breathing. The experimental protocol addressed the difficulties inherent in previous work on respiratory muscles (Kadono et al., 1963; Fedde et al., 1964) by using non-anaesthetised and unrestrained giant Canada geese (*Branta canadensis maximus*). The external intercostal muscles occupy the spaces between adjacent ribs (Figure 6). No ventilatory role was determined by Codd (2005), in contrast to earlier work (Kadono et al., 1963; Fedde et al., 1964). Activity of the portion of external intercostal muscle adjacent to the uncinate process was instead consistent with contralateral limb support. This result supports earlier research in dogs, amphibians and reptiles that demonstrated that external intercostal muscles are involved in locomotion (De Troyer et al., 1985; Carrier, 1990, 1991, 1993, 1996). The appendicocostales muscle (Shufeldt, 1890) originates along the caudoventral edge of the uncinate process and inserts onto the following vertebral rib (Figure 6). The insertion point often passes along the cranial edge of the rib merging into the external intercostal muscle, of which it has therefore traditionally been considered an extension (George and Berger, 1966; Vanden Berge and Zweers, 1993). Codd *et al* (2005) demonstrated that appendicocostal activity was correlated with inspiration and locomotion. Activity was recorded during the inspiratory phase of ventilation in the sitting, standing and running bird. Appendicocostal activity increased during sitting, where it is likely to have an important role in laterally flaring of the rib cage thereby facilitating inspiration. Biphasic activity was apparent during locomotion, consistent with a dual locomotor and respiratory role. Therefore in addition to facilitating inspiration, EMG activity indicated a role in contralateral limb support, perhaps stabilising the trunk during running. The third muscle studied by Codd *et al* (2005) was the external oblique muscle (Figure 6). Previous EMG studies demonstrated that the external oblique muscle is activated in phase with expiration (Kadono et al., 1963; Fedde et al., 1964). Codd *et al* (2005) confirmed these results, suggesting that the oblique muscle aids expiration by dorsal movement of the sternum. The insertion points of the muscle suggest that uncinate processes act as a brace for movement of the sternum during expiration. Therefore the potential action of the external oblique muscle in elevating the sternum during expiration provides evidence of a functional link between the uncinate processes and the sternum.

The conclusions drawn from this study of muscle function forms the foundation for much of the research presented in this thesis. Hypotheses of uncinate process function tested in this thesis build on the work of Codd *et al* (2005), where interaction of breathing and locomotion in thoracic muscles was reported.

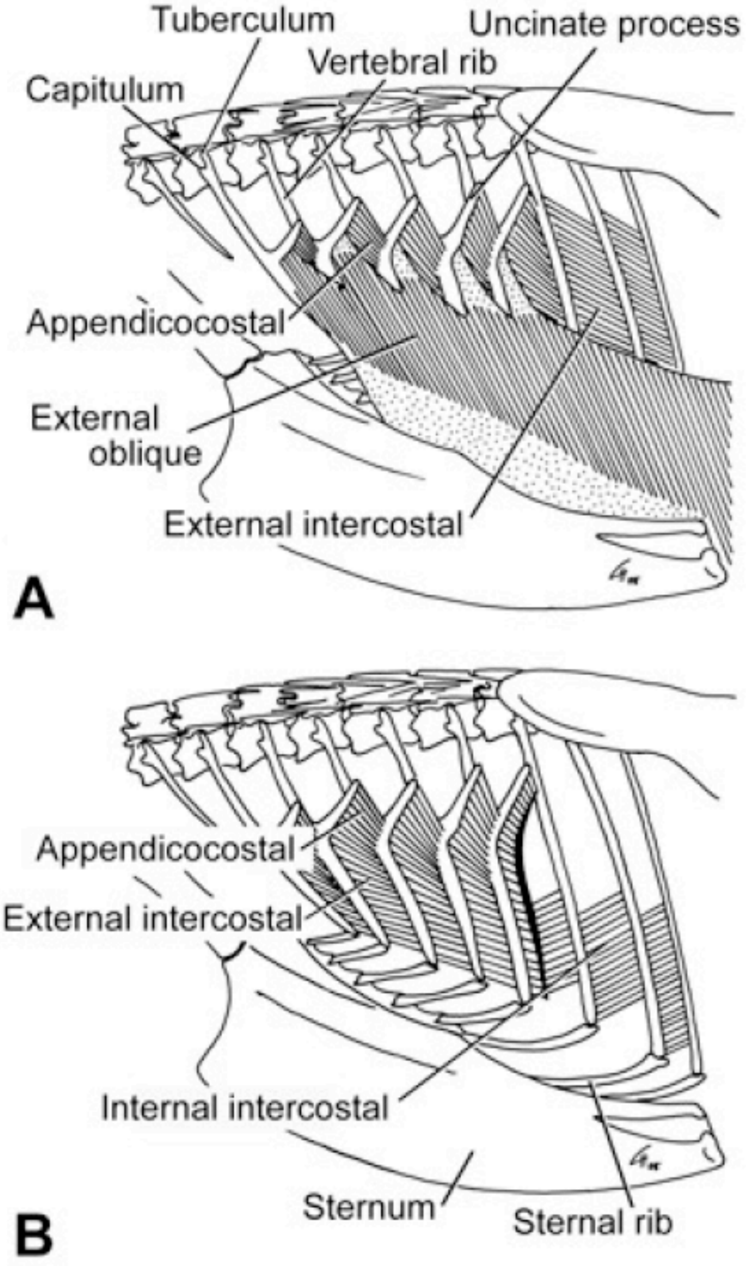

Figure 6: Diagram showing the musculo-skeletal anatomy of the avian thorax. **A)** Uncinate processes project from the proximal surface of the vertebral rib and are associated with appendicocostal, external intercostal and external oblique musculature. **B)** Appendicocostal muscle fibres merge into the external intercostal muscles. Anterior is to the left (Perry et al, 2005).

1.2.1 Uncinate process morphology and biomechanics

While Codd *et al.* (2005) provided evidence for the activity of muscles during respiration and locomotion, a model to explain the mechanism by which the ribs may be moved remains unreported. Therefore Chapter 2 (Tickle *et al*., 2007) presents a mathematical model to determine the mechanical advantage of the uncinate processes for movements of the ribs and therefore sternum during respiration. Furthermore, it has been suggested that the length of the process is proportional to the magnitude of the proposed uncinate lever action on the ribs (Fedde, 1987). I therefore present experimental evidence to show the effect of varying uncinate process morphology on movement of the ribs in birds.

Extant birds include species which specialise in a variety of locomotor behaviours. For example, the emu (*Dromaius novaehollandiae*) is morphologically adapted to walking and running (Patak and Baldwin, 1993) while others have specialisations to flying, swimming and diving (Tucker, 1993; Dyke and Rayner, 2001; Rayner and Couldrick, 2003). Interestingly, variations in uncinate process morphology have been linked to differences in locomotor mode. Duncker (1971) and Welty (1988) both reported anecdotally that uncinate processes appear to be elongated in diving species such as penguins and guillemots. This observation may be of critical importance to our understanding of breathing mechanics in birds. A longer process would have a greater area available for the insertion and attachment of muscles, potentially affecting the mechanics of inspiration, expiration or both. Varying process morphology may affect the anatomy of associated muscles suggesting the existence of functional differences in breathing mechanics. Therefore it is important to establish whether there are significant differences in ventilatory structure morphology between species adapted to different primary modes of locomotion.

1.3 Constraints on breathing in birds

1.3.1 Development

Oviparous reproduction is a defining avian characteristic. Every bird species produces eggs that are introduced into the external environment and incubated until hatching. Before musculo-skeletal development is sufficiently advanced for respiratory rib movements, oxygen and carbon dioxide are exchanged between the blood and environment using a specialised membrane. This chorioallantoic membrane is a highly vascularised structure that attaches to the inner membrane of the calcified eggshell. In conjunction with diffusion of gas through the porous eggshell, the chorioallantois meets the gas exchange requirements of respiring tissue in the developing chick until around the time of hatch (Tullett and Deeming, 1982). At this point, contribution of the chorioallantoic membrane to gas exchange reduces and is replaced by lung ventilation (Menna and Mortola, 2002). This transition period, whereby gas exchange is provided by two separate respiratory mechanisms, lasts for around a day in the chicken embryo (Dawes, 1981; Burton and Tullett, 1985). Upon hatch, the skeletal aspiration pump solely facilitates gas exchange (Menna and Mortola, 2002).

Skeletal development in the chick embryo may represent an important constraint upon respiration, since lung ventilation is dependant upon movements of the rib cage and sternum assisted by rigid uncinate processes (Codd *et al*., 2005). Bones such as uncinate processes are formed by a process of endochondral ossification, whereby a cartilage skeleton is replaced by bone during development (Hogg, 1980). Hyaline cartilage is initially synthesised during foetal development as a precursor to bone. This cartilaginous matrix foundation, produced by chondrocyte cells, is then calcified prior to cartilage cell apoptosis (Scherft, 1984). Blood vessel invasion of the matrix follows, enabling osteoblasts, which are bone-forming cells, to enter. Osteoblasts build bone on the scaffold of the matrix until ossification is complete (Fenwick, 1997). The pattern of bone ossification can vary between different bones and also within and between species (Hogg, 1980; Maxwell and Larsson, 2009). A detailed developmental account of uncinate processes formation is not currently available. Rather, the timing of process ossification is thought to occur around the time of hatch in the chicken (Hogg, 1980) and after hatching in Anseriformes (Maxwell, 2008).

The functional significance of the uncinate process ossification pattern is not clear. Precocial species of bird are capable of locomotor behaviour soon after hatch. Coupled with the energetic requirements of maintaining a high rate of growth, the elevated metabolic demands incurred during locomotion presumably require sufficient development of the costal breathing mechanism to support effective lung ventilation. Whether the timing of process ossification affects the transition in ventilatory mechanics of hatchling birds has not been resolved. The uncinate processes are an integral component of the ventilatory pump (Codd *et al.*, 2005). If this mechanism is constrained by the rigidity of the rib levers, i.e. uncinate processes, during the transition from cartilage to bone, there may be an impact upon oxygen delivery and therefore locomotor performance. Accordingly, the objective of understanding how uncinate processes develop in a precocial species forms the basis of the Chapter 3 (Tickle and Codd, 2009).

1.3.2 Locomotion

1.3.2.1 The Appendicular Skeleton

Birds have a highly modified skeleton based upon the basic tetrapod plan (Figure 4). Derived features include the fusion of thoracic vertebrae into the notarium, fusion of bones in the limbs (e.g. tarsometatarsus), loss of teeth, pneumatisation of the cranial and postcranial skeleton and strengthened wing and leg bones (Dumont, 2010). These characteristics are generally regarded as adaptations that decrease the energetic cost of flight (Feduccia, 1996). Variations in skeletal properties exist between birds adapted to different forms of locomotion. For example, volant birds generally have bones that are lighter than flightless or diving species, whose thicker bones may act as mechanical reinforcement (Currey and Alexander, 1985; Habib and Ruff, 2008). Flight is the primary form of locomotion for most birds. Consequently the majority of species have an elongated sternum that has a deep keel for the attachment of the major flight muscles, *M. pectoralis* and *M. supracoracoideus*. *M. pectoralis* is the primary downstroke muscle providing the thrust for flight and may constitute up to 35% of body mass (Dial et al., 1988). The primary upstroke muscle, *M. supracoracoideus* lies deep to the pectoralis but its tendon inserts on the upper aspect of the humerus. Therefore the supracoracoideus can elevate the wing through a pulley system (Dial et al., 1988). The pelvic limb in birds is comprised of a relatively short femur, elongated tibiotarsus (formed by the fusion of tibia and proximal tarsus) and tarsometatarsus (Figure 4). The avian femur is relatively thick for a given length compared to the mammalian equivalent, perhaps as an adaptation to withstand mechanical stresses upon landing (Prange *et al*, 1979). Differences in the morphology of the hindlimb also correspond to locomotor specialisation. For example birds capable of flying, swimming and diving behaviour have relatively light legs accounting for between 2% and 20% of overall body mass (Hartman, 1961). Contrastingly, the mass of the hindlimbs in flightless ostrich, *Struthio camelus*, constitute 29% of body mass (Alexander *et al*, 1979). Corresponding variation in the muscle properties that drive movement of the appendicular skeleton exist in birds adapted to different forms of locomotion. For example, hindlimb muscles in the emu, *Dromaius novahollandiae*, are adapted to produce greater power output during locomotion than those in primarily volant birds (Patak and Baldwin, 1993). Therefore broad adaptations in the skeleton and muscles of the limbs exist between species adapted to different forms of locomotion.

1.3.2.2 Overcoming the trade-off between breathing and locomotion

Terrestrial air-breathing vertebrates use a variety of strategies to ventilate their lungs. Anuran and caudate lissamphibians maintain pulmonary ventilation using a positive pressure buccal pump, whereby air is forced from the mouth into the lungs (Kardong 2006). In contrast, birds and mammals primarily use a costal (rib) aspiration pump to produce the pressure changes in the thorax and abdomen necessary for air to flow into the lungs. Muscles involved in driving the ventilatory buccal pump mechanism are functionally separated from the hypaxial muscles involved in producing locomotor movements. However, in species that breathe using respiratory rib movements, ventilatory muscle activity can interfere with those of locomotion and impose a constraint upon breathing (Carrier, 1987). This conflict occurs because muscles that originally had a locomotor function in the early ancestors of tetrapods are now adapted to facilitate respiration by powering rib movements (Carrier, 1987). Trade-off between locomotor and respiratory functions is obvious in the green iguana, which cannot breathe while running and therefore cannot maintain locomotion for a long duration

(Carrier 1987; 1990; 1991). Overcoming this constraint upon breathing was integral to the development of locomotor stamina in reptiles, birds and mammals.

A potential solution to this constraint is seen in some lizards that may harness undulating body movements during locomotion, so that one lung is ventilated by the other as each is compressed (Carrier, 1991). Furthermore, development of specialised structures to circumvent the trade-off between breathing and locomotion are found in a variety of species. These 'accessory' breathing mechanisms are considered to be structures that increase the efficiency of inspiration and special inspiratory muscles (Perry *et al.*, 2010b). The basal most species to experience this functional conflict have gastralia, which are abdominal ribs that aid inspiration and stiffen the ventral body wall (Carrier and Farmer, 2000; Claessens, 2004b). Extinct groups such as pterosaurs, ichthyosaurs and sauropod and theropod dinosaurs in addition to extant turtles, crocodilians and the tuatara, *Sphenodon*, all have these bony abdominal growths (Perry *et al.*, 2010b), which together with the ribs form a specialised ventilatory mechanism (Claessens, 2004a; Codd *et al.*, 2008).

Ventilatory muscles that help circumvent the functional trade-off between locomotion and respiration are present across the higher vertebrates. Crocodilians have a unique inspiratory mechanism whereby retraction of the liver is facilitated by activation of the diaphragmaticus muscle, which is attached to modified pelvis morphology (Gans and Clark, 1976). Action of this 'hepatic-piston' in coordination with rib movements facilitates expansion of the lungs due to the resulting negative pressure in the pleural cavity (Gans and Clark, 1976; Claessens, 2004b). In mammals, the diaphragm muscle allows functional separation of breathing and locomotion (Boggs, 2002). The diaphragm separates the thoracic and abdominal cavities, and is the primary inspiratory muscle. Contraction of its muscle fibres causes the diaphragm to push down the abdominal viscera and increase the volume of the thorax. The resulting thoracic negative pressure causes air to flow into the lungs (Perry *et al.*, 2010a). Birds have partitioned the mechanics of breathing and locomotion despite the absence of a respiratory diaphragm muscle. Specialised hypaxial respiratory musculature, attached to the uncinate processes, enable inspiration and expiration during locomotion, in addition to providing postural control (Codd *et al.*, 2005). Therefore, synchronous activity of muscles in the rib cage maintains respiratory movements of the skeleton and assists locomotion.

1.3.2.3 Energetics of locomotion in birds

Decoupling the musculo-skeletal functions of respiration and locomotion has enabled birds to sustain high levels of metabolism and perform energetically demanding activities such as flight. Although the physical mechanisms have been separated, there is a functional link between breathing and exercise: respiration provides the fuel to power locomotion. Given this critical interaction, the optimisation of respiratory system morphology to the metabolic requirements of exercise is intuitive. Studies of the mammalian respiratory system indicate that critical components of the oxygen delivery system determine maximal metabolic rate, or the highest attainable rate of energy metabolism (Weibel *et al*, 1991; Weibel and Hoppeler, 2005). For example, the capacity of mitochondrial volume in active muscles and blood supply from the heart are matched to the maximum rate of exercise metabolism (Weibel and Hoppeler, 2005). Economical design in the respiratory system of mammals indicates that birds may have ventilatory structures optimised to meet the energy demands of their lifestyle; high energy users would be excepted to show an anatomy that helps to sustain high levels of oxygen delivery. The Australian brush turkey (*Alectura lathami*), a species that has totally independent 'superprecocial' young, displays such morphological adaptation; a significant relationship is found between pulmonary diffusing capacity of the blood-gas barrier (related to the thickness and surface area of the gas exchange surface in the parabronchi) and metabolic rate during exercise (Seymour *et al*, 2008). Diffusing capacity and maximum metabolic rate are higher in the Brush Turkey compared to the values reported for a less active species (Seymour *et al*, 2008). Considering the integral respiratory function of uncinate processes and the link with locomotor stamina, process morphology may be linked to maintaining specific energetic requirements. Chapter 4 (Tickle *et al*., 2009) in this PhD thesis addresses whether there is a relationship between process morphology and metabolism in birds. This article considers species differences in metabolism and morphology to highlight an evolutionary pressure that may have influenced uncinate process morphology.

Clearly, the muscular work of ventilating the lungs contributes a proportion of the energetic requirements of an animal. Research efforts to define the cost of breathing as a proportion of total metabolism in birds are few, though guinea fowl ventilation is reported to consume as little as 2% of total metabolism during running (Ellerby *et al*., 2005; Markley and Carrier, 2010). This value is surprising considering that the large mass of the sternum must be moved up and down during exercise. Interactions between locomotion and ventilation may help explain this result, since coordinating the locomotor and respiratory cycles potentially imparts metabolic efficiency (Nassar *et al*., 2001). Exercising birds often show coordination between wingbeat and footfall with breathing cycle (Boggs, 2002). In effect, the energetic cost of ventilation may be offset by taking advantage of thoracic compression caused by wing stroke during flight

(Boggs *et al*, 1997) and footfall during walking/running (Brackenbury and Avery, 1980; Nassar *et al*., 2001).

Interaction between respiration and locomotion is therefore paramount in exercising birds. Considering the link between metabolism and respiration, the objective of the fourth paper presented in this thesis is to manipulate the costs of breathing and locomotion in a bird (Tickle *et al*., 2010). There is only limited understanding of the adaptations birds use to circumvent the problem of efficiently moving a heavy sternum. Chapter 5 (Tickle *et al*., 2010) considers the energetics of locomotion in birds manipulated by application of loads. Loading animals to increase body mass has been a useful research tool for studying the costs of locomotion in birds. One recent example used loads applied to the leg and back to untangle the energetic costs of locomotion in guinea fowl, a species adapted to running locomotion. (Marsh *et al*., 2006). The pattern of energy metabolism in leg muscles under these conditions indicated that muscles providing forward propulsion for the body during walking did not account for the entire energy consumption; rather the muscles that enable the passive swing limb to move forwards consumed a significant proportion of the overall energy budget (Marsh *et al*., 2006; Ellerby and Marsh, 2006). Extension of this idea allows us to manipulate the cost of breathing in birds by applying loads to the sternum, since it is likely that the metabolic cost inherent to muscular displacements of the sternum will be increased upon adding extra mass. Coupled with data from back and limb loaded birds, Chapter 5 presents evidence for the costs of locomotion in a waddling bird, the barnacle goose (*Branta leucopsis*), and the change in the metabolic costs of sternal movements with loading.

1.4 Evolution of the ventilatory pump in birds

Modern birds are the direct descendants of maniraptoran theropod dinosaurs. Evidence of shared characters in birds and theropods such as feathers (Xu *et al*, 2004), pneumatised bones (O'Connor and Claessens, 2005) and behavioural traits such as egg brooding (Norell *et al*., 1995) clearly indicate the theropod ancestry of birds. Furthermore, uncinate processes are found not only in extant birds, but also in theropod dinosaurs (e.g. Ostrom, 1969; Xu *et al*., 2000; Codd *et al*., 2008). A recent descriptive analysis of the uncinate processes in theropod dinosaurs suggested that they functioned in an avian-like ventilatory pump (Codd *et al*., 2008). This is significant since it suggests that a respiratory system which could maintain high metabolic rates was in place prior to the evolution of flight and subsequent radiation of birds. However, histological evidence suggests that the oldest bird, *Archaeopteryx*, inherited dinosaurian physiology that is characterised by low rates of growth and metabolism (Erickson *et al*, 2009). Of course, the metabolic demands of flight require a respiratory system that can maintain high rates of oxygen delivery. Therefore identifying the first appearance of a bird-like respiratory apparatus offers a pertinent perspective on the evolution of flight. Pneumatisation of the post-cranial skeleton has been used as a marker to identify presence of a lung air-sac system in pterosaurs (Claessens *et al*., 2009) and theropods (O'Connor and Claessens, 2005). However, while this soft tissue gas exchange apparatus may have resembled the avian lung and air-sac system, the significance of morphological variations in the skeletal aspiration pump are not known. Therefore an experimental analysis of fossil skeletal morphology and the implications for respiratory function is timely. Chapter 6 considers how uncinate process morphology affects the potential leverage for respiratory rib movements in basal birds and a theropod dinosaur fossil specimen. Functional significance of uncinate processes is considered and implications for the evolution of respiratory systems in numerous evolutionary lineages are considered in this paper, offering a new perspective on how rib levers may have been an important character in the diversification of terrestrial air breathers.

1.5 Overview and thesis aims

While the pattern of skeletal movements that facilitate lung ventilation in birds is recognised, there remain unknown factors that govern rib and sternal rotation. Uncinate processes are integral to breathing and may have assisted in resolving the evolutionary conflict between muscles involved in both breathing and locomotion. Therefore the objective of this thesis is to provide a description of how uncinate processes function in birds and how these structures may be linked to adaptations to locomotion. By increasing our understanding of the role of uncinate processes in extant birds I consider the evolution of respiratory structures in extinct birds, and how these may have facilitated the high metabolic rates that support demanding locomotor activities such as flight.

The overall objective of this thesis is to understand how the diversity in avian morphology and anatomy relates to aspects of their breathing and locomotion.

Specific aims of this thesis are as follows:

1) To describe the lever mechanism of uncinate processes and address how differences in locomotor behaviour affects their morphology (Chapter 2).
2) To describe the morphological and structural development of uncinate processes in birds (Chapter 3).

3) To examine the relationship between energetics and uncinate process morphology (Chapter 4).

4) To establish using respirometry the energetic cost of locomotion whilst carrying loads placed on the back, sternum and legs. Loads provide a means to manipulate the costs of biomechanical functions, in this case the cost of locomotion and breathing (Chapter 5).

5) To describe the anatomy of uncinate processes in basal bird species and consider the potential to elicit ventilatory movements of the skeleton (Chapter 6).

Chapter 2

Functional significance of the uncinate processes in birds

This chapter is as a reprint of an article published in the *Journal of Experimental Biology:*

Tickle, P. G., Ennos, A. R., Lennox, L. E., Perry, S. F. and Codd, J. R. (2007) Functional significance of the uncinate processes in birds. *J. Exp. Biol.* **210,** 3955-3961

§The Journal of Experimental Biology 210, 3955-3961
Published by The Company of Biologists 2007
doi:10.1242/jeb.008953

Functional significance of the uncinate processes in birds

Peter G. Tickle[1], A. Roland Ennos[1], Laura E. Lennox[1], Steven F. Perry[2] and Jonathan R. Codd[1,*]

[1]Faculty of Life Sciences, University of Manchester, Jackson's Mill, PO Box 88, Sackville Street, Manchester M60 1QD, UK and [2]Institute for Zoology, Bonn University, Germany

*Author for correspondence (e-mail: jonathan.codd@manchester.ac.uk)

Accepted 29 August 2007

Summary

The functional significance of the uncinate processes to the ventilatory mechanics of birds was examined by combining analytical modeling with morphological techniques. A geometric model was derived to determine the function of the uncinate processes and relate their action to morphological differences associated with locomotor specializations. The model demonstrates that uncinates act as levers, which improve the mechanical advantage for the forward rotation of the dorsal ribs and therefore lowering of the sternum during respiration. The length of these processes is functionally important; longer uncinate processes increasing the mechanical advantage of the Mm. appendicocostales muscle during inspiration. Morphological studies of four bird species showed that the uncinate process increased the mechanical advantage by factors of 2–4. Using canonical variate analysis and analysis of variance we then examined the variation in skeletal parameters in birds with different primary modes of locomotion (non-specialists, walking and diving). Birds clustered together in distinct groups, indicating that uncinate length is more similar in birds that have the same functional constraint, i.e. specialization to a locomotor mode. Uncinate processes are short in walking birds, long in diving species and of intermediate length in non-specialist birds. These results demonstrate that differences in the breathing mechanics of birds may be linked to the morphological adaptations of the ribs and rib cage associated with different modes of locomotion.

Supplementary material available online at
http://jeb.biologists.org/cgi/content/full/210/22/3955/DC1

Key words: biomechanics, breathing mechanics, morphology, uncinate.

Introduction

Birds lack the muscular diaphragm of mammals (Brackenbury, 1972) and do not ventilate their lungs by expanding the lung itself, but through the bellows-like movement of air through the air sacs (Brackenbury, 1972; Brackenbury, 1973). Uncinate processes are bony projections that extend from the vertebral ribs of most extant birds (Fig. 1). In 1935, Zimmer postulated that the uncinate processes played some role during inspiration (Zimmer, 1935). Contemporary hypotheses have linked these processes with stiffening or strengthening the rib cage (Kardong, 1988; Walker and Liem, 1994), providing attachment sites for muscles stabilizing the shoulder (Hildebrand, 1982), or serving as an adaptation for flight (Welty and Baptista, 1988). Existing hypotheses on uncinate function appear to have been based on the general morphology of these structures rather than experimental analyses. However, recent electromyographic studies in the giant Canada goose confirmed Zimmer's hypothesis by demonstrating that these processes are integral component of the ventilatory mechanics of birds being involved in both inspiration and expiration (Codd et al., 2005). The processes are associated with fleshy parts of the Mm. intercostales externi, the Mm. appendicocostales that originates from the proximal edge of the uncinate and inserts onto the following vertebral rib (Shufeldt, 1890). The Mm. appendicocostales is active during inspiration in the giant Canada goose, suggesting the processes facilitate the craniad movement of the ribs, which would in turn move the sternum ventrally (Codd et al., 2005). The base of the uncinate processes serves as a brace for the insertions of the 'finger-like' projections of the M. externus obliquus abdominus that pull the sternum dorsally during expiration (Codd et al., 2005). Given that the processes provide attachment sites for these important respiratory muscles, any change in uncinate morphology may have a significant effect on ventilation. Here we develop a mathematical mechanical model to examine the mechanics of ventilation in birds. This model will then be used to determine the mechanical advantage of the uncinate process system for movements of the ribs and therefore sternum during respiration.

Extant birds are diverse and include species that specialise in running, walking, swimming, flying and diving. As with any animal, morphological alterations in birds are commonly associated with differences in locomotor mode (Tucker, 1993; Patak and Baldwin, 1993; Dyke and Rayner, 2001; Rayner and Couldrick, 2003; Zeffer and Norberg, 2003). Furthermore, variations in uncinate morphology have previously been

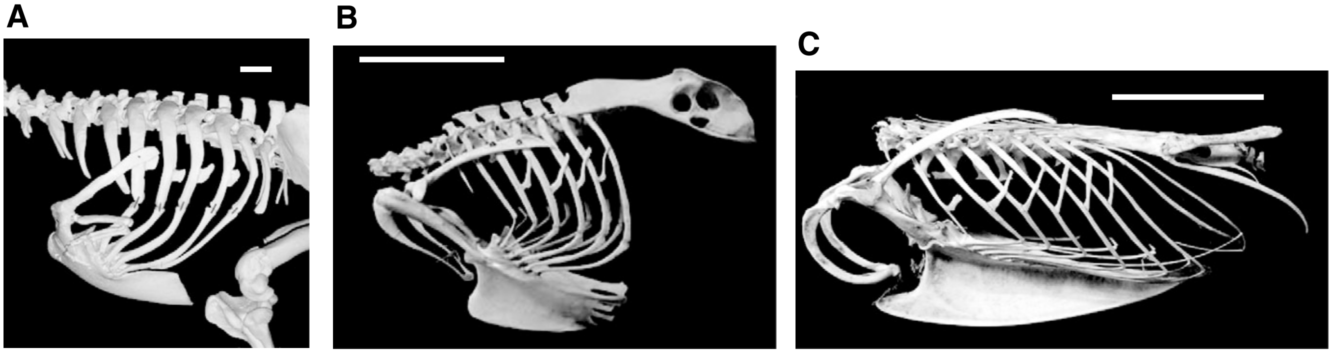

Fig. 1. Representative skeletons showing the morphological differences in the rib cage associated with different forms of locomotion in (A) a walking species, cassowary (*Casuaris casuaris*); (B) a non-specialist, eagle owl (*Bubo bubo*); and (C) a diving species, razorbill (*Alca torda*). Uncinate processes are short in walking species, of intermediate length in non-specialists and long in diving species. In all photographs cranial is to the left; scale bar, 5 cm.

anecdotally linked to differences in locomotor mode, and long uncinate processes noted in diving species (Welty, 1988; Duncker, 1971); however, there has been no further examination or testing of these observations. Here we use morphometric analysis to test the hypothesis that the length of the uncinate processes is predominantly correlated with the locomotor mode of birds. We will then use our mechanical model to examine the functional significance of these differences in uncinate length. In light of our mechanical model, a demonstrable link between the locomotor mode and the length of the uncinate processes will enable us to gain a better understanding of breathing mechanics in Aves.

The geometrical model of uncinate function

At a first approximation, the ribcage of a bird can be considered to be composed of two sets of dorsal and ventral ribs, which are held the same distance apart at the backbone and sternum, and at the same angle. Hence the dorsal and ventral ribs can be regarded as mirror images, which are separated where they join by the same distance as at the backbone and sternum. Therefore two adjacent dorsal ribs can be modeled as the opposite sides of a parallelogram (Fig. 2), running at an angle θ to the backbone and separated from each other by a distance *D*. Moving such a mechanism is clearly very different from rotating a single bone about a single joint. Any muscle can only alter the angle θ of the ribs to the backbone, and its mechanical advantage is best described by determining how much it changes in length for a given change in the rib angle; the bigger the length change, the more powerful its action and the greater its mechanical advantage.

Consider the effect of a muscle that joins the two ribs, and which is attached to the posterior rib a distance *P* further from the backbone than it is to the anterior rib (Fig. 2A). The length of the muscle, *L*, can be readily determined by Pythagoras's theorem:

$$L = x^2 + y^2 = \sqrt{[(D\cos\theta+P)^2 + (D\sin\theta)^2]}\ . \qquad (1)$$

For the Mm. intercostalis externus, which attaches the same distance down the ribs, *P* equals zero and the muscle runs

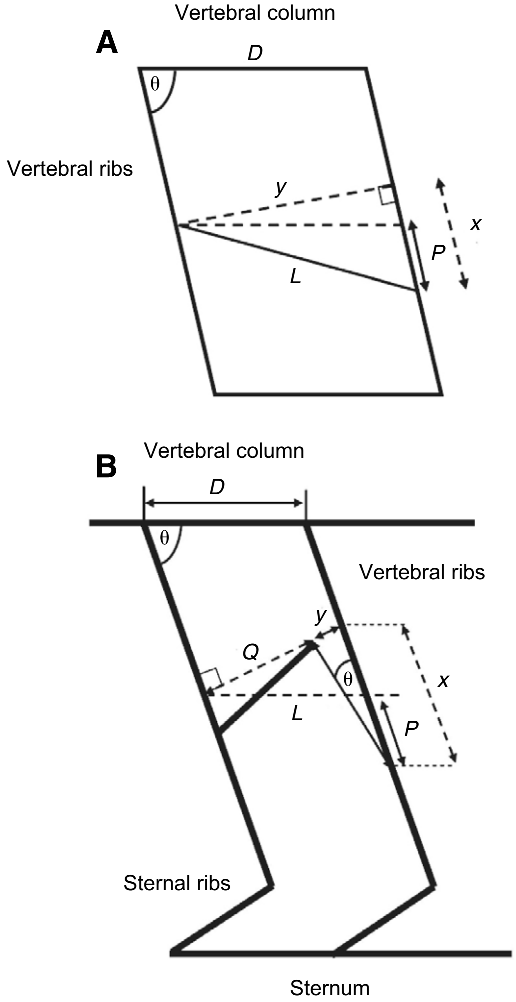

Fig. 2. Geometric model of uncinate function. (A) The situation in birds without an uncinate process. The length of the Mm. appendicocostales, *L*, changes with the rib angle, θ, depending on the distance down the rib, *P*, of the posterior attachment. (B) The situation with an uncinate process of perpendicular length *Q* behind the anterior rib. Cranial is to the left.

approximately parallel to the backbone. Its length is therefore given by the simplified equation:

$$L = \sqrt{[(D\cos\theta)^2 + (D\sin\theta)^2]} = D\,. \tag{2}$$

Whatever the angle of the ribs, the muscle length is constant. It cannot therefore act to move the ribs. The mechanical model supports previous experimental work (Codd et al., 2005), which demonstrated that the Mm. intercostalis externus had no activity related to either inspiration or expiration but was active during contralateral limb support, suggesting it plays a role acting as a brace to stabilise the thorax during locomotion (Codd et al., 2005).

For the appendicocostales muscle, however, for which P is positive, the length of the muscle will vary with the angle of the ribs according to the modified version of Eqn 1.

$$L = \sqrt{[D^2+P^2+2DP\cos\theta)]}\,. \tag{3}$$

The muscle will shorten as θ increases, so the appendicostales muscle will act to swing the ribs forward. Two examples of how the muscle's length will vary with θ are shown in Fig. 3A for P=0.5D and P=D. It can be seen that the length changes more rapidly with θ for larger values of P (the higher the angle of the muscle to the backbone) and at higher values of θ (the higher the angle of the ribs to the backbone). Therefore the mechanical advantage of the muscle will alter with both P and θ. Mechanical advantage (MA) is defined as the relative change in muscle length per unit change in angle and is given by the formula:

$$\mathrm{MA} = L_\theta - L_{\theta+1} / L_\theta\,. \tag{4}$$

The mechanical advantage is shown in Fig. 3A. It rises with the rib angle, θ, and is higher for larger values of P.

Effect of the uncinate process

Consider now the same ribcage, but with an uncinate process on the anterior rib that extends back a perpendicular distance, Q, from it, and that has the Mm. appendicostales attached to its end (Fig. 2B). The length of this muscle is now given by the expression:

$$L = \sqrt{[(D\cos\theta + P)^2 + (D\sin\theta - Q)^2]}\,. \tag{5}$$

The effect of the uncinate process is to increase the length change of the muscle as the ribs are moved, because although as θ rises the reduction in the distance x parallel to the ribs ($D\cos\theta+P$) is unaffected, the increase in the distance perpendicular y to the ribs ($D\sin\theta-Q$) is reduced. Indeed if Q is sufficiently large that the uncinate process extends behind the posterior rib, swinging the ribs forward will actually reduce the perpendicular distance. The effect of uncinate processes of length Q=0.5D and Q=D on the length of the appendicocostales at different angles are shown in Fig. 3A, and the mechanical advantage at different angles is shown in Fig. 3B. It can be seen that the change in muscle length and the mechanical advantage of the muscle is greatly increased by the uncinate process, giving a good mechanical advantage even at low values of θ. The uncinate acts as a mechanical lever, being most effective when it is longer and, surprisingly, when P is smaller.

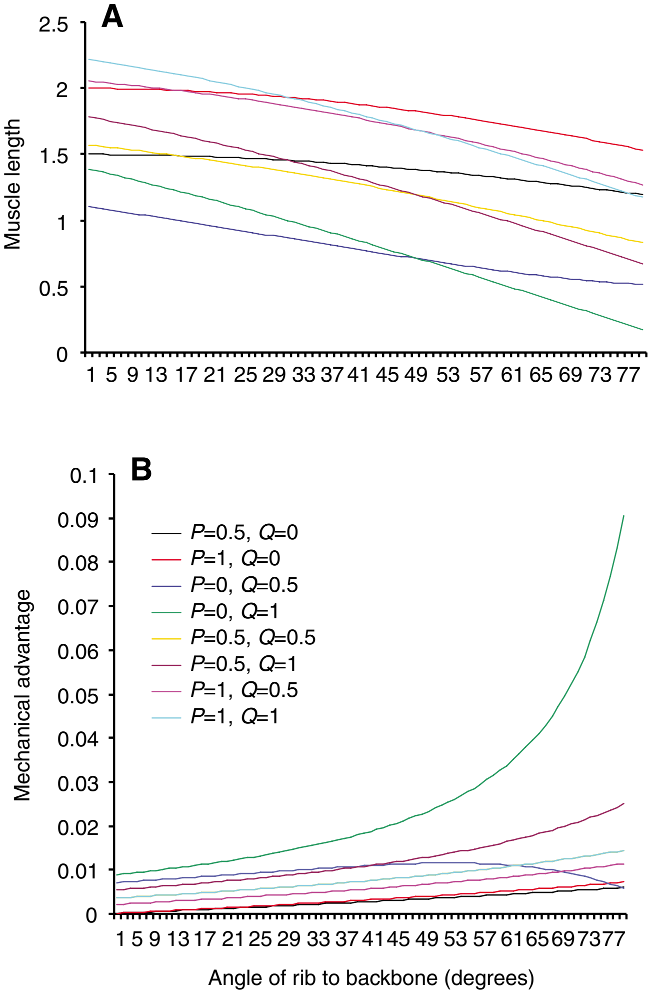

Fig. 3. (A) Changes in length of the Mm. appendicocostales muscle with rib angle, θ, for various relative values of uncinate length, Q, and distance of posterior attachment, P. (B) Changes in mechanical advantage of the Mm. appendicocostales muscle with rib angle, θ, for various relative values of uncinate length, Q, and distance of posterior attachment, P. It can be seen that mechanical advantage increases with θ, and with higher values of Q.

Materials and methods

Mechanical advantage of the Mm. appendicocostales

The uncinate length, Q, the distance between the ribs, D, the distance of the posterior insertion, P, and the rib angle θ of the ribs were measured in four randomly chosen representative bird species: the diving razorbill *Alca torda* L.; the non-specialist locomotors kestrel *Falco tinnunculus* L. and barnacle goose *Branta leucopsis* Bechstein 1803; and the walking red-legged partridge *Alectoris rufa* L.

All lengths were measured on the left hand side of the skeleton using a digital caliper (16EX 150 mm, Product No: 4102400, Mayr GmbH, Berlin, Germany), while the angle was measured using an image analysis system of digital images. Using our mechanical model (Eqn 4), we then calculated the mechanical advantage for each appendicocostales muscle, with and without the uncinate processes.

Skeletal morphology

Data were collected from the skeletons of 100 birds representing examples from all major taxa and orders (see Appendix in supplementary material). To establish if within-species variation in uncinate process length on different ribs was significantly different, the lengths of the processes from ten skeletons of adult barnacle geese *Branta leucopsis* were examined. Birds were then grouped according to specialization to a primary mode of locomotion. (1) Walking, including birds that are either flightless (e.g. cassowary) or incapable of sustained flight (e.g. capercallie); (2) diving, including all birds that actively forage under water by either plunge (e.g. kingfisher) or sustained, deep diving (penguin); and (3) non-specialists, including all other birds flying or swimming that are not facultative diving or walking birds. We collected measurements of the length of the vertebral and sternal ribs, and the length and width of the uncinate processes. Sternal morphology was also examined by measuring the total length and depth of the sternum (height of keel). Correcting for body size is problematic in birds as many species have disproportionably long necks, meaning the traditional snout–vent measurements to scale for size are not feasible. Therefore all data collected were corrected for variations in body size by dividing total length by the length of the vertebral column spanning the thoracic ribs. All data were collected from the left hand side of the skeleton using a Mayr digital caliper (16EX 150 mm, Product No: 4102400, Mayr GmbH).

Statistical analysis

Relationships between the groups were determined using canonical variate analysis (CVA), which maximises the variation between groups relative to the variation within groups (Campbell and Atchley, 1981). Values used in the CVA were: uncinate length and width at base, midpoint and tip; sternal width, length and depth; vertebral and sternal rib length. A one-way ANOVA with a Tukey *post-hoc* test was used to establish if mean uncinate length varies according to mode of locomotion. Within-species uncinate comparison and the ratio of sternal length to depth were analysed using a repeated-measures ANOVA with Bonferroni comparisons. All analyses were completed using the statistical package SPSS (SPSS v.13.0; SPSS Ltd, Chicago, IL, USA).

Results

Mechanical advantage of the Mm. appendicocostales

Measurements on the four bird species were taken and analysed using our mathematical model, with or without the uncinate process. The results of the output from the model are given in Table 1 and Fig. 4. It can be seen that in each species without the uncinate processes the mechanical advantage of the Mm. appendicocostales was low, whereas the presence of uncinate processes improved the mechanical advantage for rib movements by a factor of 2–4. The model therefore demonstrates that uncinate processes act as levers for movements of the ribs (see Table 1, Fig. 4).

Rib cage morphology

Rib number does not always correlate with locomotor mode, although walking species generally tend to have the fewest ribs and the diving species the most. For birds used in this study, 8 had 6 ribs, 43 had 7 ribs, 25 had 8 ribs, 22 had 9 ribs and only 2 had 10 ribs (see Appendix in supplementary material). Our

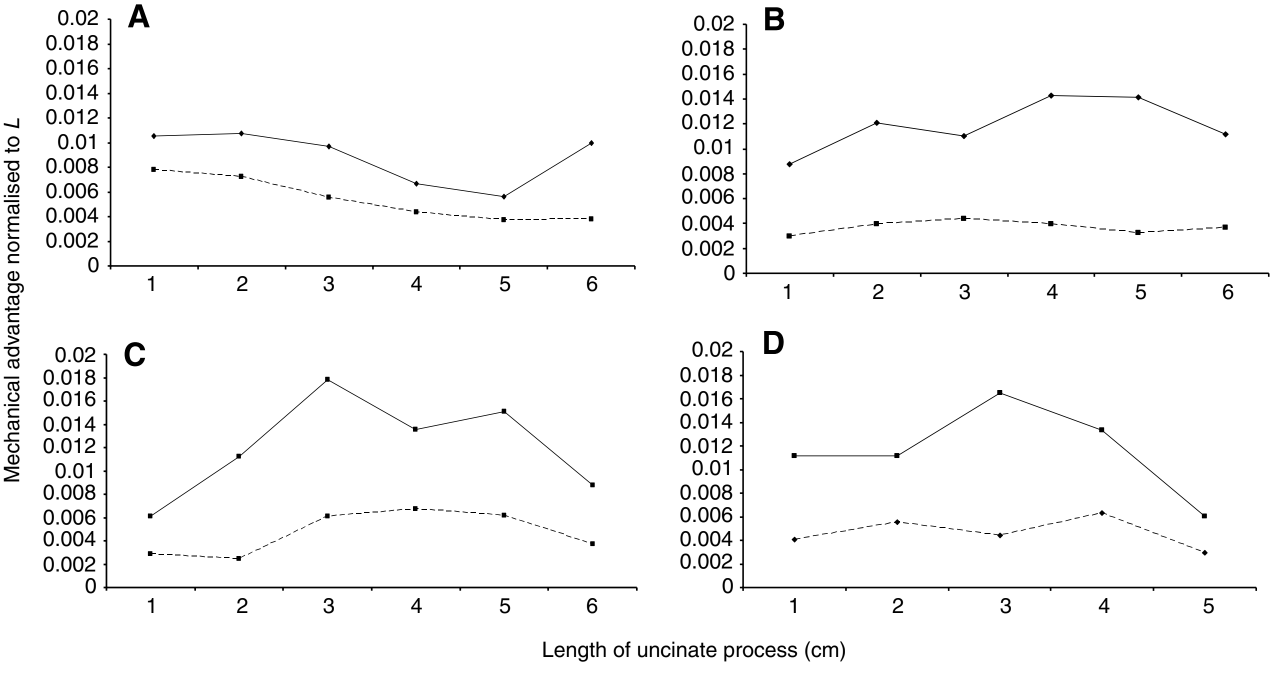

Fig. 4. Mechanical advantage (corrected for muscle length *L*) for representative species calculated with (solid line) and without (broken line) the uncinate processes. (A) A diving bird, the razorbill *Alca torda*; (B,C) non-specialist birds, (B) barnacle goose *Branta leucopsis* and (C) kestrel *Falco tinnunculus*; and a walking bird (D) the red-legged partridge *Alectoris rufa*.

Table 1. *Measurements of the uncinate process on the anterior rib that extends back a perpendicular distance (Q), the distance between the ribs (D), the distance of the posterior insertion (P) and the rib angle (θ) of the ribs in bird species representative of different types of locomotion*

	Barnacle goose	Razorbill	Kestrel	Red-legged partridge
D (mm)	14.9±0.59	7.94±0.44	7.51±1.57	7.6±1.99
P (mm)	4.54±0.43	13.08±1.29	3.79±1.91	3.81±1.13
Q (mm)	7.21±0.43	10.50±1.3	4.50±0.36	3.87±0.50
θ (degrees)	71.19±1.88	64.79±6.77	76.85±3.66	74.26±0.41

Species include the diving razorbill *Alca torda*; the non-specialists kestrel *Falco tinnunculus* and barnacle goose *Branta leucopsis*; and the walking red-legged partridge *Alectoris rufa.*

Values are means ± s.e.m. (N=6–10).

correction for body size will tend to make comparisons less different rather than more. The general morphology of the rib cage was similar in all birds examined, as indicated by a within-species comparison of relative uncinate process length (mean ± s.e.m.) for 10 barnacle geese *Branta leucopsis*. Aside from the first rib, sternal ribs connect the vertebral ribs to the sternum and these become increasingly thinner and longer as one moves down the vertebral column. Using one-way ANOVA and Tukey *post-hoc* tests the mean length (± s.e.m.) of the uncinate processes are significantly shorter on the first (0.16±0.02) and last (0.14±0.02) ribs on which they occur. Therefore data from these processes were not used in the canonical analysis. The processes on the remaining ribs are not significantly different in length (rib 2: 0.22±0.03; rib 3: 0.23±0.02; rib 4: 0.22±0.02; rib 5: 0.21±0.03). Therefore the mean length of processes 2–5 was used in all subsequent analyses.

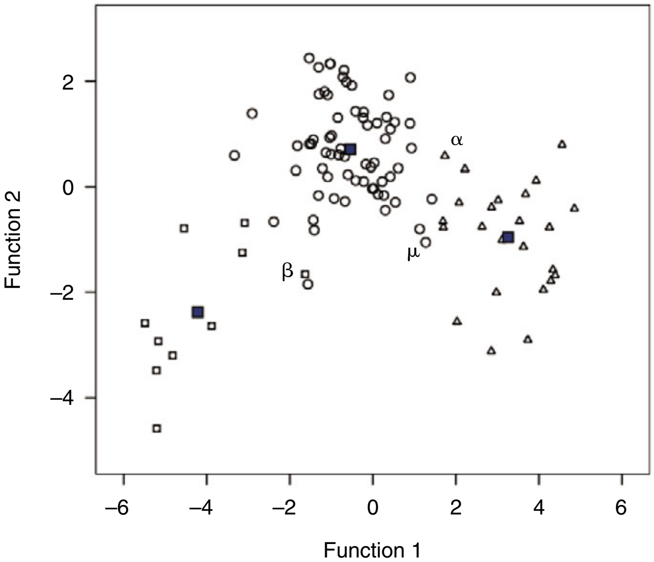

Fig. 5. Canonical variate analysis (CVA) of skeletal morphology in birds. Function 1 against function 2 for walking species (squares, N=10); non-specialists (circles, N=66); diving birds (triangles, N=24). Functions 1 and 2 were primarily functions of relative uncinate length and width and rib length, respectively. Solid black squares represent significantly different group centroids. Letters highlight borderline species of respective groups: the fulmar (α), the green woodpecker (β) and the swallow (μ).

Canonical variate analysis

There was distinct clustering in the data corresponding to locomotor mode and significant differences between group means (Wilks' Lambda=0.82, P<0.001, Fig. 5). Some overlap is present, indicating that there are species on the boundary of our classification. Canonical discriminant function 1 accounts for 80.2% of the variation while function 2 accounts for 19.8%. Functions 1 and 2 were primarily functions of relative uncinate length and width and rib length, respectively.

Uncinate morphology

The relative length of the uncinate processes was found to be more similar in birds with the same locomotor mode. They were shortest in the walking (0.11±0.02, N=10, P<0.01), of intermediate length in non-specialist (0.17±0.01, N=66, P<0.01) and the longest in diving species (0.23±0.01, N=24, P<0.01). The processes of the walking birds typically reach about halfway across to the following rib. In non-specialists the processes have a characteristic L-shaped morphology and reach across to the following rib. In diving species the uncinate processes are long, thin and taper towards the end (Fig. 1C), and may overlap the following rib. There is no significant difference between relative uncinate length in the deep (0.21±0.01, N=8) and shallow divers (0.19±0.02, N=16, P=0.32, two-sample t-test).

Sternal morphology

The relative ratio of sternal length to depth of walking birds was significantly lower (1.12±0.44, N=10, P<0.001) than that of non-specialist (2.16±0.07, N=66, P<0.01) and diving species (2.75±0.20, N=24, P<0.01).

Discussion

Role of the uncinate process

The mechanical model developed in this paper suggests that the uncinate process acts as a lever, increasing the mechanical advantage of the Mm. appendicocostales, particularly when the ribs are at a low angle to the backbone, helping them rotate the dorsal ribs forwards, pushing the sternum down, and so inflating the lungs. The results of actual mechanical advantage of the four representative species measured, based on the model, confirms this interpretation. In all cases the mechanical advantage increased by a factor of 2–4 compared with what it would have been had an uncinate process not been present, though the effect was least pronounced in the diving species, the razorbill.

These results can help shed light on the two main findings of the morphometric study: first that the anterior and posterior uncinates are shorter than the intermediate ones; and second that the uncinates and sternum of diving birds were relatively longer than those of walking birds, with non-specialist birds having uncinates and sternum of intermediate length. The sternum in birds is the site of attachment for the large flight muscle, the pectoralis and supracoracoideus (Duncker, 1971). The pectoralis can account for up to 35% of the body mass of some birds (Dial et al., 1988). This large muscle mass, together with the abdominal viscera, must be moved up and down during breathing (Brainerd, 1999). The importance of movements of the sternum is highlighted by the entrainment of wing beat with sternal movements (Jenkins et al., 1998) and the fact that birds can suffocate if movements of the sternum are restricted (Ludders et al., 2001). The uncinate processes also act as a brace for the insertion of the M. obliquus externus, which pulls the sternum dorsally to effect expiration (Codd et al., 2005), meaning there is a functional link between sternal and uncinate morphology and the breathing mechanics in birds. The sternum of walking birds is reduced and this group has the shortest length processes, while the elongated sternum of diving birds correlates with the longest length processes. Differences in uncinate morphology may translate into anatomical differences in the associated musculature such as the Mm. appendicocostales and M. obliquus externus, meaning that different patterns of muscle activity facilitate breathing; this, however, remains to be determined.

The Mm. appendicocostales attaches to the proximal edge of the process, meaning that the total length of the process is the most significant characteristic in uncinate morphology. The width of the process along its length may contribute to the overall strength. However, the process is rigidly fixed from above to the rib it extends from by a strong triangular aponeurotic membrane that is attached from the anterior edge of the process along its entire length (Shufeldt, 1890). This ligament provides a strong anchorage for the lever action on the ribs and may negate any thickening of the process itself. Aside from the walking birds, the uncinate processes are also typically thin and taper towards the tip of the process. Alterations in uncinate length may also have implications for the area available for muscle insertion, given the role of the processes during expiration, as thickening of the base would increase the area for attachment for the insertion of the M. obliquus externus (Codd et al., 2005). In all birds examined the anterior and posterior uncinates are siginficantly shorter than the remaining processes. Aside from the diving species, the mechanical advantage for the anterior and posterior processes is also correspondingly lower, suggesting these processes and their associated muscles probably have little function in moving the ribcage during breathing.

Determination of locomotor modes

The locomotor modes used in the morphometric study are broadly defined into walking, diving and non-specialist birds. Although within each group there remain potentially significant differences between the birds, i.e. foot and wing propelled divers, these modes can be considered to be representative as there are broad mechanical differences between specialization for running *versus* diving and/or non-specialists (all other birds). Swimming birds were not categorized as a separate grouping as there are no birds that swim but do not fly. The results of the CVA analysis indicate that there are species that overlap or are near the border of the locomotor groups. These species represent birds that have intermediate morphology; for example, the fulmar (Fig. 5α), which is classed as a diving species, is a strong flyer, which may explain why it borders the non-specialist group. The green woodpecker (Fig. 5β), which clusters close to the walking species, can be considered an atypical bird as it has pronounced broadening of the vertebral ribs as an adaptation to head banging (Kirby, 1980). Swallows (Fig. 5μ) have highly streamlined bodies, which may explain why they cluster close to the diving species.

Contrast in uncinate morphology between diving and walking species

Longer processes have previously been assumed to play a role in preventing collapse of the rib cage by counteracting the increased pressure with increased depth during dives (Welty, 1988). However, aside from the penguins (*Aptendytes patagonicus*, *Spheniscus demersus* and *S. humbolti*) and auks (*Pinguinis impennis*, *Alca torda* and *Alle alle*), the vast majority of diving birds investigated in this study do not dive to depths likely to encounter large increases in pressure. Species from diverse groups such as the kingfisher (*Alcedo atthis*), the white throated dipper (*Cinclus cinclus)*, the gulls (*Larus argentatus* and *L. canus*), the ducks (*Clangula hyemalis* and *Mergus merganser*) and the terns (*Sterna paradisaea* and *S. hirundo*) have nominal diving depths of less than 10 m; i.e. approximately 1 atmosphere of pressure (Jones and Furilla, 1987). Despite this, there is no significant difference between uncinate length in the deep and shallow divers; all diving birds have significantly longer uncinates than the non-specialist and walking birds (see Appendix in supplementary material). Any muscle pulling on the uncinate processes will facilitate movement of the associated rib rather than prevent it. Furthermore, given that the uncinate processes are not found on every rib, it seems unlikely that they are essential in stiffening the body cavity against increased pressure. The caudally located thin and long ribs, i.e. those that would need the most stiffening as pressure increased on the rib cage, lack uncinates (Fig. 1C). Diving birds have a streamlined body form, long ribs and sternum, to reduce resistance on entry to the water. In diving birds the greater relative length of the uncinate processes is probably related to the greater length of the sternum and the lower angle of the ribs to the backbone and sternum (Fig. 1C). As indicated by our model, without an uncinate process the mechanical advantage of the Mm. appendicocostales in lowering the sternum is low, while the force needed to lower the sternum against the large pectoralis muscle in these species would be extremely high. Interestingly, in the razorbill the effectiveness of the uncinate process at increasing the mechanical advantage was actually rather low. This is probably due to the large angle between the ribs and the vertebral column in this species, which may make the uncinate less important, but it contrasts strongly with the low angle seen in its relative the guillemot (J.R.C., unpublished observations). During surfacing both penguins (Wilson et al., 2003) and tufted ducks (Parkes et al., 2002) maximise gas exchange by increasing breathing frequency. The increased mechanical advantage of longer uncinates may be especially important upon resurfacing when inspiration occurs against the pressure of water against the body. In walking birds, in contrast, the sternum is relatively small (Fig. 1A) and the ribs are at a large angle to the backbone and sternum (Fig. 2A). Even without an uncinate process the appendicocostales muscle could have a reasonable mechanical advantage, and little force needs to be exerted against the tiny pectoralis muscle. In any case the dorsal and ventral ribs tend towards being parallel, meaning that rotating the dorsal rib forward would have little effect in increasing the volume of the chest cavity.

Conclusion

The morphology of the rib cage and the length of the uncinate processes varies with locomotor mode. The reduction in uncinate length found in the walking species suggests that they may play a reduced role during breathing in these species, meaning muscles such as the Mm. intercostalis externi may play a significant role during inspiration in walking birds; this, however, remains to be determined. The elongation of the ribs, rib cage and sternum associated with streamlining in diving species suggests that differences may also exist in their breathing mechanics. Given the increased length of the processes in diving birds, the insertion of the Mm. appendicocostales towards the end of the tip of the processes may further improve the mechanical advantage for moving the elongated ribs during breathing. Future work may improve our understanding of anatomical differences in musculature associated with variations in uncinate morphology. Alternative functions of the uncinate processes remain to be determined; for example, the role of the uncinate processes in stabilizing the scapula during retraction of the wing has not been examined here. Additionally the 'finger-like' projections of the M. obliquus externus abdominus insert onto the base of the processes, and in the opposite manner the M. serratus superficialis originates at the top of the processes and inserts on the ventral margin of the scapula (Vanden Berge and Zweers, 1993), suggesting that they may act antagonistically. Variations in uncinate morphology seem likely to relate to differences in the muscles involved in breathing or in the pattern of muscle activity. Respiration in Aves is complex, with a great many axial muscles reported to be involved (Fedde, 1987). This research suggests that there may be fundamental differences in the breathing mechanics of different birds, driven in part by the morphological differences of the rib cage and sternum associated with skeletal adaptations to locomotion.

Skeletons were provided by the Ornithology Department of the Research Institute and Museum Alexander Koenig (Bonn, Germany), The Manchester Museum (Manchester, UK) and the Department of Ornithology of the American Museum of Natural History (New York, USA). The authors would like to thank Chris Klingenberg for assistance with statistical analyses, Renate van den Elzen, Henry McGhie and Paul Sweet for access to skeletons and Andrew Crooks for assistance with dissections. This work was supported by the Deutsche Forschungsgemeinschaft through the Graduiertenkolleg 'Evolution und Biodiversität in Raum und Zeit' Project No: 721/1 and the University of Manchester.

References

Brackenbury, J. H. (1972). Lung-air-sac anatomy and respiratory pressure in the bird. *J. Exp. Biol.* **57**, 543-550.

Brackenbury, J. H. (1973). Respiratory mechanics in the bird. *Comp. Biochem. Physiol.* **44**, 599-611.

Brainerd, E. L. (1999). New perspectives on the evolution of lung ventilation mechanisms in vertebrates. *Exp. Biol.* **4**, 11-28.

Campbell, N. A. and Atchley, W. R. (1981). The geometry of canonical variate analysis. *Syst. Zool.* **30**, 268-280.

Codd, J. R., Boggs, D. F., Perry, S. F. and Carrier, D. R. (2005). Activity of three muscles associated with the uncinate processes of the giant Canada goose *Branta canadensis maximus*. *J. Exp. Biol.* **208**, 849-857.

Dial, K. P., Kaplan, S. R., Goslow, G. E., Jr and Jenkins, F. A., Jr (1988). A functional analysis of the primary upstroke and downstroke muscles in the domestic pigeon (*Columba livia*) during flight. *J. Exp. Biol.* **134**, 1-16.

Duncker, H.-R. (1971). The lung air sac system of birds. A contribution to the functional anatomy of the respiratory apparatus. *Ergeb. Anat. Entwicklungsgesch.* **45**, 7-171.

Dyke, G. J. and Rayner, J. M. V. (2001). Forelimb shape and the evolution of birds. In *New Perspectives on the Origin and Early Evolution of Birds* (ed. J. Gautier and L.-F. Gall), pp. 275-282. New Haven: Peabody Museum of Natural History Press.

Fedde, M. R. (1987). Respiratory muscles. In *Bird Respiration.* Vol. 1 (ed. T. J. Seller), pp. 3-27. Boca Raton: CRC Press.

Hildebrand, M. (1982). Body skeleton. In *Analysis of Vertebrate Structure*. 2nd edn, pp. 157-158. New York: John Wiley and Sons.

Jenkins, F. A., Jr, Dial, K. P. and Goslow, G. E., Jr (1988). A cineradiographic analysis of bird flight: the wishbone in starlings is a spring. *Science* **241**, 1495-1498.

Jones, D. R. and Furilla, R. A. (1987). The anatomical, physiological, behavioural, and meatabolic consequences of voluntary and forced diving. In *Bird Respiration*. Vol II (ed. T. J. Seller), pp. 76-119. Boca Raton: CRC Press.

Kardong, K. V. (1988). Skeletal system: the axial skeleton. In *Vertebrates: Comparative Anatomy, Function, Evolution*, pp. 278-279. New York: McGraw-Hill.

Kirby, V. C. (1980). An adaptive modification in the ribs of woodpeckers and piculets (picidae). *Auk* **97**, 521-532.

Ludders, J. W. (2001). Inhaled anaesthesia for birds. In *Recent Advances in Veterinary Anaesthesia and Analgesia: Companion Animals.* New York: IVIS.

Parkes, R., Halsey, L. G., Woakes, A. J., Holder, R. L. and Butler, P. J. (2002). Oxygen uptake during post dive recovery in a diving bird *Aythya fuligula*: implications for optimal foraging models. *J. Exp. Biol.* **205**, 3945-3954.

Patak, A. and Baldwin, J. (1993). Structural and metabolic characterization of the muscles used to power running in the emu (*Dromaius navaehollandiae*), a giant flightless bird. *J. Exp. Biol.* **175**, 233-249.

Rayner, J. M. V. and Couldrick, L. B. (2003). Aerodynamic and biochemical determinants of wing shape in birds. *Comp. Biochem. Physiol.* **134A**, 38.

Shufeldt, R. W. (1890). The musculature of the trunk. In *The Myology of the Raven*, pp. 300-301. London: MacMillan and Co.

Tucker, V. A. (1993). Gliding birds: reduction of drag by wing tip slots between the primary feathers. *J. Exp. Biol.* **180**, 285-310.

Vanden Berge, J. C. and Zweers, G. A. (1993). Myologia. In *Handbook of Avian Anatomy: Nomina Anatomica Avium*. 2nd edn (ed. J. J. Baumel), pp. 209-210. Cambridge, MA: Publications of the Nuttall Ornithological Club.

Walker, W. F., Jr and Liem, K. F. (1994). Evolution of the postcranial skeleton. In *Functional Anatomy of the Vertebrates: An Evolutionary Perspective*, p. 270. New York: Saunders College Publishing.

Welty, J. C. (1988). Bones and muscle. In *The Life of Birds* (ed. J. C. Welty and L. Baptista), p. 59. London: W. B. Saunders and Co.

Welty, J. C. and Baptista, L. (1988). The appendicular skeleton. In *The Life of Birds.* 4th edn, p. 62. London: W. B. Saunders and Co.

Wilson, R. P., Simeone, A., Luna-Jorquera, G., Steinfurth, A., Jackson, S. and Falhman, A. (2003). Patterns of respiration in diving penguins: is the last gasp an inspired tactic? *J. Exp. Biol.* **206**, 1751-1763.

Zeffer, A. and Norberg, U. M. L. (2003). Leg morphology and locomotion in birds: requirements for force and speed during ankle flexion. *J. Exp. Biol.* **206**, 1085-1097.

Zimmer, K. (1935). Beitrage zur Mechanik der Atmung bei den Vögeln in Stand und Flug. Aufgrund anatomischer-physiologisher und experimenteller Studien. *Zoologica* **88**, 1-69.

Errata

Tickle, P. G., Ennos, A. R., Lennox, L. E., Perry, S. F. and Codd, J. R. (2007) Functional significance of the uncinate processes in birds. *J. Exp. Biol.* **210,** 3955-3961

- Equation (1) on page 3956 should read:

$$L = \sqrt{x^2 + y^2} = \sqrt{[(D\cos\theta + P)^2 + (D\sin\theta)^2]}\,.$$

- Angle θ in Figure 2B on page 3956 should extend between the posterior vertebral rib and the dashed line parallel to the vertebral column:

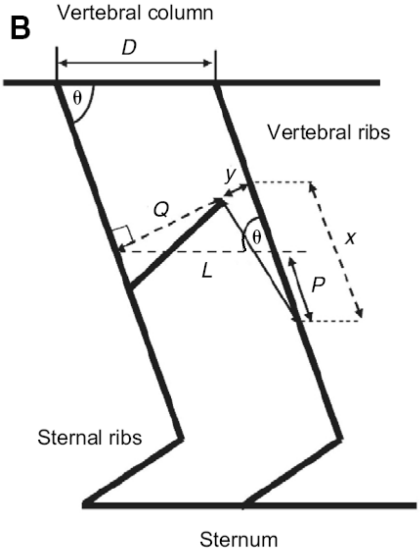

Chapter 2

Appendix

Name		Locomotor Mode	No of Ribs	Rib 2 Dorsal Rib Length to UCP	Rib 3 Dorsal Rib Length to UCP	Rib 4 Dorsal Rib Length to UCP	Rib 5 Dorsal Rib Length to UCP
Fulica	americana	**diving**	9	21.55	23.74	25.05	25.6
Gavia	arctica	**diving**	9	55.66	60.57	62.76	65.91
Fulica	atra	**diving**	9	24.29	28.15	31.31	34.11
Larus	canus	**diving**	7	24.77	23.18	21.53	22.67
Alcedo	atthis	**diving**	7	10.98	12.26	11.59	10.71
Mergus	merganser	**diving**	9	35.45	37.85	36.43	34.68
Spheniscus	demersus	**diving**	9	51.36	57.31	58.05	58.51
Sterna	hirundo	**diving**	8	19.3	20.2	19.45	18.62
Pinguinus	impennis	**diving**	10	33.72	40.51	42.61	45.22
Spheniscus	humboldti	**diving**	7	51.4	52.72	51.99	49.53
Larus	argentatus	**diving**	7	40.08	36.97	35.4	33.78
Alle	alle	**diving**	9	21.29	23.41	22.5	21.68
Clangula	hyemalis	**diving**	7	33.29	33.61	31	28.24
Gavia	stellata	**diving**	8	42.01	42.75	41.93	39
Pelecanus	rufescens	**diving**	6	72.94	69.36	64.23	60.95
Aptenodytes	patagonicus	**diving**	8	84.97	91.55	92.88	89.01
Fumarus	glacialis	**diving**	8	31.74	33.68	32.9	32.26
Alca	torda	**diving**	9	31.54	35.47	36.6	37.54
Aythya	fuligula	**diving**	9	24.53	25.51	26.29	26.29
Cinclus	cinclus	**diving**	7	12.75	14.45	14.94	14.94
Sterna	paradisaea	**diving**	8	17.5	17.42	16.94	15.17
Phalacrocorax	carbo	**diving**	8	37.6	40.83	40.23	39.37
Phalacrocorax	bougainvillii	**diving**	7	41.98	42.6	39.05	43.29
Podiceps	cristatus	**diving**	9	30.65	32.33	33.78	35.53
Tockus	nasutus	**non-specialist**	8	18.74	19.66	19.21	19.92
Hirundo	rustica	**non-specialist**	7	7.48	7.84	8.22	8.01
Gypaetus	barbatus	**non-specialist**	7	54.71	60.06	61.93	58.58
Turdus	merula	**non-specialist**	7	13.53	14.6	14.6	14.98
Eremopterix	leucotis	**non-specialist**	7	6.74	7.2	7.26	7.08
Elanus	caerulus	**non-specialist**	7	17.82	17.01	18.19	15.83
Amazona	aestiva	**non-specialist**	8	20.76	22.6	21.49	21.95
Columba	bollii	**non-specialist**	7	15.5	18.46	20.46	20.49
Melopsittacus	undulatus	**non-specialist**	8	8.54	9.79	9.8	10.15
Streptopelia	decaocto	**non-specialist**	7	12.56	15.52	17.23	16.68

Name		Locomotor Mode	No of Ribs	Rib 2 Dorsal Rib Length to UCP	Rib 3 Dorsal Rib Length to UCP	Rib 4 Dorsal Rib Length to UCP	Rib 5 Dorsal Rib Length to UCP
Columba	cayennensis	**non-specialist**	7	17.38	19.03	20.45	19.27
Corvus	corax	**non-specialist**	6	35.44	34.05	33.06	31.14
Passer	domesticus	**non-specialist**	7	7.73	8.98	8.77	8.55
Apus	apus	**non-specialist**	8	8.19	9.37	9.94	10.05
Vultur	gryphus	**non-specialist**	8	0	60.29	63.17	59.54
Chrysococcyx	caprius	**non-specialist**	7	7.83	9.02	8.67	8.36
Bubo	bubo	**non-specialist**	7	38.94	39.79	42.72	42.9
Sturnus	vulgaris	**non-specialist**	7	12.12	12.96	13.16	12.4
Agapornis	fischeri	**non-specialist**	8	9.32	9.97	9.97	9.03
Aquila	chrysaetus	**non-specialist**	8	41.02	44.5	36.94	39.35
Picoides	viridis	**non-specialist**	7	13.81	15.77	15.69	14.43
Buceros	bicornis	**non-specialist**	7	44.22	48.07	46.02	41.04
Psittacus	erithacus	**non-specialist**	8	23.44	25.77	29.32	27.31
Falco	rusticolus	**non-specialist**	8	32.01	37.52	39.37	37.61
Loriculus	galgulus	**non-specialist**	8	7.81	9.73	10	9.59
Chlamydotis	undulata	**non-specialist**	7	38.53	38.16	37.12	37.45
Phaethornis	yaruqui	**non-specialist**	7	6.29	7.14	6.61	6.62
Falco	biarmicus	**non-specialist**	8	26.83	26.75	27.43	25.43
Chordeiles	acutipennis	**non-specialist**	7	0	9.89	11.59	12.12
Athene	noctua	**non-specialist**	7	17.94	17.95	18.05	17.78
Bubo	ascalaphus	**non-specialist**	7	33.17	37.54	38.7	38.74
Agapornis	roseicollis	**non-specialist**	7	10.59	11.38	11.38	11.13
Mimus	polyglottos	**non-specialist**	7	5.59	5.88	5.73	5.38
Oena	capensis	**non-specialist**	7	8.52	10.39	10.39	10.39
Trichoglossus	haematodus	**non-specialist**	8	13.65	14.26	15.35	15.35
Chrysolampis	mosquitus	**non-specialist**	8	5.32	5.98	6.49	6.68
Polytelis	swainsonii	**non-specialist**	8	16.74	18.01	19.02	18.48
Ramphastos	tucanus	**non-specialist**	7	23.11	22.02	22.79	24
Colius	colius	**non-specialist**	7	10.25	11.29	12.27	12.55
Trogon	viridis	**non-specialist**	7	13.44	15.43	16.59	16.23
Rostratula	semicollaris	**non-specialist**	8	17.38	19.03	20.45	19.27
Perdix	perdix	**non-specialist**	7	13.21	12.49	13.68	13.37
Phoenicopterus	rubur	**non-specialist**	7	54.02	51.86	54.61	46.49
Botaurus	stellaris	**non-specialist**	7	45.23	48.12	49	47.22

Name		Locomotor Mode	No of Ribs	Rib 2	Rib 3	Rib 4	Rib 5
				Dorsal Rib Length to UCP	Dorsal Rib Length to UCP	Dorsal Rib Length to UCP	Dorsal Rib Length to UCP
Francolinus	pondicerianus	**non-specialist**	7	10.2	10.86	11.67	12.65
Ardea	alba	**non-specialist**	6	40.64	39.28	36.38	35.8
Tetraogallus	himalayensis	**non-specialist**	6	27.94	29.36	29.97	30.15
Thinocorus	rumicovorus	**non-specialist**	8	11.17	13.21	13.43	14.67
Aramus	guarauna	**non-specialist**	8	0	27.52	30.21	30.31
Ixobrychus	minutus	**non-specialist**	7	16.85	18.51	20.19	15.52
Leptoptilos	crumeniferus	**non-specialist**	6	0	47.53	56.32	51.28
Pterocles	exustus	**non-specialist**	7	14.84	15.69	16.48	16.09
Sagittarius	serpentarius	**non-specialist**	7	0	45.85	47.35	41.03
Platalea	leucorodia	**non-specialist**	7	31.13	34.15	34.36	30.3
Scolopax	rusticola	**non-specialist**	9	0	18.47	19.66	15.51
Branta	leucopsis	**non-specialist**	9	36.81	36.84	4.08	34.81
Cygnus	atratus	**non-specialist**	9	0	62.05	63.36	58.41
Somateria	mollissima	**non-specialist**	9	35.66	37.48	39.6	40.5
Anas	falcata	**non-specialist**	9	23.45	27.02	27.33	26.68
Aythya	marila	**non-specialist**	9	25.25	29.61	28.82	27.52
Gallinula	chloropus	**non-specialist**	9	18.32	19.66	21.41	21.04
Anas	acuta	**non-specialist**	9	25.22	26.2	29.9	24.33
Tadorna	ferruginea	**non-specialist**	9	24.49	27.86	28.9	27.78
Tadorna	tadorna	**non-specialist**	9	27.67	29.34	31.01	27.6
Anser	albifrons	**non-specialist**	9	34.99	37.31	35.11	32.42
Falco	tinnuculus	**non-specialist**	8	13.81	15.48	16.09	16.03
Tetrao	urogallus	**walking**	6	24.34	28.9	31.92	34.49
Casuarius	casuarius	**walking**	10	0	0	102.62	105.5
Apteryx	haastii	**walking**	8	35.49	40.91	40.91	40.57
Dinornis	maximus	**walking**	9	124.06	130.75	152.53	163.15
Struthio	camelus	**walking**	9	0	180.91	182.75	169.67
Phasianus	colchicus	**walking**	7	17.21	18.46	19.25	20.21
Geococcyx	californianus	**walking**	6	12.58	17.8	21.27	22.41
Eudromia	elegans	**walking**	7	19.84	20.93	21.09	21.95
Meleagris	gallopavo	**walking**	6	20.31	22.93	25.04	25.83
Alectoris	rufa	**walking**	7	15.24	15.72	16.77	16.95

		Rib 6	Rib 2	Rib 3	Rib 4
Name		Dorsal Rib Length to UCP	Width of Uncinate at base	Width of Uncinate at base	Width of Uncinate at base
Fulica	americana	26.37	1.63	2.14	1.87
Gavia	arctica	63.61	5.81	6.35	6.01
Fulica	atra	32.41	2.28	2.58	3.04
Larus	canus	0	2.22	2.26	1.94
Alcedo	atthis	0	1.46	1.32	1.23
Mergus	merganser	28.67	2.19	3.98	3.44
Spheniscus	demersus	57.21	5.91	6.81	5.85
Sterna	hirundo	17.47	1.46	2.06	1.73
Pinguinus	impennis	43.32	2.12	1.31	1.33
Spheniscus	humboldti	43.44	6.33	4.09	4.16
Larus	argentatus	0	4.23	3.69	2.36
Alle	alle	21.14	1.73	1.45	1.39
Clangula	hyemalis	23.66	2.81	3.47	2.7
Gavia	stellata	34.5	4.78	5.47	6.71
Pelecanus	rufescens	0	6.68	5.99	6.41
Aptenodytes	patagonicus	81.12	8.29	9.57	13.88
Fumarus	glacialis	32.54	2.13	3.08	2.64
Alca	torda	36.48	3.21	2.2	1.98
Aythya	fuligula	21.55	2.52	3.29	3.86
Cinclus	cinclus	12.77	1.41	1.54	1.01
Sterna	paradisaea	14.57	1.32	1.68	1.3
Phalacrocorax	carbo	36.82	4.3	4.13	4.35
Phalacrocorax	bougainvillii	39.2	4.89	5.22	3.66
Podiceps	cristatus	32.8	2.78	3.33	3.03
Tockus	nasutus	19.5	3.59	2.55	1.82
Hirundo	rustica	0	0.78	0.69	0.71
Gypaetus	barbatus	51.83	5.44	16.77	23.85
Turdus	merula	13.01	1.33	1.27	1.94
Eremopterix	leucotis	7.08	0.65	0.99	1.33
Elanus	caerulus	14.65	4.59	5.76	6.94
Amazona	aestiva	22.94	4.28	5.23	5.39
Columba	bollii	20.47	2.22	3.46	5.35
Melopsittacus	undulatus	9.68	1.68	2.64	2.32
Streptopelia	decaocto	16.68	1.9	3.04	3.62

		Rib 6	Rib 2	Rib 3	Rib 4
Name		Dorsal Rib Length to UCP	Width of Uncinate at base	Width of Uncinate at base	Width of Uncinate at base
Columba	cayennensis	16.91	3.96	6.26	7.2
Corvus	corax	0	6.24	5.95	4.51
Passer	domesticus	8.05	0.74	0.77	0.99
Apus	apus	9.81	0.64	0.8	0.92
Vultur	gryphus	49.87	0	10.41	23.05
Chrysococcyx	caprius	0	0.88	1.03	0.88
Bubo	bubo	41.43	4.2	4.54	3.89
Sturnus	vulgaris	11.42	1.15	1.29	1.57
Agapornis	fischeri	8.76	1.75	1.9	1.44
Aquila	chrysaetus	34.63	11.11	14.31	17
Picoides	viridis	0	3.42	4.08	2.14
Buceros	bicornis	0	5.16	5.86	5.52
Psittacus	erithacus	23.96	2.48	4.55	6.87
Falco	rusticolus	33.82	3.14	4.77	4.84
Loriculus	galgulus	8.59	0	0.84	1.18
Chlamydotis	undulata	38.7	5.83	11.38	14.39
Phaethornis	yaruqui	0	0.61	0.55	0.58
Falco	biarmicus	25.49	3.17	5.92	6.18
Chordeiles	acutipennis	11.42	0	0.91	1.15
Athene	noctua	0	1.75	1.77	1.12
Bubo	ascalaphus	0	4.4	5.02	4.47
Agapornis	roseicollis	11.42	2.2	2.45	2.74
Mimus	polyglottos	4.21	0.45	0.48	0.49
Oena	capensis	9.52	0.78	1.89	2.42
Trichoglossus	haematodus	13.36	2.05	3.42	3.99
Chrysolampis	mosquitus	6.99	0.5	0.41	0.31
Polytelis	swainsonii	19.77	1.03	2.24	3.09
Ramphastos	tucanus	20.4	3.52	3.47	2.64
Colius	colius	9.91	1.52	2.19	3.2
Trogon	viridis	0	1.51	1.7	1.45
Rostratula	semicollaris	16.91	3.96	6.26	7.2
Perdix	perdix	12.85	1.38	1.5	2.19
Phoenicopterus	rubur	42.19	9.79	6.23	9.1
Botaurus	stellaris	43.22	2.49	1.78	2.32

Name		Rib 6 Dorsal Rib Length to UCP	Rib 2 Width of Uncinate at base	Rib 3 Width of Uncinate at base	Rib 4 Width of Uncinate at base
Francolinus	pondicerianus	12.33	1.29	1.13	0.96
Ardea	alba	0	3.73	3.36	3.93
Tetraogallus	himalayensis	0	3.14	3.71	3.75
Thinocorus	rumicovorus	13.91	0	0.91	0.94
Aramus	guarauna	29.42	0	1.53	1.64
Ixobrychus	minutus	0	0.83	1.29	1.01
Leptoptilos	crumeniferus	0	0	7.44	8.33
Pterocles	exustus	15.3	1.78	2.51	3.43
Sagittarius	serpentarius	37.46	0	10.06	16.64
Platalea	leucorodia	0	4.08	4.46	4.53
Scolopax	rusticola	16.03	0	1.75	2.13
Branta	leucopsis	31.22	2.98	2.97	2.52
Cygnus	atratus	50.13	0	7	6.44
Somateria	mollissima	36.23	2.95	3.45	3.69
Anas	falcata	22.49	1.78	1.68	2.32
Aythya	marila	25.4	3.66	4.11	5.55
Gallinula	chloropus	20.14	2.39	2.15	2.45
Anas	acuta	23.54	3.1	3.32	2.53
Tadorna	ferruginea	25.55	1.9	2.32	2.76
Tadorna	tadorna	26.83	1.81	6.27	2.98
Anser	albifrons	29.53	6.36	7.41	7.25
Falco	tinnuculus	16.37	3.75	4.23	4.35
Tetrao	urogallus	36.94	1.89	2.84	3.12
Casuarius	casuarius	96.16	0	0	15.65
Apteryx	haastii	35.34	15.48	12.35	13.79
Dinornis	maximus	172.12	5.05	23.79	28.46
Struthio	camelus	0	0	16.34	17.51
Phasianus	colchicus	0	2.37	2.46	2.5
Geococcyx	californianus	0	1.94	2.95	2.91
Eudromia	elegans	0	1.54	2.41	3.5
Meleagris	gallopavo	22.03	2.5	3.12	3.84
Alectoris	rufa	18.98	1.78	1.9	1.87

Name		Rib 5 Width of Uncinate at base	Rib 6 Width of Uncinate at base	Rib 2 Width of Uncinate at Midpoint	Rib 3 Width of Uncinate at Midpoint
Fulica	americana	1.82	1.75	1.33	1.47
Gavia	arctica	5.19	5	4.3	4.28
Fulica	atra	1.77	1	1.7	1.41
Larus	canus	1.61	0	1.8	1.8
Alcedo	atthis	2.1	0	1.54	1.31
Mergus	merganser	6.3	5.46	2.24	3.58
Spheniscus	demersus	4.78	3.52	6.29	6.23
Sterna	hirundo	1.73	1.42	1.02	1.23
Pinguinus	impennis	1.12	1.27	1.86	1.82
Spheniscus	humboldti	2.37	4.11	6.15	6.03
Larus	argentatus	1.79	0	2.47	2.22
Alle	alle	1.21	0.68	0.96	0.83
Clangula	hyemalis	1.62	1.29	2.51	2.44
Gavia	stellata	6.85	2.32	2.65	3.01
Pelecanus	rufescens	5.38	0	4.25	4.54
Aptenodytes	patagonicus	10.12	8.19	8.36	15.66
Fumarus	glacialis	2.67	2.53	1.62	2.02
Alca	torda	1.97	1.42	1.89	1.39
Aythya	fuligula	3.23	2.78	2.39	2.91
Cinclus	cinclus	0.71	0.47	0.92	1.3
Sterna	paradisaea	1.02	0.83	1.09	1.02
Phalacrocorax	carbo	3.2	3.74	3.85	3.04
Phalacrocorax	bougainvillii	4.59	3.73	5.18	4.68
Podiceps	cristatus	3.4	3	2.31	2.86
Tockus	nasutus	1.1	1.1	1.71	1.99
Hirundo	rustica	0.9	0	0.62	0.63
Gypaetus	barbatus	23.77	16.49	5.32	7.24
Turdus	merula	2.01	2.07	1.09	1.53
Eremopterix	leucotis	0.7	0.28	0.55	0.39
Elanus	caerulus	5.95	3.2	3.47	2.19
Amazona	aestiva	5.38	4.28	2.67	3.09
Columba	bollii	5.62	4.48	1.83	2.84
Melopsittacus	undulatus	2.11	0.7	1.22	1.21
Streptopelia	decaocto	3.61	3.66	1.61	2.58

		Rib 5	Rib 6	Rib 2	Rib 3
Name		Width of Uncinate at base	Width of Uncinate at base	Width of Uncinate at Midpoint	Width of Uncinate at Midpoint
Columba	cayennensis	6.08	3.09	2.68	2.87
Corvus	corax	3.68	0	3.25	3.68
Passer	domesticus	0.92	0.56	0.83	0.86
Apus	apus	0.84	0.64	0.49	0.71
Vultur	gryphus	20.64	12.54	0	4.43
Chrysococcyx	caprius	0.88	0	0.73	0.83
Bubo	bubo	3.69	3.01	3.03	2.62
Sturnus	vulgaris	1.24	0.82	1.41	1.06
Agapornis	fischeri	1.23	0.8	1.15	0.9
Aquila	chrysaetus	19.58	19.57	5.37	4.88
Picoides	viridis	2.01	0	1.92	2.09
Buceros	bicornis	4.33	0	4.74	4.38
Psittacus	erithacus	8.25	2.91	2.47	2.73
Falco	rusticolus	6.21	5.88	2.89	2.79
Loriculus	galgulus	1	0.37	0.75	0.87
Chlamydotis	undulata	16	14.28	5.56	4.76
Phaethornis	yaruqui	0.59	0	0.33	0.56
Falco	biarmicus	6.17	7.29	2.4	3.07
Chordeiles	acutipennis	1.26	1.05	0	0.67
Athene	noctua	2.27	0	1.53	1.36
Bubo	ascalaphus	5.11	0	2.33	2.63
Agapornis	roseicollis	2.74	1.02	1.17	1.03
Mimus	polyglottos	0.4	0.27	0.32	0.54
Oena	capensis	2.28	1.24	0.82	1.49
Trichoglossus	haematodus	3.43	2.93	2.04	1.91
Chrysolampis	mosquitus	0.33	0.32	0.5	0.4
Polytelis	swainsonii	2.28	2.38	0.94	2.69
Ramphastos	tucanus	2.03	2.68	1.77	1.96
Colius	colius	2.51	2.32	1.23	1.38
Trogon	viridis	1.09	0	1.02	0.91
Rostratula	semicollaris	6.08	3.09	2.68	2.87
Perdix	perdix	2.03	1.8	1.41	1.38
Phoenicopterus	rubur	5.85	7.59	4.84	5.16
Botaurus	stellaris	1.71	1.31	2.12	2.09

Name		Rib 5	Rib 6	Rib 2	Rib 3
		Width of Uncinate at base	Width of Uncinate at base	Width of Uncinate at Midpoint	Width of Uncinate at Midpoint
Francolinus	pondicerianus	0.99	0.93	1.03	1.02
Ardea	alba	3.56	0	3.34	3.93
Tetraogallus	himalayensis	3.6	0	2.53	2.37
Thinocorus	rumicovorus	0.96	0.77	0.65	0.83
Aramus	guarauna	2.19	1.34	0	1.81
Ixobrychus	minutus	0.45	0	0.72	1.07
Leptoptilos	crumeniferus	7.99	0	0	5.1
Pterocles	exustus	4.31	1.77	1.59	2.17
Sagittarius	serpentarius	30.48	22.14	0	5.72
Platalea	leucorodia	2.22	0	3.16	3.04
Scolopax	rusticola	1.77	2.07	0	1.78
Branta	leucopsis	4.11	4.07	2.29	2.65
Cygnus	atratus	6.21	6.91	0	5.2
Somateria	mollissima	3.75	5.32	3.02	3.19
Anas	falcata	2.37	3.13	1.41	2.07
Aythya	marila	5.08	4.33	2.97	4.09
Gallinula	chloropus	1.93	2.65	1.11	1.29
Anas	acuta	2.13	1.67	3	2.39
Tadorna	ferruginea	2.69	1.67	2.13	2.6
Tadorna	tadorna	3.76	4.15	1.67	4.05
Anser	albifrons	6.12	3.1	5.56	4.31
Falco	tinnuculus	3.9	3.97	1.36	1.98
Tetrao	urogallus	3.02	2.46	2.25	2.6
Casuarius	casuarius	17.33	17.08	0	0
Apteryx	haastii	13.79	19.44	6.38	8.07
Dinornis	maximus	25.89	26.06	19.4	21.32
Struthio	camelus	15.02	0	0	14.5
Phasianus	colchicus	3.25	0	1.94	1.83
Geococcyx	californianus	2.44	0	1.6	1.75
Eudromia	elegans	1.68	0	1.34	1.7
Meleagris	gallopavo	2.88	0	1.85	2.33
Alectoris	rufa	1.71	1.3	1.53	1.42

Name		Rib 4 Width of Uncinate at Midpoint	Rib 5 Width of Uncinate at Midpoint	Rib 6 Width of Uncinate at Midpoint	Rib 2 Width of Uncinate at Tip
Fulica	americana	1.93	1.52	1.59	1.28
Gavia	arctica	4.17	3.22	3.02	4.99
Fulica	atra	1.72	1.58	1.27	1.6
Larus	canus	2.12	1.23	0	1.37
Alcedo	atthis	1.04	1.34	0	1
Mergus	merganser	3.68	2.66	3.12	1.87
Spheniscus	demersus	6.17	6.5	8.07	7.13
Sterna	hirundo	1.26	1.13	1.07	0.65
Pinguinus	impennis	1.36	0.81	0.96	1.89
Spheniscus	humboldti	4.23	4.56	4.32	8.37
Larus	argentatus	1.82	1.2	0	2.1
Alle	alle	0.72	0.59	0.69	1.23
Clangula	hyemalis	2.03	1.05	0.77	1.68
Gavia	stellata	2.62	2.37	1.3	1.52
Pelecanus	rufescens	3.32	4.75	0	3.48
Aptenodytes	patagonicus	13.64	10.76	5.84	14.61
Fumarus	glacialis	1.71	2.12	2.13	2.16
Alca	torda	1.52	1.46	1.14	1
Aythya	fuligula	3.36	2.35	1.77	2.03
Cinclus	cinclus	1.03	1	0.65	0.76
Sterna	paradisaea	1.1	0.96	0.67	0.79
Phalacrocorax	carbo	2.78	2.26	1.67	3.03
Phalacrocorax	bougainvillii	4.75	2.75	2.05	3.66
Podiceps	cristatus	2.2	2.73	2.54	2.3
Tockus	nasutus	1.41	0.98	0.98	1.22
Hirundo	rustica	0.51	0.44	0	0.48
Gypaetus	barbatus	8.34	6.75	5.28	5.31
Turdus	merula	1.31	1.27	1.41	0.83
Eremopterix	leucotis	0.28	0.23	0.24	0.54
Elanus	caerulus	2.18	1.9	0.96	1.38
Amazona	aestiva	3.18	2.39	1.93	1.77
Columba	bollii	3.18	3.59	3.05	1.19
Melopsittacus	undulatus	1.26	1.05	0.65	0.86
Streptopelia	decaocto	2.3	2.52	2.22	1.23

		Rib 4	Rib 5	Rib 6	Rib 2
Name		Width of Uncinate at Midpoint	Width of Uncinate at Midpoint	Width of Uncinate at Midpoint	Width of Uncinate at Tip
Columba	cayennensis	2.32	2.38	2.35	1.53
Corvus	corax	3.19	2.02	0	3.1
Passer	domesticus	0.71	0.55	0.52	0.61
Apus	apus	0.66	0.64	0.57	0.53
Vultur	gryphus	6.3	5.14	3.8	0
Chrysococcyx	caprius	0.64	0.64	0	0.42
Bubo	bubo	2.81	2.25	1.27	2.45
Sturnus	vulgaris	1	0.85	0.49	0.87
Agapornis	fischeri	0.88	0.77	0.7	1.03
Aquila	chrysaetus	5.18	5.75	5.43	4.65
Picoides	viridis	1.84	1.79	0	1.66
Buceros	bicornis	3.81	3.79	0	4.24
Psittacus	erithacus	3.92	4.11	2.78	1.41
Falco	rusticolus	2.15	2.25	1.8	1.75
Loriculus	galgulus	0.74	0.98	0.3	0.93
Chlamydotis	undulata	5.42	5.91	2	5.4
Phaethornis	yaruqui	0.4	0.4	0	0.31
Falco	biarmicus	2.4	3.05	2.83	2.15
Chordeiles	acutipennis	0.83	1.08	0.67	0
Athene	noctua	1.25	1.03	0	0.84
Bubo	ascalaphus	2.02	1.68	0	1.73
Agapornis	roseicollis	0.87	0.62	0.63	0.98
Mimus	polyglottos	0.32	0.26	0.26	0.32
Oena	capensis	1.36	0.98	1.15	0.97
Trichoglossus	haematodus	2.02	1.56	1.05	2.15
Chrysolampis	mosquitus	0.3	0.31	0.31	0.5
Polytelis	swainsonii	2.01	1.62	0.56	1
Ramphastos	tucanus	2.08	1.01	2.35	1.55
Colius	colius	1.46	1.54	1.33	1.34
Trogon	viridis	0.86	0.84	0	0.98
Rostratula	semicollaris	2.32	2.38	2.35	1.53
Perdix	perdix	1.54	1.34	1.65	1.21
Phoenicopterus	rubur	4.93	4.39	2.61	4.93
Botaurus	stellaris	1.93	2.2	2.09	1.92

		Rib 4	Rib 5	Rib 6	Rib 2
Name		Width of Uncinate at Midpoint	Width of Uncinate at Midpoint	Width of Uncinate at Midpoint	Width of Uncinate at Tip
Francolinus	pondicerianus	0.78	0.77	0.78	0.98
Ardea	alba	3.19	3.08	0	2.93
Tetraogallus	himalayensis	2.15	2.36	0	1.85
Thinocorus	rumicovorus	0.79	0.79	0.55	0.62
Aramus	guarauna	1.54	1.41	1.17	0
Ixobrychus	minutus	0.92	0.81	0	0.71
Leptoptilos	crumeniferus	6.35	5.87	0	0
Pterocles	exustus	2.26	2.05	0.95	0.96
Sagittarius	serpentarius	9.26	22.16	18.57	0
Platalea	leucorodia	3.32	2.08	0	3.01
Scolopax	rusticola	2.2	1.8	2.04	0
Branta	leucopsis	2.73	3.08	2.82	2.25
Cygnus	atratus	5.83	5.21	4.29	0
Somateria	mollissima	4.27	4.2	2.1	2.57
Anas	falcata	2.95	2.22	1.28	1.55
Aythya	marila	4.28	3.14	2.67	3.18
Gallinula	chloropus	1.01	1.1	0.9	0.79
Anas	acuta	2.8	2.15	1.49	3.12
Tadorna	ferruginea	3.02	2.01	1.45	2.73
Tadorna	tadorna	4.07	3	3.05	1.83
Anser	albifrons	3.46	3.65	3.15	3.48
Falco	tinnuculus	1.33	1.56	1.21	0.76
Tetrao	urogallus	3.08	2.38	1.28	2.04
Casuarius	casuarius	12.98	10.57	11.78	0
Apteryx	haastii	6.85	7.25	2.94	4.29
Dinornis	maximus	24.65	18.66	18.44	11.54
Struthio	camelus	11.96	10.73	0	0
Phasianus	colchicus	1.92	1.54	0	1.94
Geococcyx	californianus	1.69	1.49	0	1.55
Eudromia	elegans	1.59	1.67	0	1.39
Meleagris	gallopavo	2.2	1.67	0	2.02
Alectoris	rufa	1.68	1.12	0.97	1.81

		Rib 3	Rib 4	Rib 5	Rib 6	Rib 2	Rib 3
Name		Width of Uncinate at Tip	Width of Uncinate at Tip	Width of Uncinate at Tip	Width of Uncinate at Tip	Length of UCP	Length of UCP
Fulica	americana	1.02	1.34	2.43	1.76	6.28	14.97
Gavia	arctica	4.18	3.74	4.23	3.04	21.03	31.03
Fulica	atra	1.22	1.31	1.61	1.7	9.62	15.22
Larus	canus	1.86	1.62	1.22	0	13.19	13.59
Alcedo	atthis	1.03	0.75	0.84	0	4.47	5.04
Mergus	merganser	3.25	3.16	2.54	3.14	17.12	18.73
Spheniscus	demersus	6.69	6.68	5.96	8.04	10.52	28.77
Sterna	hirundo	1.07	1.03	0.95	0.8	7.12	9.13
Pinguinus	impennis	1.83	1.59	1.48	1.34	17.63	20.77
Spheniscus	humboldti	6.75	7.97	8.64	3.37	23.42	21.19
Larus	argentatus	1.95	1.9	0.98	0	20.57	21.16
Alle	alle	0.93	0.84	1.03	0.68	10.56	11.14
Clangula	hyemalis	2.09	1.83	1.15	0.73	18.16	19.32
Gavia	stellata	1.66	1.58	2	1.3	21.69	22.86
Pelecanus	rufescens	3.46	2.58	4.76	0	32.04	30.43
Aptenodytes	patagonicus	16.13	17.6	15.85	8.85	33.57	38.16
Fumarus	glacialis	1.61	1.64	1.74	1.84	5	15.3
Alca	torda	0.96	1.52	1.91	1.67	13.66	16.03
Aythya	fuligula	2.54	2.69	2.31	2.47	14.26	13.47
Cinclus	cinclus	0.81	0.99	0.88	0.62	5.67	6.9
Sterna	paradisaea	0.78	0.97	0.92	0.71	6.73	9.61
Phalacrocorax	carbo	3.94	2.19	1.46	1.41	12.63	20.63
Phalacrocorax	bougainvillii	3.84	3.08	4.88	2.49	19.88	21.11
Podiceps	cristatus	2.25	1.71	1.84	2.14	14.42	16.71
Tockus	nasutus	1.06	1.45	1.01	0.99	7.55	11.24
Hirundo	rustica	0.56	0.44	0.45	0	3.57	3.57
Gypaetus	barbatus	6.69	7.25	6.91	4.16	15.51	32.19
Turdus	merula	0.81	1.02	0.95	0.67	7.97	9.04
Eremopterix	leucotis	0.38	0.28	0.23	0.24	3.36	4.32
Elanus	caerulus	1.62	1.75	1.59	1.35	8.1	11.54
Amazona	aestiva	2.08	2.2	2.25	1.96	8.08	11.38
Columba	bollii	1.88	1.94	2.07	2.32	4.77	6.91
Melopsittacus	undulatus	0.96	0.86	0.65	0.65	1.96	3.71
Streptopelia	decaocto	2.03	2.24	2.24	1.65	4.27	5.55

Name		Rib 3 Width of Uncinate at Tip	Rib 4 Width of Uncinate at Tip	Rib 5 Width of Uncinate at Tip	Rib 6 Width of Uncinate at Tip	Rib 2 Length of UCP	Rib 3 Length of UCP
Columba	cayennensis	1.73	1.96	1.96	1.92	7.75	9.12
Corvus	corax	3.15	3.51	2.37	0	16.99	17.45
Passer	domesticus	0.67	0.63	0.38	0.37	4.31	5.14
Apus	apus	0.53	0.7	0.52	0.48	2.56	4.37
Vultur	gryphus	2.71	3.22	3.24	3.18	0	24.06
Chrysococcyx	caprius	0.55	0.55	0.55	0	2.14	4.03
Bubo	bubo	2.06	2.74	2.05	1.29	10.9	14.58
Sturnus	vulgaris	0.76	0.64	0.56	0.48	7.02	7.88
Agapornis	fischeri	0.78	0.72	0.6	0.7	1.97	3.95
Aquila	chrysaetus	4.33	3.74	4.78	5.06	13.49	21.28
Picoides	viridis	1.59	1.36	1.24	0	7.59	8.36
Buceros	bicornis	2.64	3.12	3.3	0	9.29	15.52
Psittacus	erithacus	2.33	2.23	2.4	1.84	1.82	5.95
Falco	rusticolus	1.43	1.9	1.97	2.21	11.43	19.17
Loriculus	galgulus	0.84	0.79	0.98	0.3	1.6	3.45
Chlamydotis	undulata	2.64	3.59	2.67	2.22	10.08	18.8
Phaethornis	yaruqui	0.5	0.38	0.37	0	1.89	1.89
Falco	biarmicus	2.31	1.71	2.36	2.91	6.3	12.5
Chordeiles	acutipennis	0.78	1.19	1.23	0.77	0	5.42
Athene	noctua	1.34	1.17	1.09	0	6.42	9.13
Bubo	ascalaphus	2.08	1.72	1.71	0	6.67	8.83
Agapornis	roseicollis	1.03	1	0.51	0.75	4.22	5.18
Mimus	polyglottos	0.29	0.32	0.25	0.24	3.02	3.38
Oena	capensis	1.03	1.24	1.25	1.05	3.7	3.89
Trichoglossus	haematodus	1.63	1.77	1.6	1.23	2.92	6.89
Chrysolampis	mosquitus	0.4	0.29	0.31	0.31	1.74	2.23
Polytelis	swainsonii	1.37	1.45	1.35	0.57	3.93	5.31
Ramphastos	tucanus	1.75	2.14	1.56	2.3	10.73	12.32
Colius	colius	1.78	1.77	1.86	1.44	4.46	6.2
Trogon	viridis	0.8	0.81	0.92	0	4.47	6.56
Rostratula	semicollaris	1.73	1.96	1.96	1.92	7.75	9.12
Perdix	perdix	1.8	1.92	2.2	1.77	6.5	6.73
Phoenicopterus	rubur	4.25	4.24	3.49	3.01	27.18	29.07
Botaurus	stellaris	2.17	2.02	1.46	1.22	6	4.16

		Rib 3	Rib 4	Rib 5	Rib 6	Rib 2	Rib 3
Name		Width of Uncinate at Tip	Width of Uncinate at Tip	Width of Uncinate at Tip	Width of Uncinate at Tip	Length of UCP	Length of UCP
Francolinus	pondicerianus	1.09	1.3	0.94	0.71	4.4	4.4
Ardea	alba	2.76	2.64	2.74	0	9.55	13.51
Tetraogallus	himalayensis	2.56	3.27	2.86	0	8.26	10.47
Thinocorus	rumicovorus	0.39	0.77	0.82	0.5	4.34	6.38
Aramus	guarauna	0.91	1.55	1.35	0.99	0	5.9
Ixobrychus	minutus	0.73	0.68	0.71	0	1.82	4.07
Leptoptilos	crumeniferus	5.11	6.85	5.9	0	0	17.26
Pterocles	exustus	1.19	1.56	1.44	0.91	3.22	5.13
Sagittarius	serpentarius	2.67	3.21	16.25	13.06	0	14.32
Platalea	leucorodia	1.73	2.01	1.96	0	6.54	12.49
Scolopax	rusticola	1.68	2.1	1.78	2.03	0	4.92
Branta	leucopsis	2.25	1.91	1.78	1.86	5.75	10.83
Cygnus	atratus	5.58	5.66	4.34	4.41	0	15.95
Somateria	mollissima	3.2	3.35	2.81	2.97	9.95	15.57
Anas	falcata	2.28	2.31	2.2	0.82	11.32	12.01
Aythya	marila	3.83	3.18	2.63	2.16	13.9	11.67
Gallinula	chloropus	1.32	1.01	1.04	1.18	8.98	10.97
Anas	acuta	2.9	3.3	3.13	1.53	12.47	12.46
Tadorna	ferruginea	2.14	2.53	1.59	1.42	8.45	10.53
Tadorna	tadorna	2.28	2.44	2.28	2.22	7.23	7.78
Anser	albifrons	3.22	3.66	3.11	3.07	12.79	13.68
Falco	tinnuculus	1.05	1.54	1.59	1.11	5.71	8.68
Tetrao	urogallus	2.04	1.94	2.5	1.3	8.22	10.81
Casuarius	casuarius	0	10.17	8.59	10.52	0	0
Apteryx	haastii	5.07	4.46	5.13	2.55	27.45	25.29
Dinornis	maximus	13.74	13.24	14.3	9.57	40.91	45.34
Struthio	camelus	7	7.3	7.84	0	0	24.83
Phasianus	colchicus	2.66	1.98	1.55	0	4.19	6.59
Geococcyx	californianus	1.91	1.2	0.72	0	3.59	6.63
Eudromia	elegans	1.8	1.64	1.56	0	3.55	5.87
Meleagris	gallopavo	2	2.07	1.32	0	7.31	7.97
Alectoris	rufa	2.21	1.91	1.87	0.83	6.03	7.42

		Rib 4	Rib 5	Rib 6	Rib 2	Rib 3	Rib 4
Name		Length of UCP	Length of UCP	Length of UCP	Dorsal length to Sternal rib	Dorsal length to Sternal rib	Dorsal length to Sternal rib
Fulica	americana	16.26	16.86	18.06	10.49	13.23	14.62
Gavia	arctica	33.89	32.78	25.69	18.39	15.33	17.35
Fulica	atra	18.19	18.61	17.43	16.14	16.86	18.05
Larus	canus	12	9.41	0	13.91	15.82	19.43
Alcedo	atthis	3.96	2.17	0	5.65	6.47	7.7
Mergus	merganser	17.44	19.34	15.62	26.72	24.32	24.87
Spheniscus	demersus	28.58	26.59	29.01	25.12	26.91	28.54
Sterna	hirundo	10.08	8.96	7.32	6.97	7.81	9.83
Pinguinus	impennis	22.63	22.4	23.45	25.03	19.52	24.22
Spheniscus	humboldti	24.55	21.35	10.7	23.95	30.78	35.36
Larus	argentatus	17.38	11.45	0	23.67	30.2	32.81
Alle	alle	12.23	10.39	8.02	13.72	13.08	19.1
Clangula	hyemalis	20.19	19.24	10.13	18.81	22.45	29.56
Gavia	stellata	21.74	16.99	10.88	12.71	13.24	15.95
Pelecanus	rufescens	22.27	6.69	0	35.71	42.81	46.83
Aptenodytes	patagonicus	46.72	41.7	30.8	56.08	55.25	58.2
Fumarus	glacialis	17.53	15.91	12.22	13.69	16.52	20.42
Alca	torda	16.66	15.5	14.1	14.35	13.63	16.15
Aythya	fuligula	14.19	12.36	9.04	17.34	17.43	19.47
Cinclus	cinclus	7.23	6.4	2.4	5.9	5.97	7.9
Sterna	paradisaea	9.6	8.75	6.51	6.05	7.57	9.03
Phalacrocorax	carbo	22.12	21.59	19.11	18.58	17.26	26.03
Phalacrocorax	bougainvillii	19.81	22.33	13.62	26.2	28.06	32.38
Podiceps	cristatus	17.83	14.77	13.99	14.61	15.64	16.57
Tockus	nasutus	9.97	6.21	5.57	9.04	9.54	12.1
Hirundo	rustica	3.81	3.13	0	4.37	4.69	4.92
Gypaetus	barbatus	41.17	40.89	28.99	35.6	32.41	31.67
Turdus	merula	8.53	8.71	4.13	6.52	6.35	8.79
Eremopterix	leucotis	4.33	4.1	2.8	2.74	3.36	4.28
Elanus	caerulus	14.26	13.1	9.57	8.51	12.27	17.52
Amazona	aestiva	11.26	13.67	14.05	7.82	10.91	14.19
Columba	bollii	8.92	9.87	6.68	8.96	7.52	8.53
Melopsittacus	undulatus	4.09	4.3	2.96	3.9	3.41	3.73
Streptopelia	decaocto	7.57	7.87	6.17	8.54	7.99	7.77

		Rib 4	Rib 5	Rib 6	Rib 2	Rib 3	Rib 4
Name		Length of UCP	Length of UCP	Length of UCP	Dorsal length to Sternal rib	Dorsal length to Sternal rib	Dorsal length to Sternal rib
Columba	cayennensis	9.45	9.45	4.86	10.17	9.23	9.32
Corvus	corax	16.87	14.21	0	19.82	25.29	27.61
Passer	domesticus	5.43	4.84	3.46	4.63	5.39	5.6
Apus	apus	4.37	4.84	3.97	4.33	5.46	6.2
Vultur	gryphus	39	33.21	23.24	0	30.88	39.54
Chrysococcyx	caprius	4.11	3.77	0	2.57	4.58	4.94
Bubo	bubo	17.44	17.19	17.16	19.07	17.31	19.59
Sturnus	vulgaris	7.35	4.74	1.79	5.93	6.98	7.1
Agapornis	fischeri	4.76	3.43	1.68	5.35	5.25	5.71
Aquila	chrysaetus	29.19	31.32	27.01	13.99	14.79	22.31
Picoides	viridis	7.14	4.8	0	7.35	10.19	12.86
Buceros	bicornis	13.95	13.64	0	24.78	27.06	34.37
Psittacus	erithacus	8.88	10.34	5.14	10.16	13.74	12.79
Falco	rusticolus	19.62	21.32	20	12.56	12.43	16.29
Loriculus	galgulus	4.6	3.31	1.71	3.09	3.41	4.9
Chlamydotis	undulata	23.34	24.99	17.1	15.27	22.42	21.42
Phaethornis	yaruqui	2.06	2.06	0	2.07	1.68	3.87
Falco	biarmicus	13.06	16.65	15.53	9.75	11.84	12.99
Chordeiles	acutipennis	6.45	7.26	5.08	0	4.68	3.65
Athene	noctua	10.13	8.23	0	3.96	6.9	7.35
Bubo	ascalaphus	11.79	12.58	0	13.11	13.74	15.85
Agapornis	roseicollis	5.17	4.47	1.85	4.44	4.55	5.3
Mimus	polyglottos	2.55	2.25	1.5	2.87	2.73	4.54
Oena	capensis	4.17	4.16	2.88	3.46	4.34	4.21
Trichoglossus	haematodus	8.9	7.52	5.28	7.05	8.37	8.46
Chrysolampis	mosquitus	2.23	2.35	1.82	1.69	1.53	1.82
Polytelis	swainsonii	6.6	6.6	6.8	0	5.43	6.97
Ramphastos	tucanus	11.17	9.54	2.45	11.81	12.91	16.54
Colius	colius	6.35	6.34	4.87	3.79	4.66	4.56
Trogon	viridis	6.54	4.87	0	7.7	6.99	7.59
Rostratula	semicollaris	9.45	9.45	4.86	10.17	9.23	9.32
Perdix	perdix	5.74	5.22	2.52	6.43	10.1	10.15
Phoenicopterus	rubur	29.05	21.37	12.1	22.05	28.29	21.56
Botaurus	stellaris	4.16	4.34	3.6	16.67	21.02	25.91

Name		Rib 4 Length of UCP	Rib 5 Length of UCP	Rib 6 Length of UCP	Rib 2 Dorsal length to Sternal rib	Rib 3 Dorsal length to Sternal rib	Rib 4 Dorsal length to Sternal rib
Francolinus	pondicerianus	4.82	4.62	2.96	5.52	7.24	7.58
Ardea	alba	13.5	9.39	0	28.31	33.99	43.02
Tetraogallus	himalayensis	11.99	10.67	0	19.06	19.3	20.51
Thinocorus	rumicovorus	5.85	6.98	3.69	5.4	4.35	5.93
Aramus	guarauna	9.15	10.63	8	0	13.86	14.56
Ixobrychus	minutus	3.8	1.97	0	9.76	12.54	11.47
Leptoptilos	crumeniferus	20.76	18.8	0	0	63.87	57.32
Pterocles	exustus	7.16	8.77	4.57	7.14	6.42	6.65
Sagittarius	serpentarius	14.84	12.98	11.17	0	22.53	25.55
Platalea	leucorodia	10.58	8.2	0	23.39	18.9	22.98
Scolopax	rusticola	5.99	6.02	7.46	0	6.61	6.64
Branta	leucopsis	11.32	11.06	12.16	16.09	21.89	57.69
Cygnus	atratus	19.58	21.59	19.54	0	39.43	49.96
Somateria	mollissima	14.12	15.15	17	26.83	25.01	25.5
Anas	falcata	9.78	9.49	6.26	12.5	18.06	15.24
Aythya	marila	10.58	12.86	13.05	21.85	20.25	24.05
Gallinula	chloropus	11.43	11.98	11.42	9.01	12.82	13.04
Anas	acuta	12.71	7.99	8.74	24.27	19.88	18.82
Tadorna	ferruginea	9.28	9.78	8.58	16.53	17.2	17.3
Tadorna	tadorna	7.18	10.08	12.87	13.89	19.59	17.87
Anser	albifrons	14.01	13.98	12.01	29.95	29.29	29
Falco	tinnuculus	10.85	11.54	8.47	6.46	5.81	4.71
Tetrao	urogallus	12.11	13.51	10.35	15.51	18.36	20.54
Casuarius	casuarius	15.34	27.32	29.53	0	0	44.18
Apteryx	haastii	29.48	21.89	11.71	21.66	20.27	26.99
Dinornis	maximus	43.8	51.83	47.81	35.77	92.83	106.47
Struthio	camelus	35.41	31.18	0	0	58.79	91.05
Phasianus	colchicus	7.46	7.85	0	5.16	7.94	7.69
Geococcyx	californianus	6.49	3.97	0	10.59	13.3	11.91
Eudromia	elegans	7.3	6.94	0	3.99	4.01	6.39
Meleagris	gallopavo	8.18	5.09	0	9.75	10.19	8.86
Alectoris	rufa	7.27	7.3	5.28	0	10.09	12.83

Name		Rib 5 Dorsal length to Sternal rib	Rib 6 Dorsal length to Sternal rib	Rib 2 Total Length of Dorsal Rib	Rib 3 Total Length of Dorsal Rib
Fulica	americana	17.81	19.35	32.04	36.97
Gavia	arctica	22.24	28.73	74.05	75.9
Fulica	atra	18.66	22.63	40.43	45.01
Larus	canus	20.69	0	38.68	39
Alcedo	atthis	8.55	0	16.63	18.73
Mergus	merganser	28.93	37.28	62.17	62.17
Spheniscus	demersus	34.32	41.79	76.48	84.22
Sterna	hirundo	11.42	12.57	26.27	28.01
Pinguinus	impennis	32.98	43.76	58.75	60.03
Spheniscus	humboldti	43.07	52.42	75.35	83.5
Larus	argentatus	35.26	0	63.75	67.17
Alle	alle	22.86	27.41	35.01	36.49
Clangula	hyemalis	34.98	45.21	52.1	56.06
Gavia	stellata	22.01	27.83	54.72	55.99
Pelecanus	rufescens	51.46	0	108.65	112.17
Aptenodytes	patagonicus	69.55	85.84	141.05	146.8
Fumarus	glacialis	23.4	23.16	45.43	50.2
Alca	torda	21.32	28.68	45.89	49.1
Aythya	fuligula	21.34	27.35	41.87	42.94
Cinclus	cinclus	8.66	8.98	18.65	20.42
Sterna	paradisaea	12.05	14.52	23.55	24.99
Phalacrocorax	carbo	26.87	31.11	56.18	58.09
Phalacrocorax	bougainvillii	25.6	34.56	68.18	70.66
Podiceps	cristatus	10.76	16.35	45.26	47.97
Tockus	nasutus	12.17	15	27.78	29.2
Hirundo	rustica	5.68	0	11.85	12.53
Gypaetus	barbatus	38.45	53.75	90.31	92.47
Turdus	merula	9.52	13.15	20.05	20.95
Eremopterix	leucotis	5.19	6.05	9.48	10.56
Elanus	caerulus	19.68	23.81	27.59	25.79
Amazona	aestiva	15.38	16.93	28.58	33.51
Columba	bollii	10.39	10.77	24.46	25.98
Melopsittacus	undulatus	5.79	7.83	12.44	13.2
Streptopelia	decaocto	7.54	9.39	21.1	23.51

Name		Rib 5 Dorsal length to Sternal rib	Rib 6 Dorsal length to Sternal rib	Rib 2 Total Length of Dorsal Rib	Rib 3 Total Length of Dorsal Rib
Columba	cayennensis	10.5	13.66	27.55	28.26
Corvus	corax	33.05	0	55.26	59.34
Passer	domesticus	5.97	7.15	12.36	14.37
Apus	apus	7.63	9.61	12.52	14.83
Vultur	gryphus	55.81	71.67	82.68	91.17
Chrysococcyx	caprius	5.23	0	10.4	13.6
Bubo	bubo	23.38	28.02	37.95	41.86
Sturnus	vulgaris	8.65	10.44	18.05	19.94
Agapornis	fischeri	6.86	8.07	14.67	15.22
Aquila	chrysaetus	22.65	28.82	55.01	59.29
Picoides	viridis	15.79	0	21.16	25.96
Buceros	bicornis	40.83	0	69	75.13
Psittacus	erithacus	15.77	22.05	33.6	39.51
Falco	rusticolus	19.78	25.49	44.57	49.95
Loriculus	galgulus	6.11	6.37	10.9	13.14
Chlamydotis	undulata	28.73	33.15	53.8	60.58
Phaethornis	yaruqui	5.1	0	8.36	8.82
Falco	biarmicus	15.55	16.98	36.58	38.59
Chordeiles	acutipennis	4.02	8.92	7.07	14.57
Athene	noctua	9.38	0	21.9	24.85
Bubo	ascalaphus	20.25	0	46.28	51.28
Agapornis	roseicollis	6.69	7.86	15.03	15.93
Mimus	polyglottos	5.85	7.42	8.46	8.61
Oena	capensis	5.03	6.51	11.98	14.73
Trichoglossus	haematodus	10.04	14.76	20.7	22.63
Chrysolampis	mosquitus	2.29	2.57	7.01	7.51
Polytelis	swainsonii	7.9	8.79	22.17	24.98
Ramphastos	tucanus	16.88	24.61	34.92	34.93
Colius	colius	5.74	9.34	14.04	15.95
Trogon	viridis	9.84	0	21.14	22.42
Rostratula	semicollaris	10.5	13.66	27.55	28.26
Perdix	perdix	11.49	12.55	19.64	22.59
Phoenicopterus	rubur	33.91	39.15	76.07	80.15
Botaurus	stellaris	30.4	0	58.42	64.79

Name		Rib 5 Dorsal length to Sternal rib	Rib 6 Dorsal length to Sternal rib	Rib 2 Total Length of Dorsal Rib	Rib 3 Total Length of Dorsal Rib
Francolinus	pondicerianus	7.63	7.93	15.72	18.1
Ardea	alba	48.61	0	68.95	73.27
Tetraogallus	himalayensis	20.95	0	47	48.66
Thinocorus	rumicovorus	6.55	8.74	16.57	17.56
Aramus	guarauna	18.47	24.9	38.84	41.38
Ixobrychus	minutus	18.53	0	26.61	31.05
Leptoptilos	crumeniferus	74.8	0	111.94	111.4
Pterocles	exustus	7.54	8.09	21.98	22.11
Sagittarius	serpentarius	33.06	38.47	56.87	68.38
Platalea	leucorodia	31.12	0	54.52	53.05
Scolopax	rusticola	14.34	13.81	24.06	25.08
Branta	leucopsis	26.96	31.61	52.9	58.73
Cygnus	atratus	58.25	70.07	95.51	101.48
Somateria	mollissima	29.55	36.83	62.49	62.49
Anas	falcata	20.55	20.18	41.51	42.26
Aythya	marila	27.84	34.54	47.1	49.86
Gallinula	chloropus	14.8	19.15	27.33	32.48
Anas	acuta	24.47	26.76	49.49	46.08
Tadorna	ferruginea	20.31	25.12	41.02	45.06
Tadorna	tadorna	21.11	27.59	41.56	48.93
Anser	albifrons	37.78	41.56	64.94	66.6
Falco	tinnuculus	7.01	7.83	21.58	23.29
Tetrao	urogallus	23.25	17.82	39.85	47.26
Casuarius	casuarius	38.28	45.25	103.24	133.52
Apteryx	haastii	30.3	39.63	57.15	61.18
Dinornis	maximus	134.35	146.62	159.83	223.58
Struthio	camelus	96.39	0	173.71	239.7
Phasianus	colchicus	8.2	0	22.37	26.4
Geococcyx	californianus	12.16	0	23.17	31.1
Eudromia	elegans	5.07	0	23.83	24.94
Meleagris	gallopavo	8.82	0	30.06	33.12
Alectoris	rufa	12.84	14.11	27.07	28.97

		Rib 4	Rib 5	Rib 6	Rib 2
Name		Total Length of Dorsal Rib	Total Length of Dorsal Rib	Total Length of Dorsal Rib	Total Length of Sternal Rib
Fulica	americana	39.67	43.41	45.72	14.96
Gavia	arctica	80.11	88.15	92.34	23.57
Fulica	atra	49.36	52.77	55.04	13.42
Larus	canus	40.96	43.36	45.41	12.73
Alcedo	atthis	19.29	19.26	19.71	8.89
Mergus	merganser	61.3	63.61	65.95	0
Spheniscus	demersus	86.59	92.83	99	0
Sterna	hirundo	29.28	30.04	30.04	7.52
Pinguinus	impennis	66.83	78.2	87.08	23.88
Spheniscus	humboldti	87.35	92.6	95.86	25.54
Larus	argentatus	68.21	69.04	69.1	19.82
Alle	alle	41.6	44.54	48.55	18.64
Clangula	hyemalis	60.56	63.22	68.87	22.5
Gavia	stellata	57.88	61.01	62.33	19.11
Pelecanus	rufescens	111.06	112.41	112.04	25.33
Aptenodytes	patagonicus	151.08	158.56	166.96	41.57
Fumarus	glacialis	53.32	55.66	55.7	13.8
Alca	torda	52.75	58.86	65.16	19.46
Aythya	fuligula	45.76	47.63	48.9	13.47
Cinclus	cinclus	22.84	23.6	21.75	4.76
Sterna	paradisaea	25.97	27.22	29.09	7.75
Phalacrocorax	carbo	66.26	66.24	67.93	0
Phalacrocorax	bougainvillii	71.43	68.89	73.76	29.4
Podiceps	cristatus	50.35	46.29	49.15	11.74
Tockus	nasutus	31.31	32.09	34.5	10.01
Hirundo	rustica	13.14	13.69	14.31	3.26
Gypaetus	barbatus	93.6	97.03	105.58	17.27
Turdus	merula	23.39	24.5	26.16	7.15
Eremopterix	leucotis	11.54	12.27	13.13	3.11
Elanus	caerulus	29.14	29.13	32.14	8.73
Amazona	aestiva	35.68	37.33	39.87	0
Columba	bollii	28.99	30.88	31.24	0
Melopsittacus	undulatus	13.53	15.94	17.51	0
Streptopelia	decaocto	25	24.22	26.07	4.48

		Rib 4	Rib 5	Rib 6	Rib 2
Name		Total Length of Dorsal Rib	Total Length of Dorsal Rib	Total Length of Dorsal Rib	Total Length of Sternal Rib
Columba	cayennensis	29.77	29.77	30.57	5.57
Corvus	corax	60.67	64.19	67.76	18.66
Passer	domesticus	14.37	14.52	15.2	2.8
Apus	apus	16.14	17.68	19.42	6.42
Vultur	gryphus	102.71	115.35	121.54	27.92
Chrysococcyx	caprius	13.61	13.59	13.06	0
Bubo	bubo	43.38	43.36	43.63	14.6
Sturnus	vulgaris	20.26	21.05	21.86	6.35
Agapornis	fischeri	15.68	15.89	16.83	4.12
Aquila	chrysaetus	59.25	62	63.45	17.1
Picoides	viridis	28.55	30.22	31.59	10.58
Buceros	bicornis	80.39	81.87	86.6	22.22
Psittacus	erithacus	42.11	43.08	46.01	0
Falco	rusticolus	55.66	57.39	59.31	0
Loriculus	galgulus	14.9	15.7	14.96	0
Chlamydotis	undulata	58.54	66.18	71.85	0
Phaethornis	yaruqui	10.48	11.72	11.82	3.74
Falco	biarmicus	40.42	40.98	42.47	11.52
Chordeiles	acutipennis	15.24	16.14	20.34	0
Athene	noctua	25.4	27.16	29.61	9.8
Bubo	ascalaphus	54.55	58.99	61.91	16.79
Agapornis	roseicollis	16.68	17.82	19.28	4.93
Mimus	polyglottos	10.27	11.23	11.63	2.43
Oena	capensis	14.6	15.42	16.03	1.58
Trichoglossus	haematodus	23.81	25.39	28.12	0
Chrysolampis	mosquitus	8.31	8.97	9.56	2.82
Polytelis	swainsonii	26.92	27.27	29.14	0
Ramphastos	tucanus	39.33	40.88	45.01	12.56
Colius	colius	16.83	18.29	19.25	0
Trogon	viridis	24.18	26.07	26.42	6.56
Rostratula	semicollaris	29.77	29.77	30.57	5.57
Perdix	perdix	23.83	24.86	25.4	0
Phoenicopterus	rubur	76.17	80.4	81.34	16.61
Botaurus	stellaris	70.02	73.13	73.62	24.84

		Rib 4	Rib 5	Rib 6	Rib 2
Name		Total Length of Dorsal Rib	Total Length of Dorsal Rib	Total Length of Dorsal Rib	Total Length of Sternal Rib
Francolinus	pondicerianus	19.25	20.28	20.26	0
Ardea	alba	79.4	84.41	89.86	11.69
Tetraogallus	himalayensis	50.48	51.1	53.55	0
Thinocorus	rumicovorus	19.36	21.22	22.65	4.72
Aramus	guarauna	44.77	48.78	54.32	10.55
Ixobrychus	minutus	31.66	34.05	0	0
Leptoptilos	crumeniferus	113.64	126.08	133.52	20.29
Pterocles	exustus	23.13	23.63	23.39	7.87
Sagittarius	serpentarius	72.9	74.09	75.93	13.6
Platalea	leucorodia	57.34	61.42	69.35	13.9
Scolopax	rusticola	26.3	29.85	29.84	11.29
Branta	leucopsis	61.77	61.77	62.83	8.68
Cygnus	atratus	113.32	116.66	120.2	24.45
Somateria	mollissima	65.1	70.05	73.06	0
Anas	falcata	47.88	46.86	49.53	13.38
Aythya	marila	52.87	55.36	59.94	0
Gallinula	chloropus	34.45	35.84	39.29	12.72
Anas	acuta	48.72	48.8	50.3	11.01
Tadorna	ferruginea	46.2	48.09	50.67	10.8
Tadorna	tadorna	48.88	48.71	54.42	0
Anser	albifrons	64.11	70.2	71.09	16.65
Falco	tinnuculus	22.6	24.62	26.35	8.04
Tetrao	urogallus	52.46	57.74	54.76	0
Casuarius	casuarius	146.8	143.78	141.41	0
Apteryx	haastii	67.9	70.87	74.97	20.6
Dinornis	maximus	259	297.5	318.74	0
Struthio	camelus	273.8	266.06	253.64	0
Phasianus	colchicus	26.94	28.41	28.41	0
Geococcyx	californianus	33.18	34.57	35.21	0
Eudromia	elegans	27.48	27.02	28.01	14.98
Meleagris	gallopavo	33.9	34.65	32.97	13.62
Alectoris	rufa	30.51	31.76	34.5	0

		Rib 3	Rib 4	Rib 5	Rib 6
Name		Total Length of Sternal Rib	Total Length of Sternal Rib	Total Length of Sternal Rib	Total Length of Sternal Rib
Fulica	americana	14.07	17.76	21.98	26.26
Gavia	arctica	30.91	37.15	67.74	78.9
Fulica	atra	17.39	23.44	29.86	35.4
Larus	canus	16.86	20.59	26.02	32.86
Alcedo	atthis	11	12.94	13.47	13.51
Mergus	merganser	19.73	24.72	33.86	41.41
Spheniscus	demersus	29.22	33.85	58.89	70.87
Sterna	hirundo	9.34	11.7	14.6	18.34
Pinguinus	impennis	32.93	42.68	58.6	69.95
Spheniscus	humboldti	34.69	43.05	55.69	68.29
Larus	argentatus	25.57	30.77	37.42	48.27
Alle	alle	24.37	30.15	37.23	43.82
Clangula	hyemalis	30.3	39.66	50.9	59.66
Gavia	stellata	26.77	33.99	45.73	57.23
Pelecanus	rufescens	36.87	49.94	67.56	85.07
Aptenodytes	patagonicus	56.97	76.31	96.22	119.27
Fumarus	glacialis	15.4	20.1	28.06	37.51
Alca	torda	24.64	32.9	41.16	50.92
Aythya	fuligula	16.49	22.24	27.89	35.13
Cinclus	cinclus	6.78	9.6	11.59	13.29
Sterna	paradisaea	10.23	13.37	17.64	22.37
Phalacrocorax	carbo	0	34.32	45.91	54.71
Phalacrocorax	bougainvillii	41.95	53.3	64.03	72.89
Podiceps	cristatus	16.47	19.58	35.08	45.58
Tockus	nasutus	14.04	18.68	20.56	13.35
Hirundo	rustica	4.66	5.89	7.89	9.5
Gypaetus	barbatus	24.86	32.33	38.89	47.58
Turdus	merula	9.35	11.45	13.03	15.62
Eremopterix	leucotis	4.2	4.84	5.71	5.7
Elanus	caerulus	10.62	16.13	20.19	25.98
Amazona	aestiva	12.15	15.65	20.03	23.98
Columba	bollii	8.14	10.65	15.89	18.77
Melopsittacus	undulatus	5.55	7.48	9.28	10.53
Streptopelia	decaocto	7.98	10.38	13.9	18.06

Name		Rib 3 Total Length of Sternal Rib	Rib 4 Total Length of Sternal Rib	Rib 5 Total Length of Sternal Rib	Rib 6 Total Length of Sternal Rib
Columba	cayennensis	11.18	14.58	18.9	22.67
Corvus	corax	25.12	31.14	36.05	36.11
Passer	domesticus	5.21	6.85	8.15	10.03
Apus	apus	7.98	9.75	12.18	14.82
Vultur	gryphus	27.92	32.58	34.95	45.61
Chrysococcyx	caprius	4.7	6.56	8.96	11.83
Bubo	bubo	24.55	31.77	38.05	46.85
Sturnus	vulgaris	7.63	11.14	13.17	15.29
Agapornis	fischeri	6.39	7.56	8.89	9.99
Aquila	chrysaetus	23.91	28.76	39.49	45.31
Picoides	viridis	13.81	18.21	22.83	22.76
Buceros	bicornis	30.52	40.68	53.52	42.61
Psittacus	erithacus	10.21	13.84	17.08	20.1
Falco	rusticolus	18.88	24.18	27.78	33.07
Loriculus	galgulus	5.41	6.4	7.9	10.89
Chlamydotis	undulata	21.61	27.18	30.53	37.59
Phaethornis	yaruqui	4.27	6.07	6.91	8.02
Falco	biarmicus	15.2	20.05	23.77	26.62
Chordeiles	acutipennis	0	6.37	7.83	15.84
Athene	noctua	12.69	15.67	18.68	20.94
Bubo	ascalaphus	19.97	27.65	33.01	36.52
Agapornis	roseicollis	6.06	8.05	9.46	10.7
Mimus	polyglottos	4.15	4.92	5.4	6.44
Oena	capensis	2.79	6.37	9.12	11.84
Trichoglossus	haematodus	8.05	11.04	14.01	16.09
Chrysolampis	mosquitus	3.2	3.55	4.07	4.99
Polytelis	swainsonii	8.19	10.24	11.91	15.9
Ramphastos	tucanus	16.4	22.7	26.85	30.63
Colius	colius	6.26	7.77	11.25	13.39
Trogon	viridis	8.66	10.8	12.47	7.14
Rostratula	semicollaris	11.18	14.58	18.9	22.67
Perdix	perdix	11.85	16.84	21.14	24.82
Phoenicopterus	rubur	25.08	34.5	49.86	58.3
Botaurus	stellaris	33.61	42.68	52.9	43.75

		Rib 3	Rib 4	Rib 5	Rib 6
Name		Total Length of Sternal Rib	Total Length of Sternal Rib	Total Length of Sternal Rib	Total Length of Sternal Rib
Francolinus	pondicerianus	9.49	14.31	19.02	20.91
Ardea	alba	20.24	24.19	32.28	45.35
Tetraogallus	himalayensis	0	0	0	0
Thinocorus	rumicovorus	5.62	8.17	11.59	14.34
Aramus	guarauna	15.54	20.75	25.74	30.23
Ixobrychus	minutus	10.98	13.81	14.02	0
Leptoptilos	crumeniferus	26.53	37.82	45.15	62.22
Pterocles	exustus	10.51	13.36	16.75	21.76
Sagittarius	serpentarius	22.92	27.76	33.7	41.61
Platalea	leucorodia	17.22	21.92	27.42	35.61
Scolopax	rusticola	13.82	13.34	15.68	18.89
Branta	leucopsis	13.85	19.6	23.15	41.25
Cygnus	atratus	30.66	49.26	63.5	79.08
Somateria	mollissima	43.8	51.06	55.82	57.07
Anas	falcata	16.47	22.52	24.84	33.87
Aythya	marila	17.28	22.53	29.33	37.84
Gallinula	chloropus	15.22	17.89	20.51	23.11
Anas	acuta	14.82	19.78	23.72	29.46
Tadorna	ferruginea	13.47	17.33	22.62	27.52
Tadorna	tadorna	9.42	13.22	16.51	23.2
Anser	albifrons	19.28	25.75	34.13	41.95
Falco	tinnuculus	12.09	13.12	15.26	17.53
Tetrao	urogallus	14.83	24.59	33.38	42.22
Casuarius	casuarius	0	81.04	98.51	126.56
Apteryx	haastii	25.75	32.7	38.78	0
Dinornis	maximus	76.18	113.78	143.4	152.85
Struthio	camelus	84.08	119.41	158.23	191.93
Phasianus	colchicus	10.98	19.74	24.08	25.23
Geococcyx	californianus	15.58	19.25	24.63	16.86
Eudromia	elegans	20.84	25.81	29.63	0
Meleagris	gallopavo	19.64	25.61	32.18	20.16
Alectoris	rufa	13.02	15.96	19.15	20.38

Name		Sternum Width at Widest Point	Sternum Length at Longest Point	Sternum Depth	Length of Vertebral Column
Fulica	americana	23.37	46.92	21.73	54.49
Gavia	arctica	83.73	187.95	46.77	115.57
Fulica	atra	23.58	57.92	24.43	65.87
Larus	canus	28.81	50.73	27.4	43.06
Alcedo	atthis	12.17	25.94	10.03	17.68
Mergus	merganser	53.11	116.25	21.82	93.18
Spheniscus	demersus	66.4	119.83	44.36	101.93
Sterna	hirundo	16.98	34.43	20.61	33.77
Pinguinus	impennis	39.03	115.09	39.77	81.54
Spheniscus	humboldti	36.83	119.42	40.47	93.21
Larus	argentatus	40.83	67.05	36.66	53.24
Alle	alle	20	56.64	22.9	39.49
Clangula	hyemalis	41.72	98.85	25.21	50.62
Gavia	stellata	56.18	140.82	30.78	81.61
Pelecanus	rufescens	85.05	86.4	58.85	106.65
Aptenodytes	patagonicus	106.95	229.86	62.55	185.31
Fumarus	glacialis	42.39	45.8	32.33	68.73
Alca	torda	34.29	99.04	33.06	73.67
Aythya	fuligula	36.49	63.72	21.31	50.98
Cinclus	cinclus	14.61	25.53	10.36	23.77
Sterna	paradisaea	16.63	32.82	18.75	33.13
Phalacrocorax	carbo	51.82	75.03	27.99	90.27
Phalacrocorax	bougainvillii	56.42	98.41	34.2	92.9
Podiceps	cristatus	38.5	61.69	26.15	67.96
Tockus	nasutus	19.72	36.79	15.21	40.83
Hirundo	rustica	9.75	15.71	6.71	13.69
Gypaetus	barbatus	87.66	111.8	55.7	108.85
Turdus	merula	16.04	29.24	14.15	27.25
Eremopterix	leucotis	7.63	9.84	4.2	11.93
Elanus	caerulus	26.17	38.43	20.65	42.95
Amazona	aestiva	26.17	64.91	28.42	51.75
Columba	bollii	27.35	58.15	31.12	38.77
Melopsittacus	undulatus	10.97	29.41	15.17	22
Streptopelia	decaocto	21.17	52.12	27.56	35.15

Name		Sternum Width at Widest Point	Sternum Length at Longest Point	Sternum Depth	Length of Vertebral Column
Columba	cayennensis	24.7	58.16	31.57	42.44
Corvus	corax	41.68	69.79	30.04	60.04
Passer	domesticus	11.23	18.21	9.22	18.97
Apus	apus	9.79	26.2	15.65	18.28
Vultur	gryphus	72.18	127.97	69.97	152.83
Chrysococcyx	caprius	8.79	14.84	8.19	20.16
Bubo	bubo	45.14	78.23	38.83	80.45
Sturnus	vulgaris	15.5	29.7	13.08	25.32
Agapornis	fischeri	11.43	31.07	13.63	20.1
Aquila	chrysaetus	57.97	104.09	48.58	105.98
Picoides	viridis	15.89	39.56	17.54	36.23
Buceros	bicornis	53.32	106.07	42.71	122.22
Psittacus	erithacus	27.83	65.98	26.74	55.51
Falco	rusticolus	47.69	81.22	34.21	77.69
Loriculus	galgulus	10.29	24.37	11.67	21.27
Chlamydotis	undulata	51.16	91.68	47.27	73.04
Phaethornis	yaruqui	5.24	14.86	10.55	11.24
Falco	biarmicus	33.88	73.7	38.28	75.12
Chordeiles	acutipennis	14.1	22.89	13.61	18.29
Athene	noctua	18.53	27.25	10.94	29.96
Bubo	ascalaphus	38.74	53.87	33	67.93
Agapornis	roseicollis	14.27	32.15	14.21	21.02
Mimus	polyglottos	6.82	12.79	6.01	11.37
Oena	capensis	12.9	29.27	18.28	22.68
Trichoglossus	haematodus	17.59	45.16	23.83	37.57
Chrysolampis	mosquitus	4.16	15.3	10.63	9.94
Polytelis	swainsonii	18.42	45.61	21.12	32.08
Ramphastos	tucanus	21.3	44.51	15.23	51.69
Colius	colius	12.18	24.82	8.95	23.43
Trogon	viridis	18.89	27.33	14.86	22.15
Rostratula	semicollaris	24.7	58.16	31.57	42.44
Perdix	perdix	48.23	20.09	37.08	40.39
Phoenicopterus	rubur	57.06	109.76	64.6	139.03
Botaurus	stellaris	31.07	69.34	29.56	104.15

Name		Sternum Width at Widest Point	Sternum Length at Longest Point	Sternum Depth	Length of Vertebral Column
Francolinus	pondicerianus	16.11	42.49	27.95	28.95
Ardea	alba	50.05	88.29	50.96	90.91
Tetraogallus	himalayensis	36.87	74.31	59.58	61.12
Thinocorus	rumicovorus	15.65	31.24	20.38	25.67
Aramus	guarauna	26.69	72.24	26.36	85.26
Ixobrychus	minutus	12.95	29.9	14.09	47.9
Leptoptilos	crumeniferus	79.97	87.89	109.68	163.83
Pterocles	exustus	19.4	57.91	33.66	36.73
Sagittarius	serpentarius	49.23	103.07	50.98	100.54
Platalea	leucorodia	46.43	83.69	38.41	101.67
Scolopax	rusticola	24.08	58.43	30.72	42.61
Branta	leucopsis	52.49	122.14	46.48	88.92
Cygnus	atratus	76.21	191.51	63.84	164.4
Somateria	mollissima	57.84	102.34	34.62	92.82
Anas	falcata	36.67	92.79	27.55	66.71
Aythya	marila	47.16	81.98	26.35	74.96
Gallinula	chloropus	15.64	40.6	16.8	55.41
Anas	acuta	39.1	94.98	25.69	84.32
Tadorna	ferruginea	41.09	88.06	27.64	76.11
Tadorna	tadorna	44.61	88.19	28.07	76.35
Anser	albifrons	56.79	125.99	48.39	97.96
Falco	tinnuculus	23.93	54.23	19.15	39.19
Tetrao	urogallus	104.77	39.67	58.97	65.99
Casuarius	casuarius	208.07	125.37	0	333.05
Apteryx	haastii	30.13	46.3	0	104.26
Dinornis	maximus	98.22	122.82	0	587.7
Struthio	camelus	207.37	218.45	0	426.62
Phasianus	colchicus	70.32	21	37.73	46.46
Geococcyx	californianus	23.13	32.28	11.45	48.49
Eudromia	elegans	20.26	83.98	0	53.07
Meleagris	gallopavo	40.33	26.76	48.91	58.23
Alectoris	rufa	43.97	73.08	18.54	41.71

Chapter 3

Ontogenetic development of the uncinate processes in the domestic turkey (*Meleagris gallopavo*)

This chapter is as a reprint of an article published in *Poultry Science:*

Tickle, P. G. and Codd, J. R. (2009) Ontogenetic development of the uncinate processes in the domestic turkey (*Meleagris gallopavo*). *Poultry Sci.*, **88**, 179-184.

Ontogenetic development of the uncinate processes in the domestic turkey (*Meleagris gallopavo*)

P. G. Tickle and J. R. Codd[1]

Faculty of Life Sciences, University of Manchester, Manchester, United Kingdom

ABSTRACT Uncinate processes extend off the vertebral ribs in most species of bird. The processes are a crucial component of ventilatory mechanics, being involved in inspiration and expiration. Here we examine the pattern of ossification of the uncinate processes using histochemistry and biomechanical testing in developing domestic turkeys (*Meleagris gallopavo*). Ossification begins just before hatching, and the processes are fully ossified in the adult bird. We suggest that the development of these processes is linked to the onset of air breathing and the increase in sternal mass that occurs after hatching.

Key words: uncinate process, galliform, ontogeny, ossification

2009 Poultry Science 88:179–184
doi:10.3382/ps.2008-00349

INTRODUCTION

Birds and mammals are the only vertebrates capable of very high rates of oxygen consumption relative to body mass. However, whereas the mechanics of breathing are well-documented for mammals, our understanding of how the avian lung is ventilated is comparatively poor. The avian respiratory system is composed of a set of rigidly fixed lungs and series of approximately 9 air sacs. The bellows-like action of the air sacs and the unidirectional passage of air through the lungs are facilitated by movements of the ribs and sternum during ventilation (Claessens, 2004). Developmental studies of the avian respiratory system are often focused on the structure and function of the parabronchial lung and air sac system (Duncker, 1978; Maina 2003a,b, 2006). The main site of gas exchange for the avian embryo is the chorioallantois, a membrane that adheres to the inner membrane of the shell and permits diffusion of oxygen and carbon dioxide between the blood and environment (Wangensteen and Rahn, 1970/71; Tullett and Deeming, 1982). As incubation progresses, an air cell forms in the blunted end of the egg through water loss across the membranes. During the period around 24 to 48 h before hatching, the embryo pips internally and begins to use pulmonary ventilation in addition to the chorioallantoic membrane for gas exchange. The relative contribution of the chorioallantoic membrane to respiration decreases rapidly after external pipping. Upon hatching, movements of the skeleton fulfill respiratory requirements by pumping air around the air sacs (Menna and Mortola, 2002).

Uncinate processes (**UP**) are bony projections that extend off the posterior edge of the vertebral ribs in most species of extant birds. Although UP were previously thought to be adaptations for flight (Welty, 1988) or to strengthen the ribs and rib cage (Kardong, 1988), these processes have recently been demonstrated to be integral components of the ventilatory mechanics of birds. The UP are involved in both ventilation and running locomotion in the giant Canada goose (Codd et al., 2005). The appendicocostales muscle originates from the caudal surface of the processes and facilitates cranial and ventral movements of the ribs and sternum, respectively, during inspiration. The UP also act as a brace for the externus obliquus abdominus that inserts onto the base of the processes and pulls the sternum dorsally during expiration (Codd et al., 2005). Geometric modeling of the rib cage demonstrated that the UP function as levers for the forward movement of the ribs and ventral rotation of the sternum during respiration (Tickle et al., 2007). Given the lever action of the processes on the ribs and sternum, changes in length will have a significant functional impact. For example, a longer process provides a greater surface area for muscle attachment and a greater mechanical advantage for movements of the ribs and sternum (Tickle et al., 2007).

The avian pattern of skeletal development is typical of amniotes. A cartilaginous skeleton is subsequently replaced by bone mineralisation. The majority of developmental studies have focused on the sequence of ossification in galliform birds, such as the domestic chick-

---

©2009 Poultry Science Association Inc.

Received August 14, 2008.
Accepted September 23, 2008.

[1] Corresponding author: jonathan.codd@manchester.ac.uk

en (*Gallus gallus*) and the Japanese quail (*Coturnix coturnix*). Fell (1925) undertook the first detailed investigation of histogenesis of bone and cartilage in the developing fowl, and subsequent research has tended to focus on the long bones (e.g., Simmons and Pankovich, 1963; Blom and Lilja, 2004). An understanding of the skeletal changes during ontogeny has been used to model avian growth (Starck, 1994) and to examine the significance of developmental patterns in phylogenetics (Burke and Feduccia, 1997). However, existing research into the ontogeny of skeletal development in birds provides sparse information on the chondrification and ossification of UP. Recent comparative analyses of the embryonic skeleton in galliform birds suggest that although ossification of the UP occurs in the quail (Nakane and Tsudzuki, 1999) and the chicken (Hogg, 1980), it is absent in stage 40+ turkeys (Maxwell, 2008). Hogg (1980) highlighted the uncertainty surrounding the sequence of UP ossification in the chicken embryo; onset of bone growth has been reported from as early as d 17 (Fujioka, 1952) to as late as posthatch (Hamilton, 1952). Here we examine the pattern of ossification of the UP in the developing domestic turkey using histochemical and biomechanical techniques.

MATERIALS AND METHODS

Eggs of the domestic turkey (*Meleagris gallopavo*) were purchased from a licensed breeder and placed in an incubator (Ova-Easy 190; Brinsea Products Ltd., Sandford, UK) within 1 wk of laying. Eggs were incubated for 28 d. Temperature and humidity during the initial 25 d of incubation were maintained at 37.5ºC and 50%, respectively. For the remainder of incubation humidity was increased to 65%. Eggs were turned every hour until d 25 of incubation, whereupon eggs were left undisturbed to hatch. Before hatching, embryos were culled by rapid freezing to −40°C daily from d 14 of incubation to d 28. After hatching, chicks were transferred to a brooder and given access to food (chick crumbs) and water ad libitum. Single samples for histochemical analysis were taken daily from d 29 to 35. Birds were also culled on d 42, 49, 56, 63, and 94. Posthatch birds were culled by dislocation of the cervical vertebrae. Single samples for mechanical testing were taken on d 25 and 94. Birds were frozen immediately after death for future processing.

Dissection and Histochemistry Protocol

At d 25 and 94, two specimens were taken, one for histochemical analysis and the other for biomechanical testing. At all remaining time points, one sample was collected for histochemistry. Birds were skinned and eviscerated, and the superficial thoracic musculature was carefully removed to expose the ribcage. Prepared specimens were stained for bone and cartilage according to a protocol adapted from the mouse method of Miller and Tarpley (1996). Samples were fixed in 90% ethanol for 24 h before immersion in Alcian blue solution (Acros Organics, Geel, Belgium; uptake corresponds to the presence of cartilage) for 72 h. Skeletons were then rehydrated in a series of ethanol solutions (70, 40, and 15%, respectively) for 2 h and finally rinsed in distilled water. Remaining muscle tissue was then macerated by exposure to 1% KOH solution for 24 to 48 h. Skeletons were then transferred to a solution of Alizarin red (Sigma-Aldrich, St. Louis, MO; to indicate the presence of bone) for 72 h followed by repeat exposure to 1% KOH as required. Stained skeletons were passed through a series of glycerol solutions (20, 50, and 80%, respectively) and stored in 100% glycerol. All stages of the staining protocol were conducted at room temperature (22°C).

The UP are numbered from the anterior end of the skeleton, according to the vertebral rib from which they project (i.e., the most cranial rib is rib 1, UP 1). Stained skeletons were then examined for the presence of bone and cartilage using a Leica MZ9s light microscope (Leica Microsystems, Milton Keynes, UK). Digital photographs of the ribcage and UP were then taken and analyzed using the Leica Application Suite Software. The most anterior and posterior UP are typically reduced in morphology, whereas the UP on the remaining ribs are uniform in size (Tickle et al., 2007). For comparative analyses, the relative area of bone and cartilage was calculated for the UP that extends from the fourth vertebral rib in all specimens. Areas of blue and red stain were measured and then calculated as a percentage of the total process area.

Mechanical Testing

Nanoindentation was used to calculate the elastic modulus at the base of the UP. Using the data collected from the rib histochemistry, vertebral rib 4 was dissected from the right-hand side of representative specimens obtained on d 25 and 94. Specimens were dehydrated in 95% ethanol for 24 h before embedding in a noninfiltrating polyester resin (Kleer set; Metprep Ltd., Coventry, UK). To ensure accurate calculation of mechanical properties, surface topography of the samples was imaged by atomic force microscopy, enabling the selection of relatively smooth areas for indentation. A TriboScope (Hysitron Inc., Minneapolis, MN) nanomechanical system was then used for material testing. Nanoindents were made using a maximal loading force of 5,000 μN applied via a tetrahedral diamond Berkovich indenter tip. The indenter detects force and displacement to form a nanoindentation curve. This curve consists of a loading phase (the tip is pressed into the material up to a maximal force), holding period (the tip creeps into the material), and an unloading phase (force on the sample is released; Hengsberger et al., 2001). The unloading force-displacement curve was then used to calculate reduced modulus using the equations of Oliver and Pharr (1992, 2004). Calculation of the elastic moduli assumed the Berkovich tip with an elastic modulus of 1,140 GPa and Poisson ratio of 0.07. Given the different distribution of cartilage and bone in the UP of different ages, elastic moduli were calculated using contrasting Poisson ratios. In accordance with published values we used a value of 0.3 for bone (Rho et al., 1997; Zysset et al., 1999) and 0.5 for cartilage (Mak et al., 1987; Wong et al., 2000). Mean elastic moduli values were compared using an independent sample *t*-test (SPSS 15.0).

RESULTS AND DISCUSSION

Turkey embryos and chicks had 7 vertebral ribs of which 5 were paired with a sternal rib, whereas vertebral ribs 1 and 2 were unpaired. The UP occurred on ribs 2 to 6 in all specimens. A very short UP occurred on vertebral rib 1 in specimens taken on d 15, 19, 20, 25, and 31. The UP were absent on rib 7 in all specimens. The reduced size and morphology of UP 2 and 6 indicate that their role in ventilation is limited (Tickle et al., 2007). For ease of comparison (and because the timing of ossification and morphology were similar in UP 3, 4, and 5), uncinate process 4 was considered to be representative.

Days 14 to 21

The rib cage appeared cartilaginous until d 18 of incubation when all vertebral ribs began to ossify. By d 21 the vertebral ribs were ossified except for the ventral tip, capitulum, and tuberculum. The sternal ribs that pair with the vertebral ribs 5 and 6, displayed bone growth on d 19. Ossification began on d 20 for the sternal ribs paired with vertebral ribs 4 and 7, whereas the remaining sternal rib, paired with vertebral rib 3, began bone proliferation on d 21. The sternum remained entirely cartilaginous during this period. By d 17 the characteristic adult morphology of the UP was fixed, although they remained cartilaginous. The UP 2 and 6 appeared curved and were relatively short compared with those on ribs 3, 4, and 5. Uncinate process 3 was straight with a flared base, whereas UP 4 and 5 were L-shaped with a distended tip (Figure 1A, 2). Uncinate process 4 was entirely cartilaginous during these stages (Figure 1A, 2A, 2D).

Days 22 to 28

Ossification of the UP began on d 22 with process 5. By d 23 UP 2 to 5 underwent bone growth. The timing

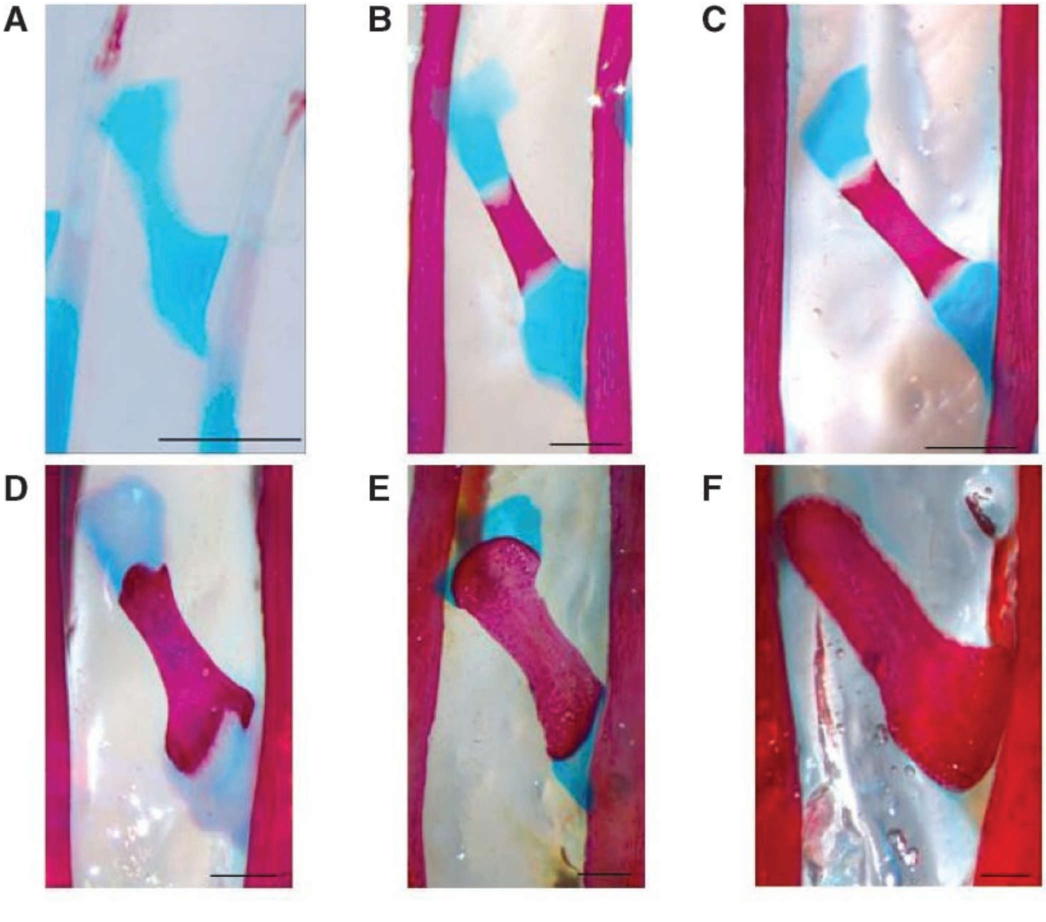

Figure 1. Pattern of ossification of uncinate process 4 from 19 to 94 d. (A) d 19 embryo, stained Alcian blue, ×25, (B) d 25 embryo, Alizarin red staining locates the ossification center, ×20 (C) d 28 chick, further bone growth apparent, ×20, (D) d 36 chick, ×20, (E) d 49 bird, ×12.5, (F) d 94, ossification of the uncinate process base to the vertebral rib, ×12.5. Scale bars represent 1 mm.

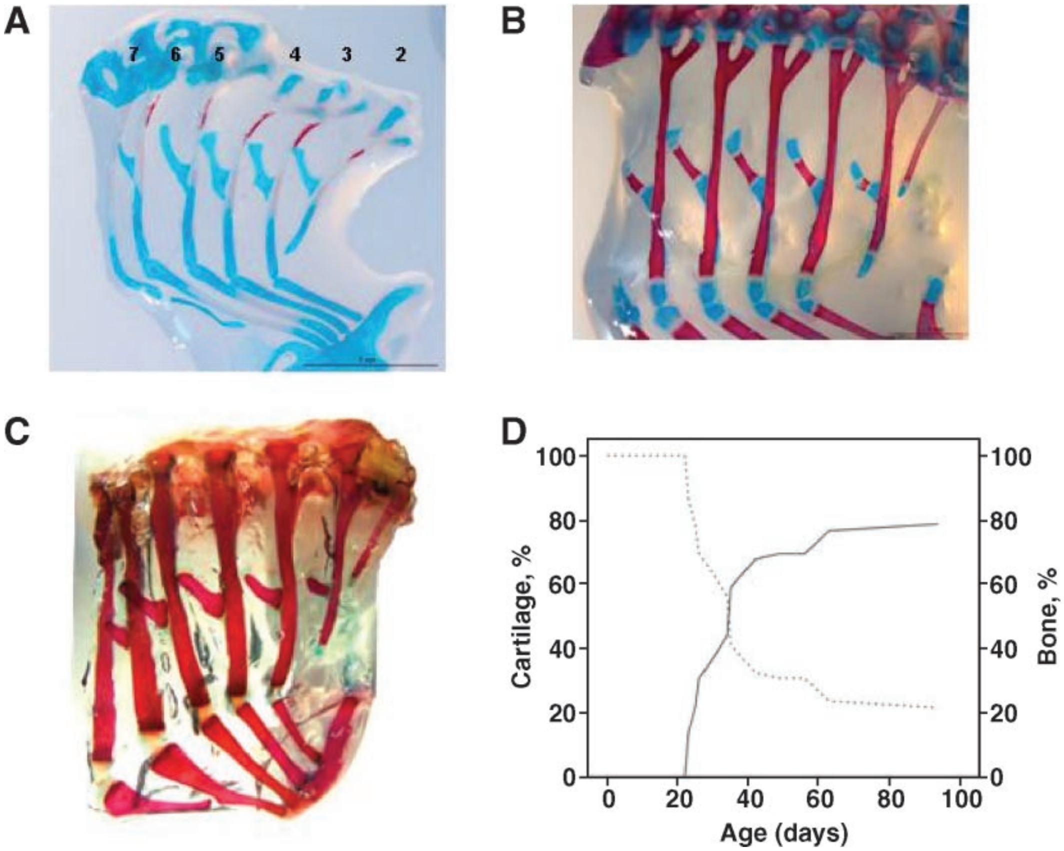

Figure 2. Representative skeletons showing the progress of ossification during ontogeny. (A) d 19 embryo, the uncinate processes (UP) are cartilaginous, whereas ossification has begun in the vertebral ribs (rib 1 is missing), ×8, (B) d 28 chick, extensive bone growth in the ribs, whereas ossification is apparent in UP, ×6.3, (C) d 90 bird, ossification is advanced in the ribs and UP. Anterior is to the right. Ribs are numbered from the anterior end. Scale bar 5 mm. (D) Percentage of cartilage (dashed line) and bone (solid line) for uncinate process 4 from d 14 to 94.

of ossification of process 2 varied between specimens, such that bone growth was not detected until hatching in some birds. Bone proliferation extended from the center of the process toward the cartilaginous tip and base. Vertebral and sternal ribs exhibit widespread ossification (Figure 2B), whereas sternal bone growth begins in the cranial aspect of the keel on d 24. During this period rapid ossification increased the bone area of process 4 from 13 to 37% (Figure 1B, 1C, 2D).

Days 29 to 35

Progressive ossification of the UP continued, including process 6 by d 31. The base and tip of each process remained cartilaginous. The ventral and dorsal tips of the vertebral and sternal ribs remained cartilaginous, whereas sternal ossification continued in the craniodorsal keel. Rapid mineralization increased the proportion of bone from 37 to 59% in process 4 (Figure 1D, 2D).

Days 36 to 63

Ossification of vertebral and sternal ribs appeared complete. Ossification of the UP appeared to slow as bone growth continued at the base; however, the tip remained predominantly cartilaginous. The ventral aspect of the tip appeared proportionally more ossified than the dorsal edge (Figure 1E and 1F). The symphysis between the UP and vertebral rib remained cartilaginous, despite extensive ossification at the process base. The relative area of bone in process 4 increased from 59 to 77% (Figure 2D).

Days 64 to 94

Ossification of the UP continued, primarily at the base. Staining of the tip remained blue in all processes, indicating that cartilage was the predominant tissue, although the relative size of this region was smaller in processes 2 and 6 (Figure 2C). The process base was seen to ossify to the bony vertebral rib by 94 d (Figure 1F). Uncinate process 4 exhibited a slight increase in bone from 77 to 79% of total area (Figure 2D).

The UP are clearly present in the developing turkey embryo and are initially cartilaginous but undergo ossification from d 22, being completely ossified to the vertebral rib from which they extend by d 94. Cartilage has a lower structural density than bone (Lyman, 1994), meaning it has different biomechanical properties. Two key changes that occur during ontogeny in birds are the switch to pulmonary ventilation and the exponential increase in the pectoralis muscle mass that occur after

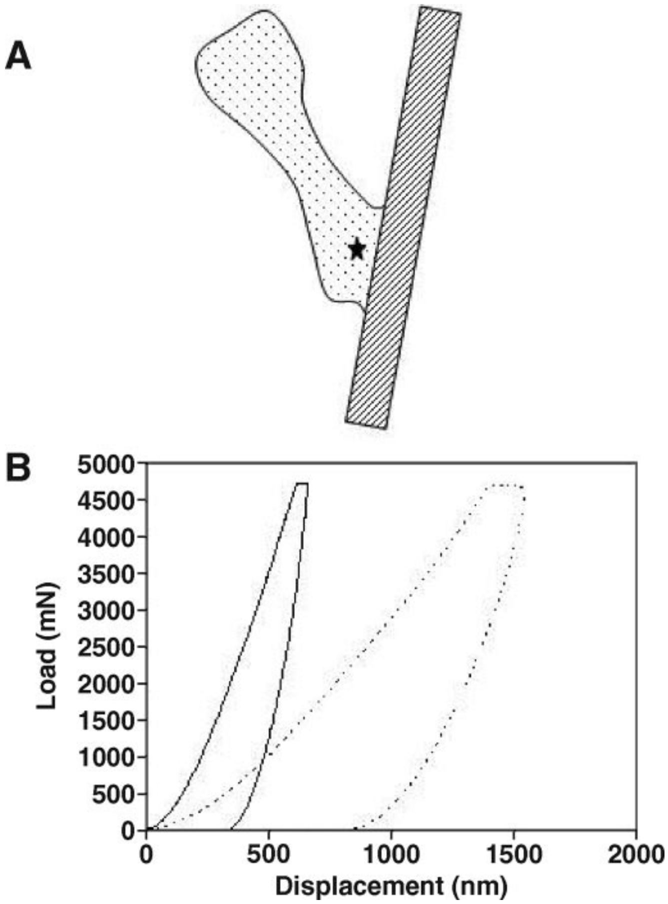

Figure 3. (A) Diagram of uncinate process 4 and adjoining vertebral rib showing location (star) used for nanoindentation, (B) Representative load displacement curves produced by indents in uncinate process 4 from d 25 (broken line) and d 94 (solid line) turkeys. The steeper unloading curve for the d-94 specimen indicates that the process is stiffer when compared with d 25. The slope of the unloading phase for each sample is used to calculate the mean elastic modulus using the equations of Oliver and Pharr (2004).

hatching (Ricklefs et al., 1994). The morphology of the UP in adult birds is linked to adaptations of the sternum to different forms of locomotion. The UP are short in walking or running birds, intermediate in nonspecialists, and long in diving species; the longer the sternum the longer the UP (Tickle et al., 2007). There may be fundamental differences in the ventilatory mechanics of different species of bird linked to morphological specializations to different forms of locomotion (Tickle et al., 2007). For example, the mass of the flight muscles accounts for up to 35% of the total BW in some species of flying birds (Dial et al., 1988), which may affect the timing of UP ossification. However, it remains to be determined if the pattern of ossification also varies during ontogeny in species adapted to diving, flying, or running.

Maxwell (2008) did not report ossification of the UP for stage 40+ (before hatch) *M. gallopavo* but did report that accelerated ossification of the UP is characteristic of galliforms. Endochondral bone formation is associated with mechanical stimulation (Carter et al., 1996). For the turkeys used in this study, ossification began just before hatching; therefore, we suggest that the onset of respiratory movements, around the time of internal pipping, may be the trigger for the initialization of bone formation in the UP. Similarly, ossification of the UP has been shown to occur at the time of internal pipping in the Japanese quail (Nakane and Tsudzuki, 1999) and at hatch in the domestic chicken (Hogg, 1980). Therefore, the timing of ossification in the UP may be conserved within the galliformes.

Biomechanical Testing

A section toward the base of the UP on d 25 and 94 specimens (Figure 3A) was exposed by grinding and polishing the resin. Representative force-displacement curves from which the elastic moduli were calculated for each sample are shown in Figure 3B. The disparity between the curves is indicative of a difference among the samples in response to loading. The relatively steep slope in the d 94 specimen indicates a higher elastic modulus when compared with d 25. The mean elastic modulus of the uncinate process base from d 25 (n = 7; 1.20 GPa ± 0.07) was significantly reduced compared with d 94 (n = 8, 6.72 GPa ± 0.31; $P <$ 0.001). Mechanical testing indicated that the stiffness increased as the process ossified, meaning the UP in older birds would function as a more effective lever and brace during respiration. The UP with a cartilaginous attachment to the vertebral rib would also be more likely to flex during muscle shortening, therefore reducing its effectiveness. Given the key role UP have during avian ventilation, an examination of the developmental changes in UP ossification across a wider range of species during ontogeny may shed new light on the mechanics of avian ventilation.

ACKNOWLEDGMENTS

The authors thank Grenham Ireland and Nick French (Aviagen, Cheshire, UK) for providing the eggs used in this research. Frances Colman (University of Manchester, UK) provided assistance in the development of the staining technique. The nanoindentation work was performed at the School of Materials, University of Manchester, and we would like to thank Paul Mummery, Riaz Akhtar, Andrew Forrest, and Ken Gyves for training and assistance with sample preparation. This research was funded by the Biotechnology and Biological Sciences Research Council through a postgraduate stipend to P. G. Tickle and the University of Manchester.

REFERENCES

Blom, J., and C. Lilja. 2004. A comparative study of growth, skeletal development and eggshell composition in some species of birds. J. Zool. 262:361–369.

Burke, A. C., and A. Feduccia. 1997. Developmental patterns and the identification of homologies in the avian hand. Science 278:666–668.

Carter, D. R., M. C. H. Van Der Meulen, and G. S. Beaupré. 1996. Mechanical factors in bone growth and development. Bone 18:5S–10S.

Claessens, L. P. A. M. 2004. Archosaurian respiration and the pelvic girdle aspiration breathing of crocodyliforms. Proc. R. Soc. B: Biol. Sci. 271:1461–1465.

Codd, J. R., D. F. Boggs, S. F. Perry, and D. R. Carrier. 2005. Activity of three muscles associated with the uncinate processes of the giant Canada goose *Branta canadensis maximus.* J. Exp. Biol. 208:849–857.

Dial, K. P., S. R. Kaplan, G. E. Goslow Jr., and F. A. Jenkins Jr. 1988. Functional analysis of the primary upstroke and downstroke muscles in the domestic pigeon. J. Exp. Biol. 134:1–16.

Duncker, H.-R. 1978. Development of the avian respiratory and circulatory systems. Pages 260–273 in Respiratory Function in Birds, Adult and Embryonic. J. Piiper, ed. Springer-Verlag, Berlin, Germany.

Fell, H. B. 1925. The histogenesis of cartilage and bone in the long bones of the embryonic fowl. J. Morphol. 40:417–460.

Fujioka, T. 1952. Time and order of appearance of ossification centres in the chicken skeleton. Acta Anatomica Nipponica 30:140–150.

Hamilton, H. L. 1952. Lillie's Development of the Chick. 3rd ed. Henry Holt & Co., New York, NY.

Hengsberger, S., A. Kulik, and Ph. Zysset. 2001. A combined atomic force microscopy and nanoindentation technique to investigate the elastic properties of bone structural units. Eur. Cell. Mater. 1:12–17.

Hogg, D. A. 1980. A re-investigation of the centres of ossification in the avian skeleton at and after hatching. J. Anat. 130:725–743.

Kardong, K. V. 1988. Skeletal system: The axial skeleton. Pages 278–279 in Vertebrates: Comparative Anatomy, Function, Evolution. McGraw-Hill, New York, NY.

Lyman, R. L. 1994. Structure and quantification of vertebrate skeletons. Page 79–84 in Vertebrate Taphonomy. Cambridge Univ. Press, Cambridge, UK.

Maina, J. N. 2003a. A systematic study of the development of the airway (bronchial) system of the avian lung from days 3 to 26 of embryogenesis: A transmission electron microscopic study on the domestic fowl, *Gallus gallus* variant *domesticus.* Tissue Cell 35:375–391.

Maina, J. N. 2003b. Developmental dynamics of the bronchial (airway)- and air sac systems of the avian respiratory system from days 3 to 26 of life: A scanning electron microscopic study of the domestic fowl, *Gallus gallus* variant *domesticus.* Anat. Embryol. (Berl.) 207:119–134.

Maina, J. N. 2006. Development, structure, and function of a novel respiratory organ, the lung-air sac system of birds: To go where no other vertebrate has gone. Biol. Rev. Camb. Philos. Soc. 81:545–579.

Mak, A. F., W. M. Lai, and V. C. Mow. 1987. Biphasic indentation of articular cartilage—I. Theoretical analysis. J. Biomech. 20:703–714.

Maxwell, E. E. 2008. Comparative embryonic development of the skeleton of the domestic turkey (*Meleagris gallopavo*) and other galliform birds. Zoology 111:242–257.

Menna, T. M., and J. P. Mortola. 2002. Metabolic control of pulmonary ventilation in the developing chick embryo. Respir. Physiol. Neurobiol. 130:43–55.

Miller, D. M., and J. Tarpley. 1996. An automated double staining procedure for bone and cartilage. Biotech. Histochem. 71:79–83.

Nakane, Y., and M. Tsudzuki. 1999. Development of the skeleton in Japanese quail embryos. Dev. Growth Differ. 41:523–534.

Oliver, W. C., and G. M. Pharr. 1992. An improved technique for determining hardness and elastic modulus using loading and displacement sensing indentation experiments. J. Mater. Res. 7:1564–1583.

Oliver, W. C., and G. M. Pharr. 2004. Measurement of hardness and elastic modulus by instrumented indentation: Advances in understanding and refinements to methodology. J. Mater. Res. 19:3–20.

Rho, J.-Y., T. Y. Tsui, and G. M. Pharr. 1997. Elastic properties of human cortical and trabecular lamellar bone measured by nanoindentation. Biomaterials 18:1325–1330.

Ricklefs, R. E., R. E. Shea, and I.-H. Choi. 1994. Inverse relationship between functional maturity and exponential growth rate of avian skeletal muscle: A constraint on evolutionary response. Evolution 48:1080–1088.

Simmons, D. J., and A. M. Pankovich. 1963. Bone development in Japanese quail. Anat. Rec. 147:325–336.

Starck, J. M. 1994. Quantitative design of the skeleton in bird hatchlings: Does tissue compartmentalization limit posthatching growth rates? J. Morphol. 222:113–131.

Tickle, P. G., A. R. Ennos, L. E. Lennox, S. F. Perry, and J. R. Codd. 2007. Functional significance of the uncinate processes in birds. J. Exp. Biol. 210:3955–3961.

Tullett, S. G., and D. C. Deeming. 1982. The relationship between eggshell porosity and oxygen consumption of the embryo in the domestic fowl. Comp. Biochem. Physiol. 72A:529–533.

Wangensteen, D., and H. Rahn. 1970/71. Respiratory gas exchange by the avian embryo. Respir. Physiol. 11:31–45.

Welty, J. C. 1988. Bones and muscle. Page 59–61 in Life of Birds. J. C. Welty and L. Baptista, ed. W. B. Saunders and Co., London, UK.

Wong, M., M. Ponticiello, V. Kovanen, and J. S. Jurvelin. 2000. Volumetric changes of articular cartilage during stress relaxation in unconfined compression. J. Biomech. 33:1049–1054.

Zysset, P. K., X. E. Guo, E. Hoffler, K. E. Moore, and S. A. Goldstein. 1999. Elastic modulus and hardness of cortical and trabecular bone lammelae measured by nanoindentation in the human femur. J. Biomech. 32:1005–1012.

Chapter 4

Uncinate process length in birds scales with resting metabolic rate

This chapter is as a reprint of an article published in *PLoS ONE:*

Tickle, P. Nudds, R. and Codd, J. (2009) Uncinate process length in birds scales with resting metabolic rate. *PLoS ONE* **4(5)**: e5667

Uncinate Process Length in Birds Scales with Resting Metabolic Rate

Peter Tickle, Robert Nudds, Jonathan Codd*

Faculty of Life Sciences, University of Manchester, Manchester, United Kingdom

Abstract

A fundamental function of the respiratory system is the supply of oxygen to meet metabolic demand. Morphological constraints on the supply of oxygen, such as the structure of the lung, have previously been studied in birds. Recent research has shown that uncinate processes (UP) are important respiratory structures in birds, facilitating inspiratory and expiratory movements of the ribs and sternum. Uncinate process length (UPL) is important for determining the mechanical advantage for these respiratory movements. Here we report on the relationship between UPL, body size, metabolic demand and locomotor specialisation in birds. UPL was found to scale isometrically with body mass. Process length is greatest in specialist diving birds, shortest in walking birds and intermediate length in all others relative to body size. Examination of the interaction between the length of the UP and metabolic demand indicated that, relative to body size, species with high metabolic rates have corresponding elongated UP. We propose that elongated UP confer an advantage on the supply of oxygen, perhaps by improving the mechanical advantage and reducing the energetic cost of movements of the ribs and sternum.

Citation: Tickle P, Nudds R, Codd J (2009) Uncinate Process Length in Birds Scales with Resting Metabolic Rate. PLoS ONE 4(5): e5667. doi:10.1371/journal.pone.0005667

Editor: Alejandro Lucia, Universidad Europea de Madrid, Spain

Received February 23, 2009; **Accepted** April 20, 2009; **Published** May 27, 2009

Copyright: © 2009 Tickle et al. This is an open-access article distributed under the terms of the Creative Commons Attribution License, which permits unrestricted use, distribution, and reproduction in any medium, provided the original author and source are credited.

Funding: This research was funded by the BBSRC (G011338/1) and The Leverhulme Trust (F/00 120/BH). The funders had no role in study design, data collection and analysis, decision to publish or preparation of the manuscript.

Competing Interests: The authors have declared that no competing interests exist.

* E-mail: jonathan.codd@manchester.ac.uk

Introduction

The avian respiratory system consists of a relatively rigid lung coupled with a series (in most birds) of nine compliant air-sacs [1]. The anatomical arrangement of these air-sacs facilitates the bellows-like movement of inspired air unidirectionally across the parenchymal tissue [2,3]. Like all tetrapods birds face a possible mechanical constraint during simultaneous locomotion and ventilation [4,5]. However, almost all extant birds and some non-avian maniraptoran dinosaurs exhibit osteological characters known as uncinate processes (UP). These bony projections on the vertebral ribs (oriented in the caudo-dorsal direction) play a key role in enabling simultaneous ventilation and locomotion. The function of the UP was thought to be linked with stiffening the rib cage [6,7] or as a site for attachment of flight muscles [8]. However, their role as accessory breathing structures, first suggested by Zimmer [9], was confirmed in recent research [10]. The *Mm. appendicocostales* projects from the proximal edge of the uncinate process, and inserts onto the following vertebral rib [11]. Activity of the *Mm. appendicocostales* is associated with craniad movement of the ribs and a ventral displacement of the sternum during inspiration [10]. UP also provide a site for the attachment of projections from the *M. externus obliquus abdominus*, which pull the sternum dorsally during expiration [10]. Geometric modelling of the avian rib cage indicated that UP act as levers that improve the mechanical advantage for forward rotation of the dorsal ribs and therefore ventral movement of the sternum during inspiration [12]. Morphological variations in UP have been demonstrated to correspond to adaptations to different forms of locomotion [12]. Birds adapted to diving have the longest processes, flying and swimming birds have UP of intermediate length whilst the shortest UP occur in walking species [12]. Given the important respiratory function of the UP, variation in morphology suggests that differences in ventilatory mechanics may be driven by adaptation to locomotion. The presence of these processes in some non-avian maniraptoran dinosaurs has also been linked to avian-like breathing mechanics in these theropod ancestors of modern birds [13].

Respiration powers locomotion by providing metabolic energy. Resting metabolic rate (RMR) is often used to investigate the relationship between metabolism and body weight [14]. Lasiewski and Dawson [15] provided a review and re-analysis of published values of bird RMR. Using data from a range of species, RMR was reported to scale to the two-thirds power of body mass ($\mathrm{RMR} \propto M_b^{2/3}$), i.e. in proportion to body surface area [15,16]. However, by re-analysing the scaling relationship in separate passerine and non-passerine groups, Lasiewski and Dawson [15] calculated that RMR scales as $M_b^{0.72}$. The projected 0.72 scaling coefficient found by Lasiewski and Dawson [15] is very similar to the ⅔ [17] or ¾ [16,18] scaling component often used to describe the relationship between basal metabolic rate and body size for mammals. A common relationship between metabolism and body weight may therefore exist amongst endothermic vertebrates. Avian RMR has been reported to vary according to phylogeny, circadian rhythms and ecological variables [15,19–23]. Furthermore, passerines have an elevated metabolic rate when compared to non-passerine species [15], while RMR is greater for birds during their period of normal activity [19,20]. However, some controversy exists on the scaling relationship between passerine and non-passerine birds with studies either reporting [24] or not reporting [22,25] a difference. The rate of energy metabolism in species adapted to life in aquatic environments is relatively high compared to arboreal birds, while nocturnal species have relatively low RMR [21]. Variation in energy metabolism within Aves suggests that adaptations in breathing mechanics may have occurred to meet the oxygen demands of varied lifestyles.

The supply of oxygen to gas exchange tissue is critically important for sustaining the metabolic rate of an animal. Numerous studies across a range of phyla have addressed the constraints upon oxygen delivery imposed by body size. For example, an examination of avian respiration by Lasiewski and Calder [26] highlighted the relative efficiency of the unique lung air-sac system.

UP are now confirmed to be important respiratory structures in birds involved in inspiration and expiration [10]. Here we disentangle the relationships between uncinate process length (UPL), M_b and RMR in birds adapted to different modes of primary locomotion. An understanding of the relationship between the UPL and metabolic rate will shed further light on the evolution of morphological variation in these processes.

Materials and Methods

(a) Specimens

Measurements of UPL were taken from the left-hand side of skeletons from 112 species using a Mayr digital calliper (16EX 150 mm, Product No: 4102400, Mayr GmbH, Germany). The length of process 4 was used in all statistical analyses. This process occurs in all specimens and has a relatively stable morphology [27]. Following the classification of Tickle et al [12], birds were grouped based upon their primary mode of locomotion and assigned to a single category; (1) walking (n = 13); birds which are flightless or incapable of sustained flight: (2) diving (n = 27); birds which are capable of diving underwater using foot or wing propulsion; and (3) non-specialist (n = 72); all other birds which fly and swim but are not flightless or capable of diving underwater. Body masses were taken from records of intact specimens or literature values [28].

(b) Uncinate process length and body size

Reduced major axis (RMA) regression [29] was used to examine the relationship between UPL and M_b. This procedure is appropriate for analysis of morphological characters because the variation in both x and y variables is taken into account [29,30]. The slope and confidence intervals of the regression line were calculated as described by Sokal and Rohlf [29]. RMA equations for $\log_{10}$ transformed data were independently generated in each locomotor category. ANCOVA was used to test for significant differences between regression lines.

The potentially confounding effects of the birds having a shared phylogenetic ancestry were controlled by calculating independent contrasts [31]. The phylogeny of Livezey and Zusi [32] was used to generate contrasts for $\log_{10}$ transformed M_b and UPL data, with the CRUNCH facility in the Comparative Analysis of Independent Contrasts (CAIC) software, version 2.6.9 [33]. A punctuational model of evolution was assumed and therefore all branch lengths were set as equal. RMA regression equations were calculated [29] to explore the linear relationship between phylogenetically corrected UPL and M_b. RMA regressions of independent contrasts were performed through the origin [33] for each locomotor mode.

(c) Uncinate process length and metabolic rate

The relationship between RMR and UPL was studied in a subset of 35 species, taken from the previous dataset. These species were selected because corresponding RMR values are available [21,34]. These species were again assigned to locomotor categories, walking, non-specialist and diving. Body masses and values of RMR (taken from [21,34]) were $\log_{10}$ transformed, and only data corresponding to true RMRs, as defined by them, were used. To ensure that the regression equations describing the relationship between UPL and M_b in the species subset did not differ significantly from those in the larger dataset, RMA analyses were repeated. This procedure is important for validating the assumption that an association between process length and RMR can be extrapolated to the larger dataset. RMA regression was used to investigate the linear relationship between M_b and RMR. Finally, the scaling of RMR with UPL was explored using RMA regression.

General linear models (GLM) were used to assess the influence of locomotor mode, UPL and M_b on RMR. By accounting for the variation attributable to M_b and group structure, the GLM provides an estimate of the association between RMR and process length independent of M_b. In the first analysis, locomotor category (diving, non-specialist and walking) was designated as a group factor, while M_b and UPL were the covariates (RMR = locomotor group+UPL+M_b). A second GLM analysis repeated the prior method with the group factor comprising diving and non-specialist species. Lastly, the influence of UPL and M_b on RMR, in the absence of a grouping variable, was examined (RMR = UPL+M_b).

A phylogenetically controlled analysis in the form of the GLM (above) was not possible. Therefore, to assess the influence of locomotor mode, UPL and M_b on RMR whilst controlling for phylogeny we employed the following method: first the linear relationship between $\log_{10} M_b$ and $\log_{10}$ UPL was determined (UPL = 0.2137 M_b+0.4336). Residual UPL was then calculated by subtracting the length predicted from the $\log_{10} M_b/\log_{10}$ UPL relationship from actual UPL for each species. The relationship between $\log_{10}$ RMR and residual uncinate process length was then calculated for each of the three locomotor groups using CAIC. RMA regressions were calculated to assess the linear relationship between the independent contrasts generated for RMR and residual UPL within each locomotor mode.

GLM analyses were conducted in SPSS (SPSS v.15; SPSS Ltd, Chicago, IL, USA) and ANCOVAs, and RMA regressions in MATLAB® 2007b (The MathWorks, Inc., 3 Apple Hill Drive, Natick, MA). Ninety five percent confidence limits are displayed in parentheses immediately after the scaling exponent.

Results

Uncinate process length and body size

Analyses of 112 species indicated that, for all three locomotor modes investigated, uncinate process length scales isometrically with body mass (Figure 1a; Table 1), i.e. in all cases the regression line exponent did not differ significantly from 0.33. The regression line intercept differed between locomotor groups, indicating that processes are longest relative to M_b in diving birds, intermediate in non-specialists and shortest in walking birds (Figure 1a; Table 1) (ANCOVA: group, $F_{2,108} = 14.16$, $P<0.001$; M_b, $F_{1,108} = 169.54$, $P<0.001$). Greater variation around the regression line was evident for the walking category, as indicated by the lower correlation coefficient, r (Figure 1a; Table 1). Scaling of UPL against M_b using independent contrasts suggested that when phylogeny is taken into account the effects were minimal and scaling was isometric ($M_b^{0.33}$) for all locomotor groups (Figure 1b; Table 1). Similar to the corresponding values estimated using the species level analysis above, variation around the regression line was greatest within the walking category (Table 1).

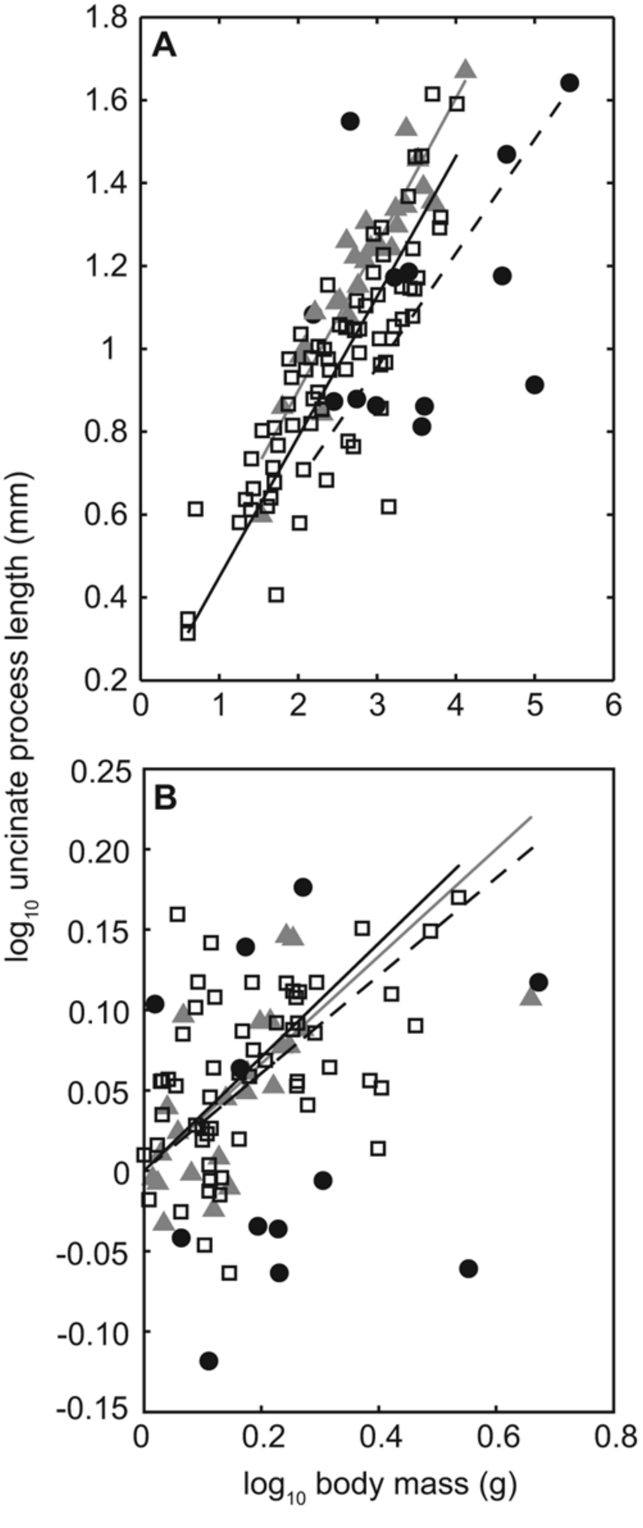

Figure 1. The relationship between uncinate process length (UPL) and body mass (a) species level analysis, b) comparative analysis using independent contrasts and the phylogeny of Livezey and Zusi [31]. Diving birds (grey solid triangles and grey regression lines), non-specialists (open squares and black regression lines) and walkers (solid circles and dashed regression lines). The equations describing the lines of best fit were $y = 1.96\ x^{0.35\ (0.30-0.41)}$ ($t = 12.80$, $n = 27$, $r^2 = 0.85$, $p < 0.001$) and $y = x^{0.33\ (0.25-0.42)}$ ($t = 8.47$, $n = 23$, $r^2 = 0.68$, $p < 0.001$) for diving birds, $y = 1.29\ x^{0.34\ (0.29-0.38)}$ ($t = 14.94$, $n = 72$, $r^2 = 0.71$, $p < 0.001$) and $y = x^{0.35\ (0.30-0.41)}$ ($t = 12.47$, $n = 57$, $r^2 = 0.63$, $p < 0.001$) for non-specialists, and $y = 1.34\ x^{0.28\ (0.07-0.48)}$ ($t = 2.99$, $n = 13$, $r^2 = 0.15$, $p < 0.02$) and $y = x^{0.30\ (0.12-0.49)}$ ($t = 3.57$, $n = 12$, $r^2 = 0.06$, $p < 0.005$) for walkers in a & b respectively.
doi:10.1371/journal.pone.0005667.g001

Within the data subset of species where RMR values are also available ($N = 35$: diving = 8; non-specialist = 21; walking = 6) UPL scaled isometrically with M_b in the diving and non-specialist birds (Table 1). In contrast, the relationship between UPL and M_b in the walking group (Table 1) was not significant. Nonetheless, the overall trend is similar to that in the full data set.

While a significant positive relationship was found between RMR and M_b, this relationship did not differ between groups (ANCOVA: group, $F_{2,29} = 1.19$, $P = 0.317$; M_b, $F_{1,29} = 762.18$, $P < 0.001$; group*M_b, $F_{2,29} = 0.13$, $P = 0.882$). The group and M_b interaction term was included to ensure that the slope of RMR against M_b for the three groups was not significantly different. The regression line exponents for RMR regressed on M_b did not match the expected (1.0) for geometric similarity (Table 1), but corresponded to the results reported in previous studies [15,21], where $\mathrm{RMR} \propto M_b^{0.67}$ (Table 1). As $\mathrm{RMR} \propto M_b^{0.67}$ and $\mathrm{UPL} \propto M_b^{0.33}$, RMR should be proportional to $\mathrm{UPL}^{2\ (\text{i.e.,}\ 0.67/0.33)}$. The scaling exponent determined for RMR against UPL was significantly less than 2 for both diving and non-specialist groups ($\mathrm{UPL}^{1.78\ \&\ 1.53}$; Table 1). For the walkers, however, RMR did not change predictably with UPL (Table 1).

A GLM suggested that after controlling for the well-established relationship between size (M_b) and RMR, and the group differences determined above, UPL is significantly positively correlated (coefficient = 6.77) with RMR (group: $F_{2,30} = 5.238$, $P = 0.011$; M_b: $F_{1,30} = 336.108$, $P < 0.001$; UPL: $F_{1,30} = 43.481$, $P < 0.001$, model $r^2 = 0.954$). Given the non-significant association between RMR and UPL for walking birds (RMA: Table 1), the GLM was repeated with non-specialist and diving species only. Again, locomotor group did not explain any variation in RMR (group: $F_{1,25} = 0.429$, $P = 0.518$; M_b: $F_{1,25} = 86.1441$, $P < 0.001$; UPL: $F_{1,25} = 15.387$, $P = 0.001$, model $r^2 = 0.973$). Therefore, the group factor was removed from the GLM, leaving M_b and UPL as covariates. As found for the GLM including all three groups, after accounting for the variation in RMR attributable to M_b, the length of the UP was again significantly positively correlated (coefficient = 3.21) with RMR (M_b: $F_{1,26} = 88.035$, $P < 0.001$; UPL: $F_{1,26} = 17.706$, $P < 0.001$, model $r^2 = 0.972$).

A similar result was found when using the RMR and residual uncinate process phylogenetically independent data. The length of the UP was positively correlated with RMR and this relationship varied between locomotor groups (Figure 2). Therefore, a longer uncinate process (when controlled for body mass) is found in birds with high RMRs relative to M_b.

Discussion

Our analysis indicates that the length of the uncinate process increases with body mass irrespective of the mode of locomotion used by the bird. UP are important structures for moving the ribs and sternum during ventilation. Sternal mass is primarily composed of the major flight muscles, the pectoralis and supracoracoideus. Geometric scaling of the major flight muscles to body mass has been calculated [35], although subsequent reports have suggested that pectoral mass scales with a slight negative allometry when looking at the non-passerines only [36]. An increase in rib length and sternal mass will necessitate a corresponding increase in process length [12]. Therefore, the increase in process length proportional to body mass is necessary

Table 1. Parameters described in the table are for scaling relationships of the form $y = m\ x^c$.

y	*x*	Analysis	Locomotor mode	*n*	*r*	m	RMA slope	95% CI
UPL	M_b	Species	Walkers	13	0.38	1.34	0.28	0.07–0.48
			Non-specialists	72	0.84	1.29	0.34	0.29–0.38
			Divers	27	0.92	1.56	0.35	0.30–0.41
		Phylogenetically controlled	Walkers	12	0.24		0.30	0.12–0.49
			Non-specialists	57	0.80		0.35	0.30–0.41
			Divers	23	0.82		0.33	0.25–0.42
		Species (RMR subset)	Walkers	6	0.26	1.90	0.18‡	−0.13–0.49
			Non-specialists	21	0.91	1.20	0.38	0.30–0.46
			Divers	8	0.96	1.16	0.39	0.29–0.50
RMR			Walkers	6	0.98	0.64	0.68*	0.51–0.84
			Non-specialists	21	0.98	0.62	0.71*	0.63–0.79
			Divers	8	1.00	0.65	0.70*	0.66–0.75
	U_p		Walkers	6	0.17	0.06	3.69‡	−2.92–10.30
			Non-specialists	21	0.89	0.43	1.53*	1.11–1.95
			Divers	8	0.96	0.50	1.78*	1.30–2.27

‡Indicates the regression was not significant at p = 0.05 (i.e., the slope of the relationship did not differ from zero).
*Indicates the slope differs from that expected for isometric similarity.
doi:10.1371/journal.pone.0005667.t001

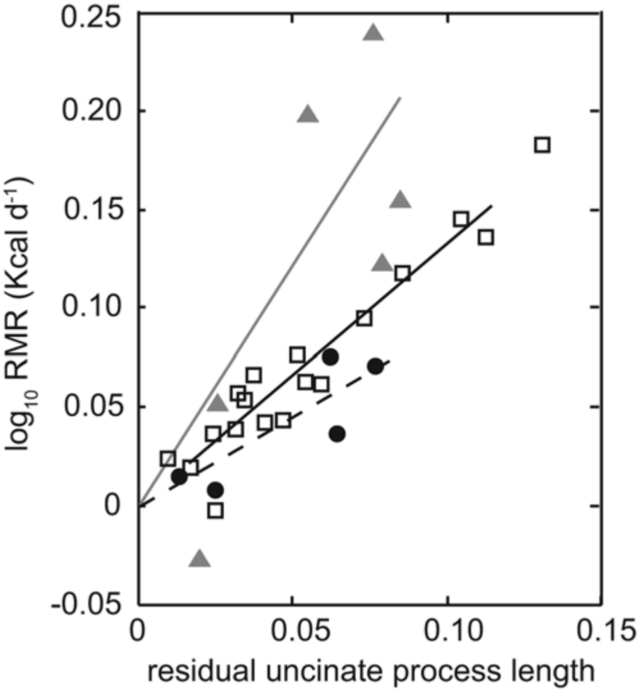

Figure 2. The relationship between RMR and residual uncinate process length (UPL). Plotted are the phylogenetically independent values derived using CAIC [32] and the phylogeny of Livezey and Zusi [31]. Diving birds (grey solid triangles and grey regression lines), non-specialists (open squares and black regression lines) and walkers (solid circles and dashed regression lines). The equations describing the lines of best fit were $y = x^{2.43\ (1.31-2.96)}$ ($t = 6.42$, $n = 6$, $r^2 = 0.85$, $p < 0.001$) for diving birds, $y = x^{1.32\ (1.21-1.42)}$ ($t = 26.69$, $n = 18$, $r^2 = 0.97$, $p < 0.001$) for non-specialists, and $y = x^{0.91\ (0.57-1.24)}$ ($t = 7.48$, $n = 5$, $r^2 = 0.91$, $p < 0.005$) for walkers respectively.
doi:10.1371/journal.pone.0005667.g002

as sternal mass increases. While process length scales isometrically with mass in all locomotor groups, UP are longest in diving birds, intermediate in non-specialists and shortest in walking species (Figure 1a; Table 1). The relationship between the locomotor mode of the bird and UPL was described by Tickle et al [12]. Elongated processes are likely to relate to the increased sternal length and low angle of the ribs to the backbone in diving birds [12]. These adaptations for a streamlined body facilitate efficient entry into, and locomotion in water and accordingly a greater mechanical advantage is required for respiratory movements of the relatively long sternum in divers. The relative increase in process length provides the necessary increase in effectiveness of the *Mm. appendicocostales* [12]. Contrastingly, walking species often have a relatively small sternal mass, relating to a reduction in flight muscle mass. This reduction coupled with a larger angle of the ribs to the backbone, means that a relatively small mechanical advantage may be sufficient for rib movements [12].

In this paper we have used the RMR of birds as a proxy for energy demand. For the birds used in this study, RMR scaled with M_b as expected and in line with previous predictions. While data for RMR is widely available in the literature, the validity of many reports has been questioned [21]. The lack of a standardised experimental protocol means that it is unclear how measures of BMR and/or RMR relate to each other. For example, metabolic rate is influenced by temperature and activity cycle [19,20], variables which have not always been standardised between experiments. Although these are obvious limitations in the dataset, we consider RMR to be a valid measure of energy metabolism. However, considering that the form and function of the respiratory system may be adjusted to the demands of maximum exertion [37], maximal metabolic rate (MMR) may represent a more appropriate measure of metabolic demand. Unfortunately, the relative lack of MMR data prevents its use in comparative analyses like those presented in this study. However, the use of RMR as a proxy for MMR may be considered valid in the light of recent work in avian energetics. Comparative analyses have suggested a correlation between RMR and cold induced MMR [24,38]. After removing the effect of body mass, RMR and MMR show similar scaling exponents [24]. It is unclear whether this relationship will hold for the wider range of species used in this study, since the Rezende et al, [24] analysis was dominated by data for passerines. The relationship does appear to hold ontogenetically for at least one species, however, the Australian Brush Turkey [39]. The relationship between RMR and flight MR, however, has not been extensively examined in birds, with the exception of some attempts to estimate the relationship [40,41]. Therefore, while we must interpret our results carefully, it seems that RMR may be an adequate proxy for maximum metabolic demand.

A combination of the small RMR dataset that is available for walking species and the diversity within this group (a mixture of flightless and ground dwelling birds) may explain why there is no association between uncinate process length, body size, and RMR in these birds. The GLM analysis indicates that when we control for body size, increases in the length of the UP correspond to an increase in RMR. Therefore, birds with higher RMR for a given body mass have proportionately longer UP. Consequently, relatively longer UP appear to be associated with an elevated metabolic rate. Perhaps elongation of the UP facilitates an increase in metabolic demand by improving ventilation via the action of the UP in moving the ribs and sternum. Improving the work involved in ventilation may also explain the long UP found in diving species such as the penguins [42] and tufted ducks that have an elevated breathing frequency upon resurfacing after dives [43].

Of course, if it is advantageous, the question of why all birds don't have proportionally longer UP arises. Presumably, process elongation comes at a cost, possibly in terms of changing the shape of the associated musculature. Furthermore, UP act as levers for rib and therefore sternal movement and longer levers will not always provide a mechanical advantage depending on the overall body shape of the birds. Crucially, the rib cage, sternal morphology and associated musculature, appear to be driven by adaptations to different forms of locomotion.

Acknowledgments

Skeletons were provided by the Ornithology Dept of the Research Institute and Museum Alexander Koenig (Bonn, Germany), The Manchester Museum (Manchester, UK), and the Dept of Ornithology of the American Museum of Natural History (New York, USA). The authors would like to thank Paul Sweet, Mark Norell, and Henry McGhie for facilitating access to skeletons. An earlier draft of this manuscript was greatly improved by the comments of Craig White and an anonymous referee.

Author Contributions

Conceived and designed the experiments: JRC. Performed the experiments: PGT RN JRC. Analyzed the data: PGT RN JRC. Wrote the paper: PGT RN JRC.

References

1. Powell FL (2000) Respiration. In: Causey Whittow G, ed. Avian Physiology, 5th edition. New York: Academic Press. pp 233–264.
2. Brackenbury JH (1972) Lung-air-sac anatomy and respiratory pressure in the bird. J Exp Biol 57: 543–550.
3. Brackenbury JH (1973) Respiratory mechanics in the bird. Comp Biochem Physiol 44: 599–611.
4. Carrier DR (1991) Conflict in the hypaxial musculo-skeletal system: documenting an evolutionary constraint. Amer Zool 31: 644–654.
5. Nassar PN, Jackson AC, Carrier DR (2001) Entraining the natural frequencies of running and breathing in guinea fowl (*Numida meleagris*). J Exp Biol 204: 1641–1651.
6. Walker WF Jr, Liem KF (1994) Evolution of the postcranial skeleton. In: Functional Anatomy of the Vertebrates: An Evolutionary Perspective. New York: Saunders College Publishing. 270 p.
7. Zhang F, Zhou Z, Lianhai H, Gang G (2001) Early diversification of birds: evidence from a new opposite bird. Chin Sci Bull 46: 945–949.
8. Welty JC, Baptista L (1988) The appendicular skeleton. In: The Life of Birds. 4th ed. London: W. B. Saunders and Co. 62 p.
9. Zimmer K (1935) Beitrage zur Mechanik der Atmung bei den Vögeln in Stand und Flug. Aufgrund anatomischer-physiologisher und experimenteller Studien. Zoologica 88: 1–69.
10. Codd JR, Boggs DF, Perry SF, Carrier DR (2005) Activity of three muscles associated with the uncinate processes of the giant Canada goose *Branta canadensis maximus*. J Exp Biol 208: 849–857.
11. Schufeldt RW (1890) The musculature of the trunk. In: The Myology of the Raven. London: MacMillan and Co. pp 300–301.
12. Tickle PG, Ennos AR, Lennox LE, Perry SF, Codd JR (2007) Functional significance of the uncinate processes in birds. J Exp Biol 210: 3955–3961.
13. Codd JR, Manning PL, Norell MA, Perry SF (2008) Avian-like breathing mechanics in maniraptoran dinosaurs. Proc Roy Soc B 275: 157–161.
14. White CR, Phillips NF, Seymour RS (2006) The scaling and temperature dependence of vertebrate metabolism. Biol Lett 2(1): 125–127.
15. Lasiewski RC, Dawson WR (1967) A re-examination of the relation between standard metabolic rate and body weight in birds. Condor 69: 13–23.
16. Schmidt-Nielsen K (1984) Scaling: why is animal size so important? UK: Cambridge University Press.
17. White CR, Seymour RS (2003) Mammalian basal metabolic rate is proportional to body mass$^{2/3}$. Proc Natl Acad Sci U S A 100: 4046–4049.
18. Kleiber M (1932) Body size and metabolism. Hilgardia 6: 315–353.
19. Aschoff J, Pohl H (1970a) Der Ruheumsatz von Vögeln als Funktion der Tageszeit und der Körpergrösse. J Ornithol 3: 38–48.
20. Aschoff J, Pohl H (1970b) Rhythmic variations in energy metabolism. Fed Proc 29: 1541–1552.
21. Bennett PM, Harvey PD (1987) Active and resting metabolism in birds: allometry, phylogeny and ecology. J Zool Lond 213: 324–363.
22. Jetz W, Freckleton RP, McKechnie AE (2007) Environment, migratory tendency, phylogeny and basal metabolic rate in birds. PLoS ONE 3: e3261.
23. White CR, Blackburn TM, Martin GR, Butler PJ (2007) Basal metabolic rate of birds is associated with habitat temperature and precipitation, not primary productivity. Proc Roy Soc B 274: 287–293.
24. Rezende EL, Swanson DL, Novoa FF, Bozinovic F (2002) Passerine versus non-passerines: so far no statistical differences in the scaling of avian energetics. J Exp Biol 205: 101–107.
25. McKechnie AE, Freckleton RP, Jetz W (2006) Phenotypic plasticity in the scaling of avian basal metabolic rate. Proc Roy Soc B 273: 931–937.
26. Lasiewski RC, Calder Jr WA (1971) A preliminary allometric analysis of respiratory variables in resting birds. Resp Physiol 11: 152–166.
27. Tickle PG, Codd JR (2009) Ontogenetic development of the uncinate processes in the domestic turkey (*Meleagris gallopavo*). Poultry Sci 88: 179–184.
28. Dunning Jr JB (1993) CRC handbook of avian body masses. CRC Press LLC.
29. Sokal RR, Rohlf FJ (1995) Biometry: the principles and practice of statistics in biological research. New York: W. H. Freeman and Company.
30. Rayner JMV (1985) Linear relations in biomechanics: the statistics of scaling functions. J Zool Lond 206: 415–439.
31. Felsenstein J (1985) Phylogenies and the comparative method. Am Nat 125: 1–15.
32. Livezey BC, Zusi RL (2007) Higher-order phylogeny of modern birds (Theropoda, Aves: Neornithes) based on comparative anatomy. II. Analysis and Discussion. Zool J Linn Soc 149: 1–95.
33. Purvis A, Rambaut A (1995) Comparative analysis by independent contrasts (CAIC): an Apple Macintosh application for analysing comparative data. CABIOS 11: 247–251.
34. McKechnie AE, Wolf BO (2004) The allometry of avian basal metabolic rate: Good predictions need good data. Physiol Biochem Zool 77: 502–521.
35. Greenewalt CH (1962) Dimensional relationships for flying animals. Smithsonian misc Coll 144: 1–46.
36. Carrier DR, Auriemma J (1992) A developmental constraint on the fledging time of birds. Biol J Zool Soc 47: 61–77.
37. Taylor CR, Weibel ER (1981) Design of the mammalian respiratory system. I. Problem and strategy. Respir Physiol 44: 1–10.
38. Dutenhoffer MS, Swanson DL (1996) Relationship of basal to summit metabolic rate in passerine birds and the aerobic capacity model for the evolution of endothermy. Physiol Zool 69: 1232–1254.
39. Seymour RS, Runciman S, Baudinette RV (2008) Development of maximum metabolic rate and pulmonary diffusing capacity in the superprecocial Australian Brush Turkey Alectura lathami: An allometric and morphometric study. Comp Biochem Physiol A 150(2): 169–175.
40. Bishop CM (1997) Heart mass and the maximum cardiac output of birds and mammals: implications for estimating the maximum aerobic power input of flying animals. Phil Trans Roy Soc Lon B 352: 441–456.

41. Bishop CM (1999) The maximum oxygen consumption and aerobic scope of birds and mammals: Getting to the heart of the matter. Proc Roy Soc B 266: 2275–2281.
42. Wilson RP, Simeone A, Luna-Jorquera G, Steinfurth A, Jackson S, Fahlman A (2003) Patterns of respiration in diving penguins: is the last gasp an inspired tactic? J Exp Biol 206: 1751–1763.
43. Parkes R, Halsey LG, Woakes AJ, Holder RL, Butler PJ (2002) Oxygen uptake during post dive recovery in a diving bird Aythya fuligula: implications for optimal foraging models. J Exp Biol 205: 3945–6954.

Chapter 5

Load carrying during locomotion in the barnacle goose (*Branta leucopsis*): the effect of load placement and size.

This chapter is as a reprint of an article published in *Comparative Biochemistry and Physiology Part A: Molecular and Integrative Physiology:*

Tickle, P. G., Richardson, M. F. and Codd, J. R. (2010) Load carrying during locomotion in the barnacle goose (*Branta leucopsis*): the effect of load placement and size. *Comp. Biochem. Physiol. A* **156**, 309-317.

Comparative Biochemistry and Physiology, Part A 156 (2010) 309–317

Contents lists available at ScienceDirect

Comparative Biochemistry and Physiology, Part A

journal homepage: www.elsevier.com/locate/cbpa

Load carrying during locomotion in the barnacle goose (*Branta leucopsis*): The effect of load placement and size☆

Peter G. Tickle, Mark F. Richardson, Jonathan R. Codd *

Faculty of Life Sciences, University of Manchester, Manchester, M13 9PT, UK

ARTICLE INFO

Article history:
Received 27 November 2009
Received in revised form 22 January 2010
Accepted 25 January 2010
Available online 11 February 2010

Keywords:
Locomotion
Birds
Respiration
Load carrying
Metabolic rate
Respirometry

ABSTRACT

Load carrying has been used to study the energetics and mechanics of locomotion in a range of taxa. Here we investigated the energetic and kinematic effects of trunk and limb loading in walking barnacle geese (*Branta leucopsis*). A directly proportional relationship between increasing back-load mass and metabolic rate was established, indicating that the barnacle goose can carry back loads (up to 20% of body mass) more economically than the majority of mammals. The increased cost of supporting and propelling the body during locomotion is likely to account for a major proportion of the extra metabolic cost. Sternal loads up to 15% of body mass were approximately twice as expensive to carry as back loads. Given the key role in dorso-ventral movement of the sternum during respiration we suggest that moving this extra mass may account for the elevated metabolic rate. Loading the distal limb with 5% extra mass incurred the greatest proportional rise in metabolism, and also caused increases in stride length, swing duration and stride frequency during locomotion. The increased work required to move the loaded limb may explain the high cost of walking.

© 2010 Elsevier Inc. All rights reserved.

1. Introduction

The constraints on locomotion, driven by natural selection, are perhaps the most significant influence on an animal's morphology. The metabolic requirements of locomotion have a substantial effect on an animal's energy balance and are consequently of critical importance to the fitness of an individual (Tolkamp et al., 2002). Therefore it follows that the physiology of locomotion is integral to our understanding of animal behaviour and evolution.

Experimental manipulation of the biomechanics and physiology of locomotion by applying loads has been undertaken in a wide range of taxa. Remarkable physiological accomplishments have been reported in some invertebrates, such as the rhinoceros beetle, which can carry enormous loads with five times the economy predicted from research in mammals (Kram, 1996). Studies of human locomotion have also highlighted the extraordinary ability of some African tribeswomen (Maloiy et al., 1986) and Nepalese porters (Bastien et al., 2005) to carry loads equivalent to 70% and 183% of their body mass, respectively. When compared to European control subjects, the tribeswomen and porters carry loads with superior economy, indeed loads up to 20% of body mass are transported without an increase in metabolic rate. For these African women it is thought that greater conservation of mechanical energy during each step may facilitate the more efficient load carriage (Heglund et al., 1995), although the mechanisms allowing for such economy in porters remain unclear.

Muscles provide the propulsive and braking forces that are necessary for moving the body and limbs during locomotion in addition to forces developed passively in the skeleton and ligaments. The energetic cost of supporting and accelerating the body can be increased by attaching loads to the trunk, independent from the cost of moving the limb during the swing phase (Taylor et al., 1980). Generating muscular force to support body weight has been considered as the main factor contributing to total metabolism during locomotion (Taylor et al., 1980). Studies of load carrying in mammals have indicated that the cost of supporting extra mass is the same as the weight-specific cost of locomotion, i.e. the cost increases in direct proportion to the additional mass (Taylor et al., 1980; Kram and Taylor, 1990; Wickler et al., 2001). Therefore the muscle force exerted on the ground during the stance phase of the stride may determine the energetic cost of locomotion. Further work in running mammals supports this prediction since the duration of foot contact against the ground corresponds to energy expenditure (Kram and Taylor, 1990). Consequently, limb movement during the swing phase, when the foot is not in contact with the ground, can be considered to have a minimal metabolic cost.

However, recent analyses using an avian model of terrestrial locomotion have challenged this principle. The metabolic activity of individual hind-limb muscles in the guinea fowl (*Numida meleagris*) suggests that rather than being a passive process, swinging the limb

---

☆ This paper derives from a presentation given at the International Congress of Respiratory Science (ICRS) symposium *Breathing, Locomotion and Everything in between*, held in Bad Honnef, Germany, August 10, 2009.

* Corresponding author. Tel.: +44 161 275 5474.
E-mail address: jonathan.codd@manchester.ac.uk (J.R. Codd).

1095-6433/$ – see front matter © 2010 Elsevier Inc. All rights reserved.
doi:10.1016/j.cbpa.2010.01.022

consumes around 25% of the energy used during locomotion (Marsh et al., 2004; Ellerby and Marsh, 2006). Further experiments using guinea fowl have loaded the tarsometatarsal segment to manipulate the energetic costs associated with swinging the hind-limb during locomotion. Increasing the mass of the hind-limb incurs a rise in metabolic rate equivalent to over 300% of the applied load (Marsh et al., 2006), providing further evidence for the energetic cost of limb swinging. An increase in the mechanical energy of the tarsometatarsal segment with loading may explain the corresponding rise in metabolism (Marsh et al., 2006). The application of trunk loads to evaluate the cost of producing muscle force to support and propel the bird, resulted in an increase in metabolic rate equivalent to 74% and 77% of the mass increase (Marsh et al., 2006) and McGowan et al. (2006), respectively. This constitutes a less than proportional increase in metabolism and indicates that guinea fowl are able to carry loads more economically than the majority of tested mammalian species (Taylor et al., 1980; Wickler et al., 2001). Further research into the diversity of locomotor biomechanics and physiology is required to explain this variation in metabolic response to load carrying.

Application of loads to additional locations may provide valuable insights into the costs of mechanical functions other than those directly associated with locomotion; for example, the avian sternum, which may be loaded to examine the costs associated with breathing. Birds have a highly derived respiratory system that delivers inspired air to the parenchymal gas exchange tissue via a series of interconnected air sacs and bronchioles. Dorsal and ventral movements of the ribs and therefore sternum driven by respiratory muscles (Codd et al., 2005) facilitate the necessary pressure changes for inspiration and expiration (Zimmer, 1935; Claessens, 2008). The avian sternum is the site of the major flight muscles, *M. pectoralis* and *M. supracoracoideus*, which account for up to 35% of body mass (Dial et al., 1991). Breathing therefore requires movement of a heavy load that may contribute to a suggested relatively high cost of ventilation in birds. Interestingly, recent studies have estimated this cost to be similar to that reported in other amniotes. Using unidirectional artificial ventilation, Markley and Carrier (2010) calculated the cost of ventilation as 1.43% of total running metabolism in the guinea fowl. Similarly, Ellerby et al. (2005) estimated the cost as 2% of whole-animal metabolism in exercising guinea fowl by measuring blood flow to respiratory muscles. It is surprising that the cost of ventilation in guinea fowl is low, especially when considering that the mass of the sternum and abdominal viscera which must be moved is equivalent to 25% of total body mass (Markley and Carrier, 2010). Perhaps the entrainment of breathing with locomotion which is widespread in birds (Brackenbury and Avery, 1980; Boggs et al., 1998; Nassar et al., 2001) assists in mitigating the energetic demand of ventilation, and consequently the reported costs may have been underestimated, however this remains to be determined. The application of additional loads to the sternum will increase the mechanical work of ventilation. Furthermore the individual application of trunk and limb loads may allow us to disentangle the energetic cost of ventilation from overall metabolism, which includes the energy required to support and move the body and limbs. The behavioural and metabolic responses to sternal loading may therefore further illuminate the inherent costs and plasticity of avian breathing.

Here we report the energetic cost and kinematics of carrying artificial loads on the back, sternum and hind-limbs in the barnacle goose (*Branta leucopsis*). Barnacle geese are non-specialist birds and therefore provide an interesting comparison with the cursorial guinea fowl in terms of locomotor specialisation (Tickle et al., 2007). Barnacle geese show adaptation to terrestrial and aquatic habitats (Portugal et al., 2009), in addition to being excellent flyers that undergo long-distance migrations (Butler et al., 1998). Barnacle geese also experience a natural annual body mass cycle of up to 25% (Portugal et al., 2007; Portugal et al., 2009). We hypothesised that natural changes in the physiology of barnacle geese associated with seasonal variation in body mass would be reflected in a metabolic response to loading different from that observed in the guinea fowl, which do not undergo such mass fluctuations.

2. Materials and methods

2.1. Animals

Barnacle goose (*B. leucopsis*) eggs were obtained from a local supplier and hatched within the BSF Animal Unit at the University of Manchester. Goslings were maintained indoors on a 13 h : 11 h light–dark cycle, housed within a 12 m^2 room with access to a grass turf area and pond with *ad libitum* access to food (Poultry Grower Pellets, Small Holder Range, Norfolk, UK: fat 4.8%, protein 16%, carbohydrate 73.7%, and fibre 5.5%) and water. At the time of experiments, birds were between 10 and 21 months old. Body mass was recorded throughout the experimental trials and averaged 1.86 kg ± 0.01 (mean ± SE). All experimental procedures were approved by the University of Manchester Ethics Committee and conducted in accordance with the Animals (Scientific Procedures) Act (1986) working under a UK Home Office Licence held by Dr Codd (40/3001).

2.2. Training

Birds were trained to walk inside a Perspex® box (respirometry chamber) on a motorised treadmill (Tunturi T60, Turku, Finland) at a range of speeds (0.25–1.25 ms^{-1}). Treadmill training commenced around 3 months after hatching. Pairs of birds were taken into the experimental rooms during the course of each individual experiment to limit any stress caused by removal from their social group. We found that the birds were the most calm and ran well when a companion bird was visible alongside the test goose at all times, while a mirror attached to the front of the box facing the walking goose further gave the illusion of being in a large social group. During training the geese were found to walk comfortably at 0.75 ms^{-1} for over 10 min without displaying signs of exhaustion, so this speed was selected for use in subsequent load bearing trials. We trained the birds to carry loads on the trunk, sternum and leg while resting and during treadmill locomotion for two weeks prior to any experimental data collection.

2.3. Load attachment

2.3.1. Back loads

A soft cotton backpack (mass = 30 g) was used to apply trunk loads to 6 geese. Two elastic straps sewn into the front of the backpack were passed around the shoulders, under the wings and attached to Velcro® strips at the rear of the pack to secure load placement above the estimated centre of mass. Lead weights were then placed inside the backpack and this combined mass was adjusted to 5%, 10%, 15% and 20% of body mass as required.

2.3.2. Sternal loads

Contour feathers overlying the breast were trimmed to reveal the semiplume layer under the birds' estimated centre of mass, to which small Velcro® strips were attached using superglue. Sternal loads were then attached to this area using a corresponding Velcro® strip attached to a lead weight. Duct tape was used to further secure and prevent any movement of the load during locomotion. Sternal loads were adjusted to 5%, 10% ($N = 6$) and 15% ($N = 4$) of body mass.

2.3.3. Leg loads

Distal limb loading was accomplished by applying lead rings to the tarsometatarsal segment of the foot ($N = 6$). Cotton wool was glued inside the rings to prevent irritation or injury, while duct tape was used to secure the loads in place at the distal portion of the tarsus. Total mass of leg loads was adjusted to 2% and 5% of body mass.

2.4. Respirometry

We used flow-through respirometry to collect and analyse respiratory gases during rest and locomotion. A Perspex® respirometry chamber (66 × 48.5 × 46.5 cm; volume = 148 L) was placed over the treadmill belt into which room air was pumped at a flow rate of 255 L min^{-1}. Excurrent airflow was then sub-sampled and pumped through the gas analysis system at a flow rate of 105 ml min^{-1} using a FoxBox® sub-sampling pump (Sable Systems, Las Vegas, NV, USA). Prior to gas analysis water vapour pressure of the sub-sample airstream was measured using a RH-300 humidity meter (Sable Systems, Las Vegas, NV, USA) before passing through a column of magnesium perchlorate (Acros Organics, NJ, USA) to remove water vapour. The carbon dioxide (CO_2) content was then measured and removed by passing the gas through a column of Ascarite (Acros Organics, NJ, USA) before the oxygen (O_2) content of the scrubbed gas was measured. Respiratory gas measurements were recorded continuously using a FoxBox® (Sable Systems, Las Vegas, NV, USA) integrated O_2 and CO_2 analyser connected to a laptop computer. Ambient temperature inside the respirometry chamber was monitored throughout and found to be within the thermoneutral zone for barnacle geese (Calder and King, 1975). The excurrent flow rate was mathematically corrected for the presence of water vapour, which would otherwise cause an overestimation of flow rate. O_2 consumption ($\dot{V}_{O_2}$) and CO_2 production ($\dot{V}_{CO_2}$) were then calculated using the appropriate upstream flow equations (Lighton, 2008) inputted into ExpeData® respirometry software (Sable Systems, Las Vegas, NV, USA). Respiratory quotient (RQ) values for resting and exercising geese were calculated as $\dot{V}_{CO_2}$:$\dot{V}_{O_2}$. $\dot{V}_{O_2}$ was then converted to rate of energy metabolism (W) using a conversion factor calculated from measured RQ values (Brody, 1945). For each trial the resting metabolic rate was subtracted from the total rate measured during locomotion. This net metabolic rate is presented for all unloaded and loaded experiments.

The data collection protocol established during training was followed in all experiments. Pairs of birds were selected at random and left to settle in holding cages in the experimental room for a period of 10 min prior to any experimentation. The body mass of the test bird was taken and loads prepared and applied while room baseline gas traces were recorded for 5 to 10 min. Once a steady baseline trace was observed, the goose was allowed to walk from the holding cage into the respirometry chamber. Following steady resting O_2 and CO_2 readings, the treadmill was started and the speed increased to 0.75 ms^{-1}. $\dot{V}_{O_2}$ during exercise stabilised after 2 min of walking although geese were typically exercised for a further 2 to 3 min to ensure stable readings. After walking, the test bird was allowed to rest in the chamber until fully recovered, as observed by steady respiratory gas traces. Stable O_2 and CO_2 traces were observed 5 min post-exercise, after which a further 1 to 2 min of data were recorded to ensure full recovery. Loads were removed immediately after the bird was taken from the chamber. To account for any change in the background gas fractions, a final baseline measurement of room air was recorded for between 5 and 10 min following the removal of the bird. A change in the baseline measurement of O_2 and CO_2 during a trial was corrected in the ExpeData® software package, which enables adjustment of a selected gas dataset to take into account linear drift. A representative gas trace obtained during experimentation is included in Appendices A and B. The accuracy of the respirometry system was calibrated using the nitrogen flow-through method and found to be accurate to 4% in line with previous studies (White et al., 2008). Metabolic rate during locomotion was calculated using a plateau on the trace that corresponded to steady walking. The precise duration of the selected plateau varied between trials according to the behaviour of the geese during experimentation (mean ± SE: 90.2 s ± 2.8) Resting metabolic rate was calculated from the recovery period that followed exercise since this value was typically lower than the resting period before walking (mean ± SE duration of period for analysis: 50.9 s ± 1.6). Experiments were designed so that the bird and load were selected randomly. The number of trials of each loading condition per bird and experimental protocols are presented in Appendices A and B.

2.5. Kinematics

High-speed footage (frame rate: 120 Hz) of the walking geese was recorded using a Sony SR12E HD video camera (Sony, Japan). Measurements of stance and swing durations, stride frequency and stride length were taken from footage in which the bird maintained a steady position on the treadmill belt. Mean measurements for each bird were calculated from between 9 and 29 strides. Videos were analysed in Tracker Video Analysis software (v.2.60:http://www.cabrillo.edu/~dbrown/tracker/tracker/.com).

2.6. Statistical analyses

The effects of load magnitude and placement on metabolic and kinematic measurements were tested using ANOVA with Tukey post-hoc tests and general linear models (GLM), with load, goose identity and body mass included as covariates. The linear relationship between the fractional increase in mean net metabolic rate and load was calculated using least-squares linear regression. Tests for differences between the slopes of regression lines were calculated using one- and two-sample *t*-tests. Regression lines were forced through the origin in all cases.

3. Results

3.1. Back loads

When compared to the mean result for unloaded locomotion, loading the back with 5% body mass caused a 3.19% increase in net metabolic rate, while a 10% load was associated with a rise of 10.19%. Neither of these values was significantly different from the unloaded condition (5% load: Tukey: $P = 0.951$; 10% load: $P = 0.187$) (Table 1). Loads of 15% caused an 18.29% increase in net metabolic rate, while 20% loads caused a rise of 16.50% (Table 1). These results were significantly different to the unloaded trials (15% load: Tukey: $P < 0.01$; 20% load: $P < 0.05$) (Table 1). When controlling for the effects of bird identity and body mass using GLM, increasing mass of the back load was associated with an increase in net metabolic rate, although there was no influence of load upon resting metabolic rate (Table 2). A one-sample *t*-test indicated that there was no significant difference between the slope of the regression line (calculated from the mean net metabolic rate measured at each load) ($y = 0.953x$, $r^2 = 0.439$) and direct proportionality (one-sample *t*-test: $t = 0.393$, $df = 81$, $P > 0.05$) (Fig. 1). GLM indicated that loading did not affect kinematic parameters during locomotion (Table 3).

3.2. Sternal loads

Compared to the values for unloaded trials, all sternal loads were associated with a significant increase in net metabolic rate. 5% loads were associated with a 13.71% increase in net metabolic rate (Tukey: $P < 0.01$) (Table 1). Addition of 10% load caused an increase in net metabolism of 25.40% (Tukey: $P < 0.001$), while loads of 15% were associated with a rise of 30.65% (Tukey: $P < 0.001$) (Table 1). No significant difference between the rise in metabolic rate caused by 10% and 15% loads was detected (Tukey: $P = 0.59$). After controlling for the variation in body mass and individual goose using GLM, there was a strong relationship between increasing load and metabolic rate during locomotion, while resting rate was unaffected by loading condition (Table 2). Linear regression indicated that net metabolic rate increased by over twice the fractional mass increase ($y = 2.289x$, $r^2 = 0.814$). The slope of this line was significantly higher than the equivalent line for back loading (2-sample *t*-test: $t = 6.7477$, $df = 127$,

Table 1
Summary data for loading trials. Load is described as a percentage of body mass (M_b). Metabolic rate during rest and exercise is presented as oxygen consumption (ml min^{-1}) and after transformation to metabolic power (W). For each trial the resting metabolic rate (W) was subtracted from the total rate (W) measured during locomotion. This net metabolic rate is presented for all unloaded and loaded experiments, in addition to the change from unloaded rate. *P* values calculated using Tukey tests are included to indicate statistical differences between loaded and unloaded metabolic rate.

Location	Load (%M_b)	*n* (kg)	Mean M_b (kg) (ml O_2 min^{-1})	Resting MR (ml O_2 min^{-1})	Exercise MR	Resting MR (W)	Exercise MR (W)	Net metabolic rate (W)	% Δ net metabolic rate	*P*
Back	0	20	1.80 ± 0.04	28.35 ± 1.58	72.72 ± 1.88	9.60 ± 0.50	24.80 ± 0.64	15.20 ± 0.51		
	5	24	1.84 ± 0.04	29.52 ± 1.78	75.37 ± 2.41	9.89 ± 0.54	25.56 ± 0.74	15.69 ± 0.42	3.19 ± 2.78	0.951
	10	20	1.83 ± 0.05	30.00 ± 1.55	78.59 ± 2.01	9.95 ± 0.47	26.70 ± 0.67	16.75 ± 0.57	10.19 ± 3.75	0.187
	15	18	1.82 ± 0.05	24.75 ± 1.57	77.59 ± 2.28	8.42 ± 0.45	26.40 ± 0.69	17.98 ± 0.50	18.29 ± 3.28	<0.01
	20	20	1.81 ± 0.04	30.51 ± 1.42	82.51 ± 2.02	10.43 ± 0.44	28.13 ± 0.64	17.71 ± 0.47	16.50 ± 3.11	<0.05
Sternum	0	18	1.89 ± 0.04	25.93 ± 1.51	72.16 ± 1.88	8.78 ± 0.46	24.70 ± 0.62	15.93 ± 0.44		
	5	19	1.91 ± 0.04	25.51 ± 0.94	77.96 ± 1.61	8.66 ± 0.28	26.77 ± 0.50	18.11 ± 0.27	13.71 ± 1.71	<0.01
	10	18	1.89 ± 0.04	27.82 ± 1.24	85.57 ± 1.93	9.11 ± 0.37	29.08 ± 0.57	19.97 ± 0.41	25.40 ± 2.57	<0.001
	15	12	1.89 ± 0.04	26.13 ± 1.51	86.32 ± 1.42	8.75 ± 0.49	29.55 ± 0.44	20.81 ± 0.70	30.65 ± 4.40	<0.001
Leg	0	19	1.87 ± 0.03	28.57 ± 1.61	72.07 ± 2.37	9.48 ± 0.45	24.16 ± 0.70	14.68 ± 0.62		
	2	20	1.88 ± 0.03	30.95 ± 1.65	77.22 ± 2.30	10.12 ± 0.50	25.84 ± 0.74	15.72 ± 0.60	7.05 ± 4.07	0.48
	5	21	1.87 ± 0.03	27.37 ± 1.21	77.77 ± 2.27	9.22 ± 0.38	26.58 ± 0.75	17.36 ± 0.65	18.25 ± 4.44	0.01

$P < 0.001$) (Fig. 1). Kinematic parameters were not found to change significantly with load attachment, although stance duration varied between geese (Table 3).

3.3. Distal leg loads

Although loading the tarsal segment by 2% of body mass increased the metabolic cost of locomotion by 7.05%, this effect was not statistically different from unloaded trials (Tukey: $P = 0.483$) (Table 1). Increasing the combined load to 5% caused a significant 18.25% rise in metabolic rate (Tukey: $P = 0.010$) (Table 1). After accounting for the variation in metabolic rate caused by bird mass, a clear relationship with increasing load was established using GLM, while no effect upon resting metabolic rate was detected (Table 2). The slope of the regression line between load and metabolic rate ($y = 3.634x$, $r^2 = 0.354$) was significantly different from the back loading line (2-sample *t*-test: $t = 3.416$, $df = 119$, $P < 0.001$) (Fig. 1). However, no difference between the slopes of leg and sternal regression lines was found (2-sample *t*-test: $t = 1.6983$, $df = 86$, $P > 0.05$).

Tarsal loading caused a significant increase in stride length (Table 3). Adding a 5% load caused stride length to increase by 9.62% (ANOVA: $P = 0.03$). Correspondingly, swing duration was found to significantly increase with load (Table 3), with a 5% load associated with a 15.68% swing time increase (ANOVA: $P < 0.001$). GLM failed to detect an effect of load upon the duration of the stance phase (Table 3). Load had a significant effect on stride frequency (Table 3), for example a 5% load caused a significant reduction in stride frequency of 8.89% (ANOVA: $P = 0.026$).

Table 2
Outcome of GLM analyses which determined the proportion of variation in metabolic rate attributable to load condition, body mass and goose identity. Load has no effect on resting rate but has a considerable influence on the metabolic rate during locomotion.

Location		*df*	*F*			*P*		
			Load	Goose	Mass	Load	Goose	Mass
Back	Resting	102	0.008	4.746	27.43	0.93	0.032	<0.001
	Exercise	102	24.337	0.767	0.383	<0.001	0.383	0.112
		102	21.899	*	*	<0.001	*	*
Sternum	Resting	67	0.344	6.968	4.645	0.559	0.010	0.035
	Exercise	67	71.347	2.123	3.928	<0.001	2.123	0.052
		67	67.624	*	*	<0.001	*	*
Leg	Resting	60	0.567	1.402	20.196	0.454	0.241	<0.001
		60	0.587	*	21.474	0.447	*	<0.001
	Exercise	60	11.067	1.372	11.307	0.002	0.246	0.001
		60	10.896	*	10.697	0.002	*	0.001

Parameters which had a non-significant effect on metabolic rate were removed from subsequent GLM analyses, and are denoted by an asterisk.

4. Discussion

Net metabolic rate (the difference between metabolic rate during locomotion and resting metabolic rate) was calculated for each unloaded and loaded trial. During our experiments the applied loads had no effect on resting metabolic rate. Previous research in birds suggests that there is little change in blood flow to tissues that are not directly involved in locomotion from rest to exercise (Ellerby et al., 2005). Therefore we regard the increase in metabolic rate during exercise to be the most appropriate measure of load-carrying economy. Our use of net metabolic rate is in line with previous research investigating the effects of loading in humans and guinea fowl (Griffin et al., 2003; Grabowski et al., 2005; Marsh et al., 2006). By using the metabolic rate calculated from birds during the day, our measure of resting rate is likely to be higher than a comparable resting rate taken during the inactive night phase (Aschoff and Pohl, 1970a; Aschoff and Pohl, 1970b). Therefore, the net metabolic rate presented in this paper will be lower than if we had used the

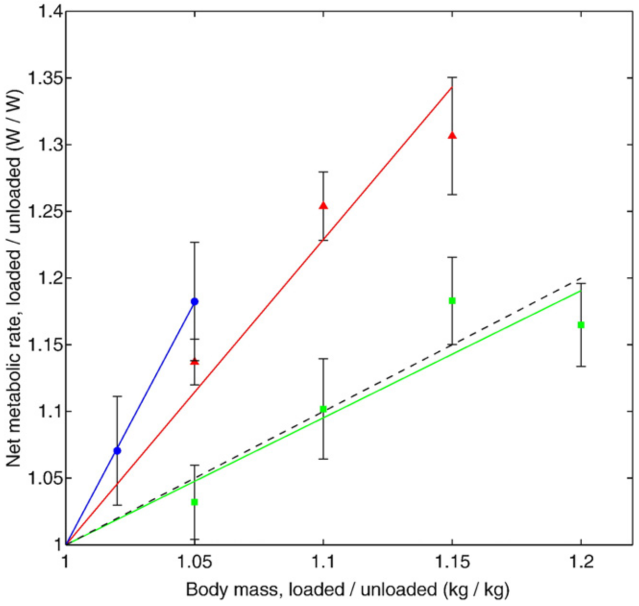

Fig. 1. Loaded/unloaded net metabolic rate plotted against loaded/unloaded body mass during walking at 0.75 ms^{-1}. Vertical bars represent the standard error of the means for net metabolic rate. Green squares represent data from back-loaded geese; red triangles represent data on sternally loaded birds; blue circles show the results of distal limb loading. Each loading condition has a corresponding regression line which was calculated from mean metabolic mass values. The dashed line is included for comparison and represents direct proportionality between increasing metabolic rate and increasing mass.

Table 3
Results of GLM analyses which described the variation in kinematic parameters caused by load condition, body mass and goose identity.

Location	Parameter	*df*	*F*			*P*		
			Load	Goose	Mass	Load	Goose	Mass
Back	Stance duration	30	2.435	25.184	3.067	0.131	<0.001	0.092
		30	2.622	28.714	*	0.144	<0.001	*
	Swing duration	30	0.593	1.870	6.722	0.448	0.183	0.015
		30	0.574	*	5.833	0.455	*	0.028
	Stride frequency	30	1.310	16.611	1.862	0.263	<0.001	0.184
		30	1.269	20.324	*	0.270	<0.001	*
	Stride length	30	1.351	18.088	1.558	0.256	<0.001	0.223
		30	1.324	24.245	*	0.260	<0.001	*
Sternum	Stance duration	23	0.708	7.723	0.066	0.411	0.012	0.800
		23	0.695	0.414	*	0.414	0.001	*
	Swing duration	23	0.042	1.556	4.459	0.840	0.227	0.048
		23	0.003	*	2.963	0.957	*	0.100
	Stride frequency	23	0.587	1.802	0.147	0.453	0.195	0.705
		23	0.477	*	*	0.497	*	*
	Stride length	23	0.434	2.600	0.148	0.123	0.148	0.704
		23	0.309	*	*	0.584	*	*
Leg	Stance duration	18	2.531	3.979	0.277	0.134	0.066	0.607
		18	1.817	*	*	0.196	*	*
	Swing duration	18	30.900	1.178	9.063	<0.001	0.296	0.009
		18	30.537	*	8.463	<0.001	*	0.011
	Stride frequency	18	7.385	1.911	1.141	0.017	0.188	0.304
		18	5.566	*	*	0.031	*	*
	Stride length	18	7.062	2.229	1.275	0.019	0.158	0.278
		18	5.071	*	*	0.039	*	*

Non-significant parameters were removed from subsequent GLM analyses and are denoted by an asterisk.

overnight values. Since the objective of this study was to quantify the energetic costs of load carrying in day-active birds, we consider the use of resting rates taken immediately after treadmill locomotion to be appropriate. Indeed, the mean resting rates presented here closely correspond to the season-controlled daylight resting data of Portugal et al. (2007) (approx. 13.5 ml O_2 min^{-1} kg^{-1}), suggesting that oxygen consumption was not unduly affected by the preceding bout of exercise. Furthermore, our data are comparable to the Marsh et al.'s (2006) study of avian load carrying, since both use a resting rate measured during the daylight active phase to calculate net metabolic rate.

4.1. Back loading

The general relationship between net metabolic rate and load magnitude did not differ from direct proportionality, i.e. the cost of carrying additional mass on the back was the same as the weight-specific cost of locomotion. Our results correspond to the relationship described in quadrupedal mammals and humans (Taylor et al., 1980), but differ from the more economical load carrying reported in guinea fowl (Marsh et al., 2006; McGowan et al., 2006). Taylor et al.'s (1980) relationship uses total metabolic rate which, after correction to net metabolic rate (Marsh et al., 2006), indicates that the fractional energetic cost of transporting loads by quadrupedal mammals and humans is slightly greater than the fractional increase in mass, i.e. not directly proportional. Barnacle geese are able to carry back loads with greater metabolic economy than most recorded mammals but more expensively than guinea fowl. No effect of back load on locomotor kinematics was found in the geese, corresponding to previous work in mammals (Taylor et al., 1980; Griffin et al., 2003) and guinea fowl (McGowan et al., 2006). Consequently it seems that back-load carrying in birds is intrinsically cheaper than for the majority of bipedal and quadrupedal mammals. The mechanisms that allow for this economy are not immediately obvious. Birds have anatomical and physiological adaptations to sustain energetically demanding locomotion, such as flight. It may be that an interaction of the highly efficient avian respiratory system (Maina, 2000) with a capability for maintaining high intensity exercise facilitates economical load carrying during terrestrial locomotion. Oxygen delivery to active muscles is likely to be important factor for consideration however more research on the physiology of avian locomotion is required before we can partition the factors that allow economical load carrying.

A conspicuous locomotor difference between these birds and other avian species is their walking gait. While the guinea fowl moves with minimal body roll, the goose has a waddling gait characterised by lateral displacements of the trunk. Anatomical adaptations to swimming, such as relatively short hind-limbs and webbed feet, in the barnacle goose may necessitate the adoption of this seemingly energetically expensive gait. The high cost of locomotion in animals which employ a waddling gait has been attributed to these side-to-side excursions (Fedak et al., 1974; Pinshow et al., 1977), although recent work using penguins also indicates that having a relatively high stride frequency also increases cost (Griffin and Kram, 2000). A consequence of using back loads is a dorsal displacement of the birds' centre of mass. It is conceivable that the magnitude of lateral movements during locomotion may be exaggerated due to the destabilising effect of the additional mass. Assuming a standard avian condition of relatively cheap load carriage, an increase in energy use associated with stabilising body roll may explain the disparity between the results for guinea fowl and barnacle geese. It is possible that the activity of trunk muscles contributes to the elevated energetic requirements of walking and running. For example, the metabolic activity of external intercostal muscles, which help to stabilise body roll in the Canada goose (*Branta canadensis maximus*) (Codd et al., 2005), increases during locomotion in the guinea fowl (Ellerby et al., 2005). Given the paucity of data in the literature, further load-carrying experiments represent an opportunity to quantify the biomechanics and energetics of body roll during locomotion. The superior carrying economy reported for guinea fowl when compared to the barnacle goose may be accounted for by considering the differences in anatomy and physiology. Fibre type and metabolic qualities of the sartorius muscle have been shown to differ between the domestic goose and guinea fowl (Kiessling, 1977). Furthermore, the high cost of locomotion in ducks has been linked to a relative lack of tendon elastic savings, which play an important role in economical locomotion in more cursorial birds (Biewener and Corning, 2001).

Studies in humans indicate that rather than levelling off, the energetic cost of carrying heavy loads increases out of proportion with load mass (Soule et al., 1978; Marsh et al., 2006). Contrastingly, the results presented in this paper suggest no such curvilinear response exists in the barnacle goose. Reports of economical carrying in guinea fowl used back loads equivalent to around 23% of body mass (Marsh et al., 2006; McGowan et al., 2006), rather than a series of loads increasing in mass.. Therefore we cannot ascertain whether cursorial birds have a linear metabolic response to loading such as that seen in the geese. However, the metabolic data from loaded locomotion in guinea fowl and geese suggest that fundamental differences in the anatomy and physiology of birds may enable superior load-carrying economy. Elastic energy storage in the hind-limbs (Baudinette and Biewener, 1998), for example, and increased active stretching of locomotor muscles (McGowan et al., 2006) may assist the relative reduction in load-carrying cost, but the exact mechanisms accounting for this economy remain equivocal.

4.2. Sternal loading

During locomotion with sternal loads the fractional increase in metabolic rate was approximately double the fractional increase in mass. This contrasts with the directly proportional relationship between increasing metabolism and load in back-loaded geese. Both back and sternal loads can be considered to be ‘trunk’ loads according to their location directly above and below the birds' centre of mass. Trunk loads may increase the overall energetic cost of applying force against the ground during locomotion (Taylor et al., 1980). It follows that the elevation in metabolism associated with carrying back and sternal loads is comparable if kinematic parameters do not differ. We found no difference between the kinematics of unloaded and back and sternally loaded birds, although it is possible that changes in the biomechanics and energetics of posture may represent a significant proportion of the elevated metabolic rate. The difference in metabolic rate between back and sternal loads may therefore derive from factors other than those involved in locomotion. Since ventilation in standing birds is intrinsically linked to sternal movements (Zimmer, 1935; Claessens, 2008), we suggest that the extra cost associated with carrying a sternal load may be attributable to the increased work of breathing. Despite reports of the ventilatory costs in birds not exceeding 2% of whole-animal metabolism (Ellerby et al., 2005; Markley and Carrier, 2010), the results presented here suggest that moving a heavy sternum represents a greater energetic burden. However, although we have measured the cost of carrying a sternal load during locomotion, the energetics of specifically moving the sternum cannot be ascertained in this study. Therefore the cost of breathing in the barnacle goose remains unknown and the potential impact of loading at the level of respiratory musculature requires further research.

Given that the metabolic cost of carrying a trunk load is likely to be associated with changes in the forces required for accelerating and decelerating the body, no energetic effect associated with carrying back loads was expected while the bird was resting. However, the increased work of ventilatory movements in geese carrying a sternal load was expected to cause an elevated resting metabolic rate when compared to the unloaded birds. Surprisingly, the expected metabolic increase was not found, suggesting that the confounding effect of bird posture was important. Barnacle geese carrying a sternal load were often observed to sit on the treadmill belt before and after exercise. By moving the centre of mass ventrally, sternal loads may affect postural biomechanics such that the energetic cost of standing is increased. Furthermore, postural differences in breathing mechanics have been described by Codd et al. (2005), who monitored respiratory muscle activity in the giant Canada goose (*B. canadensis maximus*). Standing birds breathe by dorsal–ventral excursion of the ribs and sternum, however, when sternal movement is restricted, for example during sitting, geese can instead ventilate the lungs by lateral flaring of the ribs (Codd et al., 2005). Although the cost of breathing is unknown in the barnacle goose, the change from a standing to sitting posture may indicate a switch to an energetically favourable strategy. Stressing the avian ventilatory system by applying sternal loads may therefore offer an insight into the plasticity of bird breathing. For example, given the complexity of the anatomy and activity of trunk muscles in birds, geese may be able to limit the cost of moving the sternum by recruiting in additional accessory respiratory muscles. For example, ventilatory function has been identified in abdominal muscles by movements of the pelvic region in phase with breathing (Baumel et al., 1990; Carrier and Farmer, 2000).

The plasticity of the respiratory system may also prove essential to meet the energetic demands of locomotion. Constraints upon ventilation by locomotion have been suggested to limit the metabolic stamina of modern lizards (Carrier, 1987). Birds have largely circumvented this mechanical constraint by separating respiratory and locomotor functions (Carrier, 1991). However, the division of labour in hypaxial muscles between these functions remains complicated. While exclusively inspiratory in the resting bird, *Mm. appendicocostales* has a dual locomotor and ventilatory function in walking Canada geese (Codd et al., 2005). Furthermore, abdominal muscles which are respiratory in resting ducks and penguins have a locomotor function during exercise (Boggs et al., 1998; Boggs, 2002). Therefore recruitment of accessory respiratory muscles may not be possible for the walking barnacle goose due to conflict with locomotor requirements. Birds are able to adjust the basic respiratory variables of tidal volume, breathing frequency and the amount of oxygen extracted from inspired air. Knowledge of the physiology of hypaxial muscles under stress coupled with data on these ventilatory parameters may help to unravel the factors limiting locomotor performance in birds.

While the regression analysis indicated a relatively high cost of carrying extra mass on the sternum, there was no significant difference between the metabolic rate for 10% and 15% loads. A lack of statistical power due to a reduced sample size ($N=4$) is a potentially confounding factor since the general trend indicates energy expenditure to increase with a 15% load. We found that geese carrying the heaviest sternal load struggled to maintain the duration of exercise necessary to obtain steady state respirometry traces and often panted at the end of the trial. Previous research using barnacle geese reported even greater rates of oxygen consumption during walking at higher velocities (Ward et al., 2002), suggesting that the maximum metabolic rate attainable during terrestrial locomotion had not been reached in our trials. It therefore seems that factors other than the energetic demand of hind-limb muscles were limiting exercise performance. Fatigue in respiratory muscles has been shown to impose a constraint on locomotor stamina in exercising humans (Mador and Acevedo, 1991). Furthermore, increasing the work of breathing in humans causes redistribution of blood flow away from leg muscles to active respiratory muscles (Harms et al., 1997), thereby limiting the performance of locomotion. It is possible that intense activity of respiratory musculature may therefore constrain oxygen uptake and locomotor stamina in the loaded barnacle geese.

Since we have assumed that the increased cost of ventilation may account for the difference in metabolic rate between trunk-loaded birds, we rely upon the assumption of similar hind-limb muscle dynamics in loaded geese. However a number of factors suggest that this may not be the case. For example, distribution of energy use between muscles in the leg and fibre type recruitment may differ depending upon where loads are placed. Furthermore, despite similar walking kinematics in trunk-loaded geese, potential differences in the magnitude of body roll were not quantified. Conservation of mechanical energy during walking has been demonstrated to increase via the lateral movements in waddling penguins (Griffin and Kram, 2000). Disruption of this energy saving mechanism due to the potentially destabilising effect of load placement may account for a fraction of the increased cost of sternally loaded locomotion. Sternal loads may therefore increase the metabolic rate of locomotion in part due to additional stabilisation requirements for controlling roll and pitch. Further research is necessary to unravel the effects of loading upon stability during locomotion from other potential factors, such as relatively expensive breathing costs. Changes in the pattern of locomotor muscle activation and intensity due to corresponding alterations in breathing mechanics may also account for a proportion of the energetic difference between birds carrying back and sternal loads. Division of whole-organism metabolism into the energetic cost of individual functions is therefore confounded by the integration of ventilation and locomotion.

4.3. Distal limb loading

Research on the energetics of vertebrate locomotion has provided often-contradictory reports on the metabolic cost of moving the legs. Using trunk loads, Taylor et al. (1980) suggested that the force supporting the body while the foot is in contact with the ground accounted for the majority of energy expended during locomotion, thereby indicating that limb movement is metabolically insignificant. Following the rationale of Taylor et al. (1980), which is based upon an analysis of total metabolic rate, the directly proportional relationship between back load and net metabolic rate described in this paper could be interpreted as evidence for an insignificant cost of swinging the hind-limb in barnacle geese. However, the activity of individual hind-limb muscles during locomotion indicates that the cost of swinging the limb accounts for a significant proportion of total energy expenditure (Marsh et al., 2004; Ellerby et al., 2005; Ellerby and Marsh, 2006). The relatively high cost of carrying distal limb loads in barnacle geese corresponds with data from humans, dogs and guinea fowl (Martin, 1985; Steudel, 1990; Marsh et al., 2006). The increased mechanical work required to move the loaded tarsal segment may explain the elevated energetic cost of locomotion (Martin, 1985; Steudel, 1990; Marsh et al., 2006). The large metabolic effect associated with distal limb loading may also be interpreted as further evidence for the significant cost of moving the limb. As expected, resting metabolic rate was not affected by limb loading, the extra expense is only incurred once the leg is moving. Total energy expenditure was increased approximately three-fold under limb-loading conditions, a result which is consistent with previous research in guinea fowl (Marsh et al., 2006). Carrying a 5% load corresponds to an increase of around 9% in stance and swing durations in guinea fowl (Marsh et al., 2006). The kinematics of locomotion in geese differed from these findings; while stance time was found to be unaffected, swing duration increased by almost 16% with a 5% limb load. However, a comparison of guinea fowl and barnacle goose results may be confounded by differences in the range of walking speeds used by Marsh et al. (2006). Goose stride frequency was found to decrease 9% with load, while stride length increased by the same amount. Studies in limb-loaded quadrupeds (Steudel, 1990) and humans (Martin, 1985) have also reported decreased stride frequency.

We cannot discern how the increase in energy expenditure is related to changes in individual muscle activity using whole-organism respirometry. Predicting the changes in hind-limb muscle activity with load is difficult given the anatomical adaptations associated with different primary modes of locomotion in guinea fowl (walking/running) and barnacle geese (flying, swimming). Despite the expectation that limb loads would only affect swing costs, Ellerby and Marsh (2006) highlighted the complexity of the muscular response to carrying extra mass by describing a substantial increase in both stance and swing-phase muscles in guinea fowl. The increased swing duration in the walking goose indicates that hind-limb muscles may struggle to decelerate the loaded limb. Therefore musculature which brakes the hind-limb during the swing phase may be expected to have an increased metabolic rate as seen in the guinea fowl (Ellerby and Marsh, 2006), perhaps due to a greater intensity of activity or a switch to less economical muscle fibre types. Energetic costs are clearly incurred when carrying limb loads, but the difference in kinematics between guinea fowl and geese suggests that adaptations to different forms of locomotion are associated with novel responses to loading.

5. Conclusions

(1) This study has shown that there is a directly proportional relationship between back-load mass and metabolic rate. When considered together with the data from guinea fowl, birds appear to have unique biomechanical and physiological specialisations that facilitate energetically economical loaded locomotion. This paper highlights the importance of studying a series of loads when considering the fundamental mechanisms that govern the cost of locomotion.

(2) Using sternal loads to manipulate the work of breathing, it seems that ventilatory costs in the barnacle goose may be higher than predicted from research in guinea fowl, although the actual cost of breathing remains equivocal. Our results suggest that there may be significant energetic costs associated with flight muscle hypertrophy in birds preparing for migration (Butler et al., 1998; (Dietz et al., 1999); Portugal et al., 2009). However, birds may be expected to have mechanisms that mitigate any rise in costs such as a functional plasticity in hypaxial muscles and postural changes.

(3) The relatively high energetic cost of moving distal limb loads in the barnacle goose is similar to earlier work in mammals and guinea fowl. The increased work of moving the tarsus during the swing phase suggests a cost to moving the limb, in addition to producing force to support body weight during stance.

Acknowledgements

We would like to thank Dr. Robert Nudds for assistance with respirometry and valuable comments on earlier versions of this manuscript. This research was supported by the BBRSC through G/011338/1 awarded to JRC a DTA to PGT. We are also supported by a Capacity Building Award in Integrative Biology to the University of Manchester funded by the BBSRC, BPS, HEFCE, KTN and the MRC, UK.

Appendix A

Tables containing information on the number of unloaded and loaded trials in which each bird was used. Further data is included to show the dates of trials and how often each goose was used on a specific day.

Number of trials per goose for each load.

Goose	Back load				
	0%	5%	10%	15%	20%
1	4	4	3	3	4
5	4	4	3	3	3
7	4	3	3	3	3
11	3	3	3	3	4
M	2	3	3	3	3
L	3	7	5	3	3

Goose	Sternal load			
	0%	5%	10%	15%
1	3	3	3	3
6	3	3	3	x
9	3	4	3	x
11	3	3	3	3
M	3	3	3	3
L	3	3	3	3

Goose	Leg load		
	0%	2%	5%
1	3	4	4
5	3	3	3
9	3	3	3
11	4	3	3
M	3	4	5
L	3	3	3

(continued on next page)

Appendix A (*continued*)
Number of trials by date for each goose.

Goose	Date of back-load trials													
	11/02/2009	12/02/2009	16/02/2009	17/02/2009	25/02/2009	26/02/2009	02/03/2009	04/03/2009	05/03/2009	10/03/2009	11/03/2009	12/03/2009	20/03/2009	24/03/2009
1	x	x	x	x	x	x	x	2	1	5	6	3	1	x
5	x	1	2	3	3	4	2	1	1	x	x	x	x	x
7	x	2	2	3	3	2	2	1	1	x	x	x	x	x
11	x	3	4	4	x	x	2	1	1	x	x	x	1	x
M	x	x	x	x	x	x	x	2	x	3	6	3	x	x
L	1	3	4	3	x	2	2	1	2	x	x	x	x	3

Goose	Date of sternal load trials									
	13/02/2009	18/02/2009	20/02/2009	23/02/2009	24/02/2009	25/02/2009	03/03/2009	06/03/2009	09/03/2009	10/03/2009
1	x	x	x	x	x	x	3	4	5	x
6	x	x	x	x	5	2	2	1	x	x
9	2	1	2	1	x	x	x	4	x	x
11	x	1	2	4	2	x	1	x	x	x
M	x	3	2	4	2	x	1	x	x	x
L	x	2	2	3	3	2	x	x	x	x

Goose	Date of leg load trials				
	20/03/2009	21/03/2009	23/03/2009	24/03/2009	25/03/2009
1	3	3	3	1	1
5	x	2	5	2	x
9	x	3	3	2	1
11	3	x	2	3	2
M	2	3	2	3	2
L	x	4	3	x	2

Appendix B

A typical oxygen consumption trace (goose ‘L’, 15% back load; 17/2/09) including event markers: (a) the goose is allowed to enter the respirometry chamber after a baseline measurement of ambient air is taken; (b) the treadmill belt is started and its velocity is gradually increased to 0.75 ms^{-1}; (c) the treadmill belt is stopped and the goose allowed to rest until fully recovered; (d) the goose is removed from the respirometry chamber and a baseline measurement is recorded. An increase in oxygen consumption is observed immediately after removal of the bird due to the effect of the animal handler breathing into the chamber. Highlighted areas correspond to the periods chosen for analysis of exercise and resting metabolic rate.

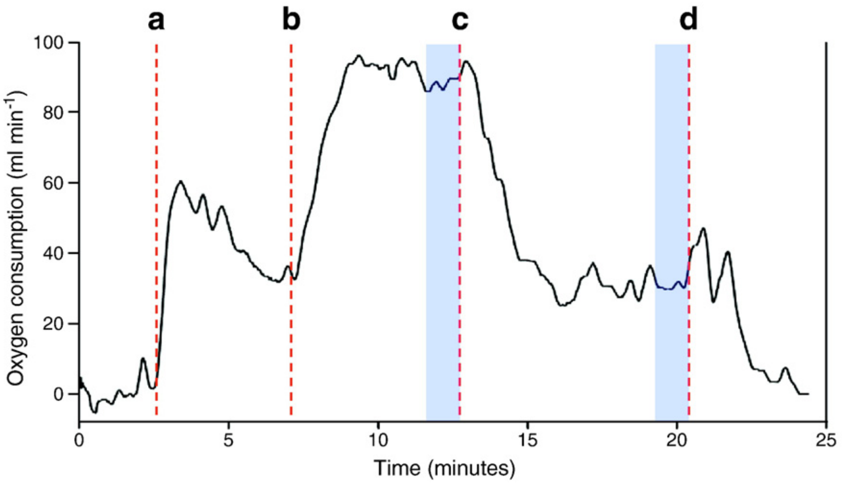

References

Aschoff, J., Pohl, H., 1970a. Rhythmic variations in energy metabolism. Fed. Proc. 29, 1541–1552.

Aschoff, L., Pohl, M., 1970b. Der ruheumsatz von vogeln als funktion der tagesziet und der korpergrosse. J. Ornithol. III, 38–47.

Bastien, G.J., Schepens, B., Willems, P.A., Heglund, N.C., 2005. Energetics of load carrying in Nepalese porters. Science 308, 1755.

Baudinette, R.V., Biewener, A.A., 1998. Young wallabies get a free ride. Nature 395, 653–654.

Baumel, J.J., Wilson, J.A., Bergren, D.R., 1990. The ventilatory movements of the avian pelvis and tail: function of the muscles of the tail region of the pigeon (*Columba livia*). J. Exp. Biol. 151, 263–277.

Biewener, A.A., Corning, W.R., 2001. Dynamics of mallard (*Anas platyrynchos*) gastrocnemius function during swimming versus terrestrial locomotion. J. Exp. Biol. 204, 1745–1756.

Boggs, D.F., 2002. Interactions between locomotion and ventilation in tetrapods. Comp. Biochem. Physiol. 133, 269.

Boggs, D.F., Butler, P.J., Wallace, S.E., 1998. Differential air sac pressures in diving tufted ducks *Aythya fuligula*. J. Exp. Biol. 201, 2665–2668.

Brackenbury, J.H., Avery, P., 1980. Energy consumption and ventilatory mechanisms in the exercising fowl. Comp. Biochem. Physiol. 66, 439–445.

Brody, S., 1945. Bioenergetics and Growth. Reinhold, New York, USA.

Butler, P.J., Woakes, A.J., Bishop, C.M., 1998. Behaviour and physiology of Svalbard Barnacle Geese *Branta leucopsis* during their autumn migration. J. Avian Biol. 29, 536–545.

Calder, W.A., King, J.R., 1975. In: Farner, D.S., King, J.R. (Eds.), Thermal and Caloric Relations of Birds. : Avian Biology, vol. IV. Academic Press, New York, pp. 259–413.

Carrier, D.R., 1987. The evolution of locomotor stamina in tetrapods: circumventing a mechanical constraint. Paleobiology 13, 326–341.

Carrier, D.R., 1991. Conflict in the hypaxial musculo-skeletal system: documenting an evolutionary constraint. Am. Zool. 31, 644–654.

Carrier, D.R., Farmer, C.G., 2000. The evolution of pelvic aspiration in archosaurs. Paleobiology 26, 271–293.

Claessens, L.P.A.M., 2008. The skeletal kinematics of lung ventilation in three basal bird taxa (emu, tinamou, and guinea fowl). J. Exp. Zool. A 311, 586–599.

Codd, J.R., Boggs, D.F., Perry, S.F., Carrier, D.R., 2005. Activity of three muscles associated with the uncinate processes of the giant Canada goose *Branta canadensis maximus*. J. Exp. Biol. 208, 849–857.

Dial, K.P., Goslow Jr, G.E., Jenkins, J.F.A., 1991. The functional anatomy of the shoulder in the European starling (*Sturnus vulgaris*). J Morphol. 207, 327–344.

Dietz, M.W., Piersma, T., Dekinga, A., 1999. Body-building without power training: endogenously regulated pectoral muscle hypertrophy in confined shorebirds. J. Exp. Biol. 202, 2831–2837.

Ellerby, D.J., Marsh, R.L., 2006. The energetic costs of trunk and distal-limb loading during walking and running in guinea fowl *Numida meleagris*: II. muscle energy use as indicated by blood flow. J. Exp. Biol. 209, 2064–2075.

Ellerby, D.J., Henry, H.T., Carr, J.A., Buchanan, C.I., Marsh, R.L., 2005. Blood flow in guinea fowl *Numida meleagris* as an indicator of energy expenditure by individual muscles during walking and running. J. Physiol. 564, 631–648.

Fedak, M.A., Pinshow, B., Schmidt-Nielsen, K., 1974. Energy cost of bipedal running. Am. J. Physiol. 227, 1038–1044.

Grabowski, A., Farley, C.T., Kram, R., 2005. Independent metabolic costs of supporting body weight and accelerating body mass during walking. J. Appl. Physiol. 98, 579–583.

Griffin, T.M., Kram, R., 2000. Biomechanics: penguin waddling is not wasteful. Nature 408, 929.

Griffin, T.M., Roberts, T.J., Kram, R., 2003. Metabolic cost of generating muscular force in human walking: insights from load-carrying and speed experiments. J. Appl. Physiol. 95, 172–183.

Harms, C.A., Babcock, M.A., McClaran, S.R., Pegelow, D.F., Nickele, G.A., Nelson, W.B., Dempsey, J.A., 1997. Respiratory muscle work compromises leg blood flow during maximal exercise. J. Appl. Physiol. 82, 1573–1583.

Heglund, N.C., Willems, P.A., Penta, M., Cavagna, G.A., 1995. Energy-saving gait mechanics with head-supported loads. Nature 375, 52–54.

Kiessling, K.-H., 1977. Muscle structure and function in the goose, quail, pheasant, guinea hen and chicken. Comp. Biochem. Physiol. 57, 287–292.

Kram, R., 1996. Inexpensive load carrying by rhinoceros beetles. J. Exp. Biol. 199, 609–612.

Kram, R., Taylor, C.R., 1990. Energetics of running: a new perspective. Nature 346, 265–267.

Lighton, J.R.B., 2008. Measuring metabolic rates. New York: OUP, USA. pp. 84–104.

Mador, M.J., Acevedo, F.A., 1991. Effect of respiratory muscle fatigue on subsequent exercise performance. J. Appl. Physiol. 70, 2059–2065.

Maina, J., 2000. What it takes to fly: the structural and functional respiratory refinements in birds and bats. J. Exp. Biol. 203, 3045–3064.

Maloiy, G.M.O., Heglund, N.C., Prager, L.M., Cavagna, G.A., Taylor, C.R., 1986. Energetic cost of carrying loads: have African women discovered an economic way? Nature 319, 668–669.

Markley, J.S., Carrier, D.R., 2010. The cost of ventilation in birds measured via unidirectional artificial ventilation. Comp. Biochem. Physiol. 155, 146–153.

Marsh, R.L., Ellerby, D.J., Carr, J.A., Henry, H.T., Buchanan, C.I., 2004. Partitioning the energetics of walking and running: swinging the limbs is expensive. Science 303, 80–83.

Marsh, R.L., Ellerby, D.J., Henry, H.T., Rubenson, J., 2006. The energetic costs of trunk and distal-limb loading during walking and running in guinea fowl *Numida meleagris*: I. organismal metabolism and biomechanics. J. Exp. Biol. 209, 2050–2063.

Martin, P.E., 1985. Mechanical and physiological responses to lower extremity loading during running. Med. Sci. Sports Exerc. 17, 427–433.

McGowan, C.P., Duarte, H.A., Main, J.B., Biewener, A.A., 2006. Effects of load carrying on metabolic cost and hindlimb muscle dynamics in guinea fowl (*Numida meleagris*). J. Appl. Physiol. 101, 1060–1069.

Nassar, P.N., Jackson, A.C., Carrier, D.R., 2001. Entraining the natural frequencies of running and breathing in guinea fowl (*Numida meleagris*). J. Exp. Biol. 204, 1641–1651.

Pinshow, B., Fedak, M.A., Schmidt-Nielsen, K., 1977. Terrestrial locomotion in penguins: it costs more to waddle. Science 195, 592–594.

Portugal, S.J., Green, J.A., Butler, P.J., 2007. Annual changes in body mass and resting metabolism in captive barnacle geese (*Branta leucopsis*): the importance of wing moult. J. Exp. Biol. 210, 1391–1397.

Portugal, S.J., Thorpe, S.K.S., Green, J.A., Myatt, J.P., Butler, P.J., 2009. Testing the use/disuse hypothesis: pectoral and leg muscle changes in captive barnacle geese *Branta leucopsis* during wing moult. J. Exp. Biol. 212, 2403–2410.

Soule, R.G., Pandolf, K.B., Goldman, R.F., 1978. Energy expenditure of heavy load carriage. Ergonomics 21, 373–381.

Steudel, K., 1990. The work and energetic cost of locomotion. I. The effects of limb mass distribution in quadrupeds. J. Exp. Biol. 154, 273–285.

Taylor, C.R., Heglund, N.C., McMahon, T.A., Looney, T.R., 1980. Energetic cost of generating muscular force during running: a comparison of large and small animals. J. Exp. Biol. 86, 9–18.

Tickle, P.G., Ennos, A.R., Lennox, L.E., Perry, S.F., Codd, J.R., 2007. Functional significance of the uncinate processes in birds. J. Exp. Biol. 210, 3955–3961.

Tolkamp, B.J., Emmans, G.C., Yearsley, J., Kyriazakis, I., 2002. Optimization of short-term animal behaviour and the currency of time. Anim. Behav. 64, 945–953.

Ward, S., Bishop, C.M., Woakes, A.J., Butler, P.J., 2002. Heart rate and the rate of oxygen consumption of flying and walking barnacle geese (*Branta leucopsis*) and bar-headed geese (*Anser indicus*). J. Exp. Biol. 205, 3347–3356.

White, C.R., Martin, G.R., Butler, P.J., 2008. Pedestrian locomotion energetics and gait characteristics of a diving bird, the great cormorant, *Phalacrocorax carbo*. J. Comp. Physiol. B 178, 745–754.

Wickler, S.J., Hoyt, D.F., Cogger, E.A., Hall, K.M., 2001. Effect of load on preferred speed and cost of transport. J. Appl. Physiol. 90, 1548–1551.

Zimmer, K., 1935. Beiträge zur Mechanik der Atmung bei den Vögeln in Stand und Flug aufgrund anatomischer-physiologischer und experimenteller Studien. Zoologica 88, 1–69.

Chapter 6

A continuum in ventilatory mechanics from early theropods to extant birds

This article is currently under review at *Proceedings of the Royal Society B: Biological Sciences* and is formatted accordingly.

Tickle, P. G., Norell, M. A., Nudds, R. L. and Codd, J. R. A continuum in ventilatory mechanics from early theropods to extant birds.

A continuum in ventilatory mechanics from early theropods to extant birds

Peter. G. Tickle[1], Mark A. Norell[2], Robert L. Nudds[1], and Jonathan R. Codd[1*]

[1]Faculty of Life Sciences, University of Manchester, Manchester, M13 9PT, UK

[2]Division of Paleontology, American Museum of Natural History, 79th Street at Central Park West, New York, NY 10024-5192, USA

*Corresponding author:

Dr. Jonathan R. Codd

Faculty of Life Sciences

University of Manchester

Manchester

M13 9PT

UK

Tel: +44 (0) 161 275 5474

Email: jonathan.codd@manchester.ac.uk

Summary

Shared behavioural, morphological and physiological characteristics are indicative of the evolution of extant birds from maniraptoran dinosaurs. One such shared character is the presence of uncinate processes, bony projections extending from the vertebral ribs. Uncinate processes are integral respiratory structures in modern birds, aiding inspiration and expiration by improving the mechanical advantage of muscles that facilitate rib and therefore sternal movements. Recent research has suggested a respiratory role for these processes in theropod dinosaurs. Here we determine the extent to which these processes are able to affect respiratory movements. Using a geometric model of the rib cage we determined the mechanical advantage, conferred by uncinate processes for movements of the ribs in a theropod dinosaur, *Oviraptor,* and basal bird species *Confuciusornis sanctus, Zhongjianornis yangi* and *Yixiaornis grabaui*, is of the same magnitude as in modern birds. Furthermore, detailed description of the thoracic skeleton in *Confuciusornis sanctus* confirmed uncinate process and sternal form that strongly resembles the morphology of modern birds. We suggest that these skeletal characteristics provide further evidence of a flow-through respiratory system in theropod dinosaurs and early birds, and indicate that uncinate processes may have been an important character in the evolution of a lung air sac system.

Keywords: bird, *Confuciusornis*, uncinate process, ventilation, respiration, sternum

1. Introduction

The origin of birds is one of the great transitions in vertebrate evolution. The discovery of *Archaeopteryx lithographica*, which lived around 150 million years ago in the Jurassic period, provided Thomas Huxley with the stimulus to propose that birds were the direct ancestors of dinosaurs. In the subsequent 150 years the phylogenetic roots of the earliest birds have been controversial. Current evidence, however, such as the fossilised remains of feathered dinosaurs [1], evidence of brooding behaviour [2] osteological traits [3, 4] and histological analysis [5-7] indicate that the origin of Aves is to be found in the maniraptoran theropods (Fig 1). Therefore, by studying the anatomy and physiology of basal birds and their ancestors, the theropod dinosaurs, we can begin to understand the evolutionary pressures that have shaped the modern avian form.

Modern birds possess a highly derived respiratory system that consists of a series of air sacs connected to a rigid, dorsally fixed lung [8]. Caudo-ventral rotation of the ribs together with a ventral excursion of the sternum facilitates inspiration by creating the low pressure necessary for air to flow into the air-sac system. Upon expiration, the ribs move cranio-dorsally, causing a dorsal displacement of the sternum [9, 10] and contraction of the air sacs. This reduction in abdominal air-sac volume causes unidirectional airflow across the parenchymal tissue, where gas exchange takes place. Movements of the sternum that are normally referred to as having a scissor-like movement [11], have been recently identified as elliptical in three basal bird species; the emu (*Dromaius novaehollandiae*), Chilean tinamou (*Nothoprocta perdicaria*) and the helmeted guinea fowl (*Numida meleagris*) [10]. Regardless of the sternum's pathway during respiration it is clear that its displacement is accomplished by an increase in the angle between sternal and vertebral ribs. This increased angle causes a ventral displacement of the distal portion of the sternal ribs. Since the caudal sternal ribs are elongated compared to the cranial sternal ribs, the caudal sternal margin is moved

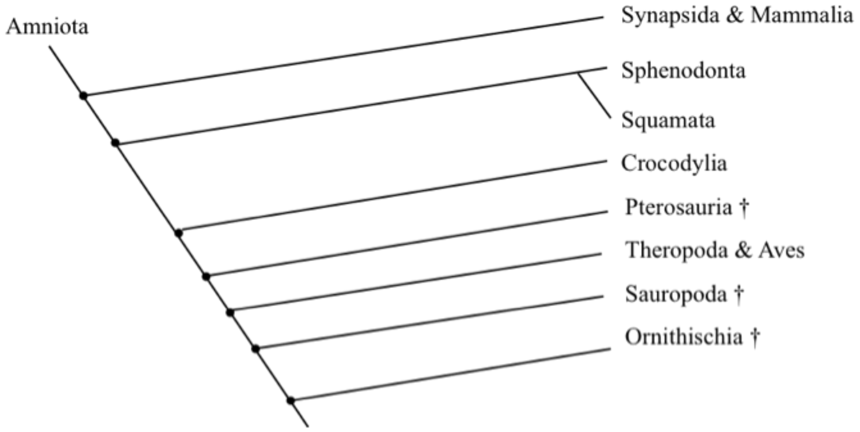

Figure 1A: Summary cladogram of surviving and extinct (†) amniotes. The relationships between *Sphenodon* (Sphenodonta), pterosaurs (Pterosauria) and *Oviraptor* and basal birds (Theropoda and Aves) are shown.

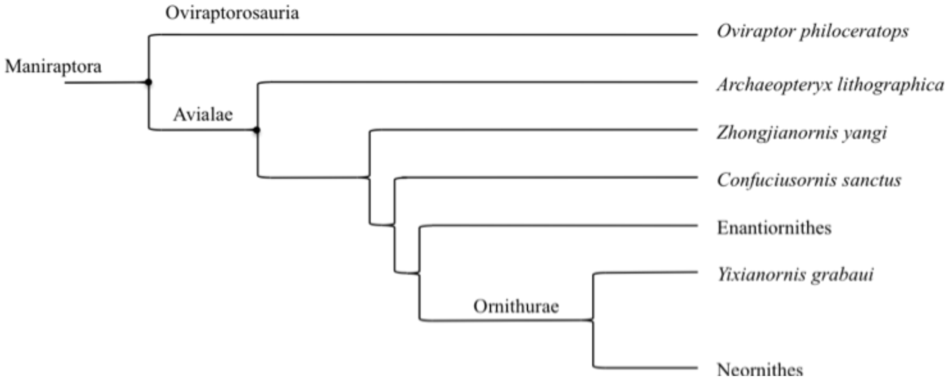

Figure 1B: Overview of the phylogenetic relationships between species used in this study.

further ventrally than the cranial margin [10]. Vertebral ribs in all birds except the screamers (Anhimidae) have ossified hook-like projections - uncinate processes (UP) - that extend caudo-dorsally. These bony structures are integral to facilitating respiratory movements in birds [12]. The *Mm. appendicocostales* project from the proximal margin of the UP and insert onto the following vertebral ribs [13]. Codd et al (2005) used electromyography to demonstrate that UP facilitate inspiration, when contraction of the *Mm. appendicocostales* rotates the ribs to ventrally displace the sternum. The *M. externus obliquus abdominus* attaches to the base of the UP and contraction of this muscle pulls the sternum dorsally during expiration [12]. A geometric model of the thoracic skeleton in extant birds has shown that UP function as levers by improving the mechanical advantage of rib and therefore sternal movement during respiration [14]. Variation in process morphology correlates with adaptations to different forms of locomotion [14]. After accounting for variation in body size, diving birds have the longest, flying and swimming birds have intermediate while walking/running species have the shortest length UP. Furthermore, relatively long UP occur in birds which maintain a high resting metabolic rate [15]. Elongated UP may confer an advantage on the supply of oxygen by improving the mechanical advantage of respiratory muscles and reducing the energetic cost of rib and sternal movements [15].

Uncovering the evolution of respiratory systems is complicated, as soft tissues are not normally preserved in the fossil record. Therefore, understanding the soft tissue anatomy and physiology of extinct species depends upon indirect evidence derived from data on living animals. Assuming that characteristics are shared in basal and derived species in a clade, evolution of the respiratory apparatus can be predicted according to the known ancestry of taxa using extant phylogenetic bracketing [16, 17]. Theropod dinosaurs are phylogenetically bracketed by birds and crocodiles (Fig 1A) [18]. The respiratory system of both birds and crocodiles is characterised by having a heterogeneous lung with an asymmetric branching pattern and it follows therefore that theropod dinosaurs may have had a similar respiratory anatomy [17]. Furthermore, unidirectional airflow in the bird [19] was recently identified in the crocodilian lung [20] suggesting that this condition was present in basal archosaurs, and therefore dinosaurs. The structure of soft tissues can also be predicted according to the osteology of extinct species [17]. For example, pneumatised vertebrae and ribs are indicative of a heterogeneous lung structure and a high compliance breathing respiratory system [21], and have been used to identify the presence of flow-through ventilation in pterosaurs [22] and theropods [23].

Reconstructing the movements of the thoracic skeleton using an analysis of the osteological features in fossils and application of biomechanical principles further adds to our understanding of the mechanics of ventilation in extinct species. Well-developed ossified UP [4] and gastralia (dermal ossifications in the ventral abdominal region: [24]) have been described in non-avian maniraptoran dinosaurs. In *Oviraptor philoceratops* and *Velociraptor mongoliensis* these processes most closely resemble (in length and morphology) those of modern flying and diving birds [4]. Gastralia are a series of narrow cranially pointing chevrons that are formed by the association of slender bony elements angling laterally and caudally from the midline [25]. Retraction and protraction of the gastralia has been suggested to act as an accessory aspiration pump in dinosaurs and primitive archosaurs [24, 25]. This model of ‘cuirassal breathing’ was updated by Codd *et al.* [4] to introduce a mechanism whereby UP facilitated respiratory movements of the skeleton in non-avian maniraptoran dinosaurs; a group hypothesised to have avian-like flow-through ventilation [23, 26]. Assuming the arrangement of abdominal musculature in non-avian maniraptorans was similar to modern birds, the *M. externus obliquus abdiminus* may have attached to the lateral margins of, and pulled dorsally, the sternum (relatively small compared to that of modern birds) and gastral basket. Coupled to the narrowing and widening of the gastralia by the ischiotruncus and rectus abdominus abdominal muscles, UP may therefore have contributed to the airflow around a maniraptoran air sac respiratory system [4]. Crocodiles also have cartilaginous processes and ossified gastralia [27]. When considering the unidirectional airflow in avian and crocodilian lungs [20] the morphology of the UP in these two groups is intriguing. While a respiratory function is known in birds [12], the role of UP in crocodilians is unclear. In addition to pelvic aspiration, facilitated by a rotation of the pubes and displacement of the viscera by shortening of the diaphragmaticus muscle [24, 28-30], it is possible that UP function to aid costal breathing in crocodilians in a manner similar to birds. The tuatara (*Sphenodon spp.*), a primitive lepidosaur, is the oldest extant amniote clade to possess functioning ribs (Fig 1B) [31]. Projecting from the ossified parts of the vertebral ribs, elongated cartilaginous UP are connected to ossified gastralia by projections from the external oblique muscle. Based upon the thoracic skeleton and musculature in *Sphenodon*, Codd *et al.* [4] hypothesised that UP work to move the gastral basket in a mechanism analogous to the sternal movements seen in birds. In contrast to the complex multi-chambered lungs of birds and crocodilians, the simple single-chambered amphibian-like lung anatomy [17] strongly indicates that in the tuatara, air does not move around a flow-through respiratory system. Therefore further examination of the function of UP in the tuatara would be especially interesting since they have developed in a species with distinctly primitive respiratory anatomy.

Understanding the evolution of the highly derived avian breathing apparatus requires an idea of how early forms may have functioned. UP and gastralia have been reported in some basal birds, indicating that a fused gastral basket may have functioned in a mechanism analogous to the sternal aspiration pump of modern birds [4, 24]. Recent research on the function of UP indicates that morphology may have a significant bearing on performance, something that has not been considered in previous reports of their occurrence in basal birds. The geometric model of UP function [14] provides a method to estimate the efficacy of the uncinate process lever action for movement of the ribs, sternum and gastral basket. Here we apply this geometric model to extinct forms that are ancestors of modern birds. Specifically, we aim to determine how the occurrence and morphology of UP may have affected the respiratory movements of the skeleton in the basal bird, *Confuciusornis sanctus*. *C. sanctus* are well described and are typically well preserved making them ideal for the current study. A better understanding of the ventilatory mechanics in extinct birds will provide insight into the evolution of the highly adapted avian respiratory system. We hypothesise that the UP improve the mechanical advantage for rib and sternal movements. Furthermore difference in process morphology is tuned to morphological differences in thoracic anatomy.

2. Methods

All specimens of *C. sanctus* used in the current study were housed in the Senckenberg collection (SMF Av 418; 419; 421; 422; 525). The preserved thoracic skeletons of *C. sanctus* and *Oviraptor philoceratops* (AMNH FR 6517) were photographed using a digital camera (Canon® EOS 350D, Canon®, UK) and analysed using Leica® Application Suite Software (Leica Microsystems, Milton Keynes, UK) to calculate the mechanical advantage provided by the UP for ventilatory movements of the ribs (using the model of Tickle *et al*. [14]). Images of an early ornithurine specimen, *Yixiaornis grabaui*, ([32], figure 4) and *Zhongjianornis yangi*, a species that is phylogenetically basal to *C. sanctus*, ([33], figure 4a) were taken from the literature and also used to estimate the effect of the UP on rib movement. Phylogenetic relationships between species use in this study are summarised in figure 1B. As avian ribcage morphology varies according to locomotor specialisation [14], a selection of extant species (diving: razorbill, *Alca torda*; non-specialists: barnacle goose, *Branta leucopsis*, and kestrel, *Falco tinnunculus*; walking: red-legged partridge, *Alectoris rufa*), were also used for comparison. These extant birds were dissected and the mean angle at which *Mm. appendicocostales* fibres projected from the UP recorded. This angle is important as it affects the predicted point of insertion of the muscle onto the following rib. Angle of muscle fibre projection was applied to the tip of the fossil. Measured (uncinate process length, distance between the ribs at the backbone, angle between the backbone, vertebral rib and distance of muscle insertion down the caudal rib – distance of process insertion down cranial rib) values were then used to calculate the mechanical advantage of the uncinate process system according to the methodology of Tickle *et al*. [14]. The geometric model requires an estimation of muscle length, (which depends upon the distance between ribs and the projection angle of the process), therefore data were only used from fossil forms in which the UP remained attached to the vertebral rib. To minimise inaccuracy in estimated muscle length arising from relative rib position, data were also only collected from UP where the rib from which they extended and the adjacent caudal rib had similar projection angles from the backbone (Table 1). Rib and processes were numbered according to their position beginning at the cranial end. Mean values for mechanical advantage were calculated based on the measurements from three *C. sanctus* specimens (SMF Av 419; 421; 422), while single fossils of *Oviraptor*, *Y. grabaui* and *Z. yangi* were analysed for comparison.

3. Thoracic morphology of *Confuciusornis sanctus*

SMF Av 418

Despite poor overall preservation of the thorax, two vertebral ribs articulate with the backbone on the left hand side. Three UP occur on the left side, extending from the three anterior-most preserved vertebral ribs (Fig. 2A: a; 2B). The first uncinate process projects to the following rib where its tip rests on the lateral costal face (Fig 2B: 1). The tip is preserved and tapers while the proximal shaft is seen as an impression in the substrate. Process morphology is similar to that of the anterior-most process in modern birds, since the process is straight and of a reduced size. There is an impression of the proximal two-thirds of the second process while the distal third is preserved and seen to overlap the following rib (Fig 2B: 2). This process has similar morphology to the first process. The proximal half of the third process is not preserved but an uncinate-shaped impression is apparent (Fig 2B: 3). The distal half overlaps the following two ribs, although they appear to have been disturbed during preservation. All UP project caudo-dorsally from around the same level from the vertebral ribs. On the right-hand side of the fossil, two disarticulated UP overlap the caudal-most preserved rib (Fig 2A: b; 1C) both of which show a characteristic distended base. There is an area of probable gastral elements cranial to the pygostyle and overlying the synsacrum (Fig. 2A: c). The medial gastral elements form a zigzag pattern in accordance with the description of *C. sanctus* by Chiappe *et al* [34]). The gastral elements on the left-hand side adjoin and slightly overlap the corresponding right-side bones, which extend to the preceding (more cranial) left element.

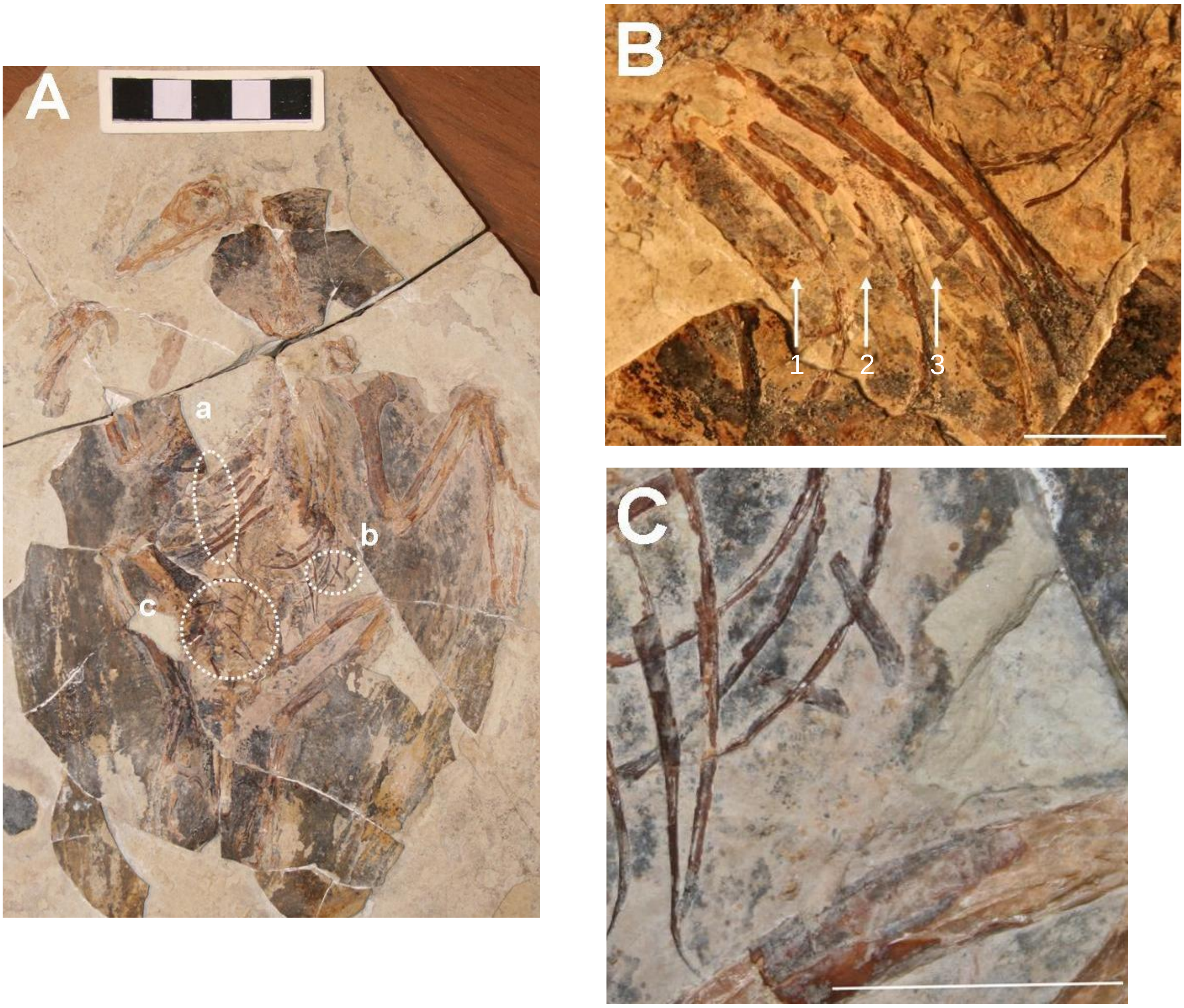

Figure 2: *C. sanctus* Av SMF 418.

(A) Entire fossil showing areas of uncinate process preservation on the left (a) and right hand sides (b). An area of gastralia (c) is preserved anterior to the legs and pelvis. Scale bar, 5cm.

(B) Three UP extending from vertebral ribs on the left side of the specimen. Scale bar, 1cm.

(C) Two disarticulated UP from the right side of the fossil. Scale bar 1cm.

SMF Av 419

There is evidence of a displaced ossified sternum to the right of the backbone immediately posterior to the deltoid crest of the right humerus (Fig 3A: a). Eleven dorsal ribs are preserved on the right side, of which the five cranial-most project from under the lateral margin of the sternal plate. Given the preserved location of two ribs (Fig. 3A: 4 and 5), it is likely that they articulated with the sternum. Impressions of four UP are identifiable on successive (III-VI) ribs on the right side (Fig. 3A: b; 2B). The base of the relatively short first process projects from the midpoint of the third rib. Moving posteriorly, UP 2, 3 and 4 are long, slender and overlap the lateral face of the following rib. Process 2 has a bell-shaped base that increases the area of attachment to the rib. Compared to UP 1, 2 and 3, process 4 projects from the rib at a flatter inclination (Fig. 3B).

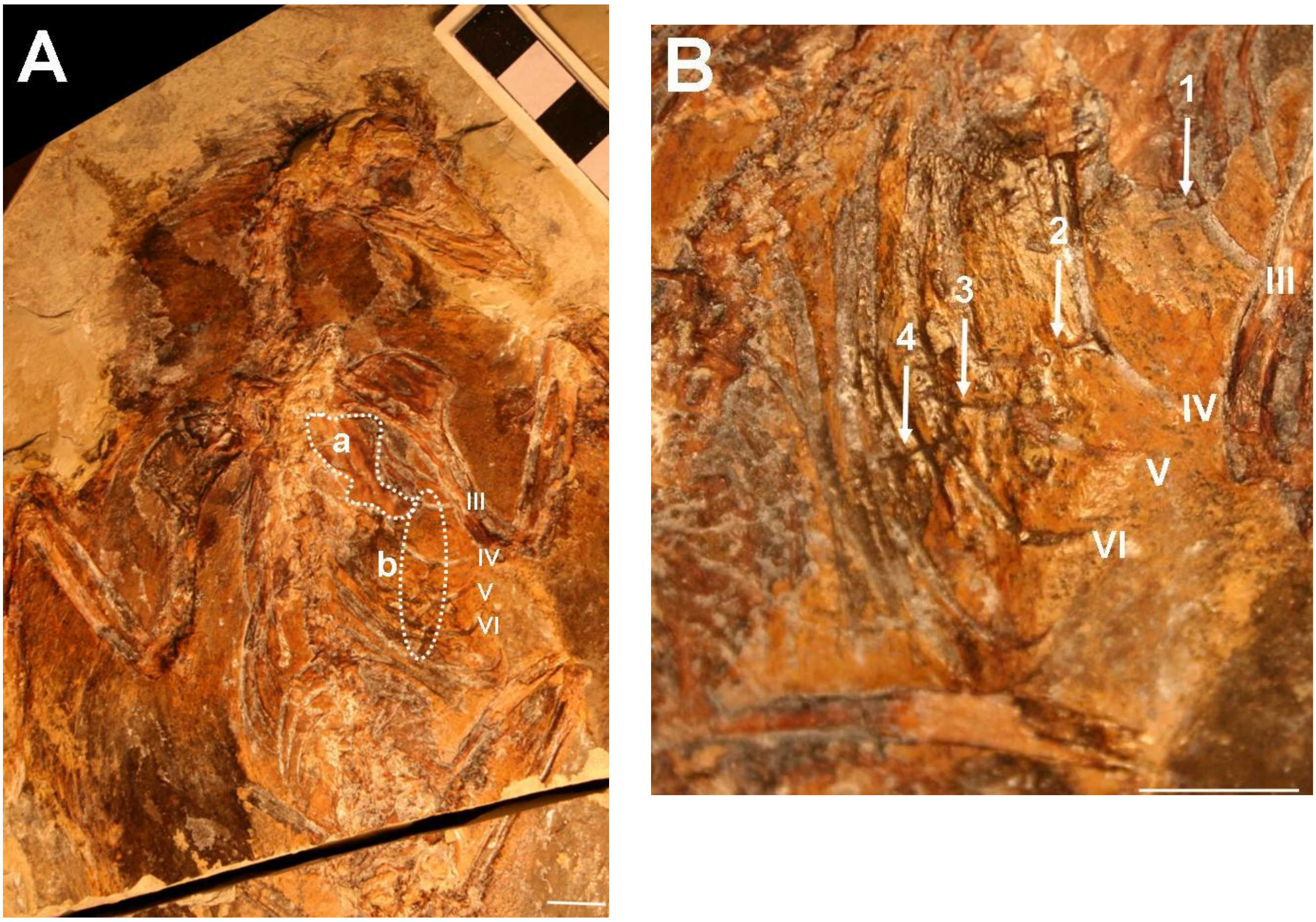

Figure 3: ***C. sanctus*** **Av SMF 419.**

(A) Preserved axial and thoracic skeleton evidence of an ossified sternum (a) and UP (b) extending from ribs III – VI. Scale bar, 1cm.

(B) Close-up view of the UP (1-4) extending from successive ribs (III-VI). Scale bar, 1cm.

SMF Av 421

The thoracic skeleton is very well preserved and is dominated by an ossified sternum (Fig. 4A). The sternum tapers caudally and has a lateral process on the left side. Five complete vertebrae bisect the sternum along the midline (potentially obscuring a sternal keel), while a further four trunk vertebrae extend to the synsacrum. The ribs are well preserved and articulation with the backbone is clearly visible. Fourteen ribs are identifiable on the left and twelve ribs on the right side of the specimen. Five UP (Fig 4B: 1-5) occur on the left side, extending from consecutive vertebral ribs from the third onwards. The first process has a relatively small base and the second process tapers distally but both are obscured by displaced sternal ribs. Process 3 is disarticulated, but in close proximity is a clear impression of an identically shaped process. This process is straight-sided, tapers towards the tip and overlaps the two following vertebral ribs. Process 4 is seen as an impression and overlies the following two ribs. It has characteristic L-shaped morphology with a distended base at the point of attachment to the rib. Process 5 also appears L-shaped but is relatively reduced in size and does not form an attachment with a rib. Two UP project from the ribs on the right-hand side of the specimen (Fig 4C). Process one on the right has identical shape to process 3 on the left side, while the right-hand second process has very similar length and width to process 4 on the left (Table 1; Figs 4B and 4C).

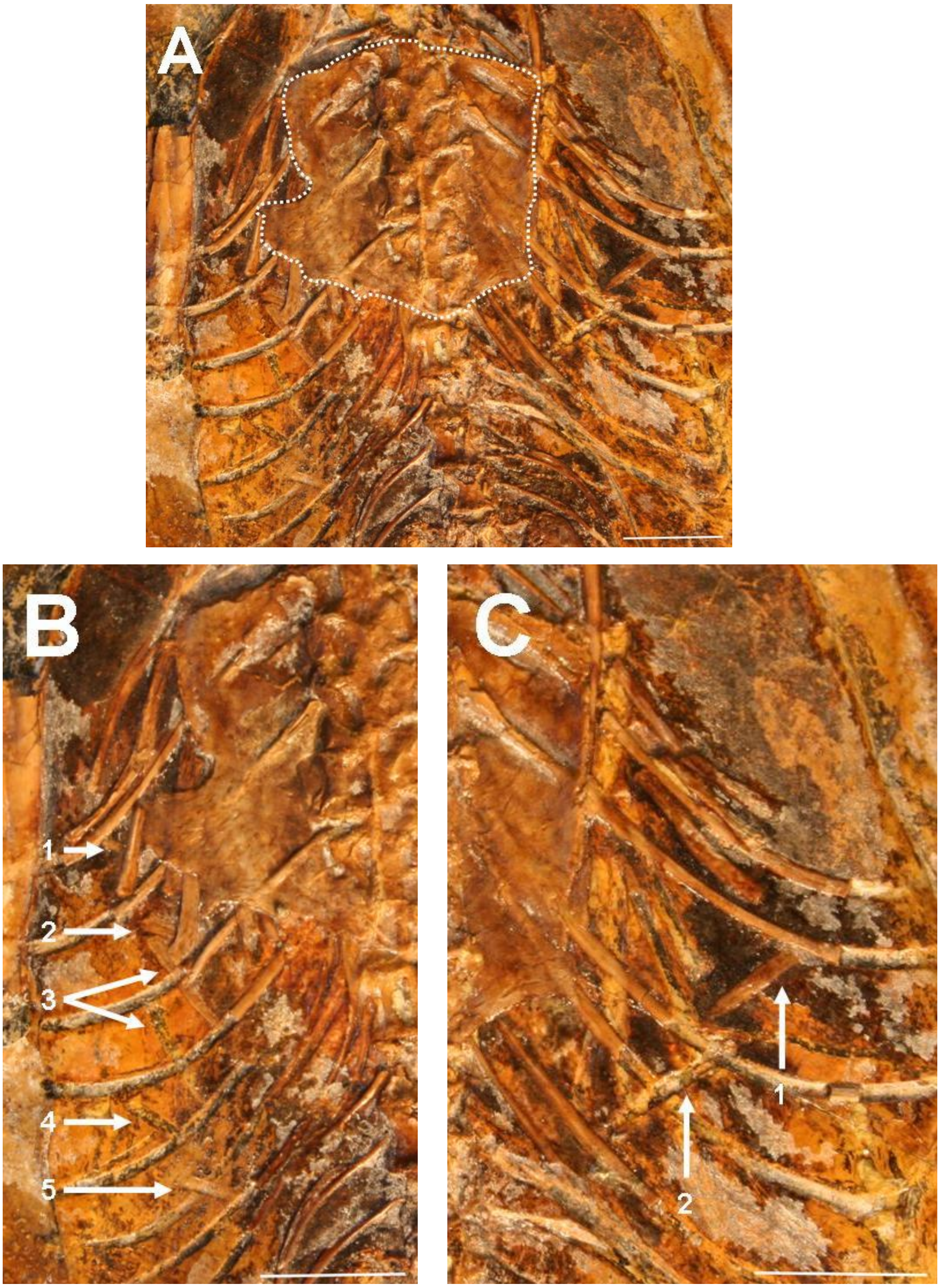

Figure 4: ***C. sanctus*** **Av SMF 421.**

(A) Close-up view of the rib cage and ossified sternum (dashed line). Scale bar, 1cm.

(B) Five UP (1-5) are preserved on the left side of the fossil. Scale bar, 1cm.

(C) Two UP (1-2) are preserved on successive ribs on the right side of the specimen. Scale bar, 1cm.

SMF Av 422

This specimen is preserved showing the right lateral aspect (Fig 5A). Seven vertebral ribs are preserved, the three anterior-most of which are associated with vertebrae. There are clear impressions of two disarticulated UP preserved amongst the vertebral ribs overlying ribs 4 -7 (Fig 5B: IV-VII). The base of the first process is not preserved but the remainder reveals a relatively long and straight morphology. The second process overlaps ribs V, VI and VII and has a reduced tip width relative to the base.

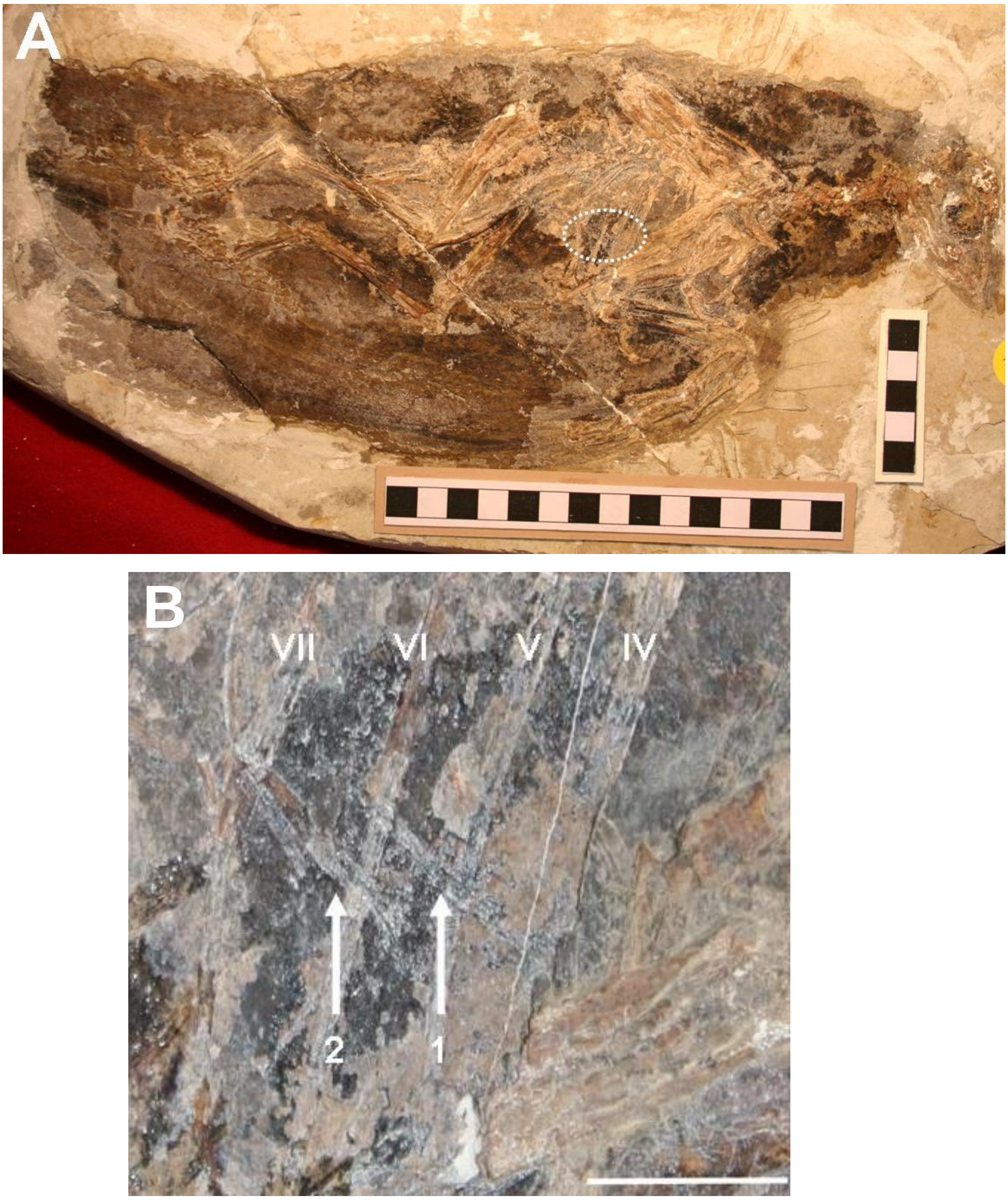

Figure 5: ***C. sanctus*** **Av SMF 422.**

(A) Lateral aspect of whole specimen showing excellent preservation of axial, appendicular and thoracic skeletal elements. Horizontal scale bar, 10cm; vertical scale bar, 5cm.

(B) Impressions of two disarticulated UP (1-2) across consecutive vertebral ribs (IV-VII). Scale bar, 1cm.

SMF Av 525

Av 525 was previously described by Peters and Qiang [35] under a different catalogue number (SMF Av 423). The fossil is characterised by the presence of a well preserved ossified ridged sternum (Fig 6: a). The left side of the sternum is well preserved and has an hourglass shape. While the depth of the keel is reduced compared with those of modern volant birds, it may have been extended by a cartilaginous outgrowth as sometimes seen in modern birds [36]. The anterior ribs are obscured by the sternal margins on the left, whilst the right side is significantly disturbed. There is only partial rib preservation posterior to the sternum on the left and no UP were located in this fossil, although there are at least three pairs of gastralia-like elements projecting caudally from the midline (Fig 6: b).

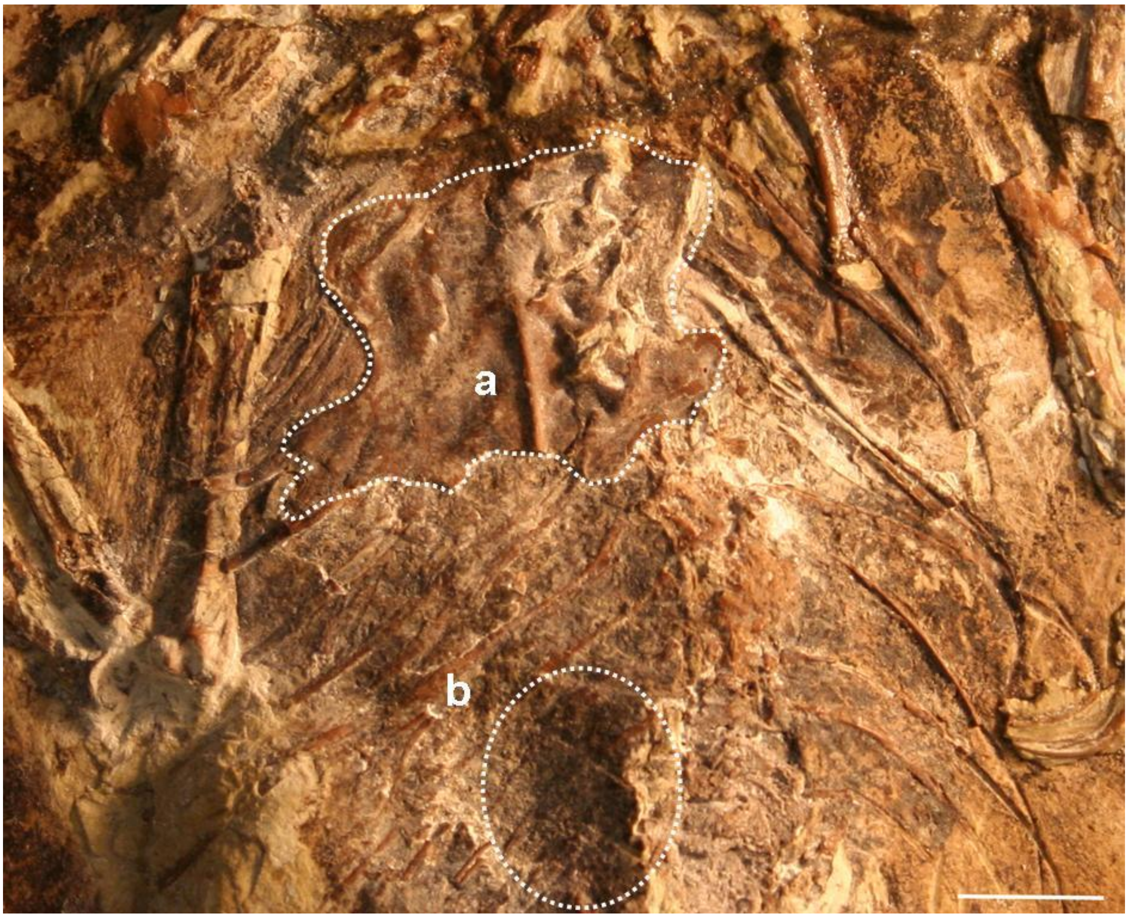

Figure 6: ***C. sanctus*** **Av SMF 525.**

Thoracic morphology is dominated by an ossified sternum (a) and an area of gastral elements (b). Scale bar, 1cm.

4. Breathing mechanics in *C. sanctus*

The characteristic morphology of the UP in *C. sanctus* is similar to that found in extant flying and swimming birds (Fig 7) [14]. Chiappe *et al*. [34] has previously documented long caudodorsally extending UP in several *C. sanctus* specimens (GMV-2130, GMV-2146, GMV-2147 and GMV-2149). Therefore, the reported lack of UP in some *C. sanctus* specimens [37, 38] seems most likely to be a taphonomic artefact. Indeed, the seemingly common disarticulation and loss of UP from fossil specimens may indicate that these elements were connected to the ribs by a cartilaginous attachment and therefore easily lost during preservation or fossil extraction [4]. Ossification and symphysis of UP and ribs is dependant upon developmental stage [39 - 41] and phylogeny (UP in modern birds directly ossify to the rib except in *Apteryx spp.* and Sphenisciformes, where processes are connected via a chondric attachment [42] in modern birds. Absence of UP in fossil birds more primitive than *C. sanctus*, may be due to poor preservation [4, 34]. For example, although UP are reported in *Archaeopteryx* [4], we consider this a misinterpretation of the fossil and conclude that none are present. The description of well-developed UP in the Early Cretaceous *Zhongjianornis yangi* [33], together with evidence from *C. sanctus* and several non-avian maniraptoran taxa [4], provides compelling evidence for conservation of UP in the lineage from theropods to modern birds, as indicated by Chiappe *et al*. [34].

Our estimation of the mechanical advantage of the UP for rib movement (described as the change in mechanical advantage *with* and *without* an uncinate process) in basal birds and *Oviraptor* suggests that the leverage of *Mm appendicocostales* would be improved, just as is found in modern birds (Table 1). Furthermore, the magnitude of increased leverage and the pattern of relatively decreased effectiveness moving caudally correspond to that seen in modern bird taxa [14, 42]. This suggests that UP were able to function as integral respiratory structures before the origin of modern birds and their

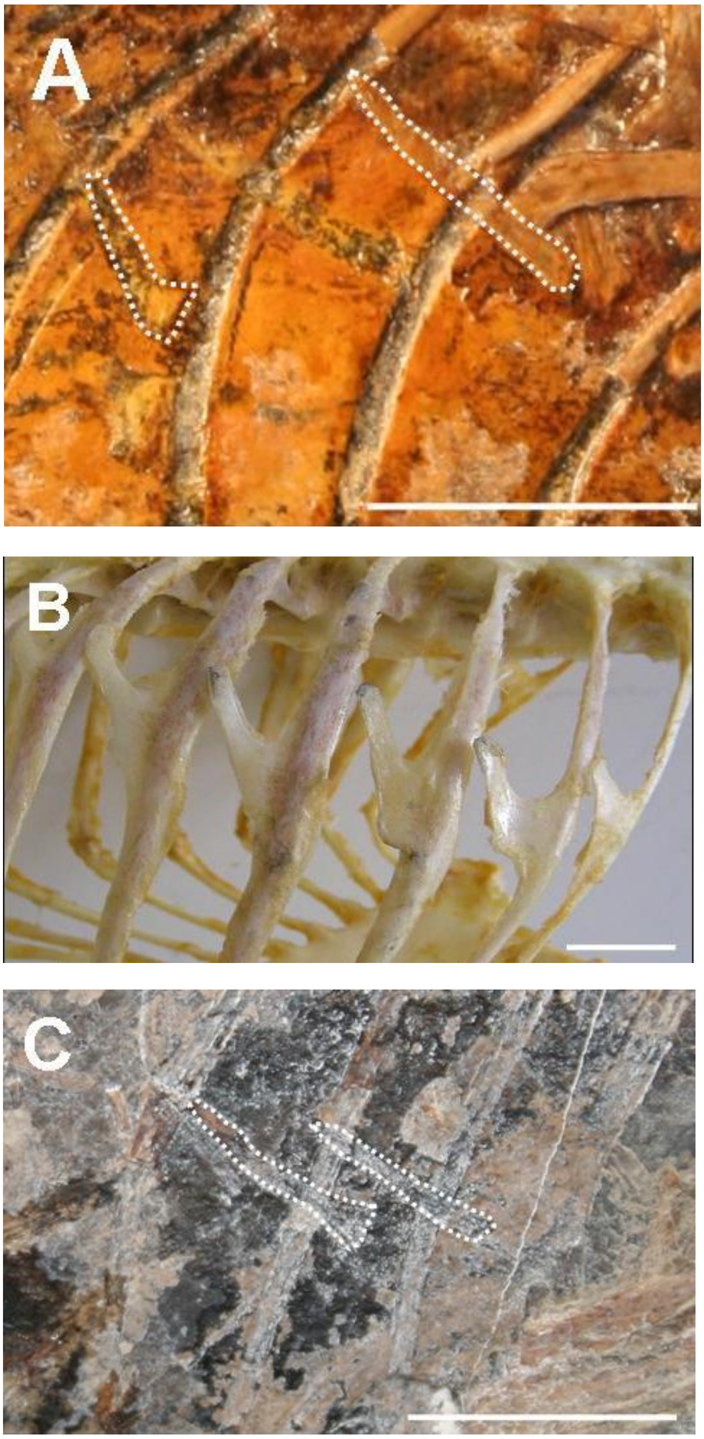

Figure 7: Comparison of UP in a basal bird (*C. sanctus*; SMF Av 421:A, SMF Av 422: C) and a modern bird, the barnacle goose (*Branta leucopsis*): (B). Scale bars, 1cm.

Species	Specimen	UP location	UP	UP length (mm)	UP base width (mm)	Rib length (mm)	Angle of parent rib	Angle of insertion rib	% improvement of M.A.
C. sanctus	SMF Av 418	left-hand side	1	4.30	1.58	12.24	rib is displaced	rib is displaced	-
			2	4.66	1.62	27.77	rib is displaced	rib is displaced	-
			3	6.65	1.43	27.25	rib is displaced	rib is displaced	-
		right-hand side	1	5.11	1.27	process is displaced	rib is displaced	rib is displaced	-
			2	4.28	1.11	process is displaced	rib is displaced	rib is displaced	-
	SMF Av 419	right-hand side	1	obscured	1.09	10.39	obscured	55.1º	-
			2	8.26	2.37	31.77	55.1º	53.5º	297
			3	5.72	1.22	28.67	53.5º	51.5º	187
			4	6.45	1.00	33.36	51.5º	42.8º	-
	SMF Av 421	left-hand side	1	obscured	1.89	26.28	50.5º	49.6º	-
			2	7.01	0.83	31.26	49.6º	50.3º	-
			3	8.54	1.98	26.21	50.3º	47.6º	402.00
			4	8.6	1.51	25.45	47.6º	48.4º	352.00
			5	7.76	1.76	30.35	48.4º	41.9º	-
		right-hand side	1	6.76	1.15	35.91	51.9º	48.9º	235.00
			2	7.87	1.52	40.42	48.9º	44.2º	196.00
	SMF Av 422	right-hand side	1	12.66	1.15	31.26	73.3º	74.3º	127.00
			2	10.84	2.61	36.42	74.3º	73.8º	116.00
Y. grabaui	IVPP V 13631	left-hand side	1	7.58	2.13	obscured	56.0º	51.5º	244.00
Z. yangi	IVPP V 15900	left-hand side	2	7.09	2.66	obscured	61.3º	56.2º	234.00
			4	10.24	2.34	obscured	81.8º	76.3º	110.00
O. philoceratops	AMNH 6517	right-hand side	1	83.89	21.77	184.7	83.1º	79.8º	274.00
			2	109.88	22.92	227.13	79.8º	70.6º	193.00

Table 1: Measurements of uncinate process and rib morphology in three basal bird species, *Confuciusornis sanctus, Yixiaornis grabaui* and *Zhongjianornis yangi* and a maniraptoran theropod, *Oviraptor philoceratops.* Estimated improvement in the mechanical advantage imparted by UP for movements of the ribs is shown.

highly derived morphology. Since the improved mechanical advantage conferred by UP is of a similar magnitude across the species studied it would seem that process morphology is optimised to enable an improved leverage for movements of the ribs and sternum. Therefore, for a given body shape, process length and shape is fine-tuned to function [42]. This optimised model may explain why the superficially similar cursorial ostrich and *Oviraptor* specimens have contrasting UP; while the ostrich has UP of reduced length, *Oviraptor* has long UP reminiscent of modern flying birds [4]. Perhaps the functional requirements of moving large sternal plates [43] and gastralia in the body wall required a longer lever arm than does the ostrich, which has a relatively small sternum and no gastral elements to rotate during breathing.

Species carrying a large sternal mass may be expected to incur relatively expensive ventilatory movements since the breastbone and heavy flight muscles must be displaced ventrally. Recent research on the energetics of load carrying in barnacle geese shows that the metabolic cost of a sternally applied mass is double that of an identical back load [44]. These relatively high energetic costs are driven by an increase in the work required to move the sternum up and down. Therefore, development of large flight muscles attached to a keeled sternum perhaps precipitated a requirement for accessory respiratory structures that decrease the cost of breathing in derived avian taxa. These skeletal structures were already in place by the time of the first birds, as indicated by the rib leverage provided by long UP. It seems that the development of UP as a means of reducing the costs associated with cuirassal ventilation in theropods [4] was later adapted by avian descendants. Therefore, avian uncinate process form is derived from the constraints upon ventilation in dinosaurs; the morphology of avian UP, optimised to help displace a heavy sternum, is a progression on the form necessary to assist movements of the functionally analogous gastral basket in theropods [4]. Interestingly, the occurrence and effectiveness of UP in *C. sanctus* indicates that maximal improvement in mechanical advantage was provided in the most cranial portion of the ribcage (Table 1). This area is adjoined to the keeled sternum, presumably where the heavy pectoral musculature was attached. The L-shape morphology of the UP in *C. sanctus*, identical to that of modern flying birds (Fig 7) [14], would have provided a large insertion area for inspiratory muscles that could offset the increased work necessary to move a heavy sternum. Furthermore, evidence to support the idea that UP initiated movements of the gastral elements in *C. sanctus*, as indicated in theropods [4], is found in specimen SMF Av 419 where UP occur on ribs caudal to those that directly interact with the sternum (Fig 3A & B). Similar preservation is also visible in specimen GMV-2147, shown in Fig. 31 of Chiappe et al [34]. Relatively high mechanical advantage in the cranial ribcage compared to the reduced effectiveness of the lever arm moving caudally is consistent with the hypothesis that UP effected gastral movement, since the mass of these elements would most likely have been lower than the sternum. In the only extant animal to have ossified UP and gastralia, *Sphenodon*, the external oblique muscles extend from the gastral basket to the UP [4, 45] suggesting a ventilatory role for gastralia [24, 25, 46, 47]. Other functions of UP in modern birds include providing stability to the trunk during terrestrial locomotion [12] and providing an attachment site for putative flight muscles [14]. Stabilising the trunk during locomotion was perhaps especially important in large theropod dinosaurs. The large rotational inertia of their trunks and long tails may have significantly impaired turning performance [48] thereby necessitating development of trunk-stabilising musculature associated with long UP. Although feather morphology indicates that *C. sanctus* may not have been capable of flapping flight, the enlarged deltopectoral crest of the humerus suggests that gliding behaviour could have been sustained [49]. Gliding with outstretched wings may have been aided by the development of serratus musculature to stabilise the scapula, which is a site of flight muscle attachment [50]. In modern birds this muscle complex attaches to the vertebral ribs and UP [14, 42, 50]. Modification of UP to enable attachment of muscles that stabilise the shoulder may represent an important step towards gliding and flapping flight. Additionally, the morphology of UP and ability to facilitate ventilatory movements in early avian species indicates that they were already equipped to cope with the demands of flight. Therefore while the origin of flapping flight in birds is unknown, the large energetic demands that are incurred as a result of powered flight were not likely to have been constrained by limits on oxygen delivery. The effective flow-through uncinate process driven ventilatory mechanism was already in place in the earliest avian taxa.

Flapping flight has only evolved in three vertebrate lineages. Pterosaurs were the first vertebrates to develop flapping flight and exhibit skeletal features that show convergent similarities to the derived avian structures associated with powered flight. In addition to the increased surface area for flight muscle attachment provided by a small sternal keel [36], pterosaurs also have ossified dorsal and ventral rib processes, termed 'sternocostapophyses' [22]. These projections are hypothesised to have worked as levers for respiratory movements [22] in a mechanism similar to that described for the UP in birds [14], indicating that ventilatory levers attached to the ribs have developed across evolutionary lineages. Regions of postcranial pneumaticity together with the proposed skeletal ventilatory pump signal the presence of flow-through lung ventilation in pterosaurs [22], analogous to the system proposed for theropods [23] and observed in modern birds and alligators [20]. Well-developed rib levers may therefore be integral components in the evolution of a skeletal aspiration pump that facilitates air-movement around an air-sac flow-through system. Alteration of process form in response to body shape changes, in part driven by locomotor behaviour [14], may be a relatively simple mechanism to maintain sufficient skeletal excursions to aspirate the lung in a highly compliant air-sac system.

A high rate of energy metabolism is characteristic of birds and helps to supply the considerable energy requirements of powered flight [51]. Since we cannot directly determine the anatomy and physiology of fossil species, we must use indirect methods to infer their respiratory biology and rates of energy metabolism. Determination of growth rates from fossil bone histology [5, 7, 52] and the discovery of feathered theropods [1] indicate an elevated metabolism, intermediate between the reptilian and modern avian condition, was likely to have been sustained in early birds and their close non-avialan ancestors. Given the positive correlation between process length and metabolic rate in birds [15], the degree of rib lever development may be considered a correlate of the rate of energy use; the presence of UP (and an efficient flow-through lung) in non-avian theropod dinosaurs may have helped to sustain a metabolic rate that was higher than found in earlier dinosaurs [23]. Therefore the development of flow-through breathing mechanics that encompass an uncinate process driven sternal aspiration pump together with rib and gastral movements may have been instrumental in the diversification from terrestrial to volant niches.

Acknowledgements

We would like to thank Rainer Brocke (Senckenberg Forschungsinstitut und Naturmuseum, Frankfurt) for access to *Confuciusornis sanctus* specimens and the American Museum of Natural History for facilitating access to *Oviraptor* specimens. Additionally, David Armson kindly provided access to a digital camera. This work was funded by the University of Manchester and the Deutsche Forschungsgemeinschaft (DFG 721/1). PGT is supported by a BBSRC DTA.

References

[1] **Xu, X., Norell, M. A., Kuang, X., Wang, X., Zhao, Q. and Jia, C.** (2004). Basal tyrannosauroids from China and evidence for protofeathers in tyrannosauroids. *Nature* **431**, 680-684. (doi: 10.1038/nature02855)

[2] **Norell, M. A., Clark, J. M., Chiappe, L. M. and Dashzeveg, D.** (1995) A nesting dinosaur. *Nature* **378**, 774-776 (doi: 10.1038/378774a0)

[3] **Padian, K. and Chiappe, L. M.** (1998) The origin and early evolution of birds. *Biol. Rev.* **73**, 1-42.

[4] **Codd, J. R., Manning, P. L., Norell, M. A. and Perry, S. F.** (2008). Avian-like breathing mechanics in maniraptoran dinosaurs. *P. Roy. Soc. B* **275**, 157-161. (doi: 10.1098/rspb.2007.1233)

[5] **Chinsamy, A., Chiappe, L. M. and Dodson, P.** (1995). Mesozoic avian bone microstructure: physiological implications. *Paleobiology* **21**, 561-574.

[6] **Erickson, G. M., Rogers, K. C., Varricchio, D. J., Norell, M. A. and Xu, X.** (2007) Growth patterns in brooding dinosaurs reveals the timing of sexual maturity in non-avian dinosaurs and genesis of the avian condition. *Biol. Lett.* **3**, 558-561. (doi: 10.1098/rsbl.2007.0254)

[7] **Erickson, G. M., Rauhut, O. W. M., Zhou, Z., Turner, A. H., Inouye, B. D., Hu, D. and Norell, M. A.** (2009). Was dinosaurian physiology inherited by birds? Reconciling slow growth in *Archaeopteryx*. *PLoS ONE* **4**, e7390. (doi: 10.1371/journal.pone.0007390)

[8] **Powell, F. L.** (2000) Respiration. *n* Avian Physiology 5th Edition (ed. Causey Whitlow, G.) pp. 233-264. Academic Press, New York.

[9] **Zimmer, K.** (1935). Beitrage zur Mechanik der Atmung bei den Vögeln in Stand und Flug. Aufgrund anatomischer-physiologisher und experimenteller Studien. *Zoologica* **88**, 1-69.

[10] **Claessens, L. P. A. M.** (2008). The skeletal kinematics of lung ventilation in three basal bird taxa (emu, tinamou, and guinea fowl). *J. Exp. Zool. A* **311**, 586-599. (doi: 10.1002/jez.501)

[11] **Kardong, K.** (2006) The respiratory system. In *Vertebrates, Comparative Anatomy, Function, Evolution*, pp. 430-433. McGraw-Hill Publishing, New York.

[12] **Codd, J. R., Boggs, D. F., Perry, S. F. and Carrier, D. R.** (2005). Activity of three muscles associated with the uncinate processes of the giant Canada goose *Branta canadensis maximus*. *J. Exp. Biol.* **208**, 849-857. (doi: 10.1242/jeb.01489)

[13] **Schufeldt, R. W.** (1890) The musculature of the trunk. In *The Myology of the Raven*, pp.300-301. London MacMillan and Co.

[14] **Tickle, P. G., Ennos, A. R., Lennox, L. E., Perry, S. F. and Codd, J. R.** (2007). Functional significance of the uncinate processes in birds. *J. Exp. Biol.* **210**, 3955-3961. (doi: 10.1242/jeb008953)

[15] **Tickle, P., Nudds, R. and Codd, J.** (2009). Uncinate process length in birds scales with resting metabolic rate. *PLoS ONE* **4**, e5667. (doi: 10.1371/journal.pone.0005667)

[16] **Witmer, L. M.** (1995) The extant phylogenetic bracket and the importance of reconstructing soft tissues in fossils. In *Functional Morphology in Vertebrate Palaeontology* (ed. J.J. Thompson), pp. 19-33. Cambridge University Press, UK.

[17] **Perry, S. F. and Sander. M.** (2004) Reconstructing the evolution of the respiratory apparatus in tetrapods. *Resp. Physiol. Neurobiol.* **144**, 125-139 (doi: 10.1016/j.resp.2004.06.018)

[18] **Sereno, P. C.** (1997) The origin and evolution of dinosaurs. *Annu. Rev. Earth Pl. Sc.* **25**, 435-489.

[19] **Hazelhoff, E. H.** (1951) Structure and function of the lung of birds. *Poultry. Sci.* **30**, 3-10.

[20] **Farmer, C. G. and Sanders, K.** (2010). Unidirectional airflow in the lungs of alligators. *Science* **327**, 338-340. (doi: 10.1126/science.1180219)

[21] **Perry, S. F.** (2001) Functional morphology of the reptilian and avian respiratory systems and its implications for theropod dinosaurs. In *New perspectives on the origin and early evolution of birds.* (eds J. Gaulthier & L. F. Gall), pp. 429-441. New Haven, CT: Peabody Museum of Natural History, Yale University.

[22] **Claessens, L. P. A. M., O'Connor, P. M. and Unwin, D. M.** (2009). Respiratory evolution facilitated the origin of pterosaur flight and aerial gigantism. *PLoS ONE* **4**, e4497. (doi: 10.1371/journal.pone.0004497)

[23] **O'Connor, P. M. and Claessens, L. P. A. M.** (2005). Basic avian pulmonary design and flow-through ventilation in non-avian theropod dinosaurs. *Nature* **436**, 253. (doi: 10.1038/nature03716)

[24] **Claessens, L. P. A. M.** (2004). Dinosaur gastralia; origin, morphology, and function. *J. Vertebr. Paleaontol.* **24**, 89-106. (doi: 10.1671/A1116-8)

[25] **Carrier, D. R. and Farmer, C. G.** (2000) The integration of ventilation and locomotion in archosaurs. *Am. Zool.* **40**, 87-100. (doi: 10.1093/icb/40.1.87)

[26] **Schachner, E. R., Lyson, T. R. and Dodson, P.** (2009). Evolution of the respiratory system in nonavian theropods: Evidence from rib and vertebral morphology. *Anat. Rec.* **292**, 1501-1513. (doi: 10.1002/ar.20989)

[27] **Hofstetter, R. and Gasc, J.-P.** (1969). Vertebrae and ribs of modern reptiles. In *Biology of the reptilian*, vol. 1 (eds C. Gans, A. d'A. Bellairs & T. S. Parsons), pp. 201-310. London, UK: Academic Press.

[28] **Gans, C. and Clark, B.** (1976) Studies on ventilation of *Caiman crocodilus* (Crocodilia: Reptilia). *Resp. Physiol.* **26**(3), 285-301.

[29] **Carrier, D. R. and Farmer, C. G.** (2000) The evolution of pelvic aspiration in archosaurs. *Palaeobiology* **26**, 271-293.

[30] **Farmer, C. G. and Carrier, D. R.** (2000) Pelvic aspiration in the American alligator (*Allgator mississippiensis*). *J. Exp. Biol.* **203**, 1679-1687.

[31] **Perry, S. F., Klein, W. and Codd, J. R.** (2010) Trade-offs in the evolution of the respiratory apparatus of chordates. In *Cardio-respiratory control in vertebrates* (eds. Glass, M. L. and Wood, S. C.) pp.193-204. Springer-Verlag, Berrlin.

[32] **Clarke, J. A., Zhou, Z. and Zhang, FG.** (2006) Insight in to the evolution of avian flight from a new clade of Early Cretaceous ornithurines from China and the morphology of *Yixianornis grabaui*. *J. Anat.* **208** 287-308.

[33] **Zhou, Z. and Li, F. Z. Z.** (2009). A new Lower Cretaceous bird from China and tooth reduction in early avian evolution. *P. Roy. Soc. B.* **277**, 219-227. (doi: 10.1098/rspb.2009.0885)

[34] **Chiappe, L. M., Shu'an, J., Qiang, J. and Norell, M. A.** (1999). Anatomy and systematics of the Confuciusornithidae (Theropoda: Aves) from the late mesozoic of northeastern China. *B. Am. Mus. Nat. Hist.* **242**, 1-89.

[35] **Peters, D. S. and Qiang, J.** (1999) Mußte *Confuciusornis* klettern? *J. Ornithol.* **140**, 41-50.

[36] **Padian, K.** (1983). A functional analysis of flying and walking in pterosaurs. *Paleobiology* **9**, 218-239.

[37] **Hou, L., Martin, L. D., Zhou, Z. and Feduccia, A.** (1996). Early adaptive radiation of birds: Evidence from fossils from northeastern China. *Science* **274**, 1164-1167. (doi: 10.1126/science.274.5290.1164)

[38] **Peters, D. S.** (1996) Ein nahezu vollständiges Skelett eines urtümlichen Vogels aus China. *Nat. Mus.* **126**(9), 298-302

[39] **Maxwell, E. E.** (2008). Ossification sequence of the avian order Anseriformes, with comparison to other precocial birds. *J. Morphol.* **269**, 1095-1113. (doi: 10.1002/jmor.10644)

[40] **Maxwell, E. E. and Larsson, H. C. E.** (2009). Comparative ossification sequence and skeletal development of the postcranium of palaeognathous birds (Aves: Palaeognathae). *Zool. J. Linn Soc-Lond.* **157**, 169-196. (doi: 10.1111/j.1096-3642.2009.00533.x)

[41] **Tickle, P. G. and Codd, J. R.** (2009). Ontogenetic development of the uncinate processes in the domestic turkey (*Meleagris gallopavo*). *Poultry Sci.* **88**, 179-184. (doi: 10.3382/ps.2008-00349)

[42] **Codd, J. R.** (2010). Uncinate processes in birds: Morphology, physiology and function. *Comp. Biochem. Phys. A* **156**, 303-308. (doi: 10.1016/j.cbpa.2009.12.005)

[43] **Clark, J. M., Norell, M. A. and Chiappe, L. M.** (1999). An Oviraptorid skeleton from the Late Cretaceous of Ukhaa Tolgod, Mongolia, preserved in an avian like brooding position over an Oviraptorid nest. *Am. Mus. Novit.* **3265**, 1-36.

[44] **Tickle, P. G., Richardson, M. F. and Codd, J. R.** (2010). Load carrying during locomotion in the barnacle goose (*Branta leucopsis*): The effect of load placement and size. *Comp. Biochem. Physiol. A* **156**, 309-317. (doi: 10.1016/j.cbpa.2010.01.022)

[45] **Maurer, F.** (1896) Die ventrale Rumpfmuskulatur einiger Reptilien. *Festschrift zum 8. Geburtstage von Carl Gegenbaur.* Engelmann, Leipzig. 1-76.

[46] **Lambe, L. M.** (1917) New genera and species from the Belly River Series (mid Cretaceous). *Contrib. Can. Palaeontol. Geol. Surv.* **3**, 25-81.

[47] **Perry, S. F.** (1983) Reptilian lungs. In *Functional anatomy and evolution*. Berlin, Germany: Springer.

[48] **Carrier, D. R., Walter, R. M. and Lee, D. V.** (2001) Influence of rotational inertia on turning performance of theropod dinosaurs: clues from humans with increased rotational inertia. *J. Exp. Biol.* **204**, 3917-3926.

[49] **Nudds, R. L. and Dyke, G. J.** (2010). Narrow primary feather rachises in *Confuciusornis* and *Archaeopteryx* suggest poor flight ability. *Science* **328**, 887-889. (doi: 10.1126/science.1188895)

[50] **Meyers, R. A.** (1992). Morphology of the shoulder musculature of the American kestrel, *Falco sparverius* (Aves), with implicaitons for gliding flight. *Zoomorphology* **112**, 91-103. (doi: 10.1007/BF01673810) **[52] Erickson, G. M., Rogers, K. C. and Yerby, S. A.** (2001). Dinosaurian growth patterns and rapid avian growth rates. *Nature* **412**, 429-433. (doi: 10.1038/35086558)

[51] **Butler, P. J.** (1991) Exercise in birds. *J. Exp. Biol.* **160**, 233-262.

Chapter 7

General Discussion

Research into the respiratory biology of birds has often overlooked the form and function of a vital component of breathing, the skeletal aspiration pump. Not until recently have researchers re-visited the work of Zimmer (1935), who undertook theoretical research on the mechanics of breathing in birds. While birds were known to breathe by movements of the ribs and therefore sternum, a mechanism in part shared with other amniotes, important characteristics that have enabled birds to develop a high rate of metabolism and a wide range of body shapes are not well understood. Prior to the onset of my PhD research it had been established that uncinate processes, ossified projections extending form the vertebral ribs in birds, were involved in breathing and locomotion in at least one species of bird, the giant Canada goose (*Branta canadensis maximus*) (Codd *et al.*, 2005). Uncinate processes facilitate inspiration and expiration through the activity of associated musculature (Codd *et al.*, 2005). The action of external intercostal musculature associated with these processes also acts to stabilize the body during locomotion (Codd *et al.*, 2005). However, the functions of the uncinate processes remain unexplored in other species. The aim of my PhD is to extend beyond this basic this research on uncinate processes and their function to investigate how diversity in avian body morphology relates to their breathing and locomotion.

Birds ventilate their respiratory system by coordinated movements of the rib cage and sternum. Uncinate processes are an integral component of the skeletal aspiration pump functioning in inspiration and expiration (Codd *et al.*, 2005). Muscles associated with the processes act upon the vertebral ribs and lateral margins of the sternum to facilitate skeletal movements during the ventilatory cycle. While a role in breathing has previously been identified, the mechanism through which uncinate processes elicit respiratory movements of the ribcage was not well understood. Therefore while much research is undertaken on avian physiology, very little is known about a fundamental aspect of their biology, i.e. how birds breathe. Without this knowledge it follows that a basic understanding of issues in avian biology and welfare are currently beyond our reach. Therefore the objective of Chapter 2 was to develop a model of uncinate process function in birds. Duncker (1971) and Welty (1988) proposed that variation in uncinate process morphology might relate to varying locomotor behaviors. Chapter 2 presents the first evidence on the relationship between uncinate process morphology and locomotor specialisation, I also consider the effects of changes in morphology upon process function.

Principal conclusions that can be drawn from the research published and presented in Chapter 2 (and in Tickle et al 2007) relating to the form and function of uncinate processes in extant birds are:

1) Uncinate processes facilitate respiratory movements of the ribs and sternum by improving the leverage of *Mm. appendicocostales* (Tickle *et al.*, 2007).
2) Uncinate processes length and sternal morphology is driven by adaptations to different forms of locomotion (Tickle *et al.*, 2007)
3) Differences in the breathing mechanics of birds may be linked to the morphological adaptations of the ribs and rib cage associated with different forms of locomotion (Tickle *et al.*, 2007).

Based upon these findings and those of Codd *et al.*, (2005), the respiratory function of uncinate processes in birds during rest and walking has now been established. Given there is a strong link between locomotor specialisation and process morphology it is appropriate that other forms of locomotion are studied. Considering their integral role during respiration at rest and during terrestrial locomotion (Codd et a 2005), it is very likely that uncinate processes have a role as respiratory structures in all birds. Therefore patterns of muscle activity may be expected to show broad similarities across birds, independent of locomotor specialisation. However, differences in the anatomy of respiratory muscles in birds adapted to various forms of locomotion (Tickle *et al*., 2007) indicate that there are subtle differences between species at the level of respiratory muscles, in terms of which muscles are active and when for example. To build a more complete picture of what changes in locomotor adaptations mean in terms of breathing mechanics, the properties of muscles should now be studied in a range of species. Changes in anatomy might be connected with alterations in force production, depending upon the mass of the sternum and degree of leverage necessary for the uncinate processes to move the ribs. Therefore by experimentally determining the pattern of muscle activity and activation intensity using EMG (based upon the methods of Codd *et al*., 2005) and muscle length changes using sonomicrometry (based upon the methods of Askew and Ellerby, 2007) we would be in a position to decipher exactly how anatomical changes in muscle size, angle, and force production affect the mechanics of ventilation. Given the switch in ventilatory mechanics due to a change in body posture from sitting to standing (Codd *et al*., 2005) it seems as though there is an inherent plasticity in the respiratory system of birds. This may extend to plasticity in the muscles responsible for producing respiratory movements of the skeleton and potentially indicates a switch in the muscles used to power ventilatory movements (Tickle *et al*., 2007). Therefore, EMG analysis of potential muscles involved in respiration, such as those in the abdomen that may facilitate pelvic aspiration (Baumel *et al*., 1990) and, based upon avian anatomy, the serratus muscles that extend from the scapula to the uncinate processes (Tickle *et al*., 2007), need to be undertaken in birds at rest and whilst undergoing various forms of locomotion, for example during terrestrial and volant locomotion.

The ventilatory movements of the ribs and sternum that are facilitated by the uncinate processes make their absence in the screamers (Anhimidae) and almost complete loss in the emu an interesting opportunity to study plasticity in ventilatory mechanics. Very little if anything in biology is absolute, meaning it is not surprising that in the absence of uncinate processes, respiration is still possible. The occurrence of processes in the dinosaur ancestors of birds (Codd *et al.*, 2008) indicates that the ancestral state of avian breathing mechanics included functioning uncinate processes for rib movements. It seems, therefore, that the subsequent loss of uncinate processes does not preclude ventilation of a lung - air sac system. EMG experiments (Codd *et al.*, 2005) suggest that the external intercostal muscles are likely to function in both locomotion and respiration to different degrees in different birds. Therefore recruitment of external intercostal muscles as the primary inspiratory muscles may provide a mechanism to move the ribs and ventilate the lung. Furthermore, additional putative respiratory muscles such as the serratus anterior and posterior muscles may be involved in enabling respiratory movements of the thoracic skeleton, so should be targeted by EMG experiments.

As demonstrated by Codd *et al.*, (2005) and Tickle *et al.*, (2007) (Chapter 2), uncinate processes are an important component of the respiratory aspiration pump in birds. Birds commence pulmonary ventilation around the time of hatch (Menna and Mortola, 2002) and must presumably rely upon the action of muscles associated with processes to move the ribs and sternum to effect breathing. However, developmental studies of the uncinate processes in birds are almost nonexistent and those that have been conducted provide conflicting information about the onset of bone growth (Fujioka, 1952; Hamilton, 1952; Hogg, 1980; Nakane and Tsudzuki, 1999; Maxwell, 2008). The objectives of Chapter 3 follow from the results on Chapter 2 and aim to provide a detailed description of the pattern of process ossification in the turkey and derive the materials properties of uncinate processes at hatch and in more mature birds. The conclusions drawn as outlined in Tickle and Codd (2009) are:

1) Uncinate processes are cartilaginous prior to hatching and ossify gradually during ontogeny beginning from day 22 of incubation in turkeys. Crucially ossification of uncinate processes begins at the onset of air breathing (Tickle and Codd, 2009).
2) However the base of the processes is chondrified at hatch and therefore may not function as effectively in assisting rib movements (Tickle and Codd, 2009).
3) Development of uncinate processes may be linked to increasing sternal mass after hatch (Tickle and Codd, 2009).

This study is the first detailed analysis of ontogenetic changes in the uncinate processes. Given their integral role in ventilation, research on the developmental changes in process ossification between species may present new perspectives on avian breathing mechanics. Differences in morphology associated with locomotion were described in Chapter 2. Whether there are broad differences between the hatchlings of birds adapted to varying primary forms of locomotion, or between altricial and precocial species is unknown. To date, studies of avian developmental biology have mainly focused on species belonging to the Galliformes and have looked at the overall development of the skeleton. While providing a useful model, species such as the turkey, as used in my study, the chicken (Hogg, 1980) and quail (Nakane and Tsudzuki, 1999) are all precocial birds that are mostly independent upon hatching. Contrastingly, there has so far been no detailed research on the developmental changes in processes of altricial species, which rely upon parental care after hatch. It may be that general differences in the pattern of ossification exist between precocial and altricial birds, perhaps related to the early onset of locomotor behaviour in precocial species and in particular related to changes in sternal muscle mass. Furthermore, differences in body morphology related to locomotor adaptation may drive species-specific ossification patterns. For example, diving birds may require a more rigid process at the onset of air breathing due to their relatively elongated morphology and potentially higher leverage forces. The need for comparative data on developmental changes in a wide range of bird species is clear.

Respiration provides the energy for locomotion in animals. This integral link between oxygen delivery and oxidative metabolism was explored in birds (Seymour *et al*., 2008) and mammals (Weibel *et al*., 1991; Weibel and Hoppeler, 2005), where there is a significant relationship between the morphology of the respiratory system. For example mitochondrial volume in exercising mammalian muscle and diffusing capacity of the avian lung is tuned to maximal rate of metabolism. Given the role of uncinate processes as levers in facilitating breathing movements, I moved on in Chapter 4 to address whether there is a relationship between process length and metabolism in birds. By exploring the interaction between these ventilatory structures and metabolism, I aim to resolve how process form may have been shaped by the physiological requirement of oxygen delivery. The major finding of this research article (Tickle *et al*., 2009) was:

1. Uncinate process length is positively correlated with resting metabolic rate; i.e. relatively longer processes occur in those species that have a correspondingly high resting metabolic rate suggesting a functional relationship between process morphology and respiratory physiology (Tickle *et al*., 2009).

While a link between process morphology and resting metabolism has been identified, it seems likely that aspects of the avian respiratory system are tuned to the demands of maximal performance (Taylor and Weibel, 1981). Therefore there is need for more data on the rates of metabolism sustained by birds exercising at maximal exertion under different locomotor modes (swimming, flying, running, walking, diving). Nevertheless, the mechanism that accounts for the correlation between process length and resting metabolic rate requires explanation. As structures that enable ventilatory movements of the ribs and sternum, uncinate processes may enable birds to effectively modify the ventilatory parameters of breathing rate, perhaps via a higher rate of muscle activity, and tidal volume, by larger displacement of the sternum. Perhaps longer processes maintain a high metabolic rate and therefore exercise performance by improving ventilation by movements of the ribs and sternum. For example, birds such as penguins (Wilson *et al*., 2003) and tufted ducks (Parkes *et al*., 2002) increase breathing frequency upon resurfacing after dives. A comparative analysis of data in the literature on respiratory parameters such as breathing frequency and tidal volume together with uncinate process measurements is an obvious first step towards explaining this result.

Locomotion incurs a rise in metabolic rate as muscles increase their use of energy to move the limbs and body. The key to understanding the factors underlying these cost are centred on *in vivo* manipulations. For example, studies of load carrying in mammals have been used to show that the main factor accounting for total metabolism during locomotion is the generation of muscle force to support body weight (Taylor *et al*., 1980). The increased cost of locomotion is in direct proportion to the extra mass added in the form of back loads (Taylor *et al*., 1980). However little research has been undertaken on loaded terrestrial locomotion in birds. Studies on guinea fowl indicate that birds are able to carry loads more economically than mammals, perhaps due to adaptation of hindlimb anatomy (Marsh *et al*., 2006). Therefore loading experiments can be used to manipulate the costs of mechanical functions and provide insight into adaptations that animals have to circumvent potentially energetically expensive activities. One such biomechanical function is avian breathing, since it relies upon dorsoventral displacements of the sternum. Given the link between respiration and locomotion identified in Chapters 2 and 4, Chapter 5 continued this research to investigate how the energetic cost of walking locomotion in the barnacle goose, *Branta leucopsis*, is affected by applying loads (Tickle *et al*., 2010). To manipulate the respective energetic costs of moving the limbs, body weight and sternum during breathing, loads were applied to the legs, back and sternum of geese trained to walk on a motorized treadmill. The main findings of this study (Tickle *et al*., 2010) are as follows:

1) There is a directly proportional relationship between increasing metabolic rate and back load mass in barnacle geese (Tickle *et al*., 2010).
2) Loads carried on the sternum were approximately twice as expensive to carry as the equivalent load carried on the back, indicating that the cost of moving the sternum, and therefore breathing, was increased (Tickle *et al*., 2010).
3) Loads applied to the legs caused the highest proportional increase in the metabolic rate of locomotion most likely due to the increase muscle work required to move the limb (Tickle *et al*., 2010).
4) Loaded locomotion is inexpensive in birds compared to equivalent trials conducted on mammals, perhaps due to adaptations in the hindlimb such as superior elastic storage in the tendons (Tickle *et al*., 2010).

Understanding the biomechanics and physiology associated with respiration and locomotion, from whole animal to individual muscles, is paramount to forming a full understanding of the results presented in Chapter 5. Measuring activity and force production of respiratory and locomotor muscles, using electromyography (Codd *et al*., 2005) and sonomicrometry (Askew and Ellerby, 2007), may offer an insight into the interaction between these systems. Determining the contribution of individual muscles to the overall energy expenditure of locomotion and respiration might help explain the rate of metabolism in birds adapted to different forms of locomotion and during seasonal changes in body mass. I demonstrated in Chapter 6 (Tickle *et al*., 2010) that by increasing the sternal mass, a considerable increase in overall metabolic rate is precipitated. This elevation in metabolism may be due to an increase in the muscular work necessary to produce ventilatory movements of the sternum. However, the cost of breathing in birds remains equivocal despite experimental efforts using guinea fowl (Markley and Carrier, 2010). Furthermore, the plasticity of ventilatory mechanisms seen during postural changes in birds (Codd *et al*., 2005) may extend to recruitment of novel muscle units under conditions of stress. For example, abdominal muscles may be recruited to assist in ventilation by movements of the pelvis (Baumel *et al*., 1990). By identifying respiratory muscles and their relative contributions to whole-animal metabolism using injections of coloured microspheres (Ellerby *et al*, 2005; Ellerby and Marsh, 2006), an estimate of breathing costs could begin to be formed and an overview of respiratory muscle recruitment formulated. This would be a key step in further elucidating the mechanics of ventilation in birds.

Whether an inherent plasticity in respiratory musculature anatomy and physiology facilitates results in differences in terms of energetic cost remains unknown. One constraint that migratory birds may have overcome is the potential for elevated ventilatory costs with sternal muscle hypertrophy, as indicated by the results in Chapter 6 (Tickle *et al*., 2010). An analysis of respiratory muscle function over the annual body mass cycle in migratory species such as the barnacle goose (Portugal *et al*., 2007) is timely in this light. Changes in force production to move a heavy sternum during breathing may correspond to increased metabolic costs, and must be factored into models of energy use during migration. Considering that the respiratory system must function during flight, the mechanical properties of ventilatory muscles may give an insight into the how birds cope with such increased muscular demands. Therefore, to better understand the ventilatory mechanics of birds the patterns of muscle strain should be identified using implanted sonomicrometry crystals to estimate fibre length changes (McGowan *et al*., 2006; Askew and Ellerby, 2007) and EMG to estimate the intensity of muscle activity (Codd *et al*., 2005).

A further expansion of my research into the effects of loading trials is to increase our understanding of the effects of selective breeding in domesticated birds. Many species (such as broiler chickens) have been artificially selected for enlarged breast muscles that are suited to the requirements of the meat industry. Respiratory problems related to rapid growth and large muscle mass are well documented in the literature (e.g. Wideman, 2001). Since the sternum must be moved up and down during breathing, it is conceivable that if respiratory muscles have not adapted to the large increase in sternal mass in some domesticated breeds, respiration may be compromised. An integrative analysis of respiratory muscle biomechanics and physiology during rest and exercise in domesticated birds and their equivalent wild ancestors would present an opportunity to quantify the effects of selective breeding on the respiratory system. Perhaps a reduced capacity for ventilation due to a sub-optimal combination of large breast muscles and comparatively underdeveloped hypaxial ventilatory muscles limits locomotor performance in domestic birds. Domesticated birds such as chickens and turkeys are among perhaps the least well-adapted group of species in terms of locomotor specialisation. These walking birds have relatively short uncinate processes that may not provide the necessary leverage to move an artificially massive sternum. Therefore quantitative dissection of respiratory muscles coupled with physiological *in vivo* measurements of muscle force production will provide us with a better understanding of the trade-off between rapid growth of sternal muscle mass and respiratory function.

Increasing metabolic rate during locomotion with load addition is lower than the corresponding mammalian value, indicating that birds may have adaptations to increase efficiency of load bearing, perhaps in the form of tendon elasticity in the legs. Future studies of the avian hindlimb should therefore consider the role of energy storage by implantation of tendon buckles to measure elastic strain energy during locomotion (Baundinette and Biewener, 1998). Additional measurements on EMG intensity recorded in hindlimb muscles together with information about underlying changes in muscle strain during loading and locomotion (McGowan *et al*, 2006) may help to unravel the mechanisms accounting for economical load carriage in birds.

Based upon shared characteristics such as behavioural traits (Norell *et al*., 1995), skeletal features (Padian and Chiappe, 1998; Codd *et al*., 2008) and physiology (Erickson et al., 2007; Erickson *et al*, 2009), birds are now confirmed to be the descendants of maniraptoran theropod dinosaurs. Comparison of the respiratory systems in the extant descendants of theropod dinosaurs, the birds and crocodilians, indicates that they shared similar heterogeneous lung anatomy (Perry and Sander, 2004). Uncinate processes also occur in maniraptoran theropod dinosaurs (Codd *et al*., 2008). Recent research into the potential role of processes in theropod dinosaurs suggested that they might function in an analogous way to the avian-like ventilatory pump consisting of vertebral ribs, an abdominal gastral basket and a relatively small sternum (Codd *et al*, 2008). The model of process function developed by Tickle *et al*., (2007) (Chapter 2) provides a method to estimate the potential of uncinate processes to elicit rib displacements in both modern birds and fossil specimens. Therefore in Chapter 6 I expanded on this by investigating how the uncinate processes may have functioned in early species of birds and a theropod dinosaur by description of the rib cage anatomy in a theropod and basal avian species. This study concluded that:

1) Uncinate processes in theropod dinosaurs and basal bird species exhibit distinctly avian morphology.
2) Uncinate processes functioned as respiratory structures in basal-most bird species by improving leverage for rib movements.
3) Development of uncinate processes may have been an important step in the evolution of the avian lung-air sac system.

The conclusions derived from my research on fossil specimens provide more evidence for the development of a flow-through respiratory system in theropod dinosaurs and early bird species. Additionally, presence of this effective respiratory mechanism driven by uncinate processes suggests that even the most basal bird taxa had the necessary respiratory adaptations in place to support the rate of energy metabolism required for powered flight. In this light it is important that the thoracic skeleton in further early avian species is analysed. Unfortunately, uncinate processes are often absent in fossil specimens, most likely due to their loss during preservation or collection (Codd *et al*., 2008; Chapter 6). However, measurements of rib, uncinate process and sternal morphology in additional basal birds would provide a better understanding of the evolution of ventilatory mechanics in Aves. A comprehensive analysis of known fossil avians may also assist towards this objective since uncinate processes are often overlooked or misidentified (Codd *et al*., 2008). Therefore current knowledge of the distribution of uncinate processes and their first appearance in the fossil record is most probably not comprehensive and should be extended by description of new species and careful analysis of museum specimens.

The model of uncinate process function provided in Chapter 2 (Tickle *et al*., 2007) demonstrates that reconstructions of a musculoskeletal mechanism can be very useful for determining effects of morphology on biomechanics. Indeed, much research on dinosaur locomotion (Carrier *et al*., 2001) and neck movement (Stevens and Parrish, 1999) has been undertaken using computer modeling. My results on the function of uncinate processes in living and extinct avian species represent an ideal starting point in the development of an accurate computer model of avian breathing. Currently there is no model of cuirassal breathing that can be used to estimate the leverage uncinate processes could exert on the gastralia (Codd *et al*., 2008). Measurement of rib, gastralia and uncinate process morphology in *Sphenodon*, the basal-most living species to have gastralia (Perry *et al*., 2010b), presents an excellent opportunity for the design of a model of cuirassal breathing, that could be adapted to the skeletons of fossil birds. While computer models of biomechanical functions are potentially informative, accurate derivation of uncinate process function in fossil specimens relies upon assumptions about the soft tissue anatomy. A primary objective for future studies of the functional morphology of uncinate processes in basal birds is to reduce the number of assumptions regarding muscle anatomy. In Chapter 6, I used an estimation of muscle fibre anatomy based upon modern bird dissections. Clearly, soft tissue remains are very rarely preserved in fossil specimens so information from modern species that have processes and gastralia, such as *Sphenodon* and crocodilians, could improve my estimation of muscle anatomy. Therefore, through careful design and interpretation of a computer model of rib, sternal and gastral movements, a deeper understanding of the evolution of breathing mechanics in birds will be made possible.

The principal findings of the five research articles presented in this PhD thesis shed important new light on the ventilatory mechanics in birds and highlight interactions between breathing and locomotion. Diversity in avian body morphology driven by adaptation to various locomotor behaviours has resulted in modification of the respiratory system. In particular, I have shown how the morphology of integral respiratory structures, the uncinate processes, is affected by adaptations to different forms of locomotion. My integral comparative approach to understanding form and function in birds has demonstrated that much research remains to be done in order to understand the pressures acting on the respiratory system. Implementing an integrative approach by researching anatomical, physiological and biomechanical adaptations may enable us to further decipher the complexities of the avian respiratory system.

References

Alexander, R. M., Maloiy, G. M. O., Njau, R. and Jayes, A. S (1979) Mechanics of the running of the ostrich (*Struthio camelus*). *J. Zool.* **187**, 169-178.

Askew, G. N. and Ellerby, D. J. (2007) The mechanical power requirements of flight. *Biol. Lett.* **3**, 445-448.

Baudinette, R. V. and Biewener, A. A. (1998) Young wallabies get a free ride. *Nature* **395**, 653-654.

Baumel, J. J., Wilson., J. A. and Bergren, D. R. (1990) The ventilatory movements of the avian pelvis and tail: Function of the muscles of the tail region of the pigeon (*Columba livia*). *J. Exp. Biol.* **151**, 263-277.

Bellairs, A. and Jenkin, C. R. (1960) The Skeleton of Birds. In *Biology and Comparative Physiology of Birds* (ed. A. J. Marshall), pp. 241-300. New York: Academic Press.

Boggs, D. F. (2002) Interactions between locomotion and ventilation in tetrapods. *Comp. Biochem. Physiol. A* **133**, 269-288.

Boggs, D. F., Jenkins. F. A. Jnr., Dial, K. P. (1997) The effects of the wingbeat cycle on respiration in black-billed magpies (*Pica pica*). *J. Exp. Biol.* **200**, 1403-1412.

Brackenbury, J. H. and Avery, P. (1980) Energy consumption and ventilatory mechanisms in the exercising fowl. *Comp. Biochem. Physiol. A* **66**, 439-445.

Bretz, W. L. and Schmidt-Nielsen, K. (1971). Bird respiration: Flow patterns in the duck lung. *J. Exp. Biol.* **54**, 103-118.

Bretz, W. L. and Schmidt-Nielsen, K. (1972). The movement of gas in the respiratory system of the duck. *J. Exp. Biol.* **56**, 57-65.

Burton, F. G. and Tullett, S. G. (1985) Respiration of avian embryos. *Comp. Biochem. Physiol. A* **82**, 735-744.

Butler, P. J. (2010) High fliers: the physiology of bar-headed geese. *Comp. Biochem. Physiol. A* **156**, 325-329.

Carrier, D. R. (1987) The evolution of locomotor stamina in tetrapods: Circumventing a mechanical constraint. *Paleobiology*, **13** 326-341.

Carrier, D. R. (1990) Activity of the hypaxial muscles during walking in the lizard *Iguana iguana*. *J. Exp. Biol.* **152**, 453-470.

Carrier, D. R. (1991) Conflict in the hypaxial musculo-skeletal system: documenting an evolutionary constraint. *Am. Zool.* **31**, 644-654.

Carrier, D. R. (1993) Action of the hypaxial muscles during walking and swimming in the salamander *Dicamptodon ensatus*. *J. Exp. Biol.* **180**, 75-83.

Carrier, D. R. (1996) Function of the intercostal muscles in trotting dogs: ventilation or locomotion? *J. Exp. Biol.* **149**, 1455-1465.

Carrier, D. R. and Farmer, C. G. (2000) The integration of ventilation and locomotion in archosaurs. *Am. Zool.* **40**, 87-100.

Carrier, D. R., Walter, R. M. and Lee, D. V. (2001) Influence of rotational inertia on turning performance of theropod dinosaurs: clues from humans with increased rotational inertia. *J. Exp. Biol.* **204**, 3917-3926.

Chappell, M. A. and Roverud, R. C. (1990) Temperature effects on metabolism, ventilation and oxygen extraction in a neotropical bat. *Respir.Physiol.* **81**, 401-412.

Claessens, L. P. A. M. (2004a). Archosaurian respiration and the pelvic girdle aspiration breathing of crocodyliforms. *Proc. R. Soc. B* **271**, 1461.

Claessens, L. P. A. M. (2004b) Dinosaur gastralia: origin, morphology and function. *J. Vert. Palaeontol.* **24**, 89-106.

Claessens, L. P. A. M., O'Connor, P. M. and Unwin, D. M. (2009). Respiratory evolution facilitated the origin of pterosaur flight and aerial gigantism. *PLoS ONE* **4**, e4497.

Claessens, L. P. A. M. (2008). The skeletal kinematics of lung ventilation in three basal bird taxa (emu, tinamou, and guinea fowl). *J. Exp. Zool. A* **311**, 586-599.

Codd, J. R., Boggs, D. F., Perry, S. F. and Carrier, D. R. (2005). Activity of three muscles associated with the uncinate processes of the giant Canada goose *Branta canadensis maximus*. *J. Exp. Biol.* **208**, 849-857.

Codd, J. R., Manning, P. L., Norell, M. A. and Perry, S. F. (2008) Avian-like breathing mechanics in maniraptoran dinosaurs. *Proc. R. Soc. B*. **275**, 157-161.

Currey, J. D. and Alexander, A. M. (1985) The thickness of the walls of tubular bones. *J. Zool.* **206**, 453-468.

Dawes, C. M. (1981) The effects of cooling the egg on the respiratory movements of the hatching fowls, *Gallus G. domesticus*, with a note on vocalization. *Comp. Biochem. Physiol. A* **68**, 399-404.

De Troyer, A., Kelly, S., Macklem, P. T. and Zin, W. A. (1985) Mechanics of intercostal space and actions of external of intercostal internal muscles. *J. Clin. Invest.* **75**, 850-857.

Dial, K. P., Kaplan, S. R. and Goslow Jr, G. E. (1988) A functional analysis of the primary upstroke and downstroke muscles in the domestic pigeon *(Columba livia*) during flight. *J. Exp. Biol.* **134**, 1-16.

Dotterweich, H. (1936) Die Atmung der Vögel. *Z. vergl. Physiol* **23,** 744-770.

Dumont, E. R. (2010) Bone density and the lightweight skeleton of birds. *Proc. Roy. Soc. B* **277**, 2193-2198.

Duncker, H-R. (1971). The Lung Air Sac System of Birds: a contribution to the functional anatomy of the respiratory apparatus, pp. 19-39. New York. Springer-Verlag.

Duncker, H-R. (1974) Structure of the avian respiratory tract. *Respir. Physiol.* **22**, 1-19.

Dyke, G. J. and Rayner, J. M. V. (2001) Forelimb shape and the evolution of birds. In *New Perspectives on the Origin and Early Evolution of Birds.* Eds J. Gaultier, L-F Gall, pp 275-282. New Haven. Peabody Museum of Natural History Press.

Ellerby, D. J., Henry, H. T., Carr, J. A., Buchanan, C. I. and Marsh, R. L. (2005) Blood flow in guinea fowl *Numida meleagris* as an indicator of energy expenditure by individual muscles during walking and running. *J. Physiol.* **564**, 631-648.

Ellerby, D. J. and Marsh, R. L. (2006) The energetic costs of trunk and distal-limb loading during walking and running in guinea fowl *Numida meleagris*: II. Muscle energy use as indicated by blood flow. *J. Exp. Biol.* **209**, 2064-2075.

Erickson, G. M., Rogers, K. C., Varricchio, D. J., Norell, M. A. and Xu, X. (2007) Growth patterns in brooding dinosaurs reveals the timing of sexual maturity in non-avian dinosaurs and genesis of the avian condition. *Biol. Lett.* **3**, 558-561.

Erickson, G. M., Rauhut, O. W. M., Zhou, Z., Turner, A. H., Inouye, B. D., Hu, D. and Norell, M. A. (2009) Was dinosaurian physiology inherited by birds? Reconciling the slow growth in *Archaeopteryx*. *PLoS ONE* **4**, e7390.

Farmer, C. G. (2006) On the origin of avian air sacs. *Respir. Physiol. Neurobiol.* **154**, 89-106.

Farmer, C. G. and Sanders, K. (2010) Unidirectional airflow in the lungs of alligators. *Science*, **327**, 338-340.

Fedde, M. R., Burger, R.E. and Kitchell, R. L. (1964) Electromyographic studies of the effects of bodily posture and anaesthesia on the activity of the respiratory muscles of the domestic cock. *Poultry Sci.* **43**, 839-946.

Fedde, M. R. (1987) Respiratory Muscles. In *Bird Respiration, Volume 1* (ed. Seller, T. J.), pp 5-16. Boca Ranton: CRC Press.

Fedde, M. R. (1998) Relationship of structure and function of the avian respiratory system to disease susceptibility. *Poultry Sci.***77**, 11330-1138.

Feduccia, A. (1996) *The origin and evolution of birds.* Yale University Press, New Haven, CT, USA.

Fenwick, S. A. (1997) Intrinsic control of vascularisation in developing cartilage rudiments. *Int. J. Exp. Pathol.* **78(3)**: 187-196.

Fujioka, T. (1952) Time and order of appearance of ossification centres in the chicken skeleton. *Acta Anatomica Nipponica* **30**, 140-150.

Gans, C. and Clark, B. (1976) Studies on ventilation of *Caiman crocodilus* (Crocodilia: Reptilia). *Respir. Physiol.* **26 (3)**, 285-301.

Gehr, P., Sehovic, S., Burri, P. H., Claassen, H. and. Weibel, E. R. (1980) The lung of shrews: morphometric estimation of diffusion capacity. *Respir. Physiol.* **40 (1)**, 33-47.

George, J. C. and Berger, A. J. (1966) Muscles of the Axial Skeleton. In *Avian Myology* pp 270-300 New York and London: Academic Press.

Habib, M. B. and Ruff, C. B. (2008) The effect of locomotion on the structural characteristics of avian limb bones. *Zool. J. Linn. Soc.* **153**, 601-624.

Hamilton, H. L. (1952) Lillie's Development of the Chick, 3rd Edition. Henry Holt & Co., New York.

Hartman, F. A. (1961) Locomotor mechanisms of birds. *Smithson. Misc. Collns.* **143**, 1-91.

Hazelhoff, E. H. (1951) Structure and function of the lung of birds. *Poultry Sci*. **30**, 3-10.

Hildebrand, M. (1982) Body Skeleton. In *Analysis of Vertebrate Structure*, 2nd Edition, pp. 157-158. John Wiley and Sons, New York.

Hogg, D. A. (1980) A re-investigation of the centres of ossification in the avian skeleton at and after hatching. *J. Anat.* **130 (4)**, 725-743.

Jones, J. H., Effmann, E. L. and Schmidt-Nielsen, K. (1981) Control of air flow in bird lungs: radiographic studies. *Respir. Physiol.* **45**, 121-131.

Kadano, H., Okado, T. and Ono, K. (1963) Electromyographic studies on the respiratory muscles of the chicken. *Poultry Sci.* **42**, 121-128.

Kardong, K. (2006) The respiratory system. In *Vertebrates, Comparative Anatomy, Function, Evolution*. McGraw-Hill Publishing, New York.

King, A. S. and McLelland, J. (1975) Skeletomuscular System. In *Outlines of Avian Anatomy*, pp. 20. London: Baillière Tindall.

Maina, J. N. and King, A. S. (1982) The thickness of the avian blood-gas barrier: qualitative and quantitative observations. *J. Anat.* **134 (3)**, 553-562.

Maina, J. N., Singh, P. and Moss, E. A. (2009) Inspiratory aerodynamic valving occurs in the ostrich, *Struthio camelus* lung: A computational fluid dynamics study under resting unsteady state inhalation. *Respir. Physiol. Neurobiol.* **169**, 262-270.

Maina, J. N. (2000) What it takes to fly: the structural and functional respiratory refinements in birds and bats. *J. Exp. Biol.* **203**, 3045-3064.

Maina, J. N. (2006) Development, structure, and function of a novel respiratory organ, the lung-air sac system of birds: to go where no other vertebrate has gone. *Biology Reviews* **81**, 545-579.

Magnussen, H., Willmer, H. and Scheid, P. (1976) Gas exchange in the air sacs: a contribution to respiratory gas exchange in ducks. *Respir. Physiol.* **26**, 129-146.

Markley, J. S. and Carrier, D. R. (2010) The cost of ventilation in birds measured via unidirectional artificial ventilation. *Comp. Biochem. Physiol A.* **155**, 146-153.

Marsh, R. L., Ellerby, D. J., Henry, H. T. and Rubenson, J. (2006) The energetic costs of trunk and distal-limb loading during walking and running in guinea fowl *Numida meleagris*: I. organismal metabolism and biomechanics. *J. Exp. Biol.* **209**, 2050-2063.

Maxwell, E. E. and Harrison, L. B. (2008) Ossification sequence of the common tern (*Sterna hirundo*) and its implications for the interrelationships of the Lari (Aves, Charadriiformes). *J. Morphol.* **269**, 1056-1072.

Maxwell, E. E. and Larsson, H. C. E. (2009) Comparative ossification sequence and skeletal development of the postcranium of palaeognathous birds (Aves: Palaeognathae). *Zool. J. Linn. Soc.* **157**, 169-196.

McGowan, C. P., Duarte, H. A., Main, J. B. and Biewener, A. A. (2006) Effects of load carrying on metabolic cost and hindlimb muscle dynamics in guinea fowl (*Numida meleagris*). *J. Appl. Physiol.* **101**, 1060-1069.

Menna, T. M. and Mortola, J. P. (2002) Metabolic control of pulmonary ventilation in the developing chick embryo. *Respir. Physiol.* **130**, 43-55.

Nakane, Y. and Tsudzuki, M. (1999) Development of the skeleton in Japanese quail embryos. *Dev. Growth Differ.* **41**, 523-534.

Nassar, P. N., Jackson, A. C. and Carrier, D. R. (2001) Entraining the natural frequencies of running and breathing in guinea fowl. *J. Exp. Biol.* **204**, 1641-1651.

Norell, M. A., Clark, J. M., Chiappe, L. M. and Dashzeveg, D. (1995) A nesting dinosaur. *Nature* **378**, 774-776.

O'Connor, P. M. and Claessens, L. P. A. M. (2005). Basic avian pulmonary design and flow-through ventilation in non-avian theropod dinosaurs. *Nature* **436**, 253-256.

Ostrom, J. H. (1969) Osteology of *Deinonychus antirurphopus*, an unusual theropod from the Lower Cretceous of Montana. *Peabody Mus. Nat. Hist. Bull.* **30**, 1-165.

Padian, K. and Chiappe, L. M. (1998) The origin and early evolution of birds. *Biol. Rev.* **73**, 1-42.

Patak, A. and Baldwin, J. (1993) Structural and metabolic characterization of the muscles used to power running in the emu (*Dromaius novaehollandiae*), a giant flightless bird. *J. Exp. Biol.* **175**, 233-249.

Parkes, R., Halsey, L. G., Woakes, A. J., Holder, R. L. and Butler, P. J. (2002) Oxygen uptake during post dive recovery in a diving bird *Aythya fuligula*: implications for optimal foraging models. *J. Exp. Biol.* **205**, 3945-3954.

Perry, S. F. and Sander, M. (2004) Reconstructing the evolution of the respiratory apparatus in tetrapods. *Resp. Physiol. Neurobiol.* **144**, 125-139.

Perry, S. F., Codd, J. R. and Klein, W. (2005) Evolutionary biology of aspiration breathing and origin of the mammalian diaphragm. *Revue de Maladies Respiratoires* **22**, 2S19-2S38.

Perry, S. F., Similowski, T., Klein, W. and Codd, J. R. (2010a) The evolutionary origin of the mammalian diaphragm. *Respir. Physiol Neurobiol.* **171**, 1-16.

Perry, S. F., Klein, W. and Codd, J. R. (2010b) Trade-offs in the evolution of the respiratory apparatus of chordates. In *Cardio-respiratory control in vertebrates* (eds. Glass, M. L. and Wood, S. C.) pp. 193-204. Springer-Verlag, Berlin.

Portugal, S.J., Green, J. A. and Butler, P. J. (2007) Annual changes in body mass and resting metabolism in captive barnacle geese (*Branta leucopsis*): the importance of wing moult. *J. Exp. Biol.* **210**, 1391-1397.

Rayner, J. M. V. and Couldrick, L. B. (2003) Aerodynamic and biochemical determinants of wing shape in birds. *Comp. Physiol. Biochem.* A **134**, 38

Scheid, P. and Piiper, J. (1970) Analysis of gas exchange in the avian lung: theory and experiments in the domestic fowl. *Respir. Physiol.* **9**, 246-262.

Scheid, P., Slama, H. and Piiper, J. (1972) Mechanisms of unidirectional flow in parabronchi of avian lungs: measurements in duck lung preparations. *Respir. Physiol.* **14**, 83-95.

Scheid, P. (1979) Mechanisms of gas exchange in bird lungs. *Rev. Physiol. Biochem. Pharmacol.* **86**, 137-186.

Scherft, J. P (1984): The amount of proteoglycans in the cartilage matrix and the onset of mineralisation. *Metab. Bone Dis. Relat. Res.* **5(4)**, 195-203.

Schmidt-Nielsen, K., Kanwisher, J., Lasiewski, R. C., Cohn, J. E. and Bretz, W. L. (1969) Temperature regulation and respiration in the ostrich. *Condor* **71**, 341-352.

Seymour, R. S., Runciman, S. and Baudinette, R. V. (2008) Development of maximum metabolic rate and pulmonary diffusing capacity in the superprecocial

Australian Brush Turkey *Alectura lathami*: an allometric and morphometric study. *Comp. Biochem. Physiol. A* **150**, 169-175.

Shufeldt, R. W. (1890) "The Myology of the Raven (*Corvus corax sinuatus*). New York: Macmillan.

Stahel, C. D. and Nicol, S. C. (1988) Ventilation and oxygen extraction in the little penguin (*Eudyptula minor*), at different temperatures in air and water. *Respir. Physiol.* **71**, 387-398.

Stevens, K. A. and Parrish, J. M. (1999) Neck posture and feeding habits of two Jurassic Sauropod dinosaurs. *Science* **284**, 798-800.

Taylor, C. R., Heglund, N. C., McMahon, T. A. and Looney, T. R. (1980) Energetic cost of generating muscular force during running: a comparison of large and small animals. *J. Exp. Biol.* **86**, 9-18.

Taylor, C. R. and Weibel, E. R. (1981) Design of the mammalian respiratory system. I. Problem and strategy. *Respir. Physiol.* **44**, 1-10.

Tickle, P. G., Ennos, A. R., Lennox, L. E., Perry, S. F. and Codd, J. R. (2007) Functional significance of the uncinate processes in birds. *J. Exp. Biol.* **210**, 3955-3961.

Tickle, P. G. and Codd, J. R. (2009) Ontogenetic development of the uncinate processes in the domestic turkey (*Meleagris gallopavo*). *Poultry Sci.*, **88**, 179-184.

Tickle, P. Nudds, R. and Codd, J. (2009) Uncinate process length in birds scales with resting metabolic rate. *PLoS ONE* **4(5)**: e5667.

Tickle, P. G., Richardson, M. F. and Codd, J. R. (2010) Load carrying during locomotion in the barnacle goose (*Branta leucopsis*): the effect of load placement and size. *Comp. Biochem. Physiol. A* **156**, 309-317.

Tucker, V. A. (1993) Gliding birds: reduction of drag by wing tip slots between the primary feathers. *J. Exp. Biol.* **180**, 285-310.

Tullett, S. G. and Deeming, D. C. (1982) The relationship between eggshell porosity and oxygen consumption of the embryo in the domestic fowl. *Comp. Biochem. Physiol. A* **72**, 529-533.

Vanden Berge, J. C. and Zweers, G. A. (1993) Myologia. In *Handbook of Avian Anatomy: Nomina Anatomica Avium*, 2nd Edition (ed. J. J. Baumel). Cambridge, MA, USA: Nuttall Ornithological Club.

Walker, W. F. Jnr. and Liem, K. F. (1994) Evolution of the Postcranial Skeleton. In *Functional Anatomy of the Vertebrates: an Evolutionary Perspective*, pp 270. New York: Saunders College Publishing.

Weibel, E. R., Taylor, C. R. and Hoppeler, H. (1991) The concept of symmorphosis: a testable hypothesis of structure-function relationship. *Proc. Natl. Acad. Sci. U. S. A.* **88**, 10357-10361.

Weibel, E. R. and Hoppeler, H. (2005) Exercise-induced maximal metabolic rate scales with muscle aerobic capacity. *J. Exp. Biol.* **208**, 1635-1644.

Welty, J. C. (1988) Bones and muscle. In *The Life of Birds* (eds. Welty, J. C. and Baptista, L.), p. 59. W. B. Saunders and Co., London.

Welty, J. C., and Baptista, L. (1988) The Appendicular Skeleton. In *The Life of Birds*, 4th Edition, pp.62. London: W. B. Saunders and Co.

West, J. B. (2006) Did evolution go the wrong path for the human lung? *Physiol. News* **65**, 17-18.

Wideman, R. F. (2001) Pathophysiology of heart/lung disorders: pulmonary hypertension syndrome in broiler chickens. *World Poultry Sci. J.* **51**, 289-307.

Wilson, R. P., Simeone, A., Luna-Jorquera, G., Steinfurth, A., Jackson, S. and Falhman, A. (2003) Patterns of respiration in diving penguins: is the last gasp an inspired tactic? *J. Exp. Biol.* **206**, 1751-1763.

Xu, X., Zhou, Z. and Wang, X. (2000) The smallest known non-avian theropod dinosaur. *Nature*, **408**, 705-708.

Xu, X., Norell, M. A., Kuang, X., Wang, X., Zhao, Q. and Jia, C. (2004). Basal tyrannosauroids from China and evidence for protofeathers in tyrannosauroids. *Nature* **431**, 680-684.

Zeuthen, E. (1942) The ventilation of the respiratory tract in birds. *K. danske Vidensk. Selsk. Biol. Medd.* **17**, 1-51 .

Zimmer, K. (1935) Beitrage zur Mechanik der Atmung bei den Vögeln in Stand und Flug. Aufgrund anatomischer-physiologisher und experimenteller Studien. *Zoologica* **88**, 1-69.